Characterisation and Protein Complexation of an Anthocyanin-Bound Pectin Extracted from New Zealand Blackcurrant (*Ribes nigrum*)

A thesis submitted in partial fulfilment of the requirements for the degree of

Doctor of Philosophy

in

Food Technology

At Massey University, Palmerston North, New Zealand

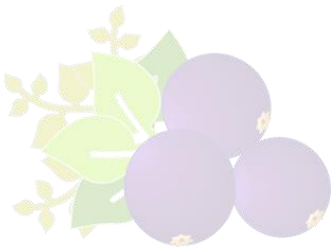

Nurhazwani Salleh

2022

Plant & Food Research
Rangahau Ahumāra Kai

MASSEY UNIVERSITY
TE KUNENGA KI PŪREHUROA
UNIVERSITY OF NEW ZEALAND

agresearch
āta mātai, mātai whetū

"O God, there is no ease except in that which You have made easy,
and You make the difficulty if You wish, easy."
(Sahih Ibn Hibban)

Dedicated to my dearest parents, Haji Salleh and Hajjah Zaimah, for being the loving and caring parents that never stop praying for her daughter

Abstract

The main objective of this thesis was to investigate the cause of physical instability in blackcurrant juice-milk system. Poor phase stability in fruit juice-milk beverages is a major challenge for the clean-label beverage industry as milk protein can interact with fruit components, like polysaccharides and polyphenols, generating unwanted characteristics such as coagulation of milk proteins and phase separation. Hence, the principal step to understand the causes of poor phase stability was to identify and study the key interactive components of the juice, which was extracted from the New Zealand blackcurrant (*Ribes nigrum*), and then investigate their interactions with milk proteins.

The key components of the blackcurrant juice were first isolated using mild extraction procedures, via ethanol precipitation and dialysis, and were identified as a complex fraction particularly rich in pectin and anthocyanins (Chapter 4). Proximate analysis revealed that the fraction contained carbohydrate (78% w/w), uronic acid (21% w/w), protein (4.8% w/w), anthocyanin (3.9% w/w) and calcium (2.2% w/w). The pectin-rich fraction had a net negative surface charge of -23.1 mV (at pH 4.8), a pK_a value of 1.7 and a relatively high degree of esterification (65.2%). Constituent sugar analysis showed that the fraction was mostly made of galacturonic acid, rhamnose, arabinose and galactose, and NMR spectroscopic analysis revealed that it was rich in rhamnogalacturonans with arabinogalactan side chains. This pectic fraction was unique as it was highly pigmented, with cyanidin 3-*O*-rutinoside as its major anthocyanin. Liquid chromatography revealed that the anthocyanins were tightly bound to the fraction as methanol used in the technique failed to separate them. Results from size-exclusion chromatography coupled with multi-angle laser light scattering showed that the blackcurrant juice contained two major pectic fractions — $\approx$ 283 kDa present at 14.6% w/w and $\approx$ 97 kDa at 85.5% w/w — with the latter producing higher $UV_{280\ nm}$ signal, signifying that proteins and/or polyphenols were present mainly in the second fraction.

Association of anthocyanins to biopolymers like pectin and protein can occur via multiple interactive forces (electrostatic, hydrophobic and hydrogen bonding forces), and pH is known to play a significant role as it can affect the associative mechanisms of anthocyanins by changing their molecular configuration and ability to electrostatically interact. An attempt to dissociate blackcurrant anthocyanins from the blackcurrant biopolymers was carried out by disrupting electrostatic interactions and changing the planarity of anthocyanins via pH adjustments and ultra-filtration (Chapter 5). Lowering the juice pH to 2 did not result in anthocyanins dissociation, likely because anthocyanins were bound to the biopolymers by other interactive forces apart from the electrostatic

bonds. Increasing the juice pH to 4.5 might have dissociated some anthocyanins from the biopolymers, but this was not reflected in the analysis of anthocyanins, probably because the freed anthocyanins had degraded before the analysis was carried out. Overall, size segregation of the juice components via ultra-filtration was relatively effective. Regardless of the pH, majority of the anthocyanins were still tightly associated with the large molecular weight biopolymers, confirming the involvement of multiple interactive forces.

In order to uncover the cause of phase instability in blackcurrant juice-milk system, a complexation study between the isolated pectin-rich fraction and whey proteins was conducted (Chapter 6). The impact of bound anthocyanins on pectin-protein interactions was studied by exploring the effects of pH (pH 3.5 and pH 4.5), heating (85 °C, 15 min) and heating sequence (mixed-heated or heated-mixed). The pH was found to influence the colour, turbidity, particle size and surface charge of the mixtures, but its impact was most drastic when heating was introduced. Heating increased the amount of blackcurrant pectin within the complexes—especially at pH 3.5, where 88% w/w of the initial pectin was found in the sedimented (insoluble) fraction. Based on physical stability measurements, the mixed-heated system at pH 4.5 displayed better stability than at pH 3.5. A noteworthy finding was that heating sequence was found to be effective in preventing the destabilisation of the systems. Mixing of components before heating produced a more stable system with small complexes (<300 nm) and relatively low polydispersity. However, heating whey proteins before mixing with blackcurrant pectin prompted protein aggregation, producing large complexes (>400 nm) that worsened the destabilisation.

The influence of bound anthocyanins on pectin-protein complexation was further studied by comparing two types of pectin-protein mixtures: (i) a mixture that is rich in anthocyanin (blackcurrant pectin-whey protein, BCP-WP) and (ii) a mixture that is free of anthocyanin (citrus pectin-whey protein, CP-WP) (Chapter 7). The mixtures were prepared at pH 4.5 with and without heat treatment at 85 °C. The study revealed that there was no direct relationship between anthocyanin presence and the destabilisation of mixtures. The Fourier-Transform Infrared (FTIR) spectrum of the heated and non-heated BCP-WP sedimented fractions showed the emergence of a peak at 800-1200 cm^{-1}, signifying the presence of anthocyanin-protein interactions. This peak, however, was absent in the spectrum of any of the anthocyanin-free CP-WP sedimented fractions, indicating that the bound anthocyanins of blackcurrant pectin provided the whey proteins with additional binding sites. The findings from FTIR analyses also indicated that non-electrostatic forces were most likely the governing forces of the heated BCP-WP mixture, via hydrophobic interactions and later reinforced by hydrogen bonds upon cooling.

Abstract

This thesis revealed that poor phase stability of the blackcurrant juice-milk system should not be attributed exclusively to the blackcurrant juice components, particularly the polyphenols. Environmental factors like pH and heat were likely the leading cause of phase instability as they could intensify the interactions that occurred in the mixed system, which eventually destabilised the mixture. This suggests that appropriate processing conditions can be applied to positively affect the blackcurrant juice-milk system.

Acknowledgements

In the name of God, The Most Gracious and The Most Merciful.

First and foremost, I would like to express my gratitude to The Almighty God for allowing me to accomplish one of my many dreams. Completing a doctoral study has taught me a lot about life and myself, not just scientific and academic knowledge. It was one of the most confronting task of my life. The journey has been emotional yet invigorating as I was 'forced' to face my strengths, passions, fears, and weaknesses.

This study would not have happened without the financial support from AgResearch and Massey University, so I would like to thank them for this once-in-a-lifetime opportunity.

I would like to give a huge Thank You to my dearest supervisor, A/P Lara Matia-Merino, for being a dedicated and patient mentor, as well as a very wise friend when I needed one. Thank you for the inspiration and continuous encouragement. I am very fortunate to have you as my professional mentor and friend.

Another huge thanks go out to my co-supervisors, A/P Kelvin Goh, Dr Lee Huffman, and Dr Mike Weeks, for helping me to complete the doctorate.

To my loving husband, thank you for the endless support that you have rendered, and thank you so much for taking care of me throughout the critical periods of my study. May God repay your kindness and generosity in bountiful sustenance.

To my supportive and awesome bunch of friends, especially to Cailing, Feng Ming, Akshay, Anynda and Marzieh, thank you so much for adding colours and spices to my doctoral life! I appreciate the unceasing tips and guidance relating to studies and life <3

To dearest Heather, thank you for the time you spent listening to my overwhelming emotions and complains.

To the very helpful lab managers, especially to Michelle and Steve, thank you for completing my purchase order in a timely manner, and for forgiving me when I left red and purple stains on equipment and lab bench.

A very special thanks to Dr Tony McGhie and Martin Hunt from Plant and Food Research for accommodating me at their laboratory and guiding me in liquid chromatography and mass spectrometry work, as well as to Dr Erin O'Donoghue for her huge help in measuring the degree of pectin esterification.

Another special thanks go out to Dr Ian Sims and Dr Tracey Bell from The Ferrier Research Institute for their contribution in structural analysis work.

Also, special thanks to Prof. Mark Waterland from the School of Natural Sciences at Massey University, for the guidance and tips on working with the Fourier-Transform Infrared spectroscopy.

Finally, thank you to all Massey personnel who has provided so much help in the laboratories, technical issues, and administrative work.

Table of Contents

Abstract ..... **i**

Acknowledgements ..... **iv**

Table of Contents ..... **v**

List of Figures ..... **xi**

List of Tables ..... **xvii**

List of Publications and Conference Proceedings ..... **xviii**

Chapter 1 Introduction **1**

Chapter 2 Literature Review **5**

2.1. Blackcurrant Fruit **5**

2.1.1. Blackcurrant Phenolic Compounds 6

2.1.1.1. Anthocyanins 7

2.1.1.2. Non-Anthocyanin Phenolic Compounds 11

2.1.2. Blackcurrant Pectin 13

2.2. Bovine Whey Protein **16**

2.2.1. β-lactoglobulin 16

2.2.2. α-lactalbumin 17

2.2.3. Heat-Induced Denaturation and Aggregation of Whey Proteins 17

2.3. Interactions Between the Reactive Components **20**

2.3.1. Pectin-Anthocyanin Interactions 20

2.3.1.1. Interactive Forces between Pectin and Anthocyanins 21

2.3.2. Pectin-Protein Interactions 22

2.3.2.1. Molecular Parameters Affecting Pectin-Protein Interactions 23

2.3.2.2. Environmental Factors Affecting Pectin-Protein Interactions 24

2.3.2.3. Interactive Forces Between Pectin and Protein 25

2.3.3. Polyphenol-Protein Interactions 25

2.3.3.1. Factors Affecting Polyphenol-Protein Interactions 26

2.3.3.1.1. Temperature and pH 26

2.3.3.1.2. Type of Protein 26

2.3.3.1.3. Polyphenol-Protein Ratio 27

2.3.3.1.4. Type of Polyphenol 27

2.3.3.2. Interactive Forces between Polyphenols and Proteins 28

Chapter 3 Experimental Techniques 29

3.1. Proximate Analysis 29

3.1.1. Total Carbohydrate Analysis 29

3.1.2. Galacturonic Acid Analysis 30

3.1.3. Protein Analysis 30

3.1.4. Composition of Blackcurrant Puree and Juice 30

3.2. Identification and Quantification of Phenolic Compounds 33

3.2.1. pH Differential Method 33

3.2.2. Reversed-Phase Ultra-Performance Liquid Chromatography 34

3.2.3. Liquid Chromatography-Mass Spectrometry 34

3.2.4. Polyphenol Profile of Blackcurrant Puree 36

3.3. Light Scattering Techniques 39

3.3.1. Size-Exclusion Chromatography-Multi-Angle Laser Light Scattering 39

3.3.2. Dynamic Light Scattering 41

3.3.3. Electrophoretic Light Scattering 42

3.3.4. Laser Diffraction 44

3.3.5. Static-Multiple Light Scattering 44

3.4. Fourier-Transform Infrared Spectroscopy 45

Chapter 4 Identification of Blackcurrant Juice Interactive Components 48

4.1. Introduction 48

4.2. Materials and Methods 50

4.2.1. Materials 50

4.2.2. Isolation of Pectin-Rich Fractions from Blackcurrant Juice 50

4.2.3. Proximate Analysis of Blackcurrant Pectin-Rich Fractions 53

4.2.3.1. Total Carbohydrate in Blackcurrant Pectin-Rich Fractions 53

4.2.3.2. Pectin in Blackcurrant Pectin-Rich Fractions 53

4.2.3.3. Anthocyanins in Blackcurrant Pectin-Rich Fractions 53

4.2.4. Polyphenol Profile of Blackcurrant Juice and Pectin-Rich Fractions 53

4.2.5. Molecular Characterisation of Blackcurrant Pectin-Rich Fractions 54

4.2.6. Constituent Sugar Composition of Dialysed Blackcurrant Pectin-Rich Fraction 55

4.2.7. Nuclear Magnetic Resonance (NMR) Spectroscopy of Dialysed Blackcurrant Pectin-Rich Fraction 56

4.2.8. Acid Dissociation Constant (pK_a) of Dialysed Blackcurrant Pectin-Rich Fraction 56

4.2.9. Zeta-Potential of Dialysed Blackcurrant Pectin-Rich Fraction 56

4.2.10. Degree of Esterification of Dialysed Blackcurrant Pectin-Rich Fraction 57

4.3. Results and Discussion 58

4.3.1. Isolation and Composition of Blackcurrant Pectin-Rich Fractions 58

4.3.2. Polyphenols in Blackcurrant Juice and Pectin-rich Fractions 61

4.3.3. Molecular Characteristics of Blackcurrant Pectin-Rich Fractions 66

4.3.4. Constituent Sugar Composition and NMR Spectroscopy of Dialysed Blackcurrant Pectin-Rich Fraction 71

4.3.5. Physico-Chemical Properties of Dialysed Blackcurrant Pectin-Rich Fraction 73

4.4. Conclusions 75

Chapter 5 Effect of pH on Blackcurrant Juice Interactive Components 76

5.1. Introduction 76

5.2. Materials and Methods 78

5.2.1. Materials 78

5.2.2. Ultra-Filtration of Blackcurrant Juice 78

5.2.3. Quantification of Protein 79

5.2.4. Quantification of Anthocyanins by pH Differential Method 79

5.2.5. Quantification of Galacturonic Acid 79

5.2.6. Molecular Profile of Compounds in Filtered Blackcurrant Juice 80

5.2.7. Quantification and Identification of Polyphenols in Filtered Blackcurrant Juice 80

5.2.8. Statistical Analysis 80

5.3. Results and Discussion 81

5.3.1. Filtered Blackcurrant Juice 81

5.3.2. Effect of pH on the Molecular Profile of Blackcurrant Juice Components 82

5.3.3. Distribution of Protein, Anthocyanin and Pectin in Filtered Blackcurrant Juice 90

5.3.4. Effect of pH on Anthocyanins and Other Phenolic Compounds 93

5.4. Conclusions 96

Chapter 6 Complexation Between Anthocyanin-Bound Blackcurrant Pectin and Whey Protein: Effect of pH and Heat Treatment 98

6.1. Introduction 98

6.2. Materials and Methods 101

6.2.1. Materials 101

6.2.2. Complexation of Blackcurrant Pectin and Whey Protein 101

6.2.3. Physical Stability Measurement 103

6.2.4. Particle Size and Zeta-Potential Measurements 103

6.2.5. Quantification of Galacturonic Acid 104

6.2.6. Fourier-Transform Infrared Spectroscopy 104

6.2.7. Statistical Analysis 105

6.3. Results and Discussion 106

6.3.1. Visual Appearance and Physical Stability of Blackcurrant Pectin-Whey Protein Mixtures 106

6.3.2. Particle Size and Zeta-Potential of Blackcurrant Pectin-Whey Protein Complexes 108

6.3.3. Insoluble Complexes in Blackcurrant Pectin-Whey Protein Mixtures 115

6.3.4. Overall Discussion: Possible Mechanism of Complexation between Blackcurrant Pectin and Whey Protein 121

6.4. Conclusions 124

Chapter 7 Comparison on Pectin-Protein Complexation Between Blackcurrant and Citrus Pectins 126

7.1. Introduction 126

7.2. Materials and Methods 128

7.2.1. Materials 128

7.2.2. Characterisation of Pectins 128

7.2.3. Preparation of Pectin-Protein Mixtures 129

7.2.4. Physical Stability Measurement 130

7.2.5. Particle Size and Zeta-Potential Measurements 131

7.2.6. Quantification of Galacturonic Acid and Protein 131

7.2.7. Fourier-Transform Infrared Spectroscopy 132

7.2.8. Statistical Analysis 132

7.3. Results and Discussion 133

7.3.1. Characterisation of Blackcurrant and Citrus Pectins 133

7.3.2. Visual Appearance and Physical Stability of Pectin-Protein Mixtures 136

7.3.3. Particle Size and Zeta-Potential of Pectin-Protein Complexes 141

7.3.4. Distribution of Pectin and Protein in Soluble and Insoluble Fractions 150

7.3.5. FTIR Assessment of Soluble and Insoluble Fractions 153

7.4. Conclusions 158

Chapter 8 Overall Conclusions and Future Work Recommendations 159

8.1. Overall Conclusions 159

8.1.1. What are the components of blackcurrant juice that can potentially interact with milk proteins? 159

8.1.2. How do whey proteins interact with the identified blackcurrant juice components? 162

8.1.3. How do blackcurrant pectin-whey protein interactions differ from citrus pectin-whey protein interactions? 164

8.2. Future Work Recommendations 167

8.2.1. Further Work on Anthocyanins Dissociation 167

8.2.2. Investigation on Blackcurrant Protein 167

8.2.3. Isolation and Characterisation of Pectin from Blackcurrant Puree 167

8.2.4. Effect of Ionic Strength on Blackcurrant Pectin-Whey Protein System 167

8.2.5. Interaction Study Between Blackcurrant Pectin and Milk Proteins 168

References 169

Appendices 188

Appendix A – Supplementary Information for Chapter 4 188

Appendix B – Supplementary Information for Chapter 7 189

List of Figures

Figure 1.1 Ultra-high temperature treated whole milk and its mixtures with blackcurrant juice at increasing juice concentration (v/v). 2

Figure 1.2 Overview of research work. 4

Figure 2.1 Concentration (mg/kg fresh fruit) and percentage of phenolic compounds in conventionally grown blackcurrant fruit. Data obtained from Anttonen and Karjalainen (2006). 7

Figure 2.2 Structure of anthocyanidin and anthocyanin with various substituent positions; R1 and R2 can be –H, –OH or –OCH3 and R3 can be –H (anthocyanidin) or –glycosyl (anthocyanin). Adapted from Schwartz et al. (2008) and Prior and Wu (2012). 7

Figure 2.3 Structure of major blackcurrant anthocyanins. 2D structures from PubChem (2022a, 2022b, 2022c, 2022d). 9

Figure 2.4 Transformation of cyanidin structure according to the pH of the medium. Adapted from Brouillard (1988), Rivas-Gonzalo (2003), Prior and Wu (2012) and Miller et al. (2013). 10

Figure 2.5 Structure of commonly found flavonol aglycones. Adapted from Zhang et al. (2013).....12

Figure 2.6 Types of interactions that can occur between blackcurrant components and whey protein. 20

Figure 2.7 Types of interactions between polysaccharide and protein in aqueous solution. Adapted from Goh et al. (2009) 23

Figure 3.1 Schematic diagram of electrospray ionisation process in mass spectrometer. Adapted from Banerjee and Mazumdar (2012). 35

Figure 3.2 Schematic diagram of a size-exclusion chromatography-multi-angle laser light scattering (SEC-MALLS) setup. Adapted from Moraes and Archer (2015). 39

Figure 3.3 Schematic diagram on size-exclusion chromatography separation of two macromolecular sizes. Adapted from Malawer and Senak (2003). 40

Figure 3.4 Zeta-potential (mV, mean ± standard deviation, n = 2) of anthocyanin solutions (cyanidin 3-*O*-rutinoside and delphinidin 3-*O*-rutinoside) at pH 3.5 and pH 4.5 and at various concentrations (% w/v). 43

Figure 3.5 Turbiscan Stability Index scale and its stability categories. Adapted from Formulaction (2018). 45

Figure 4.1 Isolation steps of blackcurrant juice pectin-rich fractions. 52

Figure 4.2 Alcohol insoluble residue (A) isolated from blackcurrant juice, undialysed pectin-rich fraction (B) and dialysed pectin-rich fraction (C). 60
Figure 4.3 Structure of delphinidin (A) and cyanidin (B) aglycone. 61
Figure 4.4 Chromatograms of blackcurrant juice (black ▬) and blackcurrant pectin-rich fractions; undialysed (blue ▪▪▪▪) and dialysed (pink ▬ ▬) at $\lambda_{530\ nm}$ and $\lambda_{280\ nm}$. The inset image show samples prepared in acidified aqueous methanol. 62
Figure 4.5 Undialysed and dialysed blackcurrant pectin-rich fraction solutions (0.1% w/v) in pH 1 and pH 4.5 buffer.....66
Figure 4.6 SEC-MALLS chromatograms of undialysed (A) and dialysed (B) blackcurrant pectin-rich fractions and citrus pectin (C) showing light scattering (LS), differential refractive index (RI) and $UV_{280\ nm}$ signal.....67
Figure 4.7 $UV_{280\ nm}$ chromatograms of undialysed and dialysed blackcurrant pectin-rich fractions and citrus pectin at retention times of 38 to 45 min. 70
Figure 4.8 HSQC spectrum of dialysed blackcurrant pectin-rich fraction recorded at 70 °C. A1: H-1/C-1 of α-L-Ara*f*; A5: H-5/C-5 of α-L-Ara*f*; G1: H-1/C-1 of β-D-Gal*p*; G5: H-5/C-5 of β-D-Gal*p*; R1: H-1/C-1 of α-L-Rha*p*; R6: H-6/C-6 of α-L-Rha*p*; GA1: H-1/C-1 of α-D-Gal*p*A; GA5: H-5/C-5 of α-D-Gal*p*A; OMe: *O*-methyl; OAc: *O*-acetyl.....73
Figure 5.1 Schematic diagram of bench-top ultra-filtration system.....79
Figure 5.2 Blackcurrant juice (initial feed) and its filtered products—permeates (PM) from cycle 1 to 4 and retentate (RTT) from the final cycle—at pH 2, pH 3 (control) and pH 4.5 along with their pH value at 20 °C. 81
Figure 5.3 SEC-MALLS chromatogram of blackcurrant juice as initial feed at pH 2, pH 3 (control) and pH 4.5 showing light scattering (LS), differential refractive index (RI), and ultra-violet ($UV_{280\ nm}$) signal. 82
Figure 5.4 SEC-MALLS chromatogram of first permeate at pH 2, pH 3 (control) and pH 4.5 showing light scattering (LS), differential refractive index (RI), and ultra-violet ($UV_{280\ nm}$) signal.....84
Figure 5.5 SEC-MALLS chromatogram of sucrose, fructose, glucose and galacturonic acid (2% w/v) showing light scattering (LS), differential refractive index (RI), and ultra-violet ($UV_{280\ nm}$) signal. 86
Figure 5.6 SEC-MALLS chromatogram of final retentate at pH 2, pH 3 (control) and pH 4.5 showing light scattering (LS), differential refractive index (RI), and ultra-violet ($UV_{280\ nm}$) signal.....87
Figure 5.7 SEC-MALLS chromatogram of final retentate at pH 3 (control) and dialysed blackcurrant pectin-rich fraction showing light scattering (LS), differential refractive index (RI), and ultra-violet ($UV_{280\ nm}$) signal.....88

Figure 5.8 Quantity (mg/100 g total solids, mean ± standard deviation) of protein, anthocyanin (expressed as cyanidin-3-*O*-glucoside) and pectin (expressed as galacturonic acid) in blackcurrant juice (initial feed) and its filtered products (first permeate and final retentate) at pH 2, pH 3 (control) and pH 4.5. Means within a group are not significantly different if the letters (a-c) are the same.....90

Figure 5.9 Quantity (mg/100 g total solids, mean ± standard deviation) of anthocyanin from pH differential method (expressed as cyanidin-3-*O*-glucoside) and individual anthocyanins from reversed-phase ultra-performance liquid chromatography (del-glu, delphinidin 3-*O*-glucoside; del-rut, delphinidin 3-*O*-rutinoside; cya-glu, cyanidin-3-*O*-glucoside; cya-rut, cyanidin-3-*O*-rutinoside) of blackcurrant juice (initial feed) and its filtered products (combined permeates and final retentate) at pH 2, pH 3 (control) and pH 4.5. Means within a group are not significantly different if the letters (a-c) are the same.....93

Figure 5.10 Quantity (mg/100 g total solids, mean ± standard deviation) of flavonols (iso-rut, isorhamnetin 3-*O*-rutinoside; kae-rut, kaempferol 3-*O*-rutinoside; myr, myricetin; myr-6-malonyl-glu, myricetin 3-*O*-(*6*-malonyl)-glucoside; myr-gal, myricetin 3-*O*-galactoside; myr-glu, myricetin 3-*O*-glucoside; que, quercetin; que-6-malonyl-glu, quercetin 3-*O*-(*6*-malonyl)-glucoside; que-glu, quercetin 3-*O*-glucoside; que-rut, quercetin 3-*O*-rutinoside), phenolic acids and flavanols in blackcurrant juice (initial feed) and its filtered products (combined permeates and final retentate) at pH 2, pH 3 (control) and pH 4.5.....95

Figure 6.1 Preparation steps for non-heated (NH) and mixed-heated (MH) blackcurrant pectin-whey protein (BCP-WP) mixtures and the measurement techniques used.....102

Figure 6.2 Preparation steps for heated-mixed blackcurrant pectin-whey protein mixture and the measurement techniques used.....103

Figure 6.3 Blackcurrant pectin (BCP), whey protein (WP) and their mixtures (NH, Non-Heated; MH, Mixed-Heated; HM, Heated-Mixed) at pH 3.5 and pH 4.5.....106

Figure 6.4 Turbiscan Stability Index (TSI) of blackcurrant pectin-whey protein mixtures (NH, Non-Heated; MH, Mixed-Heated; HM, Heated-Mixed) at pH 3.5 and pH 4.5 measured across 24-h timeframe.....107

Figure 6.5 Particle size (nm, Z-averages mean ± standard deviation) of controls (BCP, blackcurrant pectin; WP, whey protein) and their mixtures (NH, Non-Heated; MH, Mixed-Heated; HM, Heated-Mixed) at pH 3.5 and pH 4.5. Means within a group are not significantly different if the letters are same.....108

Figure 6.6 Average size distribution of aggregate-reduced whey protein (WP) at pH 3.5 and pH 4.5 based on intensity, number, and volume weighting mechanisms.....109

Figure 6.7 Average size distribution of blackcurrant pectin-whey protein mixtures (NH, Non-Heated; MH, Mixed-Heated; HM, Heated-Mixed) at pH 3.5 and pH 4.5 based on (A) intensity and (B) number weighting mechanisms. 112
Figure 6.8 Zeta-potential (mV, mean ± standard deviation) of controls—anthocyanin mix (cyanidin 3-*O*-rutinoside and delphinidin 3-*O*-rutinoside), blackcurrant pectin (BCP) and whey protein (WP)—and their mixtures (NH, Non-Heated; MH, Mixed-Heated; HM, Heated-Mixed) at pH 3.5 and pH 4.5. Means within a group are not significantly different if the letters are same. 114
Figure 6.9 Percentage of the initial pectin (w/w, expressed as mean galacturonic acid ± standard deviation) found as part of the insoluble complexes of blackcurrant pectin-whey protein mixtures (NH, Non-Heated; MH, Mixed-Heated; HM, Heated-Mixed) at pH 3.5 and pH 4.5. Means with same letter are not significantly different. 116
Figure 6.10 FTIR spectra of blackcurrant pectin (BCP), and the two major anthocyanins found in blackcurrant 118
Figure 6.11 FTIR spectra of blackcurrant pectin (BCP), whey protein (WP) and the insoluble complexes of their mixtures (NH, Non-Heated; MH, Mixed-Heated; HM, Heated-Mixed) at pH 3.5 and pH 4.5. 120
Figure 6.12 Schematic diagram of non-heated (NH) and mixed-heated (MH) blackcurrant pectin-whey protein mixtures at pH 3.5 and pH 4.5 122
Figure 7.1 Preparation steps for blackcurrant pectin-whey protein (BCP-WP) and citrus pectin-whey protein (CP-WP) mixtures (NH, Non-Heated; MH, Mixed-Heated) at pH 4.5 and the measurement techniques used. 130
Figure 7.2 Viscosity (Pa.s) versus shear rate (1/s) of blackcurrant pectin (BCP) and citrus pectin (CP) at pH 4.5 based on 0.42% w/v galacturonic acid content. 136
Figure 7.3 Percentage transmission of near-infrared LED (λ_{air}=880 nm, time 0 s) of blackcurrant and citrus pectin systems consisting of controls (BCP, blackcurrant pectin; CP, citrus pectin; 0.02% and 0.2% w/v WP, whey protein) and their mixtures (NH, Non-heated; MH, Mixed-Heated) at 1:1, 1:5 and 1:10 pectin:protein ratios (mean ± standard deviation). Means within a group are not significantly different if the letters (a-f) are the same 138
Figure 7.4 Turbiscan Stability Index of blackcurrant pectin-whey protein (BCP-WP) and citrus pectin-whey protein (CP-WP) mixtures (NH, Non-heated; MH, Mixed-Heated) at pectin:protein ratio of 1:1 measured across 24-h timeframe. 139
Figure 7.5 Turbiscan Stability Index of mixed-heated (MH) blackcurrant pectin-whey protein (BCP-WP) and citrus pectin-whey protein (CP-WP) mixtures at (A) 1:1, 1:5 and 1:10 pectin:protein ratios measured across 24-h timeframe and (B) 1:10 pectin:protein ratio showing time in minutes. 140

Figure 7.6 (A) Z-average size (nm) of blackcurrant and citrus pectin systems consisting of controls (BCP, blackcurrant pectin; CP, citrus pectin; 0.02% w/v WP, whey protein) and their mixtures (NH, Non-heated; MH, Mixed-Heated) at 1:1 and 1:5 pectin:protein ratios (mean ± standard deviation). Means within a group are not significantly different if the letters (a-c) are the same. (B) Z-average size (nm) of blackcurrant pectin-whey protein and citrus pectin-whey protein mixtures (NH, Non-heated; MH, Mixed-Heated) at 1:1 and 1:5 pectin:protein ratios (mean ± standard deviation). Means with the same letter (a–d) are not significantly different. 141
Figure 7.7 Average size distribution of blackcurrant pectin-whey protein (BCP-WP) and citrus pectin-whey protein (CP-WP) mixtures (NH, Non-Heated; MH, Mixed-Heated) at 1:1 and 1:5 pectin:protein ratios, based on (A) light scattering intensity and (B) number weighting mechanisms. 144
Figure 7.8 Average size distribution of mixed-heated (MH) blackcurrant pectin-whey protein (BCP-WP) and citrus pectin-whey protein (CP-WP) mixtures at 1:10 pectin:protein ratio, based on volume weighting mechanism..... 147
Figure 7.9 Zeta-potential (mV, mean ± standard deviation) of controls (BCP, blackcurrant pectin; CP, citrus pectin; 0.02% w/v WP, whey protein) and their mixtures (NH, Non-Heated; MH, Mixed-Heated) at 1:1, 1:5 and 1:10 pectin:protein ratios. Means within a group are not significantly different if the letters (a-c) are the same. 149
Figure 7.10 Percentage of initial pectin and protein (w/w total solids, mean ± standard deviation) found as part of the soluble and insoluble complexes of non-heated (NH) and mixed-heated (MH) mixtures of blackcurrant pectin-whey protein (BCP-WP) and citrus pectin-whey protein (CP-WP) at pectin:protein ratio of 1:1. Means within a group are not significantly different if the letters (a-c) are the same. 151
Figure 7.11 Percentage of initial pectin and protein (w/w total solids, mean ± standard deviation) found as part of the insoluble complexes of mixed-heated (MH) mixtures of blackcurrant pectin-whey protein (BCP-WP) and citrus pectin-whey protein (CP-WP) at pectin:protein ratio of 1:1, 1:5 and 1:10. Means within a group are not significantly different if the letters (a-f) are the same..... 152
Figure 7.12 FTIR spectrum of controls (BCP, blackcurrant pectin; CP, citrus pectin; WP, whey protein) and the soluble fraction of their mixtures (NH, Non-Heated; MH, Mixed-Heated) at pH 4.5. Bands between 2000 cm^{-1} and 2400 cm^{-1} are artefacts from the ATR diamond. 154
Figure 7.13 FTIR spectrum of controls (BCP, blackcurrant pectin; CP, citrus pectin; WP, whey protein) and the insoluble fraction of their mixtures (NH, Non-Heated; MH, Mixed-Heated) at pH 4.5. Some of the spectra show a carbon dioxide band (≈2340 cm^{-1}) and artefacts from the ATR diamond between 2000 cm^{-1} and 2400 cm^{-1}..... 157
Figure 8.1 Overview of Chapter 4 and Chapter 5..... 161

Figure 8.2 Overview of Chapter 6. 163
Figure 8.3 Overview of Chapter 7 166

List of Tables

Table 2.1 Substituents on carbon position 3' (R1) and 5' (R2) of commonly found anthocyanidins. Adapted from Schwartz et al. (2008) and Prior and Wu (2012). 8

Table 2.2 Substituents of commonly found phenolic acids. Adapted from Xu (2012). 13

Table 3.1 Proximate composition of blackcurrant puree and juice. 32

Table 3.2 Phenolic compounds in blackcurrant puree. 38

Table 3.3 Band assignments for blackcurrant pectin, citrus pectin, and whey protein infrared spectra. 46

Table 4.1 Proximate composition of dried undialysed and dialysed blackcurrant pectin-rich fraction. 58

Table 4.2 Phenolic compounds in blackcurrant juice and its pectin-rich fractions. 64

Table 4.3 Molecular characteristics (PDI, polydispersity index; M_w, molecular weight; RMS radius, root mean squared radius) of undialysed and dialysed blackcurrant pectin-rich fractions and citrus pectin at selected retention times (t_R). 69

Table 4.4 Constituent sugar composition (mean of duplicate analyses) of dialysed blackcurrant pectin-rich fraction. 71

Table 5.1 Average molecular weight[a] of fraction A (40-45 min) and fraction B (52-55 min) of blackcurrant juice (initial feed) and its final retentate at pH 2, pH 3 (control) and pH 4.5. 89

Table 6.1 Polydispersity index (mean ± standard deviation) of blackcurrant pectin-whey protein mixtures (NH, Non-Heated; MH, Mixed-Heated; HM, Heated-Mixed) at pH 3.5 and pH 4.5. Means with same letter are not significantly different. 113

Table 7.1 Physico-chemical and molecular properties of dialysed blackcurrant pectin (BCP) and commercial citrus pectin (CP) powder. 134

Table 7.2 Polydispersity index (mean ± standard deviation) of blackcurrant pectin-whey protein (BCP-WP) and citrus pectin-whey protein (CP-WP) mixtures (NH, Non-Heated; MH, Mixed-Heated) at 1:1 and 1:5 pectin:protein ratios. Means with the same letter (a-d) are not significantly different. 146

Table 7.3 Molar ratio of pectin (BCP, blackcurrant pectin; CP, citrus pectin) and whey protein (WP) for the insoluble complexes of non-heated (NH) and mixed-heated (MH) BCP-WP and CP-WP mixtures at 1:1, 1:5 and 1:10 pectin:protein ratios. 153

List of Publications and Conference Proceedings

1. Salleh, N., Goh, K. K. T., Sims, I. M., Bell, T. J., Huffman, L. M., Weeks, M., & Matia-Merino, L. (2021, 6th–8th July). Anthocyanin-Bound Pectin-Rich Fraction Extracted from New Zealand Blackcurrant Juice. [Poster presentation]. New Zealand Institute of Food Science and Technology Conference 2021, Palmerston North, New Zealand.
2. Salleh, N., Goh, K. K. T., Sims, I. M., Bell, T. J., Huffman, L. M., Weeks, M., & Matia-Merino, L. (2021). Characterization of Anthocyanin-Bound Pectin-Rich Fraction Extracted from New Zealand Blackcurrant (*Ribes nigrum*) Juice. *ACS Food Sci. Technol.*, *1*(6), 1130-1142.
3. Salleh, N., Goh, K. K. T., Waterland, M. R., Huffman, L. M., Weeks, M., & Matia-Merino, L. (2022). Complexation of Anthocyanin-Bound Blackcurrant Pectin and Whey Protein: Effect of pH and Heat Treatment. *Molecules*, *27*(13), 4202.
4. Salleh, N., Goh, K. K. T., Waterland, M. R., Huffman, L. M., Weeks, M., & Matia-Merino, L. (2023). The Influence of Anthocyanins in Pectin-Whey Protein Complexation Using a Natural Pigmented Blackcurrant Pectin. *Food Hydrocolloids*, *140*, 108672.

Chapter 1 Introduction

New Zealand grown blackcurrant is exceptionally rich in anthocyanins as compared to the blackcurrants grown in other countries (Heiberg & Maage, 2003; Nyanhanda et al., 2014; Scalzo et al., 2008). This is mainly due to high exposure of ultra-violet (UV) radiation that damages the plant DNA, encouraging the synthesis of antioxidants and UV absorbing compounds (i.e., phenolic compounds) that aid in the DNA repair (Henry-Kirk et al., 2018; Wargent & Jordan, 2013). Apart from anthocyanins, blackcurrant is also rich in ascorbic acid and minerals and is usually accompanied with a refreshing fruity flavour and vibrant colour. Many studies have reported the health benefits of the blackcurrant fruit that include gut health support, improvement of muscle performance, and prevention of cancer and various inflammation-related diseases (Aneta et al., 2013; Nyanhanda et al., 2014; Parkar et al., 2014; Schrage et al., 2010; Shaw et al., 2017). Due to its outstanding reported health benefits, pleasant flavour and vibrant colour, blackcurrant has become one of the sought-after functional ingredients. In the recent years, the popularity of New Zealand blackcurrant has increased, boosting its export to a combined value of $12.6 million in 2020 (New Zealand Horticulture Export Authority, 2022).

At the same time, the demand for food products containing nutraceutical ingredients is on the rise, especially those in the beverage category (Fox, 2022; Kasapoğlu et al., 2019). The current market trend shows that there is a high demand for high-protein drinks, coffee alternatives, functional carbonated drinks, and plant-based energy drinks (Fox, 2022; Kasapoğlu et al., 2019; Marcarelli, 2016). In order to achieve the beneficial effect, isolated functional ingredients like plant and dairy proteins, plant extracts, probiotics and prebiotics are added to these beverages. However, the presence of artificial and chemical-sounding additives in food products are often viewed as harmful to health by consumers. As a result, consumers are continually seeking products that are minimally processed and contain simple, recognisable, and ethically sourced ingredients. These vaguely defined sets of consumer requirements are often termed as “clean-label”, which has no official definition nor regulated. Yet, it is frequently associated to being healthy, natural, additive-free, and preservative-free (Kalantar, 2021).

Fulfilling the demand for clean-label products, including those that contain nutraceutical ingredients is a challenging task for the food industry as manufacturing a food or beverage usually requires the addition of food grade additives (i.e., refined ingredients that render specific functions, such as the enhancement of nutritional quality, improvement of taste, aesthetic and textural quality, and extension of shelf life). As a consequence, food companies are racing to find creative and alternative methods in product formulation and manufacturing. Before formulating the clean-label product,

knowledge on the interactive components of the mixed system is needed as food comprises of various constituents (carbohydrates, proteins, fats, and minor compounds like minerals, organic acids, phytochemicals, etc.) that can be physically and chemically reactive with one another, especially when they are released from the structural tissues or disrupted from their native form during processes like crushing, mashing, and heating. The interactions are influenced by the chemical groups of the food constituents and environmental factors, like temperature, pH, ionic strength, and oxidation-reduction potential. Often, interaction between these components leads to changes in appearance, texture, taste, physical stability and even nutritional quality of the final product (Zdzisław et al., 2008).

This study aimed to investigate the stability mechanism of a mixed beverage system containing New Zealand blackcurrant—in the form of puree or juice—and bovine milk that meets the "clean-label" requirements, that is, without the use of food stabilisers. Typically, mixing a fruit puree or juice with bovine milk will lead to poor phase stability due to multiple factors like pH, ionic conditions, and heat that can intensify the interactions among components like polyphenols and polysaccharides from the fruit and proteins from the bovine milk. With no food additives to stabilise the mixture, it is technologically challenging to achieve textural homogeneity and physical stability. A clear understanding of the instability mechanisms can aid in the implementation of appropriate strategies to formulate and process a stable mixed beverage system consisting of bovine milk and the blackcurrant component.

Figure 1.1 Ultra-high temperature treated whole milk and its mixtures with blackcurrant juice at increasing juice concentration (v/v).

Since the blackcurrant puree was a very complex system, blackcurrant juice was selected as the material for this experimental work; obtained simply by centrifuging the puree. Preliminary work revealed that mixing the blackcurrant juice and ultra-high temperature treated bovine milk led to a curd-like mixture with poor textural and aesthetic quality due to the coagulation of the milk proteins and phase separation (Figure 1.1). Thus, the first step in understanding the instability mechanism was

to isolate and study the main interacting components of the blackcurrant juice as knowledge in these areas is still lacking, in comparison to the extensive publications on the components of bovine milk.

In order to address the knowledge gap, interaction studies between the identified components were conducted using a model system so as to gain a clear insight into the blackcurrant juice-milk system. Instead of using two types of milk proteins—casein and whey proteins (WP)—the WPs were chosen because (i) they are soluble at the experimental conditions of pH 3.5 and pH 4.5 that simulates the pH of an acidified milk drink and (ii) they had a compact structure that would unfold during heat treatment (>60 °C) that could intensify the interactions with blackcurrant components, increasing the likelihood of observing significant changes. Furthermore, most mixed system studies have used a single type of protein, phenolic compound and/or polysaccharide, but despite their many merits, such studies are too far from the representation of the actual food systems. Therefore, instead of using individual compounds, the present study fractionated the main interacting components of the blackcurrant juice, using mild extraction processes and analysed their interactions with the globular WPs. The overarching hypotheses of this research are presented in Figure 1.2.

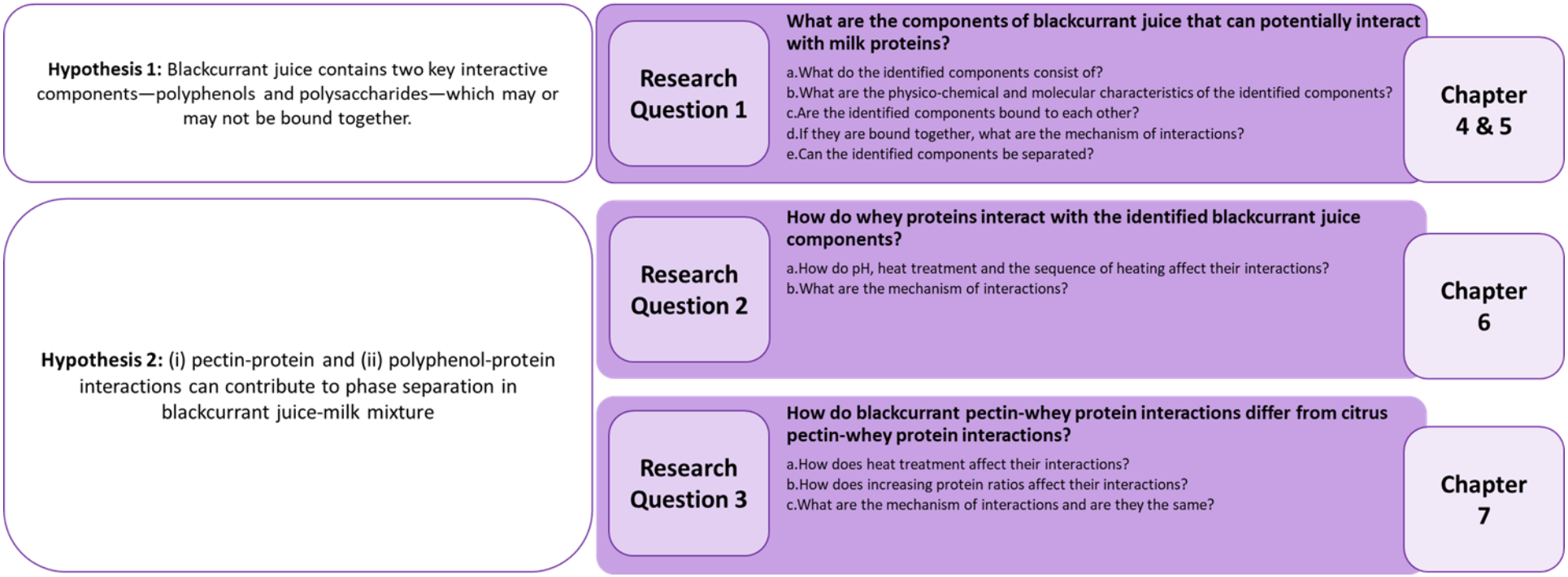

Figure 1.2 Overview of research work.

Chapter 2 Literature Review

2.1. Blackcurrant Fruit

Blackcurrant (*Ribes nigrum*) is a dark purple berry that grows on a small shrub that is native to Europe and northern Asia. Traditionally, the berries and leaves are used as an herbal medicine for treating various health issues such as fever and sore throat (Heiberg & Maage, 2003; Miller et al., 2013). Today, it is mostly consumed as a processed product in the form of juice, jams, smoothies, yoghurt, and baked goods due to its refreshing flavour and vibrant colour.

Generally, the blackcurrant fruit comprises of water (81.5%), carbohydrates (17.1%), proteins (1.3%), and a small amount of fat (0.2%) (Heiberg & Maage, 2003). Simple sugars like fructose, glucose and sucrose constitute almost half (49.7%) of the blackcurrant carbohydrates while the remaining are fibres like pectin, hemicellulose, cellulose, and lignin (Alba et al., 2018; Heiberg & Maage, 2003). Proteins that are found in blackcurrant are mostly part of the cell wall components such as extensin and arabinogalactan protein, and some enzymes (Andersson et al., 2017; Brett & Waldron, 1990a). Most of the blackcurrant lipids come from its seeds, which contain about 5% to 20% of polyunsaturated fatty acid known as γ-linolenic acid (Heiberg & Maage, 2003). Just like any other fruits, blackcurrant contains a variety of vitamins, minerals, and phenolic compounds, and it is particularly rich in ascorbic acid (1,600 mg/kg fresh fruit), potassium (3,100 mg/kg fresh fruit), and anthocyanins (1,250 mg to 2,000 mg/kg fresh fruit), respectively (Gopalan et al., 2012; Heiberg & Maage, 2003). Due to the organic acids it contains such as citric, malic and ascorbic acids, blackcurrant has a low pH that ranges between pH 2.7 and pH 3.2 (Heiberg & Maage, 2003).

Blackcurrant has been labelled as a 'superfood' for its high content of health beneficial bioactive compounds, such as ascorbic acid, cyclic glycine-proline neuropeptide, and various types of polyphenols (BCNZ, 2017; Fan et al., 2018; Vitality Wellness (NZ) Limited, 2020). In terms of phenolic compounds, blackcurrant contains higher amount of polyphenols than other major cultivated berries—like strawberry and raspberry—especially in terms of the quantity of anthocyanins (Chen et al., 2014; Heiberg & Maage, 2003; Karjalainen et al., 2009; Miller et al., 2013; Scalzo et al., 2008). Extensive research has shown that blackcurrant polyphenols have the ability to exhibit anti-inflammatory, antioxidant, and antimicrobial properties (Gopalan et al., 2012; Karjalainen et al., 2009; Nyanhanda et al., 2014; Parkar et al., 2014). These polyphenols provide therapeutic effects through common pathways that many diseases share, allowing blackcurrant to exhibit its benefits in various

conditions and illnesses (Gopalan et al., 2012). One common example is the antioxidant capacity of blackcurrant polyphenols to quench toxic oxygen radicals that are produced in the body, which if not neutralized can lead to degenerative diseases like cardiovascular and cancer (Karjalainen et al., 2009).

The bioactive compounds in blackcurrant are influenced by factors like genotype, growth conditions, pre-harvest climate, degree of maturity at harvest and post-harvest storage conditions (Krüger et al., 2012; Mattila et al., 2016; Tabart et al., 2006; Vagiri et al., 2013; Walker et al., 2010; Zheng et al., 2012; Zheng et al., 2009). Thus, it is expected that New Zealand grown blackcurrants have different amount and composition of bioactive compounds as compared to those grown in other parts of the world. Blackcurrant was first commercially grown in New Zealand in the 1970s with growers located primarily in the South Island regions like Nelson, Canterbury, Otago and Southland (BCNZ, 2022). In 2019, New Zealand became the 8th largest blackcurrant producer in the world with an average annual production volume of 6,543 tonnes (FAO, 2022). Presently, there are four main cultivars of blackcurrant in New Zealand, namely Ben Ard, Ben Rua, Blackadder, and Magnus (BCNZ, 2022; Heiberg & Maage, 2003; Schrage et al., 2010). These blackcurrant cultivars have been chosen based on their ability to synthesise a higher level of anthocyanins—960 mg to 7204 mg/kg fresh fruit (Currie et al., 2006; Scalzo et al., 2008; Schrage et al., 2010). As mentioned previously, their exposure to higher levels of UV radiation plays a crucial role in synthesising the large amounts of phenolic compounds.

This section is centred on two blackcurrant components: its phenolic compounds and pectin. They were chosen as the focus of this study as they can potentially interact with proteins and are found abundantly in blackcurrant.

2.1.1. Blackcurrant Phenolic Compounds

There are three major categories of phenolic compounds in blackcurrant (Figure 2.1): (i) anthocyanins, contributing the greatest amount of phenolic compounds (≈91.8%), (ii) flavonols (≈4.17%) and (iii) phenolic acids (≈4%) (Anttonen & Karjalainen, 2006). Some authors have also reported the presence of minor polyphenols such as condensed tannins (proanthocyanidins), hydrolysable tannins and stilbenoids, however the detection of these minor polyphenols depends on the cultivar of the blackcurrant, fraction analysed, treatments done and type of solvent used (Gopalan et al., 2012; Kapasakalidis et al., 2006). The following sub-sections present the molecular structure and chemical properties of the three major types of blackcurrant polyphenols.

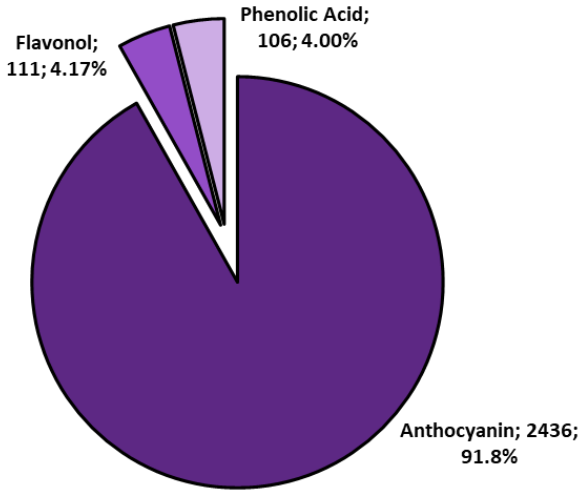

Figure 2.1 Concentration (mg/kg fresh fruit) and percentage of phenolic compounds in conventionally grown blackcurrant fruit. Data obtained from Anttonen and Karjalainen (2006).

2.1.1.1. Anthocyanins

Anthocyanin is a class of water-soluble flavonoids that displays red, purple, and blue colours. It is the compound that gives the blackcurrant skin the dark purple colour and is known to be synthesized and stored in the vacuole of the plant cell (Bae et al., 2006). Structurally, anthocyanin is made of two components: (i) the aglycone unit, known as the anthocyanidin and (ii) the sugar moiety attached to it. Anthocyanidin comprises of two aromatic rings—Ring A and Ring B—that are bonded together to an oxygen heterocyclic ring (Ring C) via carbon-carbon bonds and does not have any sugar moiety attached to it (Figure 2.2).

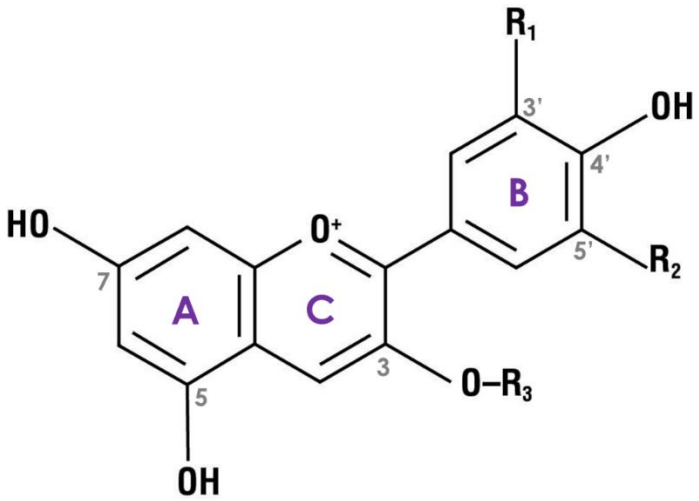

Figure 2.2 Structure of anthocyanidin and anthocyanin with various substituent positions; R1 and R2 can be –H, –OH or –OCH3 and R3 can be –H (anthocyanidin) or –glycosyl (anthocyanin). Adapted from Schwartz et al. (2008) and Prior and Wu (2012).

In nature, there are six common anthocyanidins with varying degrees of hydroxy (-OH) and methoxy (-OCH_3) groups (Table 2.1) attaching to the carbon position 3' (R_1) and 5' (R_2) of the aglycone unit (Figure 2.2). The anthocyanins are further diversified by the type and number of sugar molecules that are bonded to them, providing hydrophilicity to the otherwise hydrophobic aglycone unit, and allowing the anthocyanins to solubilize in water, ethanol, and methanol (Rivas-Gonzalo, 2003; Schwartz et al., 2008). The sugar molecule can be a monosaccharide, disaccharide or trisaccharide and the commonly bonded ones are glucose, galactose, rhamnose, arabinose, xylose, rutinose, sophorose and sambubiose (Prior & Wu, 2012; Rivas-Gonzalo, 2003). Typically, the sugar molecule is bonded at carbon position three of the aglycone unit (R_3 of Figure 2.2) via α- or β-linkages, although more sugar molecules can be attached at carbon position five, seven, 3' (R_1) and 5' (R_2) (Rivas-Gonzalo, 2003). Additionally, aliphatic, hydroxybenzoic and hydroxycinnamic acids are also reported to be linked to these sugar molecules (Goulas et al., 2012; Prior & Wu, 2012; Rivas-Gonzalo, 2003; Schwartz et al., 2008), increasing the variety of anthocyanins further.

Table 2.1 Substituents on carbon position 3' (R1) and 5' (R2) of commonly found anthocyanidins. Adapted from Schwartz et al. (2008) and Prior and Wu (2012).

Anthocyanidins	R_1	R_2
Pelargonidin	H	H
Cyanidin	OH	H
Delphinidin	OH	OH
Peonidin	OCH_3	H
Petunidin	OCH_3	OH
Malvidin	OCH_3	OCH_3

In blackcurrant, there are four major anthocyanins (Figure 2.3), comprising of two anthocyanidins—cyanidin and delphinidin—and two types of sugar moieties—glucose and rutinose. They are cyanidin 3-*O*-glucoside (cya-glu), cyanidin 3-*O*-rutinoside (cya-rut), delphinidin 3-*O*-glucoside (del-glu) and delphinidin 3-*O*-rutinoside (del-rut) (Slimestad & Solheim, 2002). The quantity and ratio of blackcurrant anthocyanins vary across the cultivars, however, several authors have reported that anthocyanin with rutinose side chain (del-rut and cya-rut) is the most abundant type of blackcurrant anthocyanin, especially in the two cultivars grown in New Zealand, Ben Ard and Magnus (Aneta et al., 2013; Kapasakalidis et al., 2006; Nyanhanda et al., 2014; Scalzo et al., 2008; Slimestad & Solheim, 2002). Several authors also reported the presence of minor anthocyanins such as petunidin 3-*O*-rutinoside, peonidin 3-*O*-rutinoside, delphinidin 3-*O*-(6"-coumaroyl)-glucoside and cyanidin 3-*O*-(6"-coumaroyl)-glucoside (Kapasakalidis et al., 2006; Slimestad & Solheim, 2002; Wu et al., 2006).

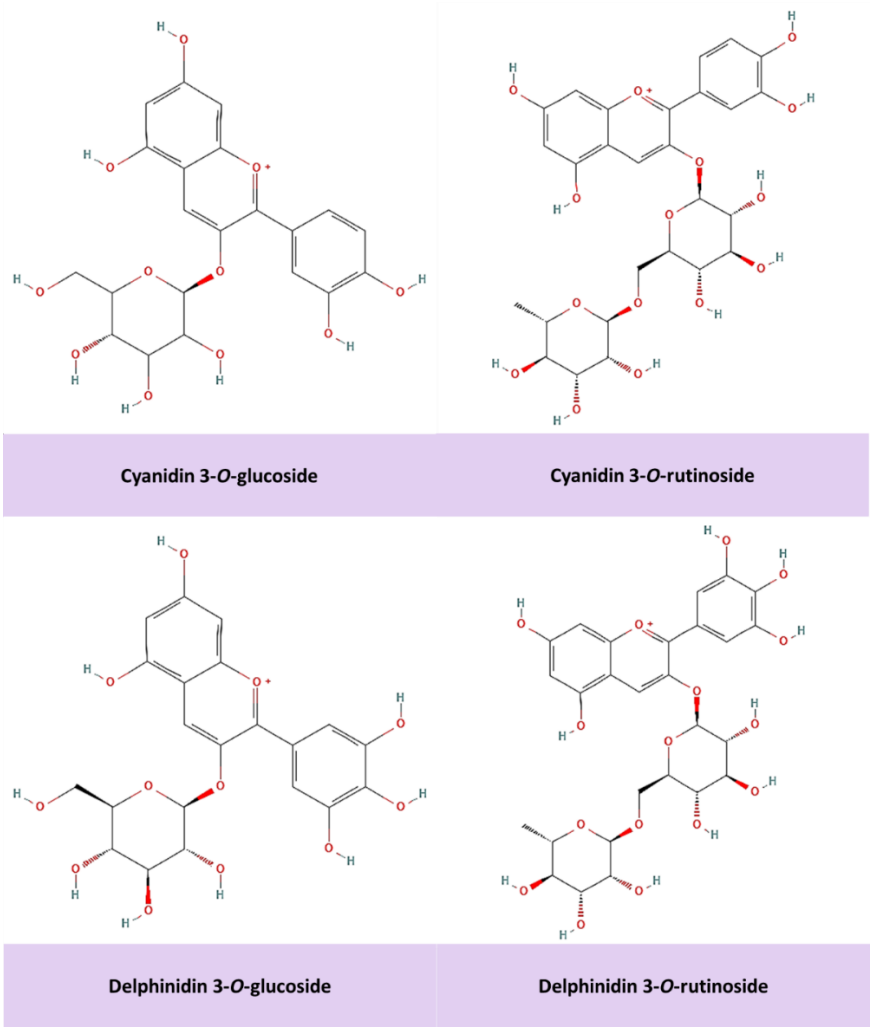

Figure 2.3 Structure of major blackcurrant anthocyanins. 2D structures from PubChem (2022a, 2022b, 2022c, 2022d).

The colour variation (redness and blueness) and stability of anthocyanins depend greatly on the substituents of the aglycone unit (Table 2.1). This includes the degree of hydroxylation and methylation, the type and number of sugar molecules as well as the acylation of the sugar moieties (Rivas-Gonzalo, 2003; Schwartz et al., 2008). Generally, the presence of methoxy group in the B ring will produce a more stable anthocyanin as they can block the reactive hydroxy group from interacting (Rivas-Gonzalo, 2003; Schwartz et al., 2008). Therefore, malvidin, petunidin and peonidin are more stable than pelargonidin, cyanidin and delphinidin as the latter group of anthocyanidins has greater number of hydroxy groups and is lacking in methoxy groups (Table 2.1). Likewise, the glycosylation of a disaccharide to an anthocyanidin will produce a more stable anthocyanin than the one glycosylated with a monosaccharide (Rivas-Gonzalo, 2003; Schwartz et al., 2008).

Apart from the substituents on the anthocyanin structure, pH also influences the colour and stability of anthocyanins. Anthocyanins are considered unstable compounds due to their flavylium core that

reacts with temperature increase and agents like hydrogen and hydroxide ions and water molecules (Prior & Wu, 2012; Rivas-Gonzalo, 2003; Schwartz et al., 2008). In an aqueous medium, depending on the pH, there can be four basic forms of anthocyanin existing in equilibrium (Figure 2.4): (i) flavylium cation, (ii) quinonoidal base, (iii) carbinol pseudobase or hemiketal, and (iv) chalcone (Brouillard, 1988; Rivas-Gonzalo, 2003; Schwartz et al., 2008). Anthocyanins are most stable when they are in the form of flavylium cations. At 25 °C, a low pH of <2 will result in a solution dominated by the red flavylium cations. As the pH increases, some of the flavylium cations will be deprotonated at carbon position five, seven or 4' to form the neutral quinonoidal base that displays a bluish hue. Between pH 3.5 and pH 4.5, the two forms of anthocyanin—flavylium cation and quinonoidal base—will coexist in the solution, and further increase of pH will favour the formation of the quinonoidal base (Rivas-Gonzalo, 2003). Once the pH crosses to pH 6, the neutral form of quinonoidal blue will ionise (Brouillard, 1988).

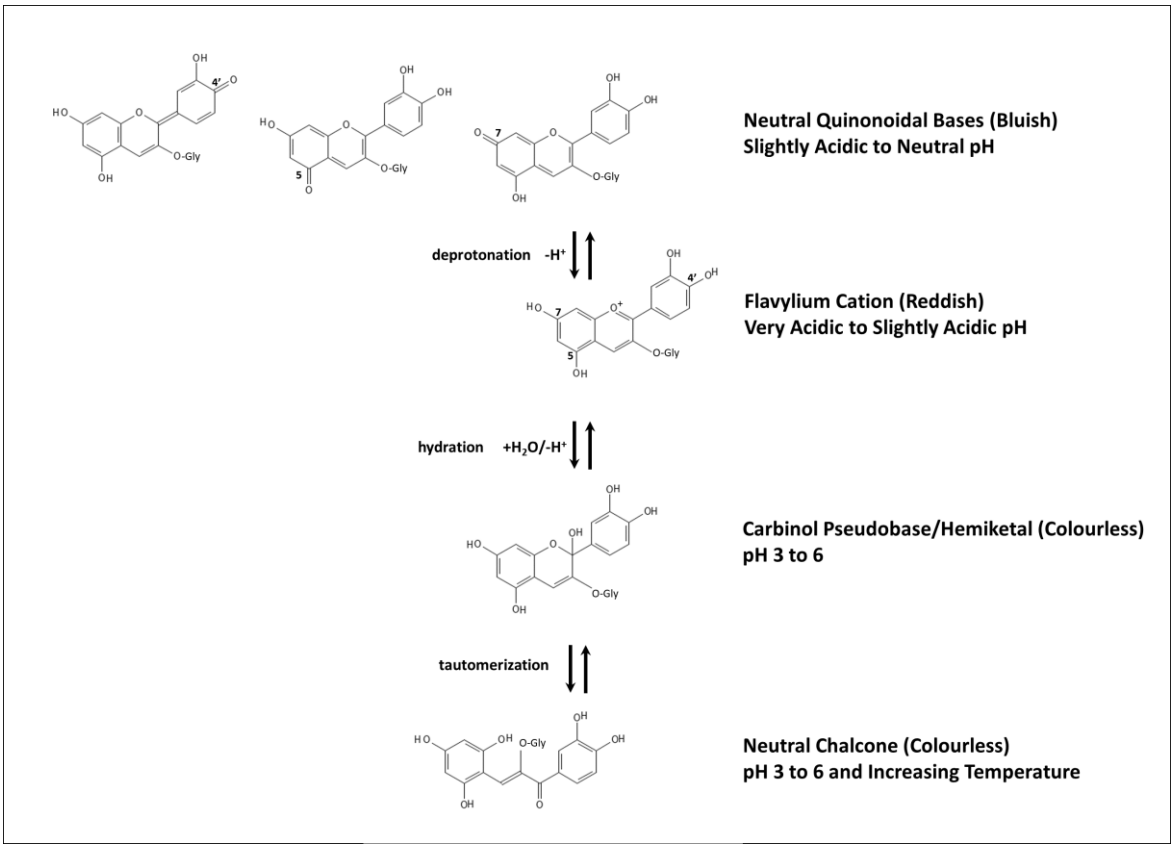

Figure 2.4 Transformation of cyanidin structure according to the pH of the medium. Adapted from Brouillard (1988), Rivas-Gonzalo (2003), Prior and Wu (2012) and Miller et al. (2013).

In the presence of water between pH 3 and pH 6, hydration of the flavylium cation will usually occur at the carbon position two of the pyrilium ring, forming the colourless carbinol pseudobase. Hydration is a slower process than protonation or deprotonation, therefore the alteration of anthocyanin colour to colourless may take several seconds to minutes before the anthocyanin structures reach equilibrium (Rivas-Gonzalo, 2003). Within the same range of slightly acidic pH, tautomerisation of the

carbinol pseudobase to the open chalcone form can happen if the temperature of the medium is increased. Although the interconversion of carbinol pseudobase to chalcone is a fast reaction, this process requires several hours before the structures can reach equilibrium (Brouillard, 1988; Rivas-Gonzalo, 2003). All three forms of anthocyanins can be reverted to the flavylium cation by lowering the pH, however, they may have different range of restoration time (Rivas-Gonzalo, 2003).

In general, the rate of anthocyanin degradation increases as the pH and temperature rise. Under physiological conditions—pH 7.4 at 37 °C—anthocyanins are significantly degraded in less than one hour (Dangles & Fenger, 2018). There are various pathways of anthocyanin thermal degradation, and they depend on the type of anthocyanin involved and the degradation temperature (Schwartz et al., 2008). One of the pathways may begin with the transformation of flavylium cation to carbinol pseudobase and then to chalcone. The sugar molecule that is attached to the chalcone is first removed from the main structure to generate anthocyanidin chalcone and sugar molecule (Oancea, 2021; Patras et al., 2010). Hydrolytic and auto-oxidative reactions will then ensue to breakdown the intermediate products into the final derivatives of aldehydes and benzoic acids as well as polymeric brown degradative products (Dangles & Fenger, 2018; Oancea, 2021; Patras et al., 2010; Schwartz et al., 2008). Furthermore, light can also leave a negative impact on anthocyanin as it can accelerate its degradation via auto-oxidative mechanism (Rivas-Gonzalo, 2003; Schwartz et al., 2008). Various steps can be taken to preserve the colour quality of anthocyanin-containing material and retard anthocyanin loss. Essentially maintaining the acidity of the medium and reducing the exposure to moisture, heat and light will keep anthocyanins stable.

2.1.1.2. Non-Anthocyanin Phenolic Compounds

Flavonol and phenolic acid are the two non-anthocyanin phenolic compounds found in blackcurrant fruit. They contribute to whiteness in some plants, browns and blacks when oxidised, as well as yellowness if present in sufficient concentration (Schwartz et al., 2008). Flavonol has similar basic aglycone structure as the anthocyanidin, but without the pyrylium ring (Ring C of Figure 2.2). Some of the commonly available flavonols are kaempferol, quercetin, myricetin and isorhamnetin, as shown in Figure 2.5 (Arts et al., 2003). Like anthocyanins, each flavonol can be distinguished by the type and number of substituents attached to the aglycone unit (hydroxylation, methylation, and glycosylation of various sugars—monosaccharides, disaccharides, trisaccharides and tetrasaccharides) as well as the substitution position (Arts et al., 2003; Schwartz et al., 2008). Typically, aglycone flavonols are not found naturally in plants but may appear as a result of food processing. Flavonols that are found abundantly in blackcurrant are quercetin, myricetin, kaempferol and their derivatives (Aneta et al., 2013; Anttonen & Karjalainen, 2006; Nyanhanda et al., 2014; Vagiri et al., 2012).

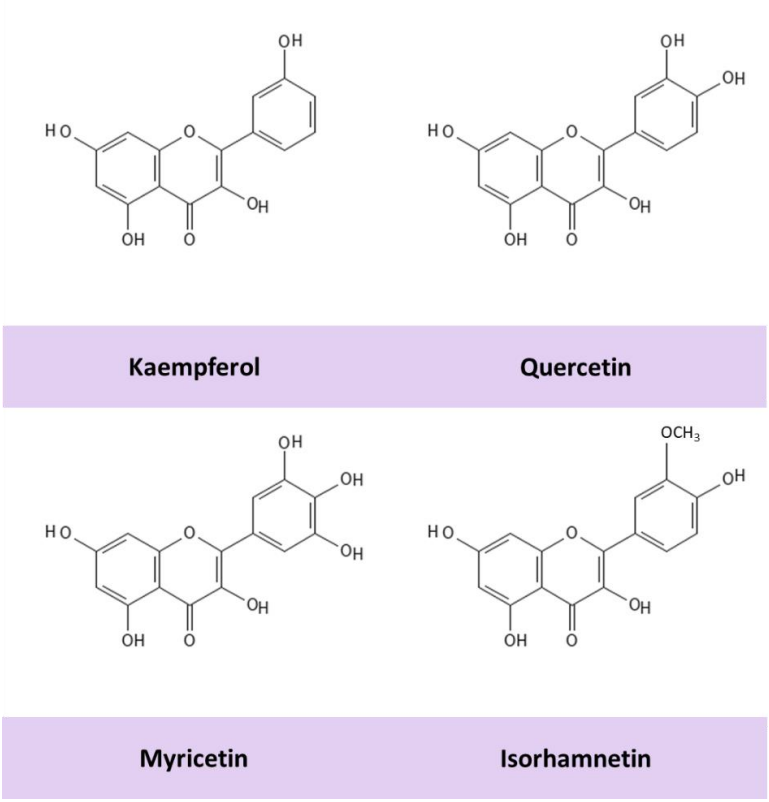

Figure 2.5 Structure of commonly found flavonol aglycones. Adapted from Zhang et al. (2013).

Phenolic acids are organic acids with an aromatic ring with at least one hydroxy group attached to it. Their primary structure is either of benzoic or cinnamic acid, hence the name hydroxybenzoic and hydroxycinnamic acids. They are differentiated by the hydroxylation and methylation of the aromatic ring as shown in Table 2.2. The formation of phenolic acid starts with the precursor amino acid, L-phenylalanine that can evolve into various phenolic acids following a series of reactions involving deamination, enzymatic conversion, and enzymatic hydroxylation (Xu, 2012). In comparison to anthocyanins and flavonols, phenolic acids have better water solubility, yet despite this, not all phenolic acids are extractable (Xu, 2012). Some of the phenolic acids are free and soluble in the liquid portion of the plant cell, while some of them are bound to small organic compounds and cell wall components such as anthocyanins and pectin, respectively (Brett & Waldron, 1990a; Dixon & Paiva, 1995; Xu, 2012). For instance, ferulic and *p*-coumaric acids are typically bound to polysaccharides (Andersson et al., 2017; Brett & Waldron, 1990a; Lopes da Silva & Rao, 2006). Rombouts and Thibault (1986) discovered that ferulic acid, a hydroxycinnamic acid, is esterified to the neutral sugar side chains of the rhamnogalacturonans of the sugar beet pectin. In blackcurrant, a variety of phenolic acids has been identified and they are mostly hydroxycinnamic acids, although some study did report the presence of hydroxybenzoic acids (Russell et al., 2009). The commonly identified phenolic acids in blackcurrant are 3-caffeoylglucoside acid, *p*-coumaric acid and its derivative *p*-coumaroylquinic acid

as well as chlorogenic and neo-chlorogenic acid (Anttonen & Karjalainen, 2006; Ochmian et al., 2014; Vagiri et al., 2012; Vagiri et al., 2013).

Table 2.2 Substituents of commonly found phenolic acids. Adapted from Xu (2012).

Hydroxybenzoic Acid		**R_1**	**R_2**	**R_3**	**R_4**
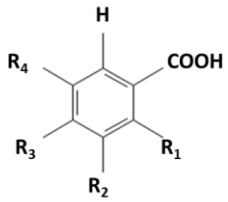	**Benzoic Acid**	H	H	H	H
	***p*-Hydroxybenzoic Acid**	H	H	OH	H
	***m*-Hydroxybenzoic Acid**	H	OH	H	H
	Salicylic Acid	OH	H	H	H
	3,5-Dihydroxybenzoic Acid	H	OH	H	OH
	Protocatechuic Acid	H	OH	OH	H
	Gentistic Acid	OH	H	H	OH
	Gallic Acid	OH	OH	OH	H
	Vanillic Acid	H	OCH_3	OH	H
	Syringic Acid	H	OCH_3	OH	OCH_3
Hydroxycinnamic Acid		**R_1**	**R_2**	**R_3**	**R_4**
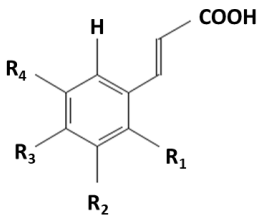	**Cinnamic Acid**	H	H	H	H
	***p*-Coumaric Acid**	H	H	OH	H
	***m*-Coumaric Acid**	H	OH	H	H
	***o*-Coumaric Acid**	OH	H	H	H
	Caffeic Acid	H	OH	OH	H
	Ferulic Acid	H	OCH_3	OH	H
	Sinapic Acid	H	OCH_3	OH	OCH_3

2.1.2. Blackcurrant Pectin

The plant cell wall is made of a group of polysaccharides—pectin, hemicellulose, and cellulose—proteins, and lignin (Andersson et al., 2017). They are normally interlinked with each other to provide the plant cell with structural integrity and shape. Besides that, the cell wall also serves as a transport and storage system for small molecules such as nutrients, minerals, and waste metabolites, and acts as a protective barrier against most pathogenic organisms (Brett & Waldron, 1990b). Unlike phenolic compounds, the blackcurrant cell wall components are not that well studied. Thus, this sub-section presents some of the available information on blackcurrant cell wall components, mainly on its pectin.

Pectin is one of the components that is found in the primary cell wall and middle lamella of a plant tissue, that is, the intercellular space between plant cell membranes (Lopes da Silva & Rao, 2006). It is a complex and diverse heteropolysaccharide that is mainly made of galacturonic acid (GalUA) units and is typically associated with other cell wall components. Structurally, there are three main configurations of pectin: homogalacturonan (HG), rhamnogalacturonan-I (RG-I) and rhamnogalacturonan-II (RG-II). The HG is an unbranched linear chain of α-(1,4)-linked D-GalUA that can be methylated and acetylated. In comparison, the RG-I is a highly branched chain of alternating rhamnose and GalUA residues with neutral sugar side chains such as arabinose and galactose (Ropartz & Ralet, 2020). Some of the HG units may be substituted with complex side chains like the RG-II domains that have branching appearance—consisting of 13 different sugars and 21 glycosidic linkages—while some may be substituted with simple side chains like the monomers and dimers of apiose and xylose (Ropartz & Ralet, 2020).

The first detailed study on blackcurrant polysaccharides was carried out by Hilz et al. (2005). The study reported on the compositions of Finland blackcurrant skin, pulp, and seeds, along with the distribution of polysaccharides over the three blackcurrant tissues. (Hilz et al., 2005). Hilz et al. (2005) reported that a 100 g of fresh Finland blackcurrant contained about 1.53 g of pectin, coinciding with the pectin concentration of United Kingdom blackcurrant (0.55 g to 1.79 g pectin/100 g fresh berries) (Money & Christian, 1950). The major carbohydrate component of the blackcurrant fruit was GalUA, followed by glucose, mannose and arabinose (Hilz et al., 2005). Sequential extraction of isolated acid soluble and calcium bound pectins revealed that the blackcurrant pectin was rich in GalUA and arabinose side chains (Hilz et al., 2005). The study also investigated the polysaccharides of a commercial blackcurrant juice, revealing that the enzymatically treated and ultra-filtered juice contained mostly pectin with minute amount of hemicellulose (Hilz et al., 2005). The pectin found in the blackcurrant juice was primarily RG-I with arabinan and arabinogalactan side chains and some RG-II (Hilz et al., 2005; Hilz, Williams, et al., 2006).

Besides the whole fruit and juice, investigation was also conducted on the polysaccharides of United Kingdom and Poland blackcurrant pomace—the by-product of commercial blackcurrant juice extraction (Alba et al., 2018). Alba et al. (2018) reported that the blackcurrant pomace contained about 30% w/w of soluble dietary fibre (42-52% pectin and 48-58% hemicellulose) and 47% w/w of insoluble dietary fibre (cellulose and lignin). The extracted pectic fractions—acid soluble and calcium bound pectins—had a wide size distribution with average molecular weight (M_w) of 30 kDa to 110 kDa (Alba et al., 2018).

Pectin can be classified simply by its degree of methyl-esterification (DE). The DE represents the amount of carboxyl groups (COOH) that have been esterified with methanol (CH_3OH) to form the methoxy group. A pectin with a DE between 25% and 50% is known as a low methoxyl (LM) pectin, while a pectin with DE between 50% and 80% is known as the high methoxyl (HM) pectin (Thakur et al., 1997). The presence of methoxy groups and functional oxygen atoms from the GalUA residues means that hydrophobic and hydrogen bonding interactions can happen amongst the pectin molecules (Oakenfull & Scott, 1984; Van Buren et al., 1988; Walkinshaw & Arnott, 1981). Classifying pectin through its DE segregates it according to its physico-chemical properties and functionalities. One of the most commonly known functionalities of LM pectin is its use as a gelling agent for products with low total solids (i.e., low sugar), whereas the HM pectin offers gelling ability for high sugar products (Lopes da Silva & Rao, 2006). There are large variations in the reported DE of blackcurrant pectin; Hilz et al. (2005) reported high DE value of acid soluble (91%) and calcium bound (58%) pectin, while two other studies reported that the pectic fraction isolated from the blackcurrant fruit and pomace had a low DE of 49.2% and 11% to 38%, respectively (Alba et al., 2018; Mierczynska et al., 2017). Variations in the reported DE value were likely due to the difference in starting material, extraction, and processing conditions (Alba et al., 2018).

Pectins from lime and sugar beet sources have acid dissociation constants (pK_a) between 2.7 to 3.2 (Ralet et al., 2001; Ralet et al., 2003). If the pH of the medium is above the pK_a of the pectin, the non-esterified carboxyl groups will dissociate to carboxyl ions (COO^-), making the pectin an anionic polysaccharide. The presence of negative charges allows pectin to interact electrostatically with small molecules that are positively charged. Below the pK_a value, pectin loses most of its negative charges and the likelihood of pectin interacting with oppositely charge molecules will be lower. So far, no study has reported the pK_a value and surface net charge of blackcurrant pectin. Such information is essential for interaction studies, particularly when one of the main complexation mechanisms is via electrostatic forces. Moreover, no study has mentioned the absence or presence of anthocyanins in any of the blackcurrant polysaccharide fractions, which poses an unknown aspect on the interaction studies, since polyphenols are known to interact with biopolymers. At this point, only one study has mentioned the presence of naturally bound anthocyanins in pectin, though it was not the focus of the study (Lin et al., 2016) and this will be discussed in later section.

2.2. Bovine Whey Protein

Whey protein constitutes around 20% of the bovine milk proteins. It is a group of small and soluble proteins that range from 4 nm to 6 nm and remain in solution even at their isoelectric point (≈5.2) (Pelegrine & Gasparetto, 2005; Swaisgood, 2008). Commercially, bovine WP powders are produced from the by-products of cheese production, using sweet and acid whey liquids (Wang & Guo, 2019b). Typically, the liquid whey contains residual caseins, cheese fines and fats, and needs to be clarified and pasteurised before continuing to powder production. Lactose and the bulk water of the clarified liquid whey is then removed via ultra-filtration to achieve a protein concentration between 20% and 80%. In order to obtain whey protein isolate (WPI), the intermediate liquid whey is micro-filtered to remove any remaining fat and boost the protein concentration to 90%. De-mineralisation is then carried out to remove majority of the minerals via ion-exchange, electrodialysis or nano-filtration, although nano-filtration is the better suited method for large scale continuous production (O'Mahony & Fox, 2013; Wang & Guo, 2019b). The low mineral, low lactose and low fat liquid whey can then be dried into WPI powder. Typically, WPI powder contains very high amount of protein (90% to 92%) with low moisture (≈4.5%) and minute amount of lactose (0.5% to 1%), fat (0.5% to 1%) and mineral (2% to 3%) (Wang & Guo, 2019a).

The two major WPs found in milk are: (i) β-lactoglobulin (β-lg) which is the primary globular protein, constituting around 60% of WPs and (ii) α-lactalbumin (α-lac), constituting around 20% of WPs (Edwards et al., 2009). Apart from these two, WPs also include immunoglobulins (10%), bovine serum albumin (BSA) (3%), and lactoferrin (<0.1%), though they are not covered in this thesis due to their minor quantity. In general, WPs are well-characterised and have been reviewed by various authors such as McKenzie (1970), Thompson et al. (2009), Fox and McSweeney (2013), O'Mahony and McSweeney (2016) and Guo (2019). Thus, the following sub-sections only focus on the two major WPs found in bovine milk, that is, β-lg and α-lac.

2.2.1. β-lactoglobulin

The β-lg is a highly ordered protein that is made up of 162 amino acids. Most of its non-polar amino acids are hidden within the calyx of the globular protein (Swaisgood, 2008; Uhrínová et al., 2000), though it has a hydrophobic site that is found on its outer surface (tryptophan61) (Albani et al., 2014; Guo & Wang, 2019). The β-lg can exist as a monomer, dimer or oligomer depending on the pH, temperature, and ionic strength of the medium (Edwards et al., 2009). At the pH of milk and WPI solution (5% w/w) (≈pH 6.7), β-lg exists as a dimer (≈36 kDa) due to the disulphide bonds that bind the monomers together (Edwards et al., 2009; O'Mahony & Fox, 2013; Otter, 2003). When the pH is

relatively close to its isoelectric point of 5.2 (i.e., between pH 3.5 and pH 5.5), β-lg becomes a larger molecule, forming an octamer (≈144 kDa) (Edwards et al., 2009; O'Mahony & Fox, 2013). However, at very acidic pH (pH <3.5) and above neutral pH (pH >7.5), the dimeric β-lg dissociates into monomers (≈18.4 kDa) (O'Mahony & Fox, 2013).

Each β-lg dimer carries five cysteine (Cys) residues; one free sulfhydryl group (Cys121) and two disulphide bonds (Cys66-Cys160 and Cys106-119) (Edwards et al., 2009). The disulphide bond Cys66-Cys160 is known to be involved in intramolecular reaction with the reactive Cys121, causing interchange reaction between the free-sulfhydryl and disulphide bonds. This interchanging reaction can create new disulphide bridges—Cys121-Cys160, Cys121-Cys60 or Cys160-Cys160—which can then form non-native dimers with one unused free sulfhydryl group (Wijayanti et al., 2014). The β-lg is also known to be a member of the lipocalin proteins due to its buried hydrophobic side chains that can unfold and bind with small hydrophobic molecules such as those with aromatic hydrocarbons (Edwards et al., 2009; O'Mahony & Fox, 2013). This makes it a protein with major interest in protein-ligands interactions studies.

2.2.2. α-lactalbumin

The second major WP found in milk is the α-lac. It has 123 amino acids and appears as a monomer with M_w of ≈14.2 kDa and has an isoelectric point that ranges between pH 4.2 and 4.5 (Guo & Wang, 2019; O'Mahony & Fox, 2013). The α-lac is a metalloprotein that carries a calcium ion—held by Lysine79 and four aspartic acid (Asp) residues (Asp82, Asp84, Asp87 and Asp88) (O'Mahony & Fox, 2013; Pike et al., 1996). It does not have a reactive sulfhydryl group like the β-lg, but it has four disulphide bonds (Cys6-Cys120, Cys28-Cys111, Cys61-Cys77, and Cys73-Cys91) (Edwards et al., 2009). Two of the disulphide groups—Cys6-Cys120 and Cys28-Cys111—are very susceptible to interactions when cleaved by heat due to their position at the surface of the protein. However, when the disulphide bond Cys28-Cys111 is cleaved, only Cys111 becomes reactive as Cys28 moves inwards into the protein structure, causing it to be unavailable for interaction (Wijayanti et al., 2014). The Cys61 residue is also accessible for interactions, but not Cys77, Cys73 and Cys91 as their position is beneath the protein surface, much like Cys28 (Wijayanti et al., 2014).

2.2.3. Heat-Induced Denaturation and Aggregation of Whey Proteins

The WPs denature and aggregate easily by heat due to their highly ordered structure. Since β-lg is the principal WP, many studies have investigated the mechanism behind β-lg denaturation and aggregation (Petit et al., 2016; Stefania et al., 1996; Verheul et al., 1998; Wijayanti et al., 2015). Essentially, heating a neutral pH β-lg solution to 70 °C will dissociate the β-lg dimers from each other

and unfold the protein, revealing its hydrophobic sites and reactive sulfhydryl group (Edwards et al., 2009; Stefania et al., 1996). These monomers will not be able to revert to their native dimeric form as the exposure of hydrophobic regions and reactive sulfhydryl groups leads to protein-protein interactions via covalent and/or non-covalent interactions (hydrophobic, hydrogen bonds and electrostatic interactions), forming dimers, trimers, and tetramers (Edwards et al., 2009; Stefania et al., 1996; Verheul et al., 1998). Further association of these polymeric molecules will produce a mixed variety of disulphide-bonded aggregates. If denaturation occurs at low pH where most of the β-lg appears as native monomers, the unfolding of protein will be reversible as long as the heating is done at <70 °C (Edwards et al., 2009; Stefania et al., 1996). Above this temperature, large protein aggregates will form via non-covalent bonds (Edwards et al., 2009). Similar findings were also reported by Verheul et al. (1998) stating that covalent bonds are prone to occur at high heating temperature (>85 °C), high pH value (>pH 6) and low ionic strength (<0.1M NaCl), while non-covalent bonds predominated at lower temperature (65 °C to 85 °C) with low pH (<pH 6) and high ionic strength (>1.0 M NaCl).

The α-lac denatures at lower temperature (64 °C) than the β-lg (70 °C to 74 °C) and has better heat-stability (Edwards et al., 2009; Guo & Wang, 2019; O'Mahony & Fox, 2013). This is because the embedded calcium ion of the α-lac helps to accelerate the rate of refolding and reformation of the right disulphide bonds once it is unfolded (Edwards et al., 2009; Fox, 2009; Otter, 2003; Wojciech et al., 2001). When α-lac is heated at acidic conditions (pH <5), the Asp residues become protonated and lose their ability to re-complex with the calcium ion, causing α-lac to be denatured and not refolded upon cooling (Fox, 2009). Irreversible denaturation can also occur in calcium-depleted α-lac or when it is heated at high temperature (≥95 °C) for at least 14 min (Chaplin & Lyster, 1986; Wijayanti et al., 2014)

Amongst the five proteins mentioned earlier, β-lg, α-lac and BSA are the common WPs that actively participate in WP aggregation (Wijayanti et al., 2014). In a WP solution, aggregation happens mainly because of β-lg and BSA ability to self-initiate via the interchanging of disulphide bonds with their free sulfhydryl group. Although α-lac is not able to aggregate on its own due to the absence of free sulfhydryl group, it can interact with β-lg and BSA by interchanging its disulphide bonds forming interprotein aggregates (Calvo et al., 1993; O'Mahony & Fox, 2013; Wijayanti et al., 2014).

Anema (2017) has shown that the degree of WP denaturation depends on the heating temperature and holding time, the higher the temperature and the longer the holding time, the greater the degree of denaturation. It takes approximately, 5 min to unfold about 80% of the WPs in milk at 80 °C. The unfolding process started at temperatures between 70 °C to 85 °C, while aggregation of the proteins occurred above 85 °C—between 85 °C and 115 °C (Anema, 2017).

The rate of heating also affects the formation of protein aggregates. Oldfield et al. (1998) pointed out that low heating rate—such as heating in water bath or by indirect heat-exchanger—unfolded WPs relatively slowly in comparison to direct steam injection, which instantly heats up and denatures the proteins. Slow heating allows the WPs to form reactive monomers and small aggregated species, instead of large aggregated ones, indicating that low heating rate can provide greater opportunity for other molecules in the solution to interact with the unfolded proteins (Oldfield et al., 1998).

2.3. Interactions Between the Reactive Components

Interactions between food constituents can occur during food processing and ingredient mixing. Amongst the components mentioned earlier (blackcurrant phenolic compounds, blackcurrant pectin and WPs), three potential interactions can occur (Figure 2.6). Interaction is likely to happen during puree or juice processing, between blackcurrant cell wall components and blackcurrant phenolic compounds, such as pectin-anthocyanin interactions. Subsequently, the mixing of WPs with the blackcurrant puree or juice, which contains pectin and phenolic compounds can bring about pectin-protein and polyphenol-protein interactions. The following sub-sections cover the fundamental and recent information on the potential interactions of blackcurrant components and WPs, which is relevant to the discussion of the experimental findings of the later chapters.

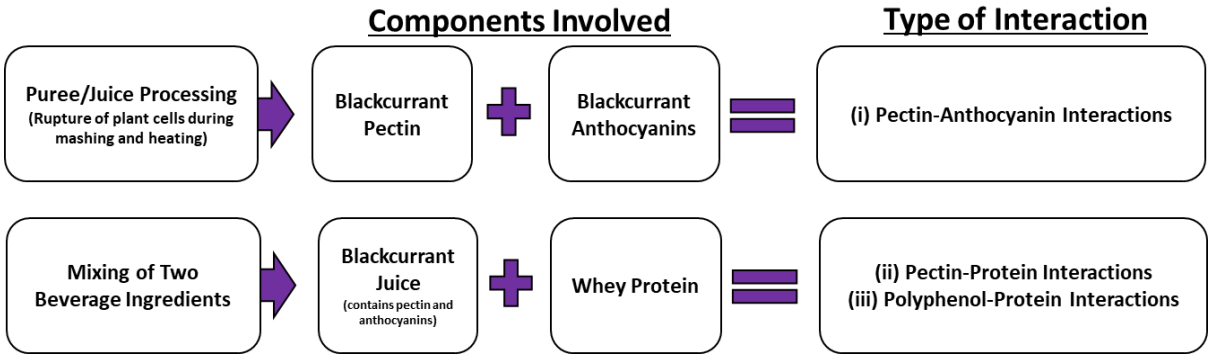

Figure 2.6 Types of interactions that can occur between blackcurrant components and whey protein.

2.3.1. Pectin-Anthocyanin Interactions

Anthocyanins are synthesized by organelles known as anthocyanoplasts, which are in the vacuole of a plant cell and protected by a network of cell walls (Bae et al., 2006; Pecket & Small, 1980). When blackcurrant is crushed and macerated during puree and juice production, the processes rupture the cells and the anthocyanoplasts contained in it, liberating anthocyanins and various other components, while leaving the cell wall network disrupted (Owuor, 2003; Takaki et al., 2021). This allows the anthocyanins to be in contact with the cell wall components like pectin, generating pectin-anthocyanin interactions. The interaction can happen between any type of cell wall components and phenolic compounds, although they have different selectivity and affinity towards each other as shown by Padayachee et al. (2012a, 2012b) and Phan et al. (2017).

The conventional production of a commercial blackcurrant puree or juice requires the use of maceration enzymes that includes pectinases, hemicellulases, cellulases and cutinases in various ratios (Buchert et al., 2005; Kashyap et al., 2001; Koponen et al., 2008; Makila et al., 2017). These enzymes aid in the extraction of phenolic compounds and the degradation of the cell wall network to

lower the viscosity and increase the yield of the puree and/or juice (Buchert et al., 2005; Kashyap et al., 2001). Since the starting material for this research was a commercially prepared blackcurrant puree, it is expected to contain blackcurrant cell wall components with possibly free and bound polyphenols. To the best of our knowledge, none of the existing blackcurrant polysaccharide studies have explicitly mentioned about the binding of blackcurrant phenolic compounds to any of the blackcurrant polysaccharide fractions, thus the need to investigate these fractions further.

2.3.1.1. Interactive Forces between Pectin and Anthocyanins

Generally, pectin-anthocyanin interactions are dependent on the structural nature of the pectin and anthocyanins and are caused by a combination of interactive forces, mostly non-covalent bonds (Dangles & Fenger, 2018). One of the early indications of pectin-anthocyanin interactions was reported by Asen et al. (1970) when a bluish pectic substance was obtained during the extraction process of anthocyanins from the petals of *Iris hollandica*. Mazzaracchio et al. (2004) suggested that the interaction between pectin and anthocyanins happened electrostatically—negatively charge GalUA with positively charged flavylium ion—and hydrophobically—between methoxy groups of pectin and anthocyanins. In agreement to that, Hubbermann et al. (2006) reported that the colour stability of elderberry and blackcurrant anthocyanins was maintained at a prolonged storage when LM citrus pectin was incorporated into the pigmented mixture. The authors attributed the protective effect to electrostatic interactions between the pectin and anthocyanins, which prevented the anthocyanins from nucleophilic water attack (Hubbermann et al., 2006).

In a more recent and detailed study, Fernandes et al. (2014) demonstrated that the interaction between a LM citrus pectin and anthocyanins (del-glu and cya-glu) depended heavily on the structure of the anthocyanins. Anthocyanins that were in the form of flavylium cations (pH 1.5) formed stronger interaction with the LM pectin than those that were in the form of hemiketals (pH 4) (Fernandes et al., 2014). The stronger interaction at lower pH was attributed to the involvement of many interactive forces—electrostatic, hydrophobic (aromatic ring stacking) and hydrogen bonding forces (Fernandes et al., 2014). Additionally, the authors found that anthocyanins with more hydroxy groups—del-glu (three hydroxy groups)—formed stronger interactions with the LM pectin than those that had lesser—cya-glu (two hydroxy groups). They ascribed the observation to the degree of hydrogen bonding between the carboxyl groups of pectin and hydroxy groups of anthocyanins, in other words, anthocyanins with more hydroxy groups lead to more hydrogen bond formations (Fernandes et al., 2014).

The binding of anthocyanins to pectin is dependent on the environmental pH as it dictates the structure of anthocyanins. Lin et al. (2016) revealed similar findings as Fernandes et al. (2014) that

cya-glu interacted more with LM blueberry pectic fractions at pH 2 and pH 3.6 than at pH 4.5, and attributed it to flavylium cations ability to electrostatically and hydrophobically (aromatic ring stacking) interact with the pectic components. The authors also pointed out that the blueberry pectic fractions had different colour following their extraction. Pectic fraction that was extracted with pH 5.2 buffered water retained its purple colour even after solvent extraction and extensive dialysis, while the fraction that was extracted with a chelating agent appeared pale pink and the alkali extracted fraction appeared brown in solution (Lin et al., 2016). The authors suggested that the endogenous anthocyanins might be tightly bound to the pectic fractions through hydrogen and/or hydrophobic interactions (Lin et al., 2016). The colour variation amongst the blueberry pectic fractions highlighted two points: (i) the difference in the degree of binding of endogenous anthocyanins to different pectin configurations (HG, RG-I and RG-II) and (ii) the impact of pectin extraction method on anthocyanins.

2.3.2. Pectin-Protein Interactions

An aqueous solution containing polysaccharide and protein may lead to segregative or associative interactions, depending on the system composition and environmental conditions (Figure 2.7) (Goh et al., 2009; Jones & McClements, 2011). Segregative interaction occurs when the biopolymers repel each other and phase separate, such as in the case of thermodynamic incompatibility and depletion interaction. Thermodynamic incompatibility takes place when the biopolymers are not interacting—between protein and neutrally charged polysaccharide or between two biopolymers with the same charges (Goh et al., 2009). As for depletion interaction, it occurs as a result of osmotic pressure difference that excludes non-adsorbing polysaccharides from the space between large colloidal particles (Maroziene & de Kruif, 2000; Matia-Merino et al., 2004). Contrary to that, associative interaction occurs when there are attractive forces drawing two biopolymers together, forming complexes that may be soluble or insoluble. The attractive forces involved may be strong or weak and specific (covalent bonding) or non-specific (electrostatic, charge-dipole, van der Waals, hydrogen bonding and hydrophobic) (Walstra, 2003). This sub-section focuses on the attractive interactions between the anionic polysaccharide pectin and protein.

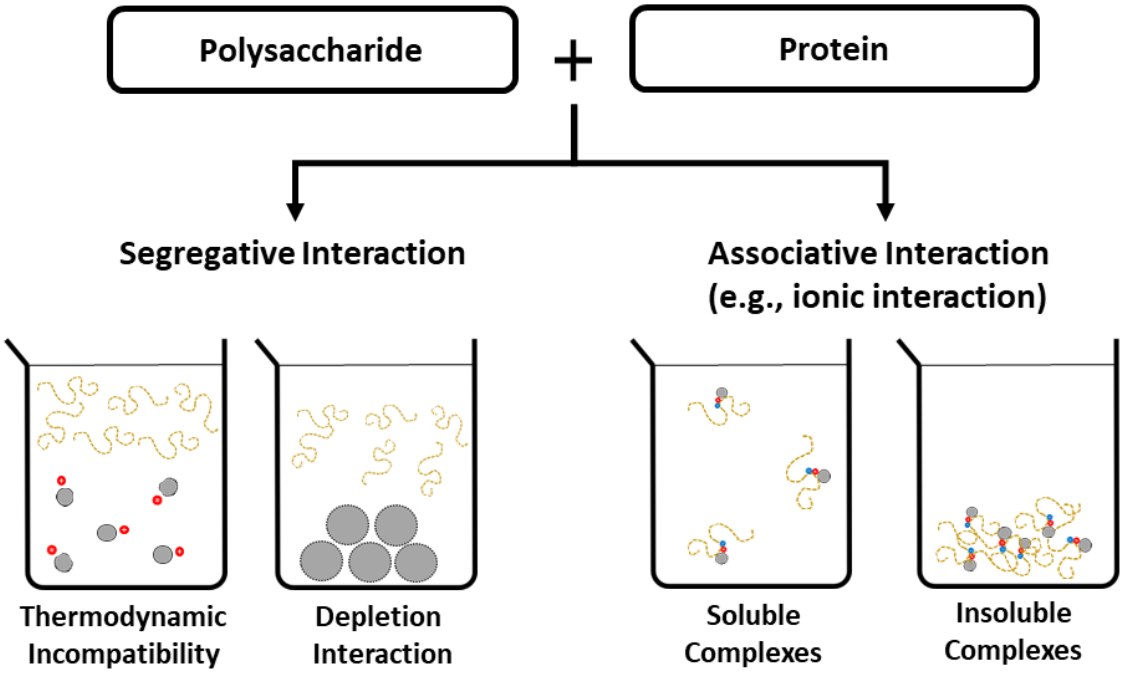

Figure 2.7 Types of interactions between polysaccharide and protein in aqueous solution. Adapted from Goh et al. (2009)

Generally, the interaction between pectin and protein is influenced by intrinsic properties of the biopolymers—M_w and surface charge—and external factors like pH and ionic strength of the mixture, temperature, biopolymers ratio, total biopolymer concentration and presence of aggregates.

2.3.2.1. Molecular Parameters Affecting Pectin-Protein Interactions

The M_w of the biopolymer determines the extent of complexation that can happen. Basically, a polyelectrolyte with high M_w enables interaction with higher number of proteins and may induce aggregation with other soluble complexes, leading to sedimentation and phase separation of the system (Schmitt et al., 2009). On the other hand, smaller M_w polyelectrolytes have limited number of binding sites, thus the complexes formed tend to be smaller and soluble as shown by the work of Laneuville et al. (2005).

Additionally, the interaction can be affected by the surface charge of the biopolymers, particularly when it is driven by electrostatic forces. In the case of pectin, the surface charge is influenced by the amount of GalUA and DE—lower DE equates to lesser methyl-esterified uronic acids; thus, LM pectin has greater number of free carboxyl groups than HM pectin and generates higher surface charge (Verkempinck et al., 2018). With higher surface charge, the proteins will have access to more binding sites, intensifying the electrostatic complexation between the pectin and protein. Although,

electrostatic interaction may be less intense for HM pectin-protein systems, other interactive forces may also be involved, depending on the experimental conditions (Girard et al., 2002, 2003a, 2003b; Jones et al., 2009).

2.3.2.2. Environmental Factors Affecting Pectin-Protein Interactions

The interactions between pectin and protein are heavily dependent on pH as pH can alter the degree of ionisation of the biopolymers charged groups (Schmitt et al., 2009). A suitable range of pH is required to generate the electrostatic attraction, that is, above the pK_a value of the pectin and below the isoelectric point of the protein (Goh et al., 2009; Schmitt et al., 2009; Schmitt et al., 1998). Essentially, the negative charges of pectin and the positive charges of protein increase as the system pH is further from the pK_a of the pectin and lower than the isoelectric point of the protein, respectively. Outside the pH range, the attractive electrostatic force will be severely weakened and the complexes may dissociate (Jones & McClements, 2011).

The presence of ions in food systems is common, however ions may cause detrimental effects while studying pectin-protein interactions as they can screen the charges of the polyelectrolytes via small ion-pairing, reducing the number of binding sites for the protein (Schmitt et al., 2009). Thus, in the present research, the ionic strength was kept at minimum for all mixed systems.

Temperature affects the participation of non-electrostatic attractive forces. Essentially, low temperature is favourable for hydrogen bonding, while high temperature promotes hydrophobic forces (Schmitt et al., 2009). Heating the pectin-protein system will promote hydrophobic interactions between the exposed hydrophobic calyx of the WPs and methoxy groups of the pectin, while upon cooling, hydrogen bonds will form, reinforcing the interacted biopolymers (Girard et al., 2002, 2003a, 2003b). The sequence of heating also plays an important role as it influences the complexes size and stability (Jones et al., 2010; Jones & McClements, 2011; Santipanichwong et al., 2008).

The ratio of pectin to protein can influence the intensity of interaction as it relates to the amount of charge pairings between the two biopolymers. At a specified pH and ionic strength, the formation of electrostatic complexes can be maximised if the optimal ratio is found (Schmitt et al., 2009). Even though the aim of this research was not to determine the optimal ratio of blackcurrant pectin and WP nor maximising the formation of complexes, varying the pectin:protein ratio can help in understanding the behaviour of the mixed system. The concentration of biopolymers is also critical in an interaction study as high concentration of biopolymers can induce phase separation through thermodynamic incompatibility due to the competition for the solvent between the biopolymers (Schmitt et al., 1998).

Therefore, a much less concentrated system was used for the interaction studies, based on the work of Sperber et al. (2009).

Moreover, the presence of protein aggregates has been reported to have a marked effect on the size, surface properties and degree of phase separation of electrostatically formed complexes and microparticles. Schmitt et al. (2000) reported that β-lg aggregates interfered with electrostatic complexation of acacia gum-β-lg by limiting the size of the complexes formed. Therefore, the removal of aggregates was carried out on the WP powder before it was used in the interaction studies.

2.3.2.3. Interactive Forces Between Pectin and Protein

The type of forces involved in a pectin-protein system depends on the experimental conditions. Covalently bonded pectin-protein complexes were formed via Maillard reaction by lyophilising a pH 7 pectin-protein mixture and dry heating it at 60 °C to 70 °C over a period of less than a day to 15 days (Hiller & Lorenzen, 2010; Mishra et al., 2001; Neirynck et al., 2004). However, in aqueous solution the participating attractive forces are mostly non-covalent in nature. The dominant force that draws the two biopolymers together is produced by the ionic or electrostatic attraction between positively charged amino groups of protein and negatively charged carboxyl groups of pectin. However, ionic force is not the only force responsible for pectin-protein complexation. Girard et al. (2002) had demonstrated that β-lactoglobulin interaction with either a LM or HM pectin at 4 °C and 40 °C was primarily driven by electrostatic interaction, and to a lesser extent, by hydrogen bonding. Hydrophobic forces can also participate if the pectin-protein interaction occurs at a temperature that is near the denaturation temperature of the protein—for example >60 °C for WPs (Law & Leaver, 2000)—particularly if it involves HM pectin as its high amounts of methoxy groups may interact hydrophobically with the exposed hydrophobic amino acids of the unfolded protein (Girard et al., 2002, 2003a, 2003b; Jones et al., 2009).

2.3.3. Polyphenol-Protein Interactions

The association of polyphenols to protein is described as a surface phenomenon where polyphenols are regarded as ligands with many interactive ends, binding at more than one point of the protein surface (Spencer et al., 1988). Generally, the interactions are influenced by temperature and pH as they affect the characteristics of the protein (Ozdal et al., 2013; Siebert et al., 1996; Yildirim-Elikoglu & Erdem, 2018). Additionally, the type of protein, ratio of polyphenol to protein, and type of polyphenol also play important roles (Hagerman, 2012; Ozdal et al., 2013; Spencer et al., 1988; Yildirim-Elikoglu & Erdem, 2018).

2.3.3.1. Factors Affecting Polyphenol-Protein Interactions

2.3.3.1.1. Temperature and pH

Similar to the effect of temperature on pectin-protein interactions, temperature influences the attractive forces of polyphenol-protein interactions by encouraging hydrophobic interactions or disrupting hydrogen bonds (Ozdal et al., 2013). If the temperature is high enough it can affect the conformation of globular protein by unfolding its structure and revealing the hydrophobic regions and other amino acids, increasing the binding sites for polyphenols. The effects of temperature were demonstrated in Prigent et al. (2003) work where the binding of chlorogenic acid to BSA decreased with increasing temperature (5 °C, 25 °C and 60 °C), indicating the detrimental effect of heat on hydrogen bonds. In another study, Hofmann et al. (2006) reported that the precipitation of BSA by hydrolysable tannins—grandinin, castalagin and pentagalloyl glucose—was increased at higher temperature due to increased hydrophobic bindings.

The precipitation of polyphenol-protein complexes is sensitive to pH because it affects the structure of protein (Hagerman & Butler, 1978). The point at which precipitation occurs varies for different proteins but typically, complexes precipitate near the isoelectric point of the protein as aggregation happens readily at that point (Hagerman, 2012; Naczk et al., 2006; Ozdal et al., 2013). Additionally, pH may also play a crucial role if the polyphenols involved are anthocyanins. This is because the structure of anthocyanins changes according to pH and different structures exhibit different binding affinity, as it has been shown by Vuong and Hongsprabhas (2021).

2.3.3.1.2. Type of Protein

The binding affinity of polyphenols to protein depends on factors like protein conformation, protein hydrophobicity—β-lg > κ-casein > BSA > lysozyme (Townsend & Nakai, 1983)—and amino acid composition of the protein (Ozdal et al., 2013; Yildirim-Elikoglu & Erdem, 2018). Phenolic compounds usually have higher binding affinity towards unstructured proteins with high proline content (e.g., casein, salivary protein, and gelatine) as compared to the highly ordered globular proteins (Baxter et al., 1997; Hagerman, 2012; Spencer et al., 1988). This is because unstructured protein has open and flexible conformation that allows greater capacity for hydrogen bonding and easy access to hydrophobic regions (Spencer et al., 1988). Jauregi et al. (2016) reported that at higher protein concentration (0.5% w/v), tannins interacted more with gelatine than with β-lg due to their large size, open structure, and high proline content.

2.3.3.1.3. Polyphenol-Protein Ratio

The ratio of polyphenols to protein can influence the size of the complexes (Siebert et al., 1996). Spencer et al. (1988) proposed a polyphenol-protein complexation model with two scenarios. In a system with low protein concentration, the polyphenols will adhere to the protein surface until most of its surface is covered. This creates a monolayer that is less hydrophilic than the protein itself, triggering complexes aggregation and then precipitation. However, when there is excess protein, the polyphenols may simultaneously bind to several protein molecules and possibly cross-link with other polyphenol-protein complexes, forming larger aggregates before precipitating out. In agreement to that model, Siebert et al. (1996) added that complexes which formed at low and high protein concentration may be smaller than those that formed when there are equal number of polyphenols and protein binding sites.

2.3.3.1.4. Type of Polyphenol

Polyphenols with high molecular weight can bind strongly and precipitate protein more readily than those with lower molecular weight and this effect is particularly prominent in proline-rich proteins (Baxter et al., 1997; Yildirim-Elikoglu & Erdem, 2018). In Jauregi et al. (2016) work, tannins were found to bind strongly with gelatine in comparison to smaller polyphenols like catechin. The binding strength is also affected by the degree of hydroxylation of the polyphenols. Xiao et al. (2010) reported that the interaction between flavones and BSA resulted in higher binding constants and number of binding sites when the ring A of the flavone was hydroxylated, likely due to increased hydrogen bonding interaction. In the case of anthocyanins, interactions with protein are believed to occur via multiple interactive forces—electrostatic, hydrophobic and hydrogen bonding forces (Vuong & Hongsprabhas, 2021; Yildirim-Elikoglu & Erdem, 2018). Generally, the interactions are dependent on the structure of the anthocyanin: flavylium cation, quinonoidal base, carbinol pseudobase, chalcone or charged quinonoidal base. Some of the anthocyanin structures are ionic like the positively charged flavylium anthocyanins that are present at pH <4.5 or the negatively charged quinonoidal anthocyanins that form at pH >6. Cheng et al. (2017) reported that the interaction between cya-glu and β-lg at ≈pH 7 was driven by hydrophobic forces and hydrogen bonding with no electrostatic interaction detected. This was likely because at neutral pH the cya-glu was in the form of neutral or negatively charge quinonoidal base, therefore the chances of them interacting electrostatically with the negatively charged β-lg was very low.

2.3.3.2. Interactive Forces between Polyphenols and Proteins

Covalent bonding between polyphenols and protein can occur as it has been shown and discussed by Ozdal et al. (2013), though it usually involves enzymatic oxidation of the phenolic compounds into quinone, which may then react covalently with the nucleophilic groups of the proteins (e.g., sulphydryl or amino groups) (Beart et al., 1985). The non-covalent binding of polyphenols to protein occurs mainly via hydrophobic and hydrogen bonding interactions (Ozdal et al., 2013; Siebert et al., 1996). Spencer et al. (1988) suggested that the interaction takes place via a two-step process: (i) attraction between the aromatic rings of polyphenols and hydrophobic regions of the protein by hydrophobic forces and (ii) stabilisation of the complexes by hydrogen bonds. Essentially, the close approximation of the aromatic rings to non-polar residues of the protein creates hydrophobic pockets that simultaneously exclude the water molecules nearby, generating hydrophobic forces, while the hydrogen bonds supervene between the amino, hydroxy and carboxyl groups of the two components (Dangles & Dufour, 2006; Hagerman, 2012; Spencer et al., 1988). However, if the interaction involves anthocyanins, the participation of electrostatic forces may be possible.

Based on the published works of blackcurrant fruit, no author has commented nor investigated on the relationship of endogenous blackcurrant anthocyanins with any of the blackcurrant cell wall components. It is vital that their relationship, especially between pectin and anthocyanins, is understood before protein interaction studies with the blackcurrant juice are conducted as presence of multiple reactive components can complicate the interaction study. The following chapters present methodical investigative works that aimed to understand the relationship between the interactive components of the juice, followed by their interaction with the WPs.

Chapter 3 Experimental Techniques

This chapter presents the main experimental techniques used in the investigative work of this thesis. The techniques are grouped into five objectives: (i) determination of material composition, (ii) identification and quantification of phenolic compounds, (iii) determination of physico-chemical characteristics, and (iv) identification of chemical groups in materials of interest.

3.1. Proximate Analysis

Various proximate tests were conducted to determine the composition of the working materials, with three of them being used repeatedly across all experimental chapters: total carbohydrate, galacturonic acid (GalUA) and protein analyses. These three techniques were important for the investigation as they measured two of the main interactive components of this study, that is, pectin and protein.

3.1.1. Total Carbohydrate Analysis

Carbohydrates were quantified using a rapid colorimetric method known as the phenol-sulphuric acid test that was based on the work of DuBois et al. (1956). This method of analysis can be used on all types of carbohydrates, including polysaccharides as it is specific to sugars with a hydroxy group at carbon position 2 (i.e., pentoses, hexoses and uronic acids) (Gerwig, 2021). The analysis uses concentrated sulphuric acid to break down the carbohydrates, usually into a mixture of monosaccharides. During acidic hydrolysis, sugars with five carbon atoms (i.e., pentoses like ribose, arabinose, xylose etc.) are dehydrated into furfural, while sugars with six carbon atoms (i.e., hexoses like glucose, fructose, galactose etc.) are dehydrated into hydroxy-methyl furfural (Nielsen, 2017b). These compounds will then bind to a chromogen known as phenol, forming yellow to golden brown compounds that can be quantified at 450 nm to 550 nm using an Ultra-Violet/Visible Light (UV/Vis) spectrophotometer (Gerwig, 2021; Nielsen, 2017b). Typically, pentoses and hexoses have maximum spectral absorption at 480 nm and 490 nm, respectively, while the uronic acids exhibit maximum absorption at 483 nm (Yue et al., 2022). In this work, the absorption was read at the average $\lambda_{485\ nm}$ as fruit pectic material consists of various saccharides. The total carbohydrate results are expressed subjectively in terms of a single monosaccharide, usually as the major monosaccharide of the sample (Nielsen, 2017b), and in this case glucose is the dominant sugar of the blackcurrant (BC) fruit (Hilz et al., 2005); thus, all carbohydrates were expressed as glucose equivalents.

3.1.2. Galacturonic Acid Analysis

A rapid colorimetric method that was based on the work of Blumenkrantz and Asboe-Hansen (1973) was used to determine the main building block of pectin, that is, GalUA. The analysis involves acidic hydrolysis of the isolated polymer and dehydration of the free uronic acids under heated conditions (90 °C, 1 h) using concentrated sulphuric acid that contains 12.5 mM of sodium tetraborate. Specific reagent used for the detection of uronic acids, known as *m*-hydroxydiphenyl (3-phenylphenol) is then added to bind with the dehydrated uronic acids, forming pink coloured compounds that can be quantified using a UV/Vis spectrophotometer at $\lambda_{520\,nm}$.

3.1.3. Protein Analysis

The determination of protein in puree and juice was carried out by the nitrogen combustion method, also known as the Dumas method. Essentially, the sample is combusted at a very high temperature that ranges between 900 °C to 1110 °C, releasing steam, nitrogen gas, and other gases. Gas chromatography is then used to quantify the released nitrogen gas. The quantified nitrogen gas is then converted to protein by multiplying it with the factor 6.25, therefore 0.16 g of nitrogen is equivalent to 1 g of protein (Nielsen, 2017a).

3.1.4. Composition of Blackcurrant Puree and Juice

According to the product specification, the commercial BC puree (BLC5100, Juice Products New Zealand Limited, Timaru, New Zealand) consisted of three BC varieties, namely Ben Ard, Ben Rua and Magnus. It is prepared by milling the fruit and then heating it at 95 °C for 60 s and followed by a two-stage refining process that removed the BC skin and seeds. There is no mention of enzyme maceration in the product specification, but the use of enzymes is typically employed in conventional production of BC puree and juice so that the viscosity is manageable, and the yield is increased (Buchert et al., 2005; Kashyap et al., 2001). The BC juice used in this work was obtained by centrifuging the puree twice at 4618 x *g* for 15 min (20 °C), which yielded about 70% w/w of juice.

The puree and juice were analysed for moisture (AOAC 925.10), total carbohydrate, GalUA, insoluble fibres (AOAC 2002.04 and 973.18)—hemicelluloses, cellulose, and lignin, fat (AOAC 922.06), protein (AOAC 968.06), ash (AOAC 942.05) and various minerals (inductively coupled plasma-optical emission spectrometry) (AOAC, 2023). All analyses were carried out by the accredited Nutrition Laboratory in the School of Food and Advanced Technology at Massey University, Palmerston North, except the analysis of moisture, total carbohydrate and GalUA.

The technique used to quantify total carbohydrate and GalUA was modified to fit a 96-well microplate. Water-soluble carbohydrates were first extracted from the puree using hot ammonium oxalate

solution (0.5% w/v, 70 °C). The extracted fraction was then analysed for total carbohydrate content. The juice, however, did not require any prior extraction as the carbohydrates it contained were soluble. Glucose solutions (20, 40, 60, 80 and 100 ug/mL) were freshly prepared to construct a standard curve and distilled water was used as a blank. In the analysis, 40 µL of blank, standard, or sample was dispensed into the microplate well followed by a 40 µL of 5% w/v phenol solution. An aliquot of 200 µL of sulphuric acid was rapidly dispensed by an electronic repetitive pipette and the microplate was shaken for 30 s after covering the plate with a clear sticky lid. The absorbance was measured after 10 min of colour development using the SPECTROstar Nano microplate reader (BMG Labtech, Ortenberg, Germany) at $\lambda_{485\ nm}$. The assay was done in two replicates in which standards and blank were measured in duplicate and samples were measured in triplicate. Results are reported as the mean and standard deviation of at least two readings and expressed as glucose equivalents.

Prior to GalUA analysis, large insoluble materials were removed from the BC juice via centrifugation (14,100 x *g*, 20 °C, 15 min). The juice and previously isolated fraction from the BC puree were mixed with ethanol (80% v/v, 4 °C, 30 min) to precipitate the solubilised pectin. Centrifugation was then conducted at the same settings to separate the alcohol insoluble residue (AIR). The AIR was washed with the same ethanol solution and then centrifuged to remove unbound sugars. The washing cycle was repeated once more before any residual ethanol was left to evaporate from the AIR. Distilled water was then added to dissolve the AIR. Five GalUA solutions (40, 80, 120, 160 and 200 µg/mL) were prepared for constructing a standard curve and distilled water was used as a blank. The blank, standard, or sample (40 µL) was dispensed into a microplate well, followed by the rapid addition of 200 µL of borax-acid mixture. The microplate was then incubated in 90 °C oven for 1 h and pre-read at $\lambda_{520\ nm}$ immediately after the incubation, using the SPECTROstar Nano microplate reader. The microplate was then cooled in an ice bath before adding 10 µL of 0.05% w/v 3-phenylphenol reagent (in 0.125M NaOH) and covering it with a clear sticky lid. After 5 min of colour development, the absorbance was read again at $\lambda_{520\ nm}$. The assay was carried out in three replicates and each time standards and blank were measured in duplicate whereas samples were measured in triplicate. The amount of uronic acid is reported as GalUA equivalents, and the mean and standard deviation of three readings.

Table 3.1 shows the overall composition of the BC puree and juice. The prominent components of the BC puree and juice were water (≈87.8% and ≈90.6% w/w, respectively) and carbohydrate (≈6.74% and ≈6.17% w/w, respectively). Both materials had a comparable carbohydrate content, but the amount of GalUA was higher in the puree (≈0.14% w/w) with only 50% of it detected in the juice (≈0.07% w/w), likely due to more pectin present in the puree. Most of the insoluble fibres were also detected in the

puree (≈2.38% w/w) with very minimal quantities found in the juice (<0.3% w/w). The fat content of the puree and juice was similar (≈0.12% and ≈0.11% w/w, respectively), and likely to be the fat-soluble vitamins of BC and/or fats liberated from the crushed BC seeds. The concentration of protein in the puree (≈0.73% w/w) was slightly lower than that of fresh blackcurrant berries (1.02% w/w) (Hilz et al., 2005), possibly due to the exclusion of berry skin and seeds during the manufacturing process of the puree. In comparison to the juice (≈0.27% w/w), the protein content of the BC puree was higher, suggesting that most of the proteins were bound to the cell wall components that were present primarily in the puree. Both the puree and juice had comparable amount of inorganic materials (≈0.42% and ≈0.40% w/w, respectively), with potassium being the dominant mineral (≈0.32% w/w for both). The puree and juice differed in the amount of calcium (≈0.033% and ≈0.024% w/w, respectively) and phosphorus (≈0.033% and ≈0.027% w/w, respectively), likely signifying calcium and phosphorus association with cell wall components such as pectin and protein, as reported by various authors (Jarvis, 1984; Kobayashi et al., 1999; Qi et al., 2022; Wu et al., 2019).

Table 3.1 Proximate composition of blackcurrant puree and juice.

Components[a]	Blackcurrant Puree % w/w	Blackcurrant Juice % w/w
Moisture	**87.8 ± 0.10**	**90.6 ± 0.02**
Total Carbohydrate	**6.74 ± 0.45**	**6.17 ± 0.20**
Galacturonic Acid[b]	0.14 ± 0.03	0.07 ± 0.01
Insoluble Fibres	**2.38**	**<0.3**
Hemicelluloses	1.12 ± 0.16	<0.1
Cellulose	0.83 ± 0.03	<0.1
Lignin	0.30 ± 0.02	<0.1
Fat	**0.12 ± 0.005**	**0.11 ± 0.004**
Protein	**0.73 ± 0.02**	**0.27 ± 0.006**
Ash	**0.42 ± 0.02**	**0.40 ± 0.018**
Calcium	0.033 ± 0.002	0.024 ± 0.001
Magnesium	0.013 ± 0.001	0.013 ± 0.001
Potassium	0.32 ± 0.015	0.32 ± 0.015
Phosphorus	0.033 ± 0.002	0.027 ± 0.001
Unknown[c]	1.81	2.15

[a]Results are expressed as % of components in blackcurrant puree and juice (mean ± standard deviation).

[b]Pectic component is represented by galacturonic acid content.

[c]Determined by subtracting moisture, total carbohydrate, insoluble fibres, fat, protein, and ash from 100%.

3.2. Identification and Quantification of Phenolic Compounds

The phenolic compounds of the BC fruit were segregated into two clusters: anthocyanins and non-anthocyanins. Quantification of anthocyanins was carried out by two techniques: pH differential method (AOAC 2005.02) and liquid chromatography, while the non-anthocyanins were quantified via mass spectrometry that was coupled to liquid chromatography (AOAC, 2023).

3.2.1. pH Differential Method

The principle behind pH differential method lies on the ability of anthocyanins to structurally change under various pH. Essentially, anthocyanins at pH 1 will appear as the coloured oxonium form (i.e., flavylium cation), while those at pH 4.5 will take the form of a colourless hemiketal (i.e., carbinol pseudobase), generating different absorbance. Absorbance difference between these two anthocyanin structures can then be linked to the concentration of anthocyanins found in the sample. Anthocyanins that are degraded and polymerised cannot structurally change from pH adjustment, therefore only monomeric anthocyanins are quantified in this method (Lee et al., 2005). The analysis uses buffers at two pH levels: pH 1 potassium chloride buffer (0.025 M) and pH 4.5 sodium acetate buffer (0.4 M). Regardless of the pH level, the maximum absorbance of most anthocyanins is at $\approx\lambda_{520\ nm}$ (Lee et al., 2005). However, in this work the anthocyanins were measured at $\lambda_{530\ nm}$ to complement the analysis done via liquid chromatography. Additionally, absorbance at $\lambda_{700\ nm}$ is also measured to offset any interferences from sample turbidity (Lee et al., 2005). Since cyanidin 3-*O*-glucoside (cya-glu) is the most common naturally occurring anthocyanins, the analysis uses its molecular weight and molar extinction coefficient to calculate the anthocyanin content of a sample (Equation 3.1). The formula is as follows:

$$\frac{\boldsymbol{A}\times\boldsymbol{MW}\times\boldsymbol{DF}\times\mathbf{10^3}}{\boldsymbol{\varepsilon}\times\mathbf{1}} \quad \text{(Equation 3.1)}$$

$\boldsymbol{A}$ is $(A_{530\,nm,\ pH\ 1} - A_{700\,nm,\ pH1}) - (A_{530\,nm,\ pH\ 4.5} - A_{700\,nm,\ pH\ 4.5})$

$\boldsymbol{MW}$ is the molecular weight of cyanidin 3-*O*-glucoside (449.2 g/mol)

$\boldsymbol{DF}$ is the dilution factor of sample

$\mathbf{10^3}$ is the factor for conversion from g to mg

$\boldsymbol{\varepsilon}$ is the molar extinction coefficient (26,900 $L \times mol^{-1} \times cm^{-1}$)

$\mathbf{1}$ is the pathlength for cuvette in cm

3.2.2. Reversed-Phase Ultra-Performance Liquid Chromatography

A detailed analysis of the anthocyanins was carried out by the reversed-phase ultra-performance liquid chromatography (RP-UPLC). The technique does not only quantify the anthocyanins but also identify the type of anthocyanins present in the sample. The pH differential method and RP-UPLC are well established methods used in the quantification of anthocyanins. Lee et al. (2005) had shown that both techniques were reliable as they demonstrated high linear correlation (r >0.925, p ≤0.05) within samples provided that the anthocyanin standard used is the same.

The RP-UPLC involves mobile and stationary phases with contrasting polarity. The mobile phase is a liquid that is relatively polar like water, dilute buffer, methanol, or acetonitrile, while the stationary phase (i.e., LC column) is a relatively non-polar material that is usually made of silica particles that are coated with C_8 or C_{18} hydrocarbon (Nielsen & Talcott, 2017). The injected sample containing compounds with varying polarity will be partitioned between the non-polar stationary phase and the polar mobile phase; those that are more polar will be eluted earlier, while those that are less polar will be retained slightly longer in the column and be eluted later. In this case, anthocyanins with more hydroxy group (e.g., delphinidin has more than cyanidin) and less methoxy group (e.g., petunidin has less than malvidin) will have greater polarity and be eluted earlier. The presence of sugar side chain also increases the polarity of anthocyanin, making anthocyanin more polar than its anthocyanidin parent (Santos-Buelga et al., 2003).

After compound separation, detection is accomplished using the diode array detector that illuminates the compounds with light in the region of $\lambda_{190\ nm}$ to $\lambda_{1100\ nm}$, and in anthocyanin case the $\lambda_{530\ nm}$ was used. Identification is then achieved by comparing the retention time (t_R) (i.e., the volume of mobile phase) of the compound of interest against the t_R of a known standard that is also chromatographed under the same conditions. The quantity is then determined by comparing the peak area of the compound of interest against the peak area of a standard at the same t_R, which in this case is cya-glu.

3.2.3. Liquid Chromatography-Mass Spectrometry

The non-anthocyanins were identified and quantified using an electrospray ionisation mass spectrometer (ESI-MS) that was connected to an RP-UPLC. The ESI-MS is suitable for the analysis of heat-labile analytes like phenolic compounds as it uses a less harsh ionization process that keeps the observed analyte intact during analysis (Banerjee & Mazumdar, 2012). Figure 3.1 shows a schematic diagram on ESI-MS. When sample is injected, the RP-UPLC partitions the analytes according to their polarity. The eluent carrying the analytes is then sprayed into the ESI chamber to produce charged droplets (circled and enlarged in Figure 3.1). During this time, the solvent is continuously evaporated

from the charged droplets causing the droplets to decrease in size. At this point, two conflicting forces predominate: (i) surface tension that holds the shape of the charged droplets, and (ii) Coulombic repulsive force—generated by akin charges—that tries to break the shape of the charged droplets (Ranque, 2022). As the solvent evaporation continues, the droplet size diminishes until it reaches the point where the repulsive Coulombic force overwhelms the surface tension after which a "Coulombic explosion" occurs, disintegrating the parent droplets into much smaller charged droplets, but with a much higher mass-to-charge ratio (Banerjee & Mazumdar, 2012). Solvent evaporation and "Coulombic explosion" happen continuously until the charged analytes reach the heated capillary, where all solvent is removed from the analytes (Ho et al., 2003).

The analytes are then transferred to the gas phase of the MS for analysis and detection, generating signals graphically known as the mass spectrum that shows relative intensity of the signals and their mass-to-charge ratio. The MS data—in positive or negative ion mode—are compiled along with the information on analytes t_R and exact mass. The information is then processed using a screening and quantitation software. The concentration of non-anthocyanin phenolic compounds (flavonols, phenolic acids and flavanols) is then determined by comparison with the standard curves of authentic compounds.

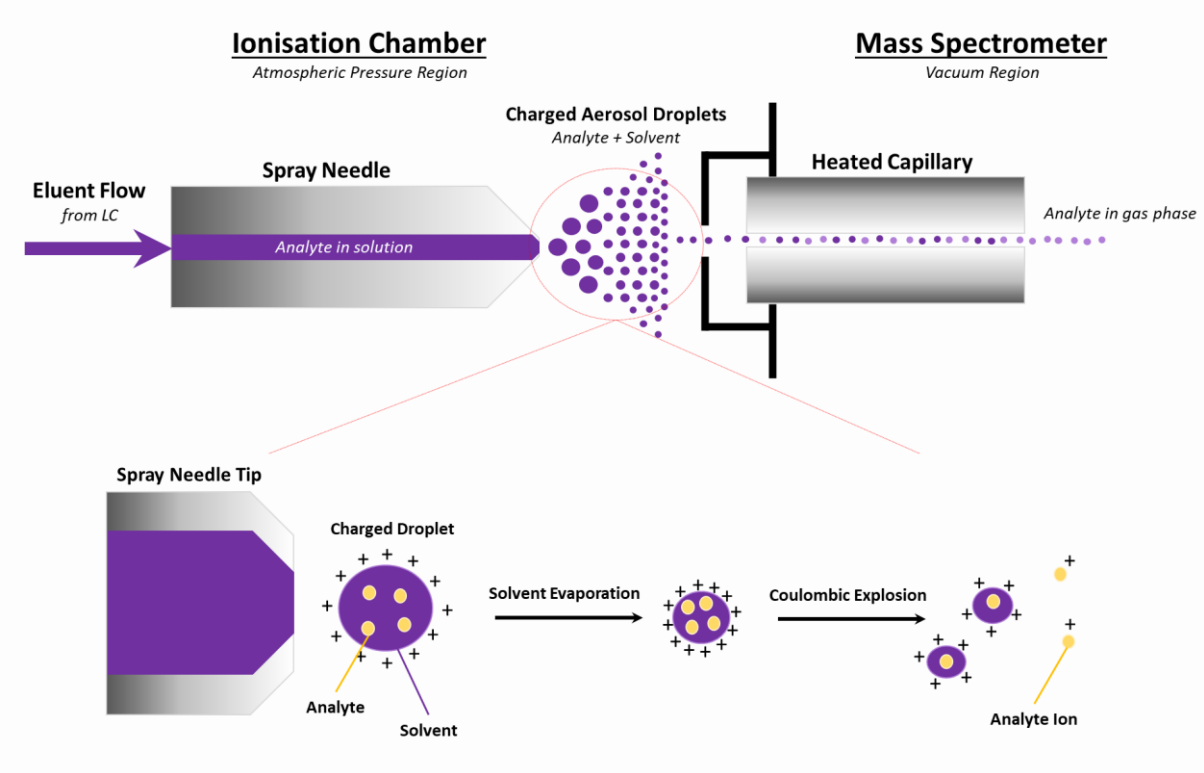

Figure 3.1 Schematic diagram of electrospray ionisation process in mass spectrometer. Adapted from Banerjee and Mazumdar (2012).

3.2.4. Polyphenol Profile of Blackcurrant Puree

An overview of BC polyphenols was obtained by analysing the phenolic compounds of BC puree (Table 3.2). The phenolic compounds were extracted from the puree by mixing it with ethanol/water/formic acid mixture (80:20:1, v/v/v) at a ratio of 1:10 (v/v) and left in the dark at 1 °C for 48 h. The mixture was then centrifuged (1620 x *g*, 10 min) and the supernatant was aliquoted and mixed with methanol/water/formic acid mixture (50:50:1, v/v/v) at a ratio of 1:4 (v/v) before sample injection.

Anthocyanins were analysed by the RP-UPLC Dionex UltiMate™ 3000 (Thermo Fisher Scientific Inc., Waltham, Massachusetts, U.S.A) that was connected to a rapid separation diode array detector. A Zorbax SB-C_{18} column (Agilent Technologies, Santa Clara, California, U.S.A) (2.1 mm x 150 mm, 1.8 µm) was used for compound separation and was set at 35 °C. The flow rate was 0.35 mL/min, and the injection volume was 5 µL. Isocratic elution was done using 5% v/v formic acid (solvent A) and acetonitrile (solvent B). The gradient was initially set to 95% A between time 0 and 0.5 min followed by 80% A between 0.5 and 10 min. At time 10–16.5 min, the gradient was changed to 5% A and finally ended with 95% A at time 20 min. Chromatograms were recorded at $\lambda_{530\ nm}$ and data were processed using Chromeleon™ Chromatography Data System version 7.2 (Thermo Fisher Scientific Inc., Waltham, Massachusetts, U.S.A). Four concentrations of the cya-glu standard (5, 10, 25, and 50 µg/mL) were prepared using the same methanol/water/formic acid solvent and its standard curve was constructed by plotting the peak area against the concentration of the compound. All results are expressed as cya-glu equivalents and reported as the mean and standard deviation of three readings.

Phenolic compounds that were not anthocyanins (flavonols, phenolic acids and flavanols) were analysed according to the method of Günther et al. (2020) using an ESI-MS micrOTOF-Q II (Bruker Daltonics, Billerica, Massachusetts, U.S.A) that was connected to the RP-UPLC. Polyphenol standards (1, 4, 10 and 20 µg/mL) containing eight phenolic compounds (kaempferol 3-*O*-rutinoside, quercetin, quercetin 3-*O*-rutinoside (que-rut), *p*-coumarylquinic acid, chlorogenic acid, catechin, epicatechin and procyanidin B2) were prepared using the same solvent mix (methanol/water/formic acid, 50:50:1, v/v/v) to generate standard curves. The injection volume of samples and standards was 1 µL. Solvent gradient was set to 95% A (0.2% v/v formic acid) and 5% B (acetonitrile) at time 0–0.5 min and then changed to 85% A up to time 4 min. Between time 4 and 8 min, the gradient was set to 60% A followed by 5% A from time 8 to 13 min. Towards the end of the analysis, the gradient was changed back to 95% A between time 13 and 15 min. The MS data in negative ion mode were compiled and processed using the Target Analysis for Screening and Quantitation software, also known as TASQ™ (Bruker Daltonics, Billerica, Massachusetts, U.S.A). Information on t_R and exact mass of the phenolic compounds of interest was used for identification. The concentrations were accomplished by

comparison with the generated standard curves of authentic compounds. Flavonols and phenolic acids that were not found in the standards were expressed as que-rut and chlorogenic acid equivalents, respectively. All results are reported as the mean and standard deviation of three readings.

As expected, anthocyanins were the dominant polyphenols of the BC puree, contributing 85.6% w/w to total phenolic compounds. However, the total concentration of anthocyanins (≈2453 mg/kg puree) was at the lower range of the reported New Zealand BC anthocyanin concentration—960 mg to 7204 mg/kg fresh fruit (Scalzo et al., 2008)—likely because the BC skin which is rich in anthocyanins has been removed from the puree during production, hence the lower anthocyanin content. Four major anthocyanins were identified in the puree and amongst them cyanidin 3-*O*-rutinoside (cya-rut) was the largest polyphenol contributor followed by delphinidin 3-*O*-rutinoside (del-rut). Overall, the results were in agreement with other publications that reported on BC anthocyanins (Aneta et al., 2013; Kapasakalidis et al., 2006; Nyanhanda et al., 2014; Scalzo et al., 2008; Slimestad & Solheim, 2002). The second major contributor of BC phenolic compounds was the flavonols (9.5% w/w), with myricetin 3-*O*-galactoside/myricetin 3-*O*-glucoside, quercetin 3-*O*-glucoside and que-rut as the main BC flavonols. The phenolic acids contributed 4.53% w/w to total phenolic compounds, with 3-caffeoylglucoside acid as the main phenolic acid. Flavanols were not the main phenolic compounds of BC, thus the detected flavanols (0.36% w/w) were very minute in comparison to other phenolic compounds of BC.

Table 3.2 Phenolic compounds in blackcurrant puree.

Phenolic Compound	Quantity
	mg/100g of total solids
Total Anthocyanin	**2004 (85.6%)**
cyanidin 3-*O*-glucoside	130 ± 3.38
cyanidin 3-*O*-rutinoside[a]	887 ± 6.72
delphinidin 3-*O*-glucoside[a]	249 ± 5.61
delphinidin 3-*O*-rutinoside[a]	738 ± 17.3
Total Flavonol	**222 (9.5%)**
kaempferol 3-*O*-rutinoside	6.22 ± 0.22
quercetin	18.5 ± 0.61
quercetin 3-*O*-rutinoside	43.5 ± 1.50
isorhamnetin 3-*O*-rutinoside[a]	2.31[b]
myricetin[a]	37.5[b]
myricetin 3-*O*-galactoside[a] myricetin 3-*O*-glucoside[a]	57.9 ± 2.60
myricetin 3-*O*-(6-malonyl)-glucoside[a]	2.24[b]
quercetin 3-*O*-(6-malonyl)-glucoside[a]	1.07[b]
quercetin 3-*O*-glucoside[a]	53.0 ± 1.05
Total Phenolic Acid	**106 (4.53%)**
p-coumaroylquinic acid	7.62[b]
chlorogenic acid	1.84 ± 0.72
caffeic acid[a]	2.11 ± 0.21
3-caffeoylglucoside acid[a]	68.6 ± 2.59
neochlorogenic acid[a]	19.4 ± 0.80
p-coumaric acid[a]	3.77 ± 0.32
sinapic acid[a]	2.83 ± 0.26
Total Flavanol/Procyanidin	**8.50 (0.36%)**
catechin	3.66 ± 0.30
epicatechin	3.32 ± 0.28
procyanidin B2	1.52 ± 0.22
Total Phenolic Compounds	**2341**

Results are expressed as milligram of phenolic compound per 100 g of total solids (mean ± standard deviation, n = 3).

[a] *Anthocyanins are expressed as cyanidin 3-O-glucoside equivalents, flavonols as quercetin 3-O-rutinoside equivalents and phenolic acids as chlorogenic acid equivalents.*

[b] *Detected in a sample only.*

3.3. Light Scattering Techniques

Light scattering is one of the major investigative techniques used in this work. It is a non-invasive and rapid technique that provides various physico-chemical information on the material of interest.

3.3.1. Size-Exclusion Chromatography-Multi-Angle Laser Light Scattering

Multi-angle laser light scattering (MALLS) is a form of static light scattering technique used to characterise macromolecules like polysaccharide and protein. It measures molecular weight and radius of gyration (root mean squared radius) of the polymers based on Rayleigh light scattering concepts, where the amount of light scattered from a given light source is proportional to the molecular weight and concentration of the polymer, and that the angular variation of the scattered light is linked to the size of the polymer (Wyatt, 1993). Essentially, larger polymers generate greater light scattering than smaller polymers. This technique is usually combined with a separation procedure known as the size-exclusion chromatography (SEC), hence the name SEC-MALLS. The SEC-MALLS system (Figure 3.2) is typically made of a high-performance liquid chromatography system that consists of SEC column(s), concentration detectors—UV and differential refractive index (RI)—a MALLS detector and a computer with data acquisition and analysis software.

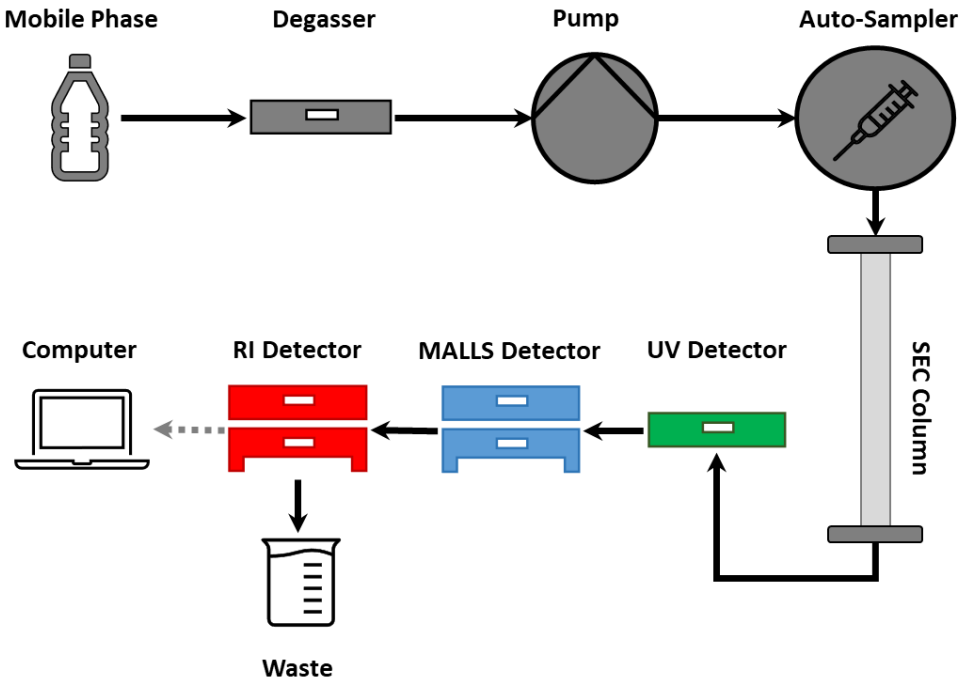

Figure 3.2 Schematic diagram of a size-exclusion chromatography-multi-angle laser light scattering (SEC-MALLS) setup. Adapted from Moraes and Archer (2015).

Prior to SEC-MALLS analysis, specific refractive index increment, also known as the *dn/dc* of the material of interest is measured. It is defined as the change in the refractive index of a solution at increasing solute concentration and is expressed as mL/g (Wyatt, 1993). The *dn/dc* value is important for the determination of molecular weight by light scattering as it can differ significantly from one polymer to another (e.g., polysaccharide vs protein) (Di Primo & Lebars, 2007).

During the analysis, analytes are carried by the mobile phase to the SEC column for compound separation via size (Figure 3.3). The SEC column is packed with porous gel beads that have uniform pore size (Barth et al., 1996). Particles that are larger than the pores are excluded from entering the gel beads and therefore, have less area to traverse and be eluted earlier. On the other hand, small particles that can enter the gel beads will traverse more distance and be eluted much later. If required, several SEC columns with different pore size can be attached consecutively to generate better separations.

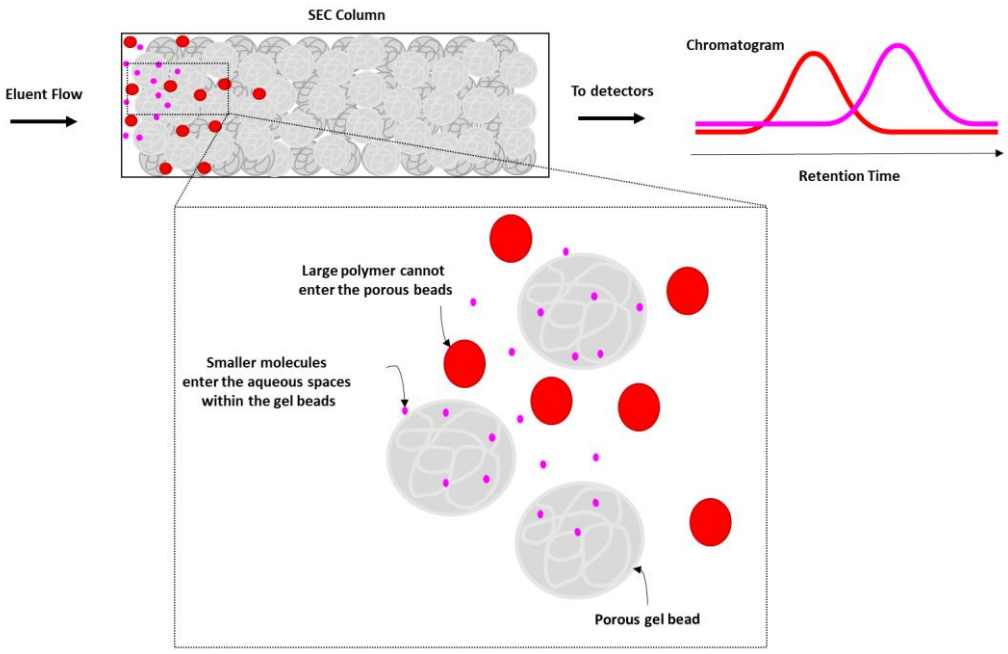

Figure 3.3 Schematic diagram on size-exclusion chromatography separation of two macromolecular sizes. Adapted from Malawer and Senak (2003).

Detection of analytes is then achieved sequentially by the UV, MALLS, and RI detectors. Data from the SEC-MALLS system is then used to calculate the average molecular weight, radius of gyration, as well as the concentration of eluting analytes in thin slices of the SEC chromatogram (Wang & Lucey, 2003). Information obtained from the UV detector is typically used to quantify UV absorbing materials at $\lambda_{280\ nm}$ like proteins, while the RI detector generates concentration information on non-UV absorbing materials like polysaccharides.

3.3.2. Dynamic Light Scattering

Dynamic light scattering (DLS) is a technique that measures the Brownian motion of particles in a dispersion system (Bhattacharjee, 2016). This random movement of particles, which results from particle collision with solvent molecules is quantified as the translational diffusion coefficient (Satoh et al., 1999). The information is used to determine the hydrodynamic size of the particle, which is described as the size of a sphere that diffuses at the same rate as the particle being measured (Lim et al., 2013). This hypothetical sphere encompasses the actual particle and components that are bound on its surface, like ions and adsorbed polymers.

A DLS system is made of three main components: the laser, the sample, and the light detector. When a laser beam is illuminated on the particles, some of the lights that hit the particles are scattered. In a dispersion system where the particles are moving constantly and randomly due to the Brownian motion, the intensity of the scattered light will fluctuate, changing overtime as the particles continue to diffuse (Lim et al., 2013). The speed of the intensity fluctuations varies with the diffusion rate of the particles, hence smaller particles diffuse more quickly and produce more rapid intensity fluctuations (Lim et al., 2013). The detector then captures the light scattering signals rapidly one after another and compares it against the original signal. Between successive signals, which are separated by ns or µs, the intensity signals will appear very similar or well correlated. However, further in time the correlation begins to decrease to the point that the signal changes entirely that there is no correlation with the original signal (Lim et al., 2013). Particles that are larger diffuse slower and lose the correlation signal at a slower rate, but smaller particles undergo faster diffusion that the correlation signal declines rapidly. This process known as the auto-correlation allows the computer to extract the translation diffusion coefficients. The hydrodynamic size can then be calculated using this information and the Stokes-Einstein equation shown below (Equation 3.2), provided the solvent viscosity and temperature are known as they influence the diffusion rate of particles (Bhattacharjee, 2016).

$$\boldsymbol{D_t} = \frac{\boldsymbol{k_B\, T}}{\boldsymbol{6\pi\eta R_H}} \quad \text{(Equation 3.2)}$$

$\boldsymbol{D_t}$ is the translational diffusion coefficient from Brownian motion

$\boldsymbol{k_B}$ is the Boltzmann constant ($1.38064852 \times 10^{-23}$ J/K)

$\boldsymbol{T}$ is the temperature

$\boldsymbol{\eta}$ is the viscosity of the solvent

$\boldsymbol{R_H}$ is the hydrodynamic radius

The main result provided by the DLS equipment is the intensity of scattered light for each size populations, and they can be converted into volume or number size distribution. Data from the light

scattering intensity can be used to determine the mean hydrodynamic size—termed as the Z-average size—and the polydispersity index of the particles. This technique is suitable for the measurement of particles that are in the range of 0.3 nm up to 10 µm (Malvern Panalytical Ltd., 2022).

3.3.3. Electrophoretic Light Scattering

Electrophoretic light scattering uses an electrical field to measure the mobility of particles in dispersion or molecules in solution. Essentially, the technique follows the concept of electrophoresis. When an electrical field is introduced to a dispersion system, particles that have a net surface charge, also known as the net zeta-potential, will be attracted to the oppositely charged electrode. This attraction causes mobility that is related to the zeta-potential of the particles. Factors like pH and ionic strength can affect zeta-potential measurements as they influence the surface charge of the particles. Changes in pH can increase or decrease the positive and negative charges of the particle of interest. Zeta-potential also varies with ionic strength, where it decreases at increasing ionic strength and vice versa. Hence, the valency of ions plays an important role in zeta-potential measurements as higher valency ions (divalent Ca^{2+} and trivalent Al^{3+}) can reduce zeta-potential drastically than the monovalent ions (Na^{+}, H^{+} and OH^{-}).

It has been established that anthocyanins carry a positive charge when they are in flavylium form at pH <4.5. Yet, no work has attempted to measure anthocyanin zeta-potential, hence one of the preliminary tasks was to determine the zeta-potential of BC anthocyanins. Two of the major BC anthocyanins were chosen for the zeta-potential measurement: cya-rut and del-rut. An anthocyanin stock solution (1.73×10^{-1} % w/v) containing 52% cya-rut and 48% del-rut was prepared by dissolving the pigments in pre-chilled pH 3.5 sodium citrate (1 mM) or pH 4.5 sodium acetate (1 mM) buffers, followed by a series of dilutions ($3.5 \times 10^{-2} – 9 \times 10^{-4}$ % w/v) using the buffer solutions. The anthocyanin solutions were prepared fresh in a dark room and kept in opaque bottles to minimise light degradation of the anthocyanins.

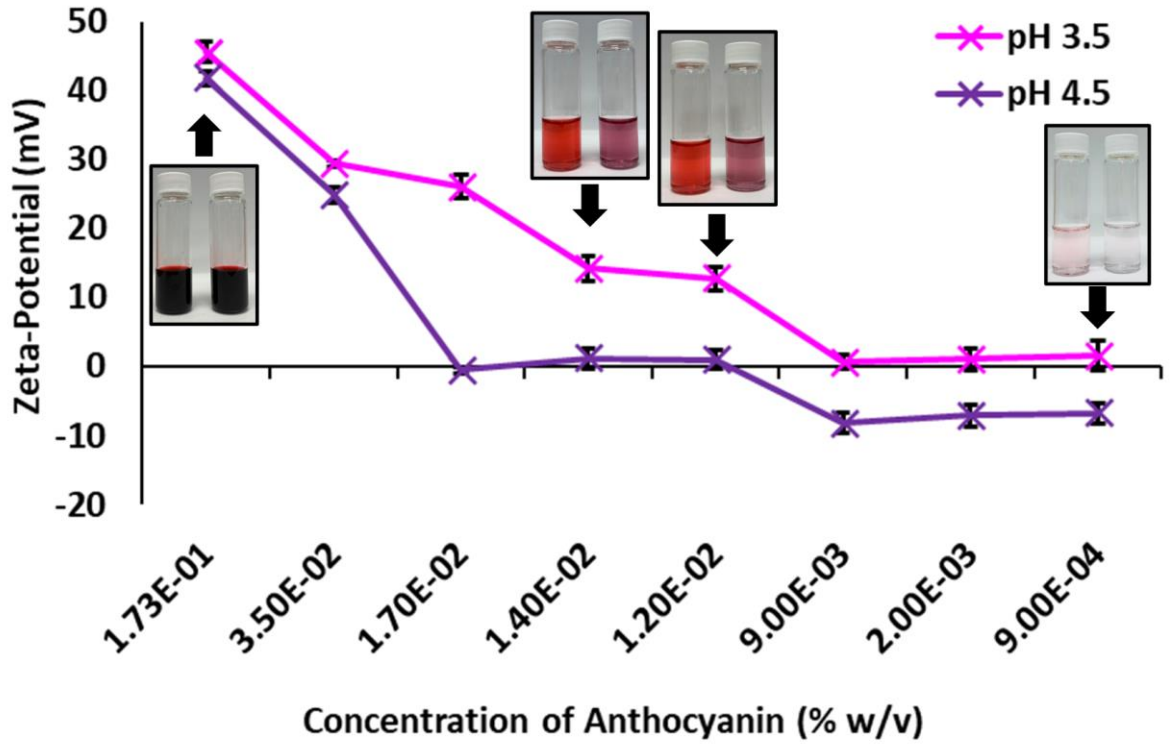

Figure 3.4 Zeta-potential (mV, mean ± standard deviation, n = 2) of anthocyanin solutions (cyanidin 3-*O*-rutinoside and delphinidin 3-*O*-rutinoside) at pH 3.5 and pH 4.5 and at various concentrations (% w/v).

Figure 3.4 shows the zeta-potential value of the anthocyanin solutions at pH 3.5 and 4.5. Irrespective of the pH level, concentrations that were > 1.7×10^{-2} % w/v show positive zeta potential value that ranged between +25 mV and +46 mV. However, the readings were unreliable as the gold-plated electrodes used for these samples (> 1.7×10^{-2} % w/v) had rapidly oxidised and blackened during the measurement. Such effect was probably caused by the high ionic strength of the solutions as the anthocyanin powders were procured as chloride salt.

The optimal concentration was found to be between 1.2×10^{-2} % and 1.4×10^{-2} % w/v. Within this range, the zeta-potential values were moderately positive at pH 3.5—≈+12.7 mV and ≈+14.3 mV at 1.2×10^{-2} % w/v and 1.4×10^{-2} % w/v, respectively—and almost neutral at pH 4.5—≈+0.95 mV and ≈+1.21 mV at 1.2×10^{-2} % w/v and 1.4×10^{-2} % w/v, respectively. This confirmed that anthocyanins were moderately positively charged at pH 3.5, validating the positive charge found on the pyrylium ring of the flavylium ion. As the pH increased to 4.5, majority of the flavylium cations transformed to the neutral quinoidal base and carbinol pseudobase, generating a neutral net zeta-potential. Diluting the anthocyanin solutions further (< 1.2×10^{-2} % w/v) reduced the zeta-potential values at both pH levels. Zeta-potential values at pH 3.5 became less positively charged, while the ones at pH 4.5 became less neutral that they crossed over to the negative region. The negative charges at pH 4.5 were

probably the result of chloride ions of the anthocyanin salts as the pH 4.5 buffer was confirmed to be neutrally charged (≈-0.32 mV).

3.3.4. Laser Diffraction

Laser diffraction is another light scattering technique used to measure particle size and particle size distribution. In comparison to dynamic light scattering, this technique can measure larger particles that are in the submicron to the millimetre size range (0.02 µm–1000 µm). It utilises the Mie theory of light, relating the scattering pattern of light to the size of particles, where large particles scatter light at small angles relative to the laser beam, while the smaller particles scatter light at wider angles (Levoguer, 2013). Data on angular scattering intensity is then used to determine the size of the particles responsible for generating the scattering pattern.

A laser diffraction system consists of three main components: the optical bench, the sample dispersion unit, and the computer (Malvern Panalytical Ltd., 2007). When sample is placed in the dispersion unit, the dispersant will deliver the particles to the optical bench. The computer will then display the percentage of laser beam obscurity to indicate the optimal level of sample addition, which is usually between 10-20% obscuration (Malvern Panalytical Ltd., 2007). During measurement, the optical bench, which contains an array of detectors, collects light scattering pattern of the particles from a range of angles at a particular time. In order to obtain a representative scattering pattern, multiple recordings were made by the equipment at each measurement. Once the measurement is complete, the raw data is analysed by the software and particle size is reported as the volume weighted mean or D [4,3], although size information can be displayed in various ways.

3.3.5. Static-Multiple Light Scattering

The physical stability of a dispersion system is evaluated by static-multiple light scattering technique using a Turbiscan Lab (Formulaction, Toulouse, France) that operates using a near-infrared LED (λ_{air}=880 nm) as its light source. When the light source projects photons to the sample, the Turbiscan measures two components: i) the light transmitted through the sample and ii) the light backscattered by the particles present in the sample (Formulaction, 2018). These two information is then used to assess particle migration and physical stability of the sample over a predetermined period. Usually, the Turbiscan Stability Index (TSI), which is calculated by the built-in software known as the TurbiSoft-Lab (Formulaction, Toulouse, France) is used as an indicator of sample stability. The TSI value represents the degree of destabilisation of a sample, essentially its resistance to physical changes like sedimentation and agglomeration (Formulaction, 2018). The TSI value can be compared against the TSI scale (Figure 3.5) that ranges from 0 (No significant destabilisation, not visible) to ≥10 (High

destabilisation, visible) (Formulaction, 2018). Apart from TSI value, the light transmission data provided by the Turbiscan can also be used as a turbidity indicator, the higher the transmission percentage, the lower the turbidity.

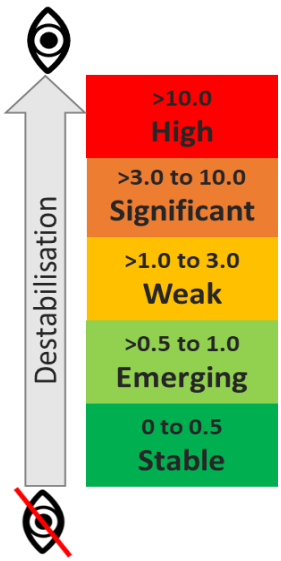

Figure 3.5 Turbiscan Stability Index scale and its stability categories. Adapted from Formulaction (2018).

3.4. Fourier-Transform Infrared Spectroscopy

The Fourier-Transform Infrared (FTIR) spectroscopy is a technique used to identify functional groups of a material and highlight any characteristic changes that have occurred. It is used for monitoring processes, identifying unknown compounds, and determining the presence of components in a mixture. The spectroscopic method is based on the concept of molecular vibrational energy, where each functional group of a sample selectively absorbs the mid-infrared radiation (wavenumber 400 cm^{-1} to 4000 cm^{-1}) at specific wavelengths and changes its vibrational energy in the bond (Moore, 2016). Each vibration—stretching or bending—has a unique frequency that corresponds to the strength of the chemical bond between the atoms of the functional group and the mass of each atom (Moore, 2016). The different molecules, functional groups and structures of a given sample generate a spectrum that is unique, akin to the uniqueness of human fingerprints or DNA. In this thesis, the spectroscopic method was used to determine the functional groups of BC pectin and whey protein, and for comparison purposes, a commercial citrus pectin was also evaluated. Table 3.3 shows the consolidated band assignments for BC pectin, citrus pectin, and whey protein infrared spectra, which is relevant to the discussion of the experimental findings of the later chapters.

Table 3.3 Band assignments for blackcurrant pectin, citrus pectin, and whey protein infrared spectra.

Compound	Position (cm^{-1})	Assignment	Source
Blackcurrant Pectin (BCP)	2400-3600 (Peak: 3327)	(i) O-H stretch from carboxylic groups of pectin	(Pretsch et al., 2009; Zaleska et al., 2000)
		(ii) O-H stretch from phenolic groups of bound anthocyanins	(Pretsch et al., 2009)
		(iii) C-H stretch of alkyl groups from pectin	(Pretsch et al., 2009; Zaleska et al., 2000)
		(iv) C-H stretch from aromatic groups of bound anthocyanins	(Pretsch et al., 2009)
	1731	C=O stretch from esterified carboxyl groups of pectin	(Mierczynska et al., 2017; Zaleska et al., 2000)
	1550-1700 (Peak: 1602)	(i) C=O stretch of non-esterified carboxyl groups of pectin	(Mierczynska et al., 2017; Zaleska et al., 2000)
		(ii) C=C stretch from alkenes in bound anthocyanins	(Pretsch et al., 2009; Wahyuningsih et al., 2017)
		(iii) C-C aromatic groups of bound anthocyanins	
	800-1200 (Peak: 1015)	(i) C-O stretch from various functional groups of BCP powder (i.e., pectic and proteic components)	(Mierczynska et al., 2017; Posé et al., 2015; Pretsch et al., 2009)
		(ii) C-C backbones (stretches, bends, and torsions) of bound anthocyanins	(Pretsch et al., 2009; Wahyuningsih et al., 2017)
		(iii) C-O stretch of bound anthocyanins	
		(iv) C-H bend of bound anthocyanins	
Citrus Pectin (CP)	2400-3600 (Peak: 3240)	(i) O-H stretch from carboxylic groups of pectin	(Pretsch et al., 2009; Zaleska et al., 2000)
		(ii) C-H stretch of alkyl groups from pectin	
	1731	C=O stretch from esterified carboxyl groups of pectin	(Mierczynska et al., 2017; Zaleska et al., 2000)
	1601	C=O stretch of non-esterified carboxyl groups of pectin	(Mierczynska et al., 2017; Zaleska et al., 2000)
	800-1200 (Peak: 1012)	C-O stretch from various functional groups of CP powder (i.e., pectic and proteic components)	(Mierczynska et al., 2017; Posé et al., 2015; Pretsch et al., 2009)
Whey Protein	3000-3600 (Peak: 3275)	O-H groups from carboxylic groups	(Zaleska et al., 2000; Zhao et al., 2020)
		N-H groups from amides and amines	(Zaleska et al., 2000; Zhao et al., 2020)
	1627	C=O stretching from amides	(Pretsch et al., 2009; Raei et al., 2018; Zaleska et al., 2000)
	1518	N-H bend from amines	(Pretsch et al., 2009; Raei et al., 2018; Zaleska et al., 2000)

MASSEY UNIVERSITY
TE KUNENGA KI PŪREHUROA
UNIVERSITY OF NEW ZEALAND

GRADUATE RESEARCH SCHOOL

STATEMENT OF CONTRIBUTION DOCTORATE WITH PUBLICATIONS/MANUSCRIPTS

We, the student and the student's main supervisor, certify that all co-authors have consented to their work being included in the thesis and they have accepted the student's contribution as indicated below in the Statement of Originality.

Student name:	Nurhazwani Salleh
Name and title of main supervisor:	Associate Professor Lara Matia-Merino
In which chapter is the manuscript/published work?	Chapter 4
What percentage of the manuscript/published work was contributed by the student?	75%

Describe the contribution that the student has made to the manuscript/published work:

Three of the experimental techniques--(i) constituent sugar composition, (ii) NMR spectroscopy and (iii) degree of esterification--were carried out with the help of researchers from Ferrier Research Institute (FRI) and Plant and Food Research (PFR), while two other techniques--HPLC and LCMS for polyphenol profile--were carried out fully by the student with the guidance from PFR researchers. Proximate analysis of fat, protein, ash and calcium were performed by the accredited Nutrition Lab at Massey University. The remaining experimental work was conducted by the student at SF&AT. The writing was done by the student with some input from the supervisors on the draft version, except the section on constituent sugar composition and NMR spectroscopy, with input from FRI researchers.

Please select one of the following three options:

- (●) **The manuscript/published work is published or in press**

  Please provide the full reference of the research output:

  Salleh, N., Goh, K. K. T., Sims, I. M., Bell, T. J., Huffman, L. M., Weeks, M., & Matia-Merino, L. (2021). Characterization of anthocyanin-bound pectin-rich fraction extracted from New Zealand blackcurrant (Ribes nigrum) juice. ACS Food Sci. Technol., 1(6), 1130-1142. https://doi.org/10.1021/acsfoodscitech.0c00128

- ( ) **The manuscript is currently under review for publication**

  Please provide the name of the journal:

- ( ) **It is intended that the manuscript will be published, but it has not yet been submitted to a journal**

Student's signature:	Nurhazwani Salleh Digitally signed by Nurhazwani Salleh Date: 2023.03.01 10:34:57 +13'00'	Main supervisor's signature:	Lara Matia-Merino Digitally signed by Lara Matia-Merino DN: cn=Lara Matia-Merino, c=NZ, ou=School of Food and Advanced Technology, email=l.matia-merino@massey.ac.nz Date: 2023.02.28 17:28:03 +13'00'

This form should be placed at the beginning of each relevant thesis chapter.

Chapter 4 Identification of Blackcurrant Juice Interactive Components

4.1. Introduction

Numerous studies have determined the phenolic profiles of blackcurrants from various countries and drawn comparisons with other types of berries (Aneta et al., 2013; Anttonen & Karjalainen, 2006; Chen et al., 2014; Slimestad & Solheim, 2002). Various research studies have also reported the health benefits of blackcurrant fruit (Aneta et al., 2013; Nyanhanda et al., 2014; Parkar et al., 2014; Schrage et al., 2010). In contrast to its polyphenols, other components of blackcurrant such as its cell wall materials have not been studied in detail. Although some studies have reported on the chemical, molecular and rheological properties of blackcurrant cell wall components (Alba et al., 2018; Hilz et al., 2005; Hilz, de Jong, et al., 2006; Hilz, Williams, et al., 2006; Mierczynska et al., 2017), there are still research gaps to be investigated such as the association of anthocyanins (ACN) to blackcurrant pectin.

Various researchers have suggested that polyphenols can interact with polysaccharides and proteins by a mixture of interactive forces such as hydrogen bonds (Buchweitz et al., 2013; Fernandes et al., 2014; Hagerman, 2012; Mazzaracchio et al., 2004; Spencer et al., 1988), electrostatic (Buchweitz et al., 2013; Lin et al., 2016; Phan et al., 2017), and hydrophobic interactions (Fernandes et al., 2014; Hagerman, 2012; Lin et al., 2016; Mazzaracchio et al., 2004; Spencer et al., 1988). Based on the authors' knowledge, no study has characterised and discussed the pigmented pectic material in blackcurrant juice. The cell wall components in blackcurrant including those found in blackcurrant juice (Hilz et al., 2005; Hilz, de Jong, et al., 2006; Hilz, Williams, et al., 2006) have been investigated; however, the presence of polyphenols particularly the ACNs that are bound to the cell wall components has not been the focus of those studies. As one of the cell wall materials found in plants, protein has been detected in various sources of commercially available pectin, such as citrus pectin (≈1.7%) (Verkempinck et al., 2018) and sugar beet pectin (≈5%) (Chen et al., 2016). In fact, the pectic material isolated from the blackcurrant fruit also contained protein (Hilz et al., 2005); however, knowledge about the type of protein and whether it is bound to the pectin is unknown. Sugar linkage analysis has shown that the pectic material isolated from ultrafiltered blackcurrant juice contained 1,3,6-linked galactose, which may indicate the presence of arabinogalactan protein (Hilz et al., 2005).

In a practical scenario, incorporating the blackcurrant juice into a beverage system can be challenging, especially if it is to be added into a clean-label, ready-to-drink, high-protein beverage. This is because the interactions between polysaccharides and proteins are known to affect the structure and stability of foods. The natural acidity of the blackcurrant juice and the presence of its interacting cell wall components that are laden with polyphenols can easily cause the beverage to coagulate, precipitate or separate, affecting its appearance and texture. Hence, it is essential to build up further knowledge on blackcurrant juice cell wall components, which can then allow food product developers to manage any undesirable interactions with proteins, especially in regard to liquid food formulations. We hypothesise that pectin and polyphenols are the key interactive components of the blackcurrant juice and that they are associated and not easily separated. The current work involved: (i) isolation of blackcurrant juice interactive components via solvent extraction; (ii) determination of proximate compositions, phenolic profile, and molecular, structural, and physico-chemical properties of the pectin fractions, given the lack of detailed information in this area.

4.2. Materials and Methods

4.2.1. Materials

As mentioned in Chapter 3, the blackcurrant juice was obtained by centrifuging the blackcurrant puree at 4618 x *g* for 15 min at 20 °C. The supernatant was collected and centrifuged once again using the same settings and all pellets were discarded.

Nine polyphenol standards were used in this study: cyanidin 3-*O*-glucoside (cya-glu), kaempferol 3-*O*-rutinoside (kae-rut), quercetin 3-*O*-rutinoside (que-rut), procyanidin B2 (Extrasynthese, Lyon, France), quercetin (Calbiochem Corp., Los Angeles, California, U.S.A), chlorogenic acid, catechin, epicatechin (Sigma-Aldrich, St. Louis, Missouri, U.S.A), and *p*-coumaroylquinic acid which was extracted in-house by Dr Tony McGhie from Plant & Food Research in Palmerston North, New Zealand. The determination of constituent sugars in pectin involved nine sugar standards: L-fucose, L-rhamnose, L-arabinose, D-xylose, D-galactose, D-glucose, D-mannose, D-galacturonic acid (GalUA) and D-glucuronic acid (Sigma-Aldrich, St. Louis, Missouri, U.S.A). Analytical grade D-glucose (BDH Limited, Dorset, United Kingdom) and D-(+)-GalUA monohydrate (Sigma-Aldrich, St. Louis, Missouri, U.S.A) were used as standards in the proximate analysis. Gibco™ bovine serum albumin (BSA) (Invitrogen Corporation, Carlsbad, California, U.S.A) was used as a reference and calibration protein in the molecular weight analysis. For comparative purposes, a citrus pectin with ≥85% degree of esterification (DE) (Sigma-Aldrich, St. Louis, Missouri, U.S.A) was used in this study. Colorimetric reagents that were used in this study were phenol (BDH Limited, Dorset, United Kingdom) and 3-phenylphenol (Sigma-Aldrich, St. Louis, Missouri, U.S.A). All other chemicals were of analytical grade and purchased from local companies. Chemical solutions, samples, and dilutions were prepared using distilled Milli-Q® water (Merck Group, Darmstadt, Germany).

4.2.2. Isolation of Pectin-Rich Fractions from Blackcurrant Juice

Pectin in blackcurrant juice was isolated based on the method of Yuliarti, Goh, et al. (2015) with some modifications (Figure 4.1). The juice was mixed with water at a ratio of 2:1 w/v followed by 99.5% ethanol to achieve a final concentration of 80% v/v ethanol. After overnight precipitation (4 °C), the mixture was centrifuged (3300 x *g* for 10 min at 4 °C) to recover the alcohol insoluble residue (AIR). Removal of free and lightly bound ACNs was done by washing the AIR with 99.5% v/v ethanol for four cycles. At each cycle, the mixture was stirred for 30 min (4 °C) before it was centrifuged as above. The final ethanol wash was carried out by stirring the mixture overnight at 4 °C. The AIR was then vacuum-dried (58 ± 3 °C, 65 cm Hg) for approximately 18 h. The dried AIR, which was also the crude fraction, was then dispersed in distilled water (1% w/w at 4 °C) and centrifuged to remove large aggregates

(30,000 x *g* for 1 h at 4 °C). The supernatant containing solubilised pectin was collected and freeze-dried. The freeze-dried fraction was redispersed in distilled water (5% w/w at 4 °C), ethanol precipitated, and ethanol washed for four more cycles before it was vacuum-dried. At this stage, the used ethanol was colourless, indicating that all free and lightly bound ACNs had been removed. This fraction was denoted as the undialysed pectin-rich fraction. The dialysed version of pectin-rich fraction was prepared by dialysing the above redispersed fraction (5% w/w) for 24 h at 4 °C using an 8 kDa molecular weight cut-off dialysis tubing (BioDesign Inc., Carmel, New York, U.S.A). The dialysate was changed at the first, second, fourth and sixth hour with fresh distilled water. The dialysed pectin solution was recovered via ethanol precipitation, ethanol washed and then vacuum dried just like its undialysed counterpart.

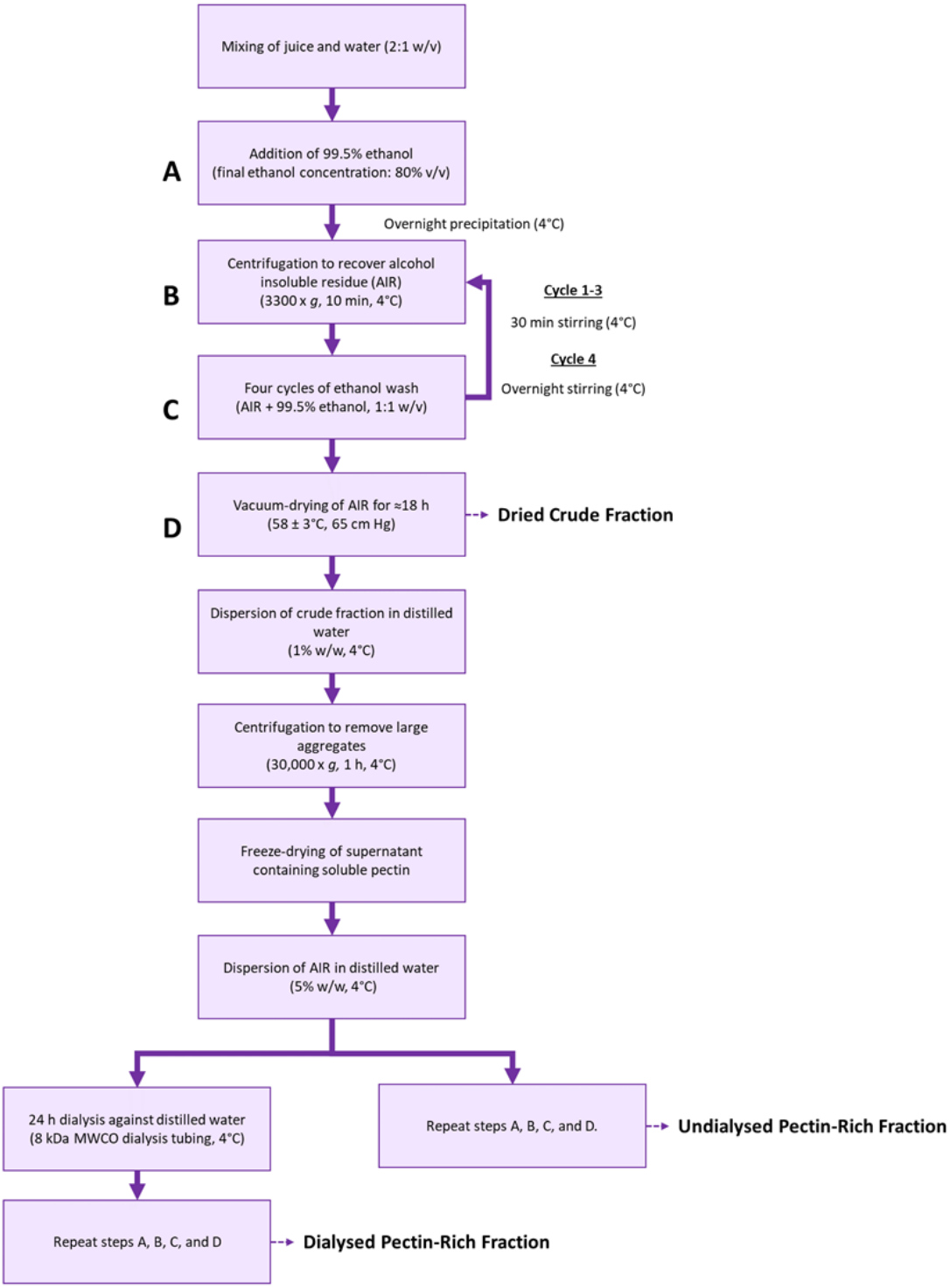

Figure 4.1 Isolation steps of blackcurrant juice pectin-rich fractions.

4.2.3. Proximate Analysis of Blackcurrant Pectin-Rich Fractions

The analysis of fat (AOAC 922.06), crude protein (AOAC 968.06), ash (AOAC 942.05) and calcium were determined at the accredited Nutrition Laboratory in the School of Food and Advanced Technology at Massey University, Palmerston North (AOAC, 2023). The amount of calcium was measured using the Inductively Coupled Plasma-Optical Emission Spectrometry technique and moisture analysis was done according to AOAC 925.10 (AOAC, 2023). All analyses were replicated three times and results are reported as the mean and standard deviation of three readings.

4.2.3.1. Total Carbohydrate in Blackcurrant Pectin-Rich Fractions

The amount of total carbohydrates was estimated by the phenol-sulphuric acid test (Nielsen, 2017b), which was modified to fit a 96-well microplate. Both pectin-rich fractions were dispersed in distilled water (1% w/v) and diluted to 0.01% w/v. The test was carried out according to the method described in Chapter 3. Results are reported as the mean and standard deviation of two readings and expressed as glucose equivalents.

4.2.3.2. Pectin in Blackcurrant Pectin-Rich Fractions

Uronic acid was determined by colorimetric method (Blumenkrantz & Asboe-Hansen, 1973) that was modified to fit a 96-well microplate (O'Donoghue et al., 2017). The dried pectin-rich fractions were dispersed in distilled water (1% w/v) and then diluted to 0.05% w/v. The test was carried out according to the method described in Chapter 3. The amount of uronic acid is reported as GalUA equivalents and the mean and standard deviation of three readings.

4.2.3.3. Anthocyanins in Blackcurrant Pectin-Rich Fractions

Monomeric ACNs were expressed as cya-glu equivalents and determined according to AOAC 2005.02 that was modified to fit a 96-well microplate (AOAC, 2023). The dried pectin-rich fraction was dispersed in distilled water (1% w/w) and diluted to 0.1% w/w with pH 1 potassium chloride (0.025 M) and pH 4.5 sodium acetate (NaOAc) (0.4 M) buffers. The absorbance of the diluted samples at pH 1 and pH 4.5 was read at $\lambda_{530\ nm}$ and $\lambda_{700\ nm}$, and distilled water was used as a blank. The assay was replicated three times and results are reported as the mean and standard deviation of three readings.

4.2.4. Polyphenol Profile of Blackcurrant Juice and Pectin-Rich Fractions

The ACNs were identified and quantified using a liquid chromatography system, while the non-ACNs were analysed using a mass spectrometer that was coupled to a liquid chromatography system. Detailed information and steps can be obtained in Chapter 3. Prior to sample injection, blackcurrant

juice was diluted to 30-fold using a methanol/water/formic acid mixture (50:50:1, v/v/v). The undialysed and dialysed blackcurrant pectin powders were first dispersed into a 1% w/v solution using distilled water and hydrated overnight (4 °C). The solutions were then diluted to 0.5% w/v with the acidified aqueous methanol. The ACNs are expressed as cya-glu equivalents, while the flavonols and phenolic acids that were not found in the polyphenol standard mix were expressed as que-rut and chlorogenic acid equivalents, respectively. All results are reported as the mean and standard deviation of three readings.

4.2.5. Molecular Characterisation of Blackcurrant Pectin-Rich Fractions

The molecular characteristics of the blackcurrant pectin were determined by size-exclusion chromatography that was coupled to multi-angle laser light scattering detector (SEC-MALLS). The analysis followed the method of Yuliarti, Goh, et al. (2015) with some modifications. The equipment LC-20AD (Shimadzu Corporation, Kyoto, Japan) was fitted with three detectors in this sequence: ultraviolet/visible light (UV/Vis) detector (SPD-20AV), a DAWN 8+ multi-angle laser light scattering detector (Wyatt Technology Corporation, Santa Barbara, California, U.S.A) and a differential refractive index (RI) detector (RID-20A). The MALLS detector uses a 50 mW GaAs linearly polarized laser (658 nm) as the light source and measures the intensity of scattered light at 8 detection angles, spanning between 23° and 155°. To study the pectin in its native state, an aqueous salt solution (0.1 M sodium chloride (NaCl) and 0.02% w/v sodium azide) was chosen as the mobile phase. The mobile phase was vacuum-filtered through 0.22 µm polyvinylidene difluoride (PVDF) and 0.025 µm mixed cellulose ester membranes and then degassed for 2 h. Samples were prepared by dissolving 0.7% w/v of blackcurrant pectin-rich fraction or 0.35% w/v of citrus pectin in the mobile phase overnight at 4 °C before filtering into a 2 mL vial using a 0.45 µm PVDF syringe filter. Sample filtration helps with aggregate removal, but it can also remove some of the material of interest, depending on the viscosity of the sample and other parameters. Nevertheless, the filtered sample will still be representative of the overall system (Corredig et al., 2000). Aliquots (100 µL) of the samples were loaded into the column and separation of the molecular fractions was achieved by combining a guard column and three polymer-based aqueous columns: Shodex SB-805 (8.0 mm x 300 mm, 13 µm), SB-803 (8.0 mm x 300 mm, 6 µm) and SB-802.5 (8.0 mm x 300 mm, 6 µm) (Showa Denko, Tokyo, Japan) connected in series. The column oven was set to 35 °C and mobile phase flow rate was set to 0.5 mL/min. The UV/Vis detector was set to $\lambda_{280\ nm}$ and 20 µL of 2% w/v BSA in mobile phase was injected into the machine. Data on standard BSA were used for alignment, band broadening and normalisation using the software Astra 6.1 (Wyatt Technology Corporation, Santa Barbara, California, U.S.A). The specific refractive index increment (*dn/dc*) of BSA in water was obtained from the literature (0.185 mL/g) (Huglin, 1965).

The determination of *dn/dc* involved the preparation of five NaCl solutions (0.025, 0.05, 0.10, 0.25 and 0.50% w/v). The salt solutions were injected into the RI detector (35 °C) to obtain the plot of RI voltage (V) versus NaCl concentration (g/mL). The gradient of this plot, which represents the RI response factor (*dV/dc*), was then divided by the known *dn/dc* of NaCl (1.74 mL/g) to obtain *dV/dn*. After that, five concentrations (0.025, 0.05, 0.10, 0.25 and 0.50% w/v) of blackcurrant pectin solutions in mobile phase were prepared and the RI signals were measured as above. The *dn/dc* of the blackcurrant pectin-rich fraction (0.132 ± 0.004 mL/g) was determined by dividing the gradient of the pectin sample (*dV/dc*) with the *dV/dn* factor obtained previously from the calibration slope of NaCl. Data collection and *dn/dc* calculation were performed by the built-in software (Astra 6.1) and the *dn/dc* value was used to determine all blackcurrant pectin molecular parameters. As for citrus pectin, the *dn/dc* value of 0.146 mL/g was used for its molecular weight analysis (Fishman et al., 2001). All samples were prepared in two replicates and all molecular characteristics (molecular weight (M_w), polydispersity index (PDI) and root mean squared (RMS) radius) were determined based on the Zimm model derived from the Astra 6.1 software.

4.2.6. Constituent Sugar Composition of Dialysed Blackcurrant Pectin-Rich Fraction

The constituent sugar composition of the dialysed pectin-rich fraction was determined by high-performance anion-exchange chromatography with pulsed amperometric detection (HPAEC-PAD) (Dionex ICS 5000, Thermo Fisher Scientific Inc., Waltham, Massachusetts, U.S.A) after hydrolysis of the polysaccharides to their component monosaccharides based the methodology of Nep et al. (2016). Briefly, samples (in duplicate) were hydrolysed in with methanolic hydrochloric acid (HCl) (3 M, 500 µL, 80 °C, 18 h), followed by aqueous trifluoroacetic acid (2.5 M, 500 µL, 120 °C, 1 h). The resulting hydrolysates were dried, redissolved in distilled water (1 mL), and diluted to 50 µg/mL. Aliquots (20 µL) of the hydrolysates were analysed on a CarboPac PA-1 (4 x 250 mm) column (Thermo Fisher Scientific Inc., Waltham, Massachusetts, U.S.A) equilibrated in 20 mM sodium hydroxide (NaOH) and eluted with a simultaneous gradient of NaOH (20 mM from 0 to 25 min, 20–100 mM from 25 to 30 min, 100–200 mM from 30 to 50 min, then held to 60 min) and NaOAc (0mM until 30 min, 0–500 mM from 30 to 50 min,500–1000 mM from 50 to 52 min, then held until 60 min) at 30 °C and a flow rate of 1 mL/min. The sugars were identified from their elution times relative to a standard sugar mix (L-fucose, L-rhamnose, L-arabinose, D-xylose, D-galactose, D-glucose, D-mannose, D-GalUA and D-glucuronic acid), quantified from the response calibration curves of each sugar and expressed as µg of the anhydro-sugar (as this is the form of sugar present in a polysaccharide) per mg of sample; the Normalised mol% of each anhydro-sugar was also calculated.

4.2.7. Nuclear Magnetic Resonance (NMR) Spectroscopy of Dialysed Blackcurrant Pectin-Rich Fraction

The dialysed pectin-rich fraction (≈40 mg) was exchanged with deuterium (D_2O) by freeze-drying with D_2O (99.9 atom%) twice and dissolved in 800 µL D_2O for analysis. Spectra were recorded on a Jeol JNM-ECZ600R 600 MHz spectrometer with a 5 mm FG/RO Digital Auto Tune Probe (Jeol USA Inc., Peabody, Massachusetts, U.S.A) at 70 °C. The ^{1}H and ^{13}C chemical shifts were measured relative to an internal standard of acetone (^{1}H, 2.225 ppm; ^{13}C, 31.45 ppm). NMR spectra were analysed and processed in MestreNova (Ver. 14.1.1) (MestreLab Research, Santiago de Compostela, Spain). Assignments were made from the heteronuclear single quantum coherence (HSQC) COSY experiment and by comparing the spectra with published data.

4.2.8. Acid Dissociation Constant (pK_a) of Dialysed Blackcurrant Pectin-Rich Fraction

The acid dissociation constant (pK_a) was determined by titrating 0.25% w/v of dialysed blackcurrant pectin and citrus pectin solution with fresh 0.1 M NaOH at 20 °C. The solution was prepared overnight (4 °C) before its pH was adjusted to pH 1.5 using 1 M and 3 M HCl. Automated titration was done by the Titrator Excellence T7 (Mettler Toledo, Columbus, Ohio, U.S.A) where the volume of titrant (V_t) and pH was recorded. The sample was titrated from pH 1.5 to pH 12.0. The titration curve (pH vs. V_t) and the first derivative ($\Delta pH/\Delta V_t$) of the titration curve were plotted to determine the volume of titrant at the maximum $\Delta pH/\Delta V_t$ also known as the equivalence point volume (V_e). Following that, a Gran plot ($V_t\,10^{-pH}\,vs\,V_t$) was also constructed to identify the linear acidic region. Using Equation 4.1, the K_a values in the linear acidic region were calculated and averaged and the pK_a of the pectin was determined using Equation 4.2. Titration was carried out in three replicates and the pK_a value is reported as the mean and standard deviation of three readings.

$$V_t \times 10^{-pH} = K_a(V_e - V_t) \rightarrow K_a = \frac{V_t \times 10^{-pH}}{V_e - V_t} \quad \text{(Equation 4.1)}$$

$$pK_a = -log_{10}K_a \quad \text{(Equation 4.2)}$$

4.2.9. Zeta-Potential of Dialysed Blackcurrant Pectin-Rich Fraction

The zeta-potential of the dialysed pectin-rich fraction was measured by the Zetasizer Pro (Malvern Panalytical Ltd., Malvern, United Kingdom). The sample was dispersed in distilled water overnight at 4 °C to achieve a concentration of 1% w/v and then diluted to a range of concentrations (0.1, 0.2, 0.3, 0.4, 0.5 and 0.6% w/v). The pH of these solutions was determined to be within the narrow range of pH 4.7–5.0 and the optimum zeta-potential readings were found to be between 0.4 and 0.5% w/v

concentration. Zeta-potential measurements at different pH levels were carried out at 0.4% w/v concentration. The pH of 0.4% w/v solution (pH 4.8) was adjusted to pH 2, pH 3 and pH 6 using 0.1 M HCl or NaOH. The samples were allowed to equilibrate overnight, and the pH values were checked once again before analysis. Approximately 1 mL of the solution was injected into the DTS1070 folded capillary cell (Malvern Panalytical Ltd., Malvern, United Kingdom) and the temperature was set at 20 °C. The zeta-potential values are reported as the mean and standard deviation of three readings.

4.2.10. Degree of Esterification of Dialysed Blackcurrant Pectin-Rich Fraction

The degree of esterification was determined based on the methods of Chen et al. (2017) and Nunes et al. (2006). The pectin fraction was dispersed in distilled water (2% w/v) to allow full hydration. The sample (100 µL) was saponified with 50 µL of 2 M NaOH for 2 h at 20 °C. After neutralisation with 50 µL of 2 M HCl, 50 µL of 25 mM of n-propanol (internal standard) and 250 µL of distilled water were added to make a total volume of 500 µL. Insoluble particles were removed by centrifugation (17,000 x *g* for 10 min at 20 °C) before an aliquot (200 µL) of the solution was placed into a micro-insert of the autosampler vial. For saponification control, water was used to replace both the NaOH and HCl. Four replicates of the control and sample were prepared. A GC17A (Shimadzu Corporation, Kyoto, Japan) gas chromatography equipped with a BP-20 column (SGE Analytical Science, Victoria, Australia) (15 m × 0.53 mm, 1 mm film thickness) was used to separate methanol at 80 °C with flame ionization detection and He as a carrier gas. Injections were Normalised with the internal standard and liberated methanol was quantified using a standard containing 3.75 µmol methanol. The DE was determined as the molar ratio of methanol to GalUA present in the blackcurrant pectin-rich fraction and expressed as the mean percentage and standard deviation of four readings.

4.3. Results and Discussion

4.3.1. Isolation and Composition of Blackcurrant Pectin-Rich Fractions

The composition of the pectin-rich fraction extracted from the blackcurrant juice is shown in Table 4.1. The undialysed fraction had a moisture content of 5.6% w/w and contained 46% w/w of total carbohydrates, of which 35% (16% w/w in the fraction) was uronic acid. The remaining was likely to be sugar residues from the pectin chains and trapped sugars that were not removed during ethanol washing. The undialysed fraction also contained a considerable amount of protein (3.6% w/w). This is similar to the findings of Hilz et al. (2005) that reported the presence of protein in blackcurrant juice pectic material (3% w/w). The presence of protein in the fraction further highlighted the complexity of the juice components and how this protein might be tightly bound to this pectin. The undialysed fraction contained minor fat (0.2% w/w), with a high percentage of inorganic materials (22% w/w), of which 22% was calcium (4.9% w/w). About 19% w/w of the fraction remained unknown. Other components such as organic acids and vitamins, which were not tested, may also account for this unknown portion of the fraction.

Table 4.1 Proximate composition of dried undialysed and dialysed blackcurrant pectin-rich fraction.

Components	Undialysed Pectin-Rich Fraction, % w/w	Dialysed Pectin-Rich Fraction, % w/w
Moisture	**5.6 ± 0.4**	**12.2 ± 0.32**
Total Carbohydrates	**46 ± 1.4**	**78 ± 4.8**
Uronic Acid (Galacturonic Acid)	16 ± 0.6	21 ± 2.9
Fat	**0.2 ± 0.01**	**Not Determined**
Crude Protein	**3.6 ± 0.1**	**4.5 ± 0.16**
Ash	**22 ± 1.0**	**5.1 ± 0.2**
Calcium	4.9 ± 0.2	2.2 ± 0.1
Anthocyanins (pH differential method)	**3.8 ± 0.3**	**3.9 ± 0.1**
Unknown	19[a]	-

Results are expressed as % of components in dry pectin-rich fraction (mean ± standard deviation).
[a] Determined by subtracting moisture, total carbohydrates, fat, crude protein, ash, and anthocyanins from 100%.

The dialysed pectin-rich fraction had a much higher moisture content (12.2% w/w) than its undialysed counterpart (5.6% w/w). This difference was likely attributed to their contrasting ash content—22% w/w and 5.1% w/w for undialysed and dialysed fraction, respectively—where large amount of minerals in the undialysed fraction might have facilitated the vacuum drying process, resulting in a much drier undialysed pectin-rich fraction. After dialysis, the purity of the fraction had increased to 78% w/w total carbohydrates, of which 27% (21% w/w in the fraction) was uronic acid. The amount

of protein (4.5% w/w) had also increased following dialysis. Despite that, the dialysis step had removed unbound molecules that were smaller than 8 kDa, such as unbound sugars, minerals, and ACNs. The ash and calcium contents of the dialysed fraction were reduced to 5.1% w/w and 2.2% w/w, respectively. The calcium content was considerably higher compared to other pectins, such as that from gold-fleshed kiwifruit (0.95% w/w), raspberry (0.78% w/w) and carrot (0.56% w/w) (Mierczynska et al., 2017; Yuliarti, Matia-Merino, et al., 2015). Moreover, the calcium content of blackcurrant pectin has been reported to be much lower (0.54% w/w) (Mierczynska et al., 2017), likely due to different blackcurrant cultivars and harsher extraction process (pH 2.5, 30 min at 90 °C) that could have hydrolysed the native structure of the blackcurrant pectin and released some of the bound calcium. Calcium and other minerals that were not removed by dialysis might be bound to the carboxyl groups of the pectic material, known as the boron-rhamnogalacturonan-II (RG-II) complex (Jarvis, 1984; Kobayashi et al., 1999). Hilz, Williams, et al. (2006) found that the blackcurrant juice contained more RG-II than the press cake of blackcurrants; therefore, the possibility of having calcium associated with the boron-RG-II complex in this fraction is high. Although, the amount of boron in the pectic material was not quantified, the presence of boron has been reported in blackcurrant fruit (Cosmulescu et al., 2015).

Both blackcurrant pectin-rich fractions appeared pigmented, signifying the presence of ACNs (Figure 4.2). The quantification of ACNs by pH differential method also confirmed that ACNs were still present in the undialysed and dialysed fractions: 3.8 % w/w and 3.9% w/w, respectively. An attempt to remove the pigments was made by washing the crude fraction with ethanol for an additional 15 cycles. In each cycle, the crude fraction was left stirring overnight at 4 °C before removing the excess ethanol. Despite the multiple ethanol washes, the crude fraction remained pigmented, suggesting the presence of tightly bound ACNs in the fraction. A similar occurrence was observed in *Mesona chinensis* polysaccharide that retained its black pigments after solvent extraction and dialysis (Yuris et al., 2019). Complexation of polyphenols with macromolecules like polysaccharides and proteins might explain the difficulty in obtaining blackcurrant pectin devoid of pigments. The difference in colour between the AIR and the undialysed pectin-rich fraction (Figure 4.2) was likely attributed to the changing proportion of hydrogen and hydroxide ions during the isolation process (i.e., pH difference). This might have affected the proportion of flavylium cations, quinonoidal bases and carbinol pseudobases, hence the colour difference between the dried products. Whereas colour difference between the undialysed and dialysed fractions (Figure 4.2) could be attributed to the ash content of the two fractions. The greater mineral content (22% w/w) of the undialysed fraction could have facilitated the drying process and produced a much lighter shade dried fraction.

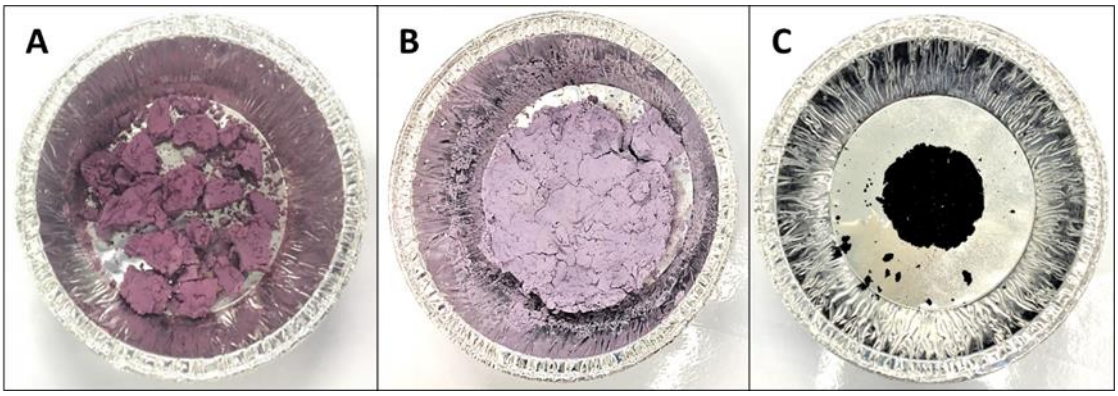

Figure 4.2 Alcohol insoluble residue (A) isolated from blackcurrant juice, undialysed pectin-rich fraction (B) and dialysed pectin-rich fraction (C).

4.3.2. Polyphenols in Blackcurrant Juice and Pectin-rich Fractions

There were four major ACNs identified in the blackcurrant juice and pectin-rich fractions: delphinidin 3-*O*-glucoside (del-glu), delphinidin 3-*O*-rutinoside (del-rut), cya-glu and cyanidin 3-*O*-rutinoside (cya-rut). The first ACN identified was cya-glu as it was the standard used for the analysis, while three other ACNs were identified based on the order of elution, with more polar compounds being eluted first (Appendix A). The delphinidins with more hydroxy groups than cyanidins (Figure 4.3) are more polar (Young & Abdel-Aal, 2009) and therefore, was eluted earlier. Glucose was a more polar sugar than rutinose (Young & Abdel-Aal, 2009), hence ACN with glucose attached was eluted first.

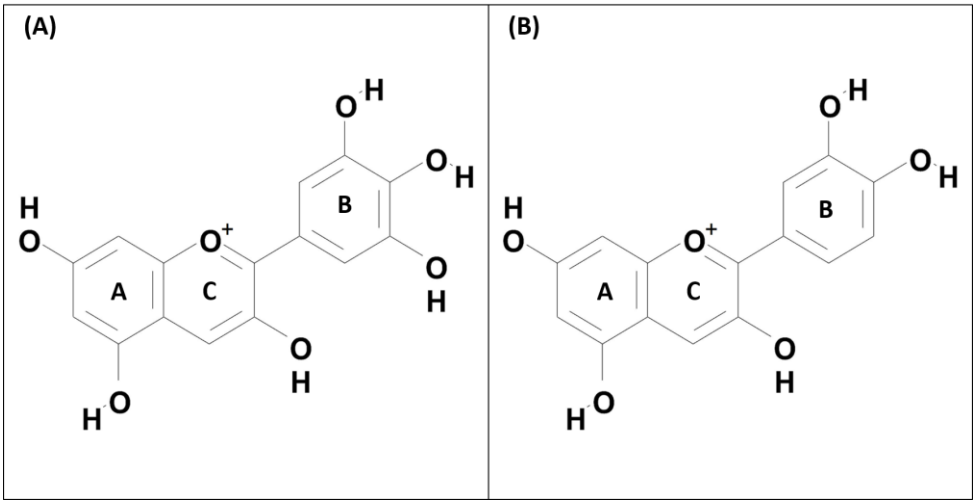

Figure 4.3 Structure of delphinidin (A) and cyanidin (B) aglycone.

The chromatograms of the juice and pectin-rich fractions at $\lambda_{530\ nm}$ and $\lambda_{280\ nm}$ are shown in Figure 4.4. Both pectin-rich samples appear to be much darker and pigmented than the juice sample (inset image of Figure 4.4); thus, stronger ACN peaks are expected for the pectin-rich samples. At $\lambda_{530\ nm}$, the chromatogram of the juice shows four distinct ACN peaks, however the absorbances of ACNs in pectin-rich fractions are much weaker. Based on the graph scale, only two peaks can be seen clearly in the chromatogram of the pectin-rich fractions, corresponding to the two major ACNs of blackcurrant (del-rut and cya-rut). In addition, both fractions have obvious broad peaks—between t_R 4 min and 10 min—that are not seen in the juice chromatogram. This may suggest two things: (i) the presence of interfering molecules that can also absorb at $\lambda_{530\ nm}$, or (ii) the absorbance of ACNs that are bound to small M_w compounds, which cannot not be freed by the solvent used (i.e., methanol). Nonetheless, the methanol managed to free some of the bound ACNs that ethanol could not, though not all of them. This was probably due to the shorter methyl radicals in methanol that interacted better with ACNs through hydrogen bonding, resulting in better solvation and extraction of ACNs (Boeing et al., 2014).

Proteins and ACNs can be detected at $\lambda_{280\ nm}$ due to the ability of phenolic rings on ACNs and aromatic ring on amino acids (e.g., phenylalanine, tryptophan, and tyrosine) to absorb UV light strongly at this wavelength (Aleixandre-Tudo & du Toit, 2018; Fátima Barroso et al., 2019). The chromatograms at $\lambda_{280\ nm}$ (Figure 4.4) have the same trend as at $\lambda_{530\ nm}$, where both pectin-rich fractions exhibit weak ACN signals that are accompanied by a broad peak. The presence of protein in the pectin-rich fractions and bound ACNs that were not freed by ethanol and methanol might be the cause of these broad peaks. This finding suggests that ACNs are bound in the pectin-rich fractions and that the presence of protein in this fraction may have a role in the binding.

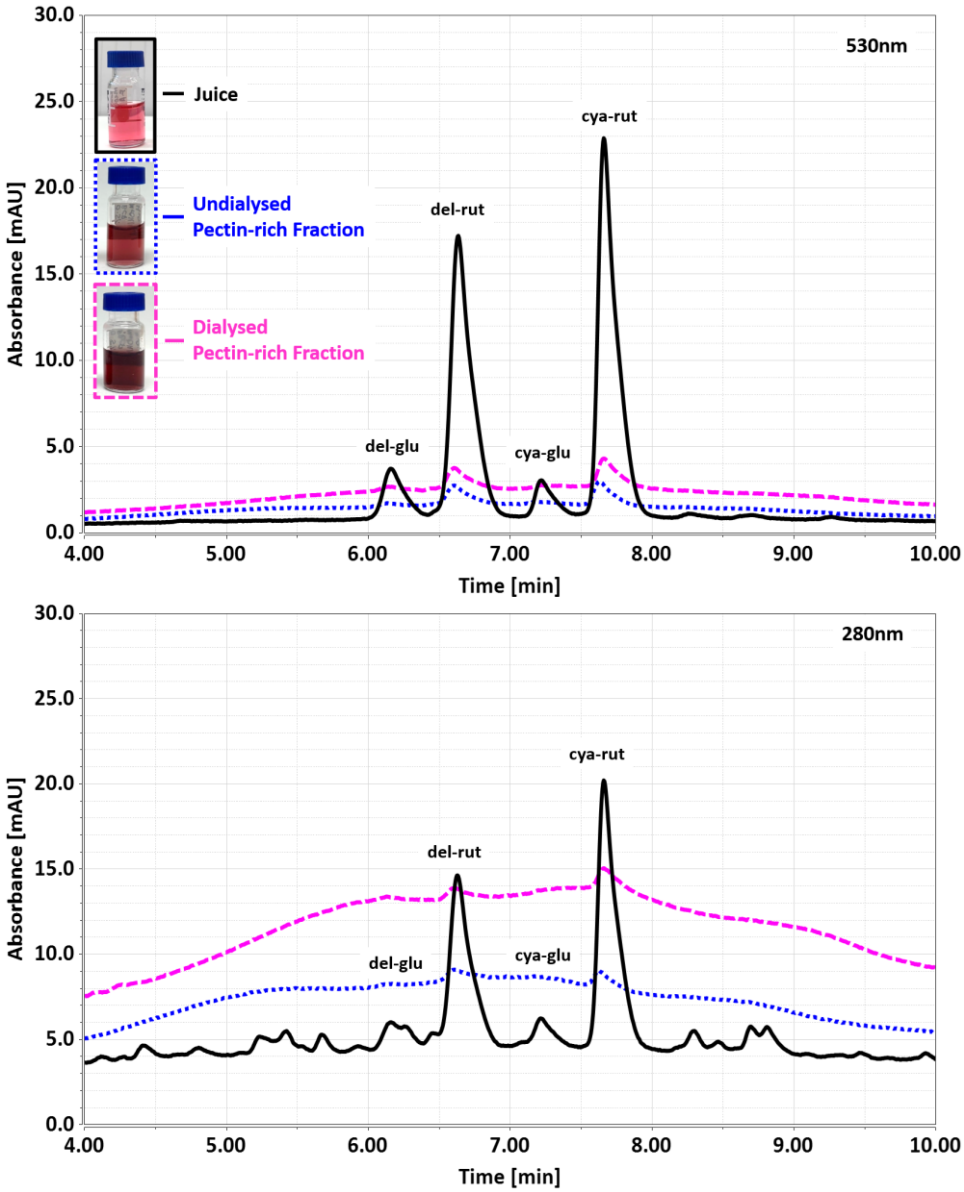

Figure 4.4 Chromatograms of blackcurrant juice (black ▬) and blackcurrant pectin-rich fractions; undialysed (blue ▪▪▪) and dialysed (pink ▬ ▬) at $\lambda_{530\ nm}$ and $\lambda_{280\ nm}$. The inset image show samples prepared in acidified aqueous methanol.

It is unclear whether the ACNs are bound to the pectic components and/or proteins of the fractions. The ACNs can interact with pectin via multiple forces. In the form of flavylium cation, ACN can complex with the negatively charged carboxylic groups of pectin through electrostatic interactions, much like the association of calcium ions to pectin (Buchweitz et al., 2013; Fernandes et al., 2014; Hubbermann et al., 2006; Lin et al., 2016; Mazzaracchio et al., 2004; Phan et al., 2017). Although Fernandes et al. (2014) and Lin et al. (2016) also reported that the binding of ACNs to pectin could also occur via hydrogen bonding and hydrophobic stacking—between the planar structure of ACNs and the ring planes of pectin. As for the interaction between polyphenols and protein, Spencer et al. (1988) described it as a surface phenomenon and proposed that the interaction occurs through hydrophobic and hydrogen bonding interactions. The aromatic rings of the polyphenols would bind themselves to the hydrophobic regions of the protein via hydrophobic forces, where hydrogen bonds would then ensue, reinforcing the protein-polyphenol residues such as the amino, hydroxy, and carboxyl groups (Hagerman, 2012; Spencer et al., 1988). Despite the various suggestions on physical interactive forces of ACN-pectin and polyphenol-protein binding, the presence of covalent bonds in this pectin-rich fraction cannot be excluded. Owing to the complexity of this fraction, a mixture of interactive forces including covalent bonds might be responsible for the binding of ACNs to the various components of the fraction.

Table 4.2 summarises the complete polyphenol profile of blackcurrant juice and its pectin-rich fractions . Overall, the juice (2048 mg/100 g total solids) contained more polyphenols than the pectin-rich fractions. Ethanol washes and dialysis reduced the amount of polyphenols in the undialysed and dialysed pectin-rich fractions to 43.8 mg/100 g total solids and 52.9 mg/100 g total solids, respectively. As a result of dialysis, the purer fraction had slightly more total polyphenols and ACNs than the undialysed fraction. The dominant type of polyphenol in all three materials was ACN, contributing 86.9%, 97.5% and 97.7% to the total polyphenols content of juice, undialysed and dialysed pectin-rich fractions, respectively. The two most abundant ACNs in these materials were cya-rut and del-rut. Cya-rut contributed between 46% and 50% of the total amount of ACNs while del-rut contributed approximately between 38% and 43%. Two other ACNs, del-glu and cya-glu, existed in smaller quantities and contributed to a lower extent of the total amount of ACNs in juice (6.74% and 4.84%, respectively), undialysed (6.79% and 4.22%, respectively) and dialysed (6.62% and 4.62%, respectively) pectin-rich fractions. Nevertheless, the ratios of ACNs in both pectin-rich fractions were comparable to the ratio of ACNs in the blackcurrant juice.

Table 4.2 Phenolic compounds in blackcurrant juice and its pectin-rich fractions.

Phenolic Compound	Quantity		
	mg/100 g Total Solids		
	Juice	Undialysed Pectin-Rich Fraction	Dialysed Pectin-Rich Fraction
Total Anthocyanin	**1780 (86.9%)**	**42.7 (97.5%)**	**51.7 (97.7%)**
Cyanidin 3-*O*-Glucoside	86.2 ± 0.803	1.80 ± 0.244	2.39 ± 0.64
Cyanidin 3-*O*-Rutinoside[a]	892 ± 2.07	19.8 ± 0.571	24.0 ± 0.455
Delphinidin 3-*O*-Glucoside[a]	120 ± 0.57	2.90 ± 0.37	3.42 ± 0.642
Delphinidin 3-*O*-Rutinoside[a]	678 ± 0.784	18.2 ± 1.81	21.9 ± 1.61
Total Flavonol	**147 (7.18%)**	**0.351 (0.801%)**	**0.323 (0.611%)**
Kaempferol 3-*O*-Rutinoside	6.49 ± 0.35	0.167 ± 0.0804	0.151 ± 0.0851
Quercetin	5.93 ± 1.16	n.d	n.d
Quercetin 3-*O*-Rutinoside	39.9 ± 0.66	0.184 ± 0.0804	0.172 ± 0.097
Isorhamnetin 3-*O*-Rutinoside[a]	n.d	n.d	n.d
Myricetin[a]	n.d	n.d	n.d
Myricetin 3-*O*-Galactoside[a] / Myricetin 3-*O*-Glucoside[a]	48.2 ± 1.44	n.d n.d	n.d n.d
Myricetin 3-*O*-(6-Malonyl)-Glucoside[a]	n.d	n.d	n.d
Quercetin 3-*O*-(6-Malonyl)-Glucoside[a]	n.d	n.d	n.d
Quercetin 3-*O*-Glucoside[a]	46.4 ± 0.67	n.d	n.d
Total Phenolic Acid	**113 (5.52%)**	**n.d**	**n.d**
p-Coumaroylquinic Acid	1.12[b]	n.d	n.d
Chlorogenic Acid	2.50 ± 0.22	n.d	n.d
Caffeic Acid[a]	2.20 ± 0.26	n.d	n.d
3-Caffeoylglucoside Acid[a]	76.7 ± 1.95	n.d	n.d
Neochlorogenic Acid[a]	22.9 ± 0.36	n.d	n.d
p-Coumaric Acid[a]	4.91 ± 0.43	n.d	n.d
Sinapic Acid[a]	2.83 ± 0.29	n.d	n.d
Total Flavanol/Procyanidin	**7.96 (0.39%)**	**0.701 (1.60%)**	**0.881 (1.67%)**
Catechin	3.24 ± 0.33	0.186[b]	0.233 ± 0.0768
Epicatechin	3.02 ± 0.29	0.211 ± 0.0795	0.382 ± 0.0287
Procyanidin B2	1.70 ± 0.28	0.304[b]	0.266[b]
Total Phenolic Compounds	**2048**	**43.8**	**52.9**

Results are expressed as milligram of phenolic compound per 100 g total solids (mean ± standard deviation, n = 3).

[a]Anthocyanins are expressed as cyanidin 3-*O*-glucoside equivalents, flavonols as quercetin 3-*O*-rutinoside equivalents, and phenolic acids as chlorogenic acid equivalents.

[b]Detected in one sample.

n.d = not detected

Three types of non-ACN phenolic compounds were also identified in the juice (Table 4.2): flavonols, phenolic acids and flavanols. Flavonol (7.18%) was the second most abundant type of polyphenol in the blackcurrant juice. Flavonols like que-rut, myricetin 3-*O*-galactoside/glucoside and quercetin 3-*O*-glucoside contributed the most to the total flavonol content of the juice except for kae-rut and quercetin aglycone, which were found in smaller quantities. Phenolic acids contributed 5.52% to the total polyphenol content of the juice. Some of these hydroxycinnamic acids might be esterified or cross-linked to the cell wall proteins and/or polysaccharides, such as pectin and arabinoxylans (Fry, 1982; Selvendran, 1985). Small amounts of flavanols (0.39%) were also detected in the juice, though the lack of flavanols being reported in blackcurrant studies might be due to the chromatography method, sample purity, or the generally low amounts of flavanols in blackcurrants (Kapasakalidis et al., 2006). The low amounts of non-ACN phenolic compounds of the pectin-rich fractions suggested that most of the compounds had been removed during extraction and ethanol washings. Two of the flavonols (kae-rut and que-rut) were detected in both fractions while phenolic acids were absent. The overall amounts of flavonols and flavanols in both fractions were small in quantities but comparable.

The pigmented appearance of the two fractions (inset image of Figure 4.4) suggests that there are unaccounted ACNs in the fractions that cannot not be freed by solvent extraction. Despite using the same ACN reference (cya-glu) in the pH differential and liquid chromatography (LC) methods, the amount of ACNs between these two methods varied greatly: 3.8 g/100 g versus 0.0403 g/100 g of the dried undialysed pectin-rich fraction and 3.9 g/100 g versus 0.0488 g/100 g of the dried dialysed pectin-rich fraction. The huge difference could be attributed to the principle of the method used. The pH differential method is based on the absorbance difference at $\lambda_{530\ nm}$ between the ACNs at pH 1 (in flavylium cationic form) and at pH 4.5 (in hemiketal form), excluding any polymerised or degraded ACNs, as they are not affected by pH changes (Lee et al., 2005). Figure 4.5 shows the colour difference of 0.1% w/v of undialysed and dialysed pectin-rich fractions in pH 1 and pH 4.5 buffers. The two buffers were able to structurally change the ACNs in the pectin-rich fractions, producing colour and absorbance differences that enabled the quantifications of all the ACNs in the fractions. Conversely, the LC method measured only the free monomeric ACNs that are extracted by the aqueous methanol, and therefore was limited by the ability of the solvent to extract the analytes. The pH differential method could be measuring both unbound and bound ACNs, but this would not be the case for the LC analysis.

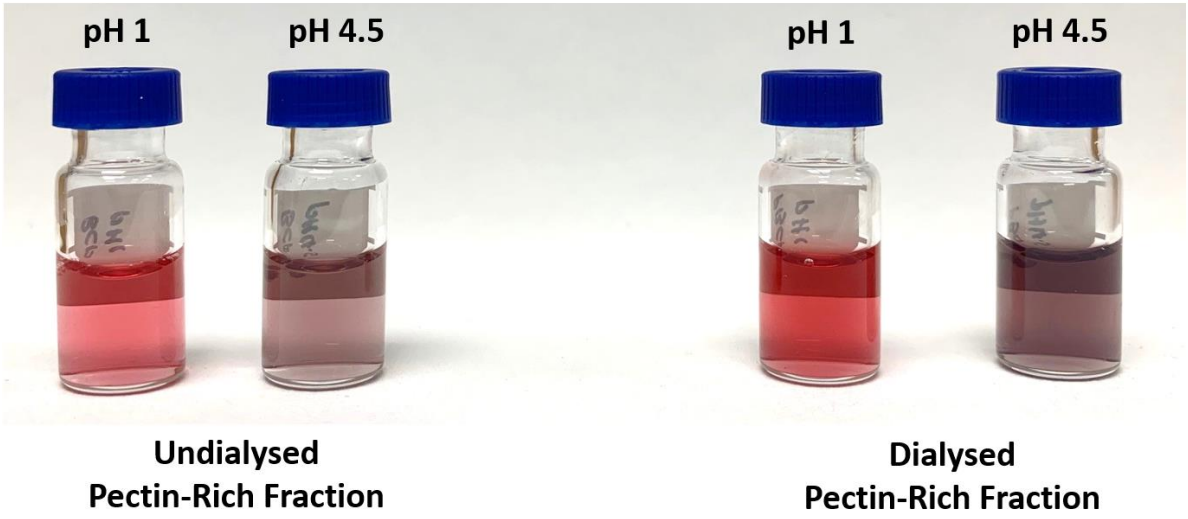

Figure 4.5 Undialysed and dialysed blackcurrant pectin-rich fraction solutions (0.1% w/v) in pH 1 and pH 4.5 buffer.

4.3.3. Molecular Characteristics of Blackcurrant Pectin-Rich Fractions

Figure 4.6 shows the chromatograms of undialysed (A) and dialysed (B) blackcurrant pectin-rich fractions. Based on the emergence of light scattering (LS) peaks in both figures, the region of interest was set to be at t_R 30–52 min. Within this t_R, the LS and refractive index (RI) signals show that there are multiple low-resolution peaks, suggesting the presence of more than one polymer species in the fractions. Analytes eluted after 52 min have little to no LS signal that are probably caused by low M_w species like unbound proteins, ACNs, oligosaccharides, sugars, or salts. Between t_R 30 min and 52 min, the dialysed fraction shows LS and RI profiles that are similar in shape to those in undialysed fraction but are twice the height. The LS and RI signals of the dialysed fraction for Peak 1 and 2 had increased 2-fold owing to the purer pectin fractions as a result of dialysis.

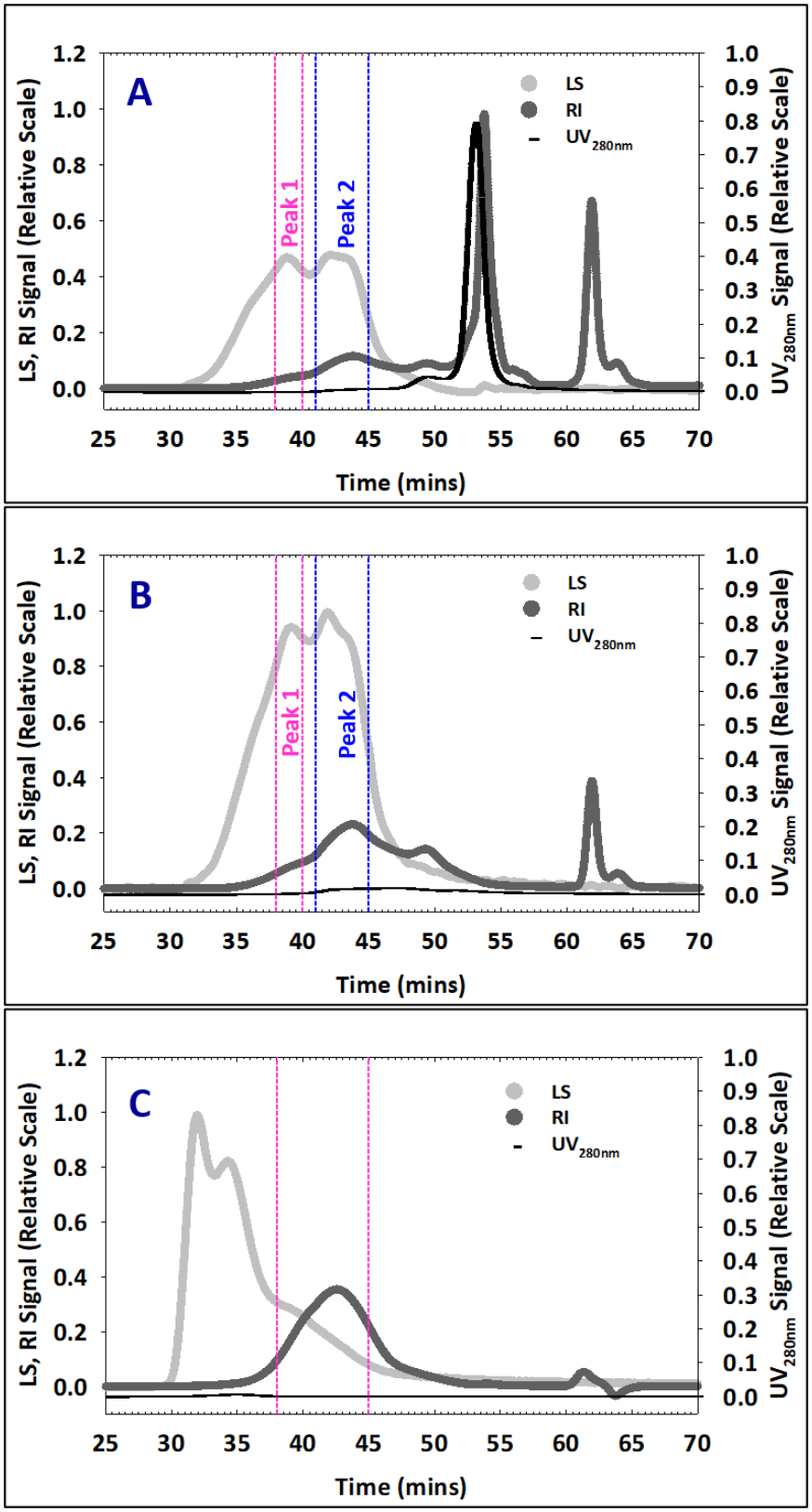

Figure 4.6 SEC-MALLS chromatograms of undialysed (A) and dialysed (B) blackcurrant pectin-rich fractions and citrus pectin (C) showing light scattering (LS), differential refractive index (RI) and $UV_{280\ nm}$ signal.

At the region of interest (t_R: 30–52 min), the high PDI value of both fractions indicated that the polymers were heterogenous (Table 4.3), especially the undialysed fraction as it was less pure than the dialysed fraction. Such heterogeneity was also seen in pectins from other plant origins (Guo et al., 2016; Muhammad et al., 2014; Yuliarti, Matia-Merino, et al., 2015). However, M_w analysis was selected based on prominent LS and RI peaks at narrower t_R range. Two regions selected for M_w analysis (Peak 1 t_R: 38–40 min, Peak 2 t_R: 41–45 min) revealed two possible pectin fractions with different M_w. In the undialysed sample, Peak 1 had a large molar mass fraction with an average M_w of ≈279 kDa and RMS radius of ≈33 nm but at a lower concentration, while Peak 2 had a smaller molar mass fraction of ≈104 kDa and a similar RMS radius of ≈32 nm, being at a higher concentration. Similar molecular characteristics and trends were observed in the dialysed sample: Peak 1 had a large average M_w (≈283 kDa) and RMS radius of ≈34 nm at a lower concentration, whereas Peak 2 had a smaller average M_w (≈97 kDa) and RMS radius of ≈30 nm at a higher concentration. Alba et al. (2018) found the M_w of pectin from blackcurrant pomace to be between 30 kDa and 110 kDa, smaller than the M_w of pectin extracted in this study. Factors such as fruit maturity, cultivar, growth conditions, climate, processing steps and extraction methods can affect the molecular characteristics of the cell wall components (Alba et al., 2018; Yuliarti, Matia-Merino, et al., 2015). The blackcurrant pomace that was generated from commercial juice production could have yielded smaller M_w pectic material than the pectin-rich fractions extracted in this study, likely owing to the various processing steps it had undergone. In addition, the acidic extraction (pH 2 at 80 °C for 2 h) carried out by the author might have hydrolysed the blackcurrant pomace pectin into low M_w pectin species, as opposed to our milder extraction where the blackcurrant juice pectin is likely to have retained its native state.

The commercial citrus pectin shows multiple LS peaks at t_R 30–52 min (Figure 4.6), signifying a heterogeneous material with high PDI value (Table 4.3). Before t_R 38 min, the region has strong LS signal that is accompanied by a weak RI signal, likely due to the presence of small amounts of pectin aggregates with large M_w (≈10^6–10^7 kDa). The majority of the polymers are eluted at t_R 38–45 min, as indicated by the distinct single RI peak. The fraction at this t_R had a comparable RMS radius (≈33 nm) to those of the blackcurrant pectins, however its M_w (≈76 kDa) was slightly smaller than those of the extracted blackcurrant pectins (Table 4.3). The different source of pectin and the harsher extraction process of a commercial pectin might have contributed to the smaller M_w. Commercial pectin is typically extracted by acid at high temperature for several hours, which may hydrolyse the native pectin to a smaller M_w pectin.

Table 4.3 Molecular characteristics (PDI, polydispersity index; M_w, molecular weight; RMS radius, root mean squared radius) of undialysed and dialysed blackcurrant pectin-rich fractions and citrus pectin at selected retention times (t_R).

Type Of Pectin	t_r, min	PDI	t_r, min	Peak 1 M_w, kDa	RMS Radius, nm	t_r, min	Peak 2 M_w, kDa	RMS Radius, nm
Undialysed Blackcurrant	30–52	6.96 ± 1.07	38–40	279 ± 2.55	32.5 ± 1.20	41–45	104 ± 3.46	32.0 ± 1.63
Dialysed Blackcurrant		2.91 ± 0.62		283 ± 7.35	33.7 ± 2.83		97.3 ± 5.23	30.1 ± 2.05
Citrus		4.95 ± 0.00	38–45	75.6 ± 1.34	32.5 ± 3.39	-	-	-

Results are reported as mean ± standard deviation (n = 2).

The $UV_{280\ nm}$ chromatogram of all three pectins at t_R 38–45 min is shown in Figure 4.7. The UV signal of both blackcurrant pectins at Peak 2 (t_R: 41–45 min) shows that it coincides with the prominent LS and RI peaks of Figure 4.6, implying that pectin, protein, and polyphenols, particularly the ACNs, were not effectively separated by the size exclusion column and suggesting that part of the pectin could be conjugated with protein and/or polyphenol moieties. Linking this with the findings from LC analysis confirms the assumption that ACNs were associated with protein and/or pectic components of the fractions. Figure 4.7 also shows that the UV peak area of Peak 2 has doubled after dialysis; 0.019 ± 0.002 AU min for the undialysed fraction and 0.044 ± 0.003 AU min for the dialysed fraction. Since the structure of the pectin was preserved, there is a possibility that the pectin-rich fractions contain hydroxyproline-rich glycoproteins such as extensin and arabinogalactan-proteins, as these have been identified as plant structural proteins known to be associated naturally to pectin (McKenna et al., 2006; Nuñez et al., 2009). Overall, the dialysis of the fraction resulted in a higher component concentration at t_R 30-52 min and significant reduction of RI and UV signals after t_R 50 min, indicating that small unbound molecules were removed during dialysis. The UV signals of both blackcurrant pectins are more apparent than that of citrus pectin, likely because the blackcurrant pectins contained protein and was rich in UV-absorbing ACNs. Nevertheless, the citrus pectin might also contain some UV-absorbing molecules because citrus peel naturally contains phenolic compounds like flavanones, flavanols and polymethoxylated flavones, though in much lesser quantity (Fátima Barroso et al., 2019; Singh et al., 2020). Moreover, a small quantity of protein, between 1.44% and 1.72%, has been detected in purified citrus pectin (Verkempinck et al., 2018) .

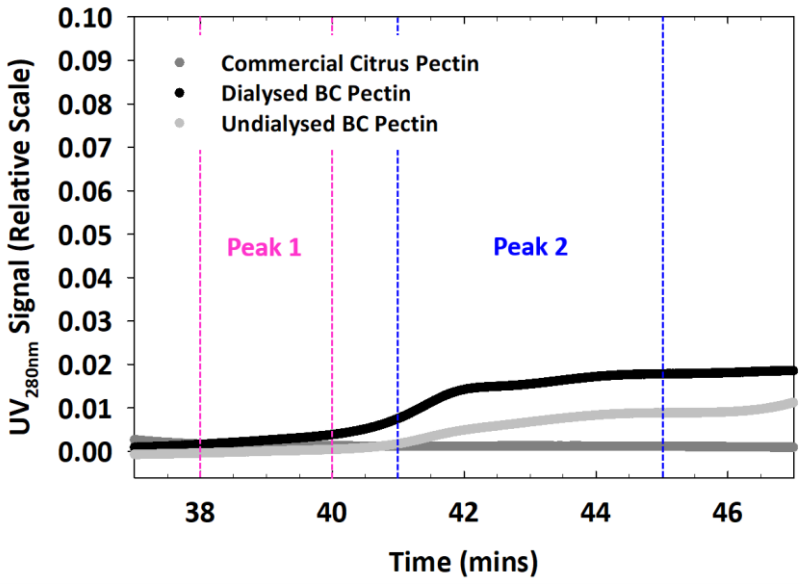

Figure 4.7 $UV_{280\ nm}$ chromatograms of undialysed and dialysed blackcurrant pectin-rich fractions and citrus pectin at retention times of 38 to 45 min.

4.3.4. Constituent Sugar Composition and NMR Spectroscopy of Dialysed Blackcurrant Pectin-Rich Fraction

The total carbohydrate content (Table 4.4) determined from the constituent sugar analysis (86% w/w) was similar to that measured by the colorimetric analysis, but the uronic acid content (33% w/w) was higher than that determined by the colorimetric analysis. The constituent sugar composition of the dialysed blackcurrant pectin-rich fraction was similar to that determined previously for ultrafiltered blackcurrant juice, although in this current study the proportion of GalUA (36.5% cf. ≈47–50%) was lower and that of galactose (24.4% cf. 6–7%) higher than reported (Hilz et al., 2005; Hilz, Williams, et al., 2006). The major monosaccharides were GalUA, galactose, and arabinose, which together with rhamnose was consistent with the presence of a high proportion of pectic polysaccharides. The amounts of rhamnose and GalUA, together with arabinose and galactose, suggested that the pectin-rich fraction was comprised of a high proportion of branched rhamnogalacturonan-I (RG-I) (Mohnen, 2008). Hilz, Williams, et al. (2006) reported that ultrafiltered blackcurrant juice was comprised of about one-third RG-II, based on the detection of 2-*O*-methyl fucose, 2-*O*-methyl xylose and other RG-II specific sugars. These sugars were not specifically analysed in the current constituent sugar analysis, but the detection of small amounts of fucose and glucuronic acid suggested that RG-II was a component of the blackcurrant pectin-rich fraction. The presence of glucose, mannose and xylose indicated that this fraction also contained small amounts of hemicellulosic polysaccharides (xyloglucan and (galacto)glucomannan) (Pettolino et al., 2012).

Table 4.4 Constituent sugar composition (mean of duplicate analyses) of dialysed blackcurrant pectin-rich fraction.

Sugar	µg/mg
Fucose	5.0
Rhamnose	65.9
Arabinose	150.6
Galactose	209.8
Glucose	49.9
Mannose	36.4
Xylose	14.9
Galacturonic Acid	314.3
Glucuronic Acid	14.2
Total	861.1

The structure of the dialysed blackcurrant pectin-rich fraction was further analysed by NMR spectroscopy. The HSQC spectrum (Figure 4.8) showed the presence of resonances that are typical of pectic polysaccharides. Anomeric resonances at δ 5.27/98.4 and at 4.96/100.0 were assigned to H-1/C-1 of rhamnose (with H-6/C-6 at 1.25/16.5ppm) and GalUA, respectively, of an RG-I backbone

(Makarova et al., 2016; Shakhmatov et al., 2020; Tang et al., 2021). The intense *O*-methyl resonance at δ 3.81/52.8 indicated a high degree of methyl-esterification of the uronic acid residues. A resonance at δ 5.07/70.6 was assigned to H-5/C-5 of →4)-α-D-Gal*p*A-6-OMe-(1→ residues, while a weak resonance at δ 4.83/71.7 was assigned to H-5/C-5 of non-esterified →4)-α-D-Gal*p*A-(1→residues. In addition, a resonance in the ^{13}C spectrum (not shown) at δ 170.6 was assigned to esterified α-D-Gal*p*A, while that for non-esterified residues (≈δ 173) was not observed (Barbieri et al., 2019; Shakhmatov et al., 2020). A weak resonance at δ 2.20/20.4 indicated a low degree of O-acetylation (Tang et al., 2021). Intense anomeric resonances at δ 5.25/109.1 and 5.08-5.14/107.1-107.5 were assigned to terminal and →5)-α-L-Ara*f*-(1→, and those at δ 4.46-4.51/102.8-103.2 were assigned to →6)-β-D-Gal*p*-(1→ and →3,6)-β-D-Gal*p*-(1→ residues (Makarova et al., 2016; Shakhmatov et al., 2020; Sims & Furneaux, 2003; Tamiello-Rosa et al., 2019). Resonances at δ 3.72-3.86/61.2 and at δ 3.79-3.95/66.9 were assigned to H-5/C-5 of both α-L-Ara*f* and H-6/C-6 of β-D-Gal*p* residues. A weak resonance at δ 4.70/103.6 was assigned to →4)-β-D-Gal*p*-(1→ (Barbieri et al., 2019; Shakhmatov et al., 2020). Other weaker anomeric resonances may be due to RG-II residues, but could not be assigned (Rodríguez-Carvajal et al., 2003).

Overall, results of the analysis of the purified pectin-rich fraction were in agreement with those reported previously (Hilz et al., 2005; Hilz, Williams, et al., 2006). It contained a high proportion of RG-I, with mostly arabinan, and/or type II arabinogalactan side chains and small proportions of hemicellulose. This fraction may also contain RG-II, as reported previously for ultrafiltered blackcurrant juice (Hilz, Williams, et al., 2006).

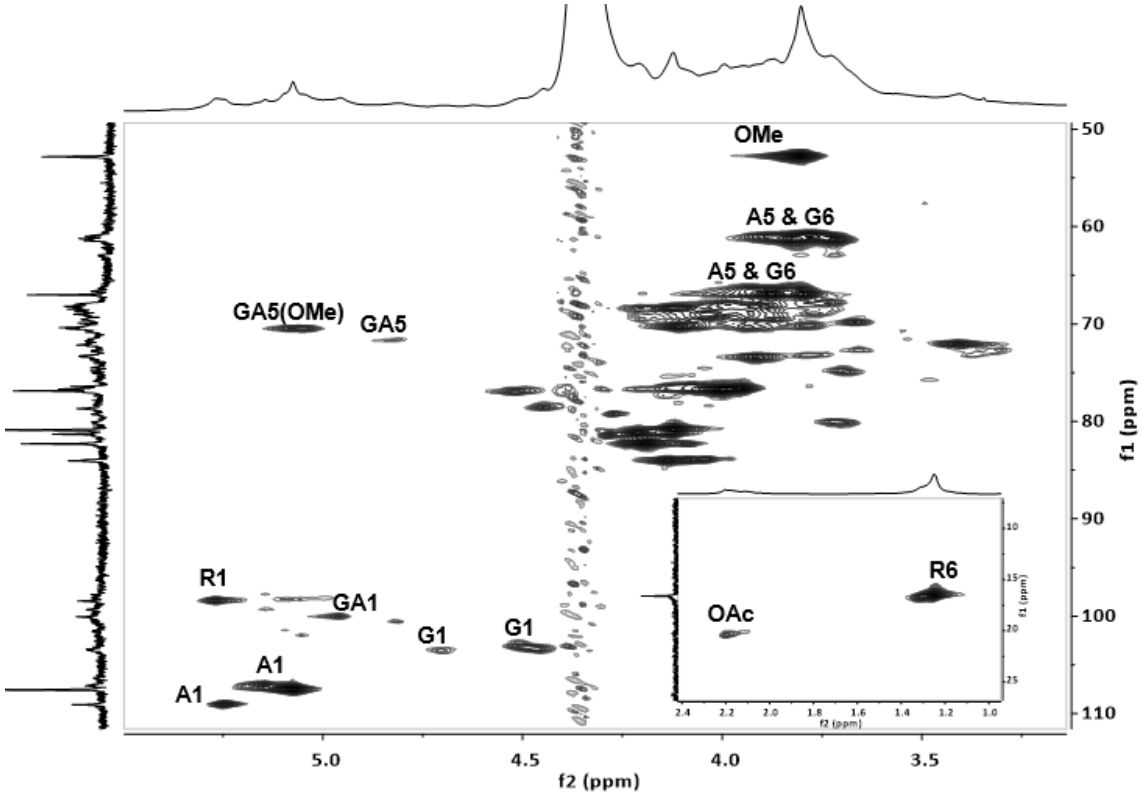

Figure 4.8 HSQC spectrum of dialysed blackcurrant pectin-rich fraction recorded at 70 °C. A1: H-1/C-1 of α-L-Ara*f*; A5: H-5/C-5 of α-L-Ara*f*; G1: H-1/C-1 of β-D-Gal*p*; G5: H-5/C-5 of β-D-Gal*p*; R1: H-1/C-1 of α-L-Rha*p*; R6: H-6/C-6 of α-L-Rha*p*; GA1: H-1/C-1 of α-D-Gal*p*A; GA5: H-5/C-5 of α-D-Gal*p*A; OMe: *O*-methyl; OAc: *O*-acetyl.

4.3.5. Physico-Chemical Properties of Dialysed Blackcurrant Pectin-Rich Fraction

Pectin is a heteropolysaccharide with a backbone that is mainly composed of GalUA units in which some of the carboxyl groups are partially acetylated or methyl-esterified. Depending on the pH of the continuous phase, these carboxyl groups can dissociate, making pectin negatively charged and hence, an anionic polysaccharide. Since the pectin-rich fraction is a composite material, determination of its pK_a can provide insight into its behaviour at different pH points. This is also useful in understanding the behaviour of blackcurrant juice when it is mixed with other ingredients. The pK_a of the dialysed blackcurrant pectin was determined to be 1.67 ± 0.17 and this was comparable to the pK_a of a high-DE citrus pectin (2.06 ± 0.08). The pK_a of this citrus pectin (DE ≥85%) was lower than the pK_a (≈3.00) of a commercial lime pectin (DE 81) reported in Ralet et al. (2001). The difference between these pK_a values might be attributed to the ionic strength and temperature of the samples during potentiometric measurements (Reijenga et al., 2013). In the study reported by Ralet et al. (2001), traces of minerals were removed from the commercial lime pectin by repeated washes with 65% aqueous ethanol and titrations were carried out at 25 °C. The citrus pectin used in this study was not

treated at all and titrations were conducted at a slightly lower temperature (20 °C). These differences might have led to a lower pK_a of the citrus pectin. Since the dialysed blackcurrant pectin-rich fraction is a composite material, the lower pK_a value might be due to the presence of large amounts of bound protein and polyphenols.

At pH > the pK_a, the pectin will appear as negatively charged because its carboxyl groups are dissociated to form COO^-. This allows it to participate in electrostatic interactions with other molecules such as proteins and other molecules that carry positive charges. The influence of the pK_a value can be seen during zeta-potential measurements at various pH points. Before pH adjustments, the pectin solution had a pH value of 4.8 with a net negative charge of -23.1 ± 0.20 mV. The zeta-potential increased slightly to -25.3 ± 0.69 mV when the pH was raised to pH 6. When the pH was adjusted to pH 3, the net electrical charge of the pectin was reduced by half, to -10.5 ± 0.53 mV. At pH 2, which was closer to its pK_a value of ≈1.7, the zeta-potential became almost negligible (-1.55 ± 0.25 mV), leaning towards zero. At this point, the likelihood of the blackcurrant pectin interacting with oppositely charge molecules will be lower.

The dialysed pectin-rich fraction was determined to be a high methyl-esterified pectin with an average DE of 65.2 ± 10.2%. This was comparable to the DE of pectic polysaccharide isolated from the blackcurrant juice (DE of 57%) in Hilz et al. (2005) study. Determining DE by quantifying the amount of methanol released by saponification was a more suitable method for this pigmented fraction than the capillary electrophoresis (CE) method (data not shown). This is because the CE method relies on absorbance at $\lambda_{192\ nm}$ and $\lambda_{235\ nm}$. An accurate measurement of DE was difficult to obtain because of interference from proteins, ACNs and other polyphenols that could also absorb UV at $\lambda_{235\ nm}$ (Fátima Barroso et al., 2019). The DE and the distribution of methyl-esters, also known as the degree of blockiness (DB), determine the overall and local charge density of the pectin, respectively (Sperber et al., 2009). Although the DB of the dialysed pectin-rich fraction was not determined, both the DE and DB can have an effect on the zeta-potential value. The effect was seen in Verkempinck et al. (2018) work, where the zeta-potential of a citrus pectin was found to be inversely proportional to the DE but directly proportional to the DB. The high DE (82%)-low DB (10.8%) citrus pectin had lower zeta-potential (-7.6 mV) than the low DE (38%)-high DB (51%) citrus pectin (-20.1 mV) (Verkempinck et al., 2018).

4.4. Conclusions

- This study demonstrated that the cell wall compounds isolated from the blackcurrant juice yielded a complex extract that was rich in pectin, protein, ACNs, and calcium.
- The results from the LC analysis indicated that there were ACNs in the extract that were not accounted for, and that the presence of proteins in the pectin-rich fractions might have a role in the binding of ACNs.
- Based on SEC-MALLS analysis, the smaller pectic fraction had a higher UV signal at $\lambda_{280\ nm}$ than the larger pectic fraction, signifying the presence of UV-absorbing molecules like protein and polyphenols.
- Interestingly, these complexes could not be separated by solvent extraction during LC analysis, nor by the size exclusion columns, likely indicating that pectin, protein, and polyphenols were interacting with each other.
- The protein identified in the pectin-rich fraction could be a type of structural protein like the hydroxyproline-rich glycoprotein and might have a role in the complexation of pectin and polyphenols.
- The use of solvents (ethanol and methanol) and physical separation, like dialysis, could not remove all the pigments from the fraction, possibly because of multiple interactive forces, like covalent, electrostatic, hydrophobic and hydrogen interactions, that bound the components together.
- Although the polyphenols and/or protein were bound to the blackcurrant pectin, the pectin-rich fraction was still negatively charged at pH > its pK_a, resembling the properties of pectin and retaining its ability to interact with other positively charged molecules.

Further investigation that focused on understanding the associative mechanism of ACNs to blackcurrant pectin is presented in the following chapter. The investigative work was based on structural and charge manipulation of ACNs by pH.

Chapter 5 Effect of pH on Blackcurrant Juice Interactive Components

5.1. Introduction

The role of pH is undoubtedly crucial in pectin-anthocyanin (ACN) interactions as it influences the binding of ACNs to pectin through structural and charge manipulation (Fernandes et al., 2014; Lin et al., 2016). Generally, ACNs favour the interaction with pectin at low pH (pH ≤3.6), that is, when the flavylium cationic ACNs are prevalent because they carry a positive charge that enables ionic interaction with the negatively charged pectin (Fernandes et al., 2014; Lin et al., 2016). In addition, the flavylium cations can also associate with pectin through hydrophobic forces via stacking of the aromatic rings due to ACN planar surface, strengthening the overall pectin-ACN interactions (Fernandes et al., 2014; Lin et al., 2016). On the contrary, the binding of ACNs to pectin are weaker and lesser at medium acidity pH (pH ≥4) (Fernandes et al., 2014; Lin et al., 2016), likely due to the transformation of majority of the flavylium cations into neutrally charged quinonoidal base and carbinol pseudobase, allowing only hydrophobic and hydrogen bonding forces to take place. Moreover, the non-planar structure of the carbinol pseudobase reduces the possibility of aromatic ring stacking of ACNs, making the overall pectin-ACN association at medium acidity pH weaker (Fernandes et al., 2014). In a more recent study, Phan et al. (2017) had reported the strong binding of cyanidin 3-*O*-glucoside (cya-glu) to apple pectin at pH 3.4 (i.e., when both components had the opposite charges). In order to validate the electrostatic interaction between the pectin and ACN, the authors compared it with a system that contained identically charged components by incubating the negatively charged ferulic acid—a type of phenolic acid—and apple pectin at pH 5. The study revealed a much weaker binding, proving that there was a lack of ionic interaction amongst the identically charged components and confirming the presence of electrostatic attractive forces between the pectin and cya-glu.

Studies on pectin-ACN interactions are typically carried out by mixing or incubating a single type of ACN with pectin at specific conditions, and then separating them via membrane separation such as dialysis or ultra-filtration (UF) (Fernandes et al., 2014; Lin et al., 2016). However, no attempts have been made to investigate their interactions through dissociation of naturally bound ACNs from pectin.

Since blackcurrant (BC) ACNs were found to be associated to the BC pectin, this finding offered an opportunity to study pectin-ACN interactions from a different perspective. Thus, an experiment was conducted to study the effect of pH on BC juice components, mainly on its ACNs and pectin. The pH levels—pH 2, pH 3 (control) and pH 4.5—were chosen based on the work of Lin et al. (2016) and Phan et al. (2017) that corresponded to the different proportion of ACN structures. Theoretically, pH 2 would have the highest amount of positively charged ACNs with minimal neutrally charged ACNs, while pH 4.5 would contain the opposite—highest amount of neutrally charged ACNs and minimal positively charged ACNs. We hypothesise that the pH adjustment of BC juice will cause ACNs to lose their planar structure and the ability to interact electrostatically with the negatively charged pectin, causing them to dissociate from the BC pectin and be separated by size via UF. We also hypothesise that some ACNs will dissociate from the BC pectin at pH 2 due to the low amounts of negative charges of BC pectin at pH close to its acid dissociation constant (pK_a) of 1.7. The current work involved: (i) UF of the BC juices at pH 2, pH 3 and pH 4.5; (ii) determination of molecular properties, compositions (protein, monomeric ACN, and pectin), and phenolic compounds of the initial feeds (BC juice), permeates (PM) and retentates (RTT).

5.2. Materials and Methods

5.2.1. Materials

The BC juice was obtained by centrifuging BC puree following the method described in Chapter 3. A Gibco™ bovine serum albumin (Invitrogen Corporation, Carlsbad, United States) was used as a reference and calibration protein in molecular weight (M_w) analysis. For comparison purposes, analytical grade D-(+)-galacturonic acid (GalUA) monohydrate, sucrose, fructose, and glucose (Sigma-Aldrich, St. Louis, United States) were also used in the M_w analysis. The same GalUA was used as a standard in pectin analysis, while 3-phenylphenol (Sigma-Aldrich, St. Louis, United States) was used as the colorimetric reagent. Nine polyphenol standards were used in this study: cya-glu, kaempferol 3-*O*-rutinoside, quercetin 3-*O*-rutinoside (que-rut), procyanidin B2 (Extrasynthese, Lyon, France), quercetin (California Corp for Biochemical Research, California, United States), chlorogenic acid, catechin, epicatechin (Sigma-Aldrich, St. Louis, United States), and *p*-coumarylquinic acid that was extracted in-house at Plant and Food Research Institute in Palmerston North, New Zealand. All other chemicals were of analytical grade and purchased from local companies. Chemical solutions, samples, and dilutions were prepared using Milli-Q® water (Merck Group, Darmstadt, Germany).

5.2.2. Ultra-Filtration of Blackcurrant Juice

The BC juice was filtered at three pH levels—pH 2, pH 3 (control) and pH 4.5—using a bench-top UF system. The system was made of a Pellicon® Mini Cassette Holder (Merck Group, Darmstadt, Germany) that was connected to a Masterflex L/S® easy-load® II peristaltic pump and a digital modular drive (Antylia Scientific, Illinois, United States). The pH of a 400 g BC juice (pH 3.08 ± 0.02) was adjusted gradually using a 3 M and 6 M HCl or NaOH at 20 °C while under stirring mode. The juice was then filtered through a Pellicon® Mini Cassette (0.1 m^2) containing Biomax® 5 kDa polyethersulfone membrane (Merck Group, Darmstadt, Germany). The filtration was done at a flowrate of 400 mL/min at 20 °C for four cycles. Following each cycle, distilled water was added to the RTT to make up the initial feed weight of 400 g. In total, PM from all four UF cycles and a RTT from the final cycle were collected. Figure 5.1 shows the schematic diagram of an UF system.

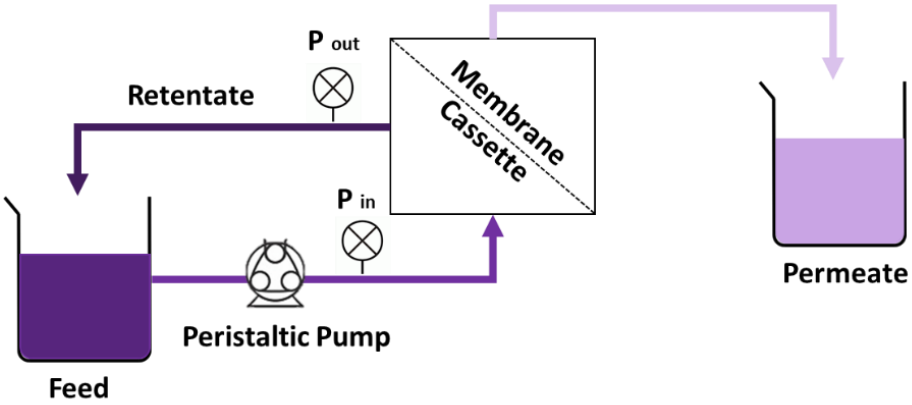

Figure 5.1 Schematic diagram of bench-top ultra-filtration system.

5.2.3. Quantification of Protein

The crude protein (AOAC 968.06) of initial feeds, first PMs and final RTTs was determined via Dumas method by the accredited Nutrition Laboratory in the School of Food and Advanced Technology of Massey University, Palmerston North (AOAC, 2023). All results are reported as the mean (w/w of total solids (TS)) and standard deviation of two samples.

5.2.4. Quantification of Anthocyanins by pH Differential Method

Monomeric ACNs were determined by the rapid pH differential method (AOAC 2005.02) that was modified to fit a 96-well microplate (AOAC, 2023). The initial feeds, PMs (1 to 4) and final RTTs were diluted to 100-fold, 10-fold, and 150-fold, respectively using pH 1 (0.025 M potassium chloride) and pH 4.5 (0.4 M sodium acetate) buffers. Other details on the analysis can be obtained from Chapter 3 and Chapter 4. All results are expressed as cya-glu equivalents and reported as the mean (w/w of TS) and standard deviation of two samples.

5.2.5. Quantification of Galacturonic Acid

Pectin was determined based on the method of Blumenkrantz and Asboe-Hansen (1973) and was modified to fit a 96-well microplate according to the work of O'Donoghue et al. (2017). Before analysis, about 1 mL of the initial feeds, first PMs and final RTTs were centrifuged (14,100 x *g*, 15 min, 20 °C) to remove any insoluble matter. The centrifuged samples were then aliquoted (0.2 mL) and washed with 80% v/v ethanol solution (0.8 mL) to remove majority of the unbound sugars that might interfere with the analysis. The mixed solution was vortexed for 30 s and placed on an ice bath for 30 min. Following that, the cooled mixture was centrifuged at the same settings and the supernatant was removed. The wash cycle was repeated three times before the alcohol insoluble residue was dissolved in 0.2 mL of distilled water. The remaining steps can be obtained from Chapter 3. All results are expressed as GalUA equivalents and reported as the mean (w/w of TS) and standard deviation of two samples.

5.2.6. Molecular Profile of Compounds in Filtered Blackcurrant Juice

The molecular profile of the initial feeds, first PMs and final RTTs was determined by size-exclusion chromatography that was coupled to a multi-angle laser light scattering detector (SEC-MALLS), based on the method described in Chapter 4. Compound separations were done by combining a guard column and three polymer-based aqueous columns that were connected in series: Shodex SB-805 (8.0 mm x 300 mm, 13 µm), SB-803 (8.0 mm x 300 mm, 6 µm) and SB-802.5 (8.0 mm x 300 mm, 6 µm) (Showa Denko, Tokyo, Japan). Large particulates were first removed from the UF samples via centrifugation (14,100 x *g*, 15 min, 20 °C). The initial feeds (0.8 mL), first PMs (0.8 mL) and final RTTs (0.8 mL) were then aliquoted for three cycles of ethanol washing to remove majority of the unbound sugars, like in the previous method. A dust free sodium chloride mobile phase (0.1 M), containing sodium azide (0.02% w/v) was used to dissolve the alcohol insoluble residue and then injected (100 µL) into SEC-MALLS. For comparison purposes, sucrose, fructose, glucose, and GalUA (2% w/v) solutions were also prepared using the same mobile phase and injected (50 µL) into the equipment. All results are reported as the mean and standard deviation of two samples.

5.2.7. Quantification and Identification of Polyphenols in Filtered Blackcurrant Juice

The polyphenol profile (ACNs and non-ACNs) of the initial feeds, PMs (1 to 4) and final RTTs was determined using liquid chromatography (LC) and mass spectrometry techniques that was described in Chapter 3. Prior to sample injection, the feeds, PMs and final RTTs were first diluted to 30-fold, 10-fold, and 50-fold, respectively, with methanol/water/formic acid mixture (50:50:1, v/v/v). The ACNs are expressed as cya-glu equivalents, while the flavonols and phenolic acids that were not found in the polyphenol standard mix were expressed as que-rut and chlorogenic acid equivalents, respectively. All results are reported as the mean (w/w of TS) and standard deviation of two samples.

5.2.8. Statistical Analysis

Statistical analyses were performed using SigmaPlot 14.5 (Systat Software, Inc., Chicago, Illinois, U.S.A). Comparison amongst samples was carried out using the One-Way Analysis of Variance. Values of $p < 0.05$ were considered statistically significant and Tukey's multiple comparisons test was used to identify significant differences among the different samples.

5.3. Results and Discussion

5.3.1. Filtered Blackcurrant Juice

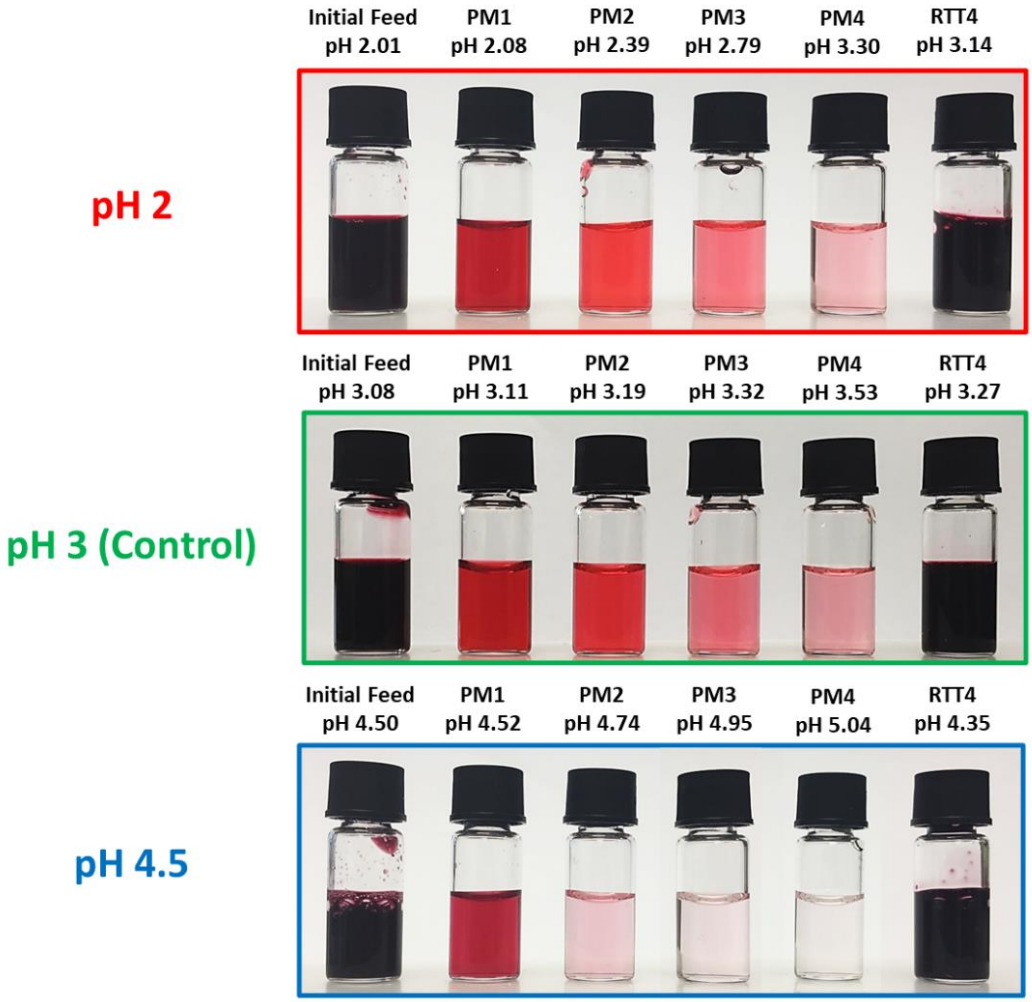

Figure 5.2 Blackcurrant juice (initial feed) and its filtered products—permeates (PM) from cycle 1 to 4 and retentate (RTT) from the final cycle—at pH 2, pH 3 (control) and pH 4.5 along with their pH value at 20 °C.

During UF, small molecules (<5 kDa) were pushed through the membrane and collected as the PM, while large molecules (>5 kDa) were retained and collected as the RTT. The image of the initial UF feeds and their respective filtered products at pH 2, pH 3 (control) and pH 4.5 is shown in Figure 5.2. The control feed had a dark reddish-purple colour that was similar to pH 2 feed, but it changed to dark purple colour at pH 4.5 due to the transformation of some flavylium ACNs to bluish quinonoidal base. Following the first cycle, all three feeds produced lighter coloured PMs, with pH 4.5 PM1 being the least red due to its higher content of quinonoidal base ACNs in comparison to the PM1 at pH 2 and pH 3. The pH of PM1s was similar to the pH of their respective feeds, increasing slightly for every subsequent PMs, likely due to the dilution effect that changed the proportion of hydrogen and

hydroxide ions in them. In addition, the colour intensity of the PMs was also altered after each cycle, where it was especially noticeable at pH 4.5 from PM2 onwards, probably because more ACNs were altered to the colourless carbinol pseudobase at pH >4.5, hence the much paler PM2, PM3 and PM4. The colour and colour intensity of the final RTTs were very much like their respective feeds except that they had pH values that were slightly higher.

5.3.2. Effect of pH on the Molecular Profile of Blackcurrant Juice Components

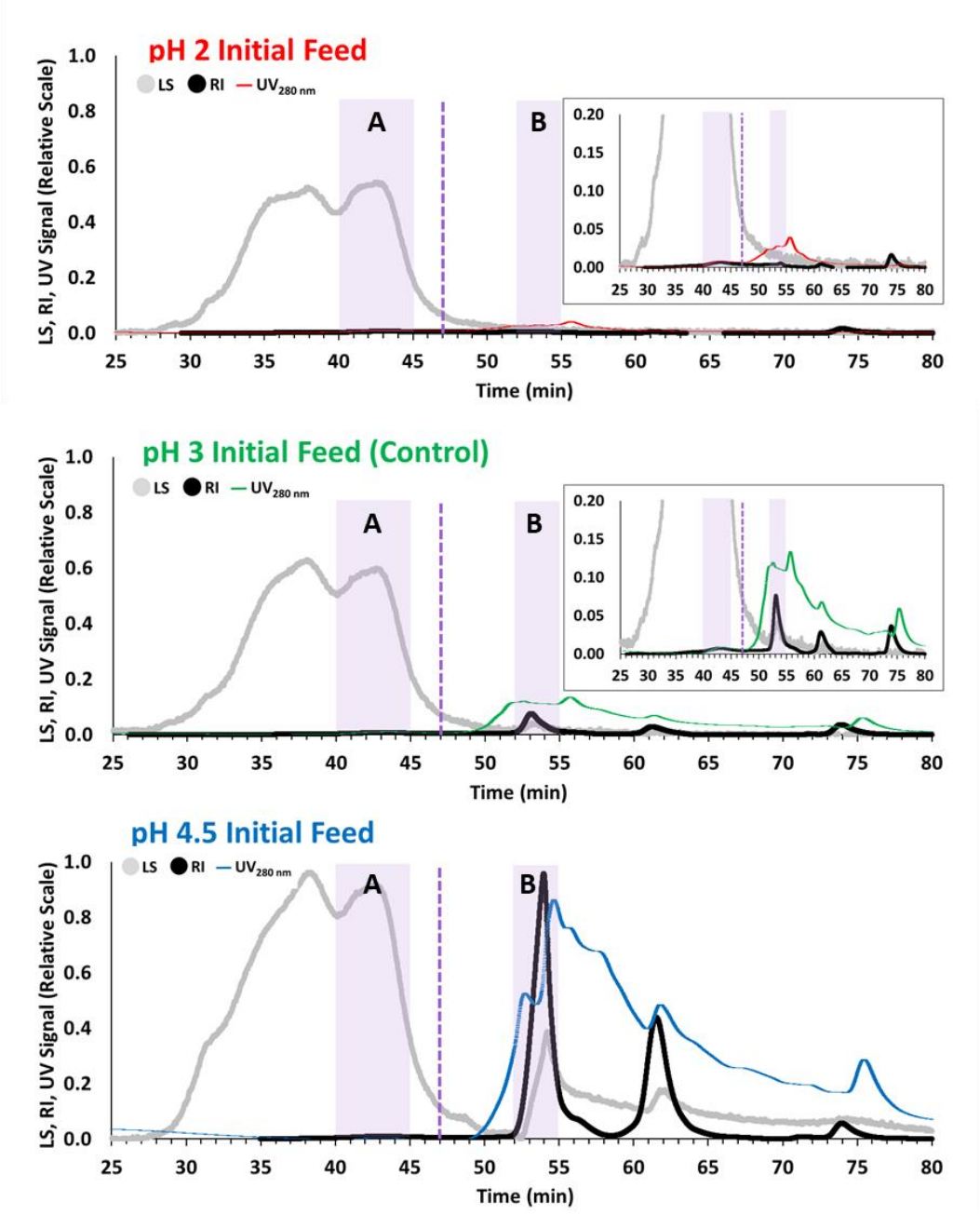

Figure 5.3 SEC-MALLS chromatogram of blackcurrant juice as initial feed at pH 2, pH 3 (control) and pH 4.5 showing light scattering (LS), differential refractive index (RI), and ultra-violet ($UV_{280\ nm}$) signal.

The filtered samples were analysed by SEC-MALLS to understand the effect of pH and membrane separation on the BC juice components. Figure 5.3 shows SEC-MALLS chromatogram of the initial feeds at pH 2, pH 3 (control) and pH 4.5. Despite the strong light scattering (LS) signal between 28 min and 50 min, only two regions are selected as the fraction of interest: fraction A at 40-45 min and fraction B at 52-55 min. Selection was made due to visible differential refractive index (RI) and ultra-violet (UV) peaks shown in the inset figure of pH 3 feed. In general, fraction A has stronger LS signal than fraction B, though it has a much weaker RI and UV signals, indicating that most of the BC juice components are found in fraction B, and are likely to be lower in M_w and contain UV absorbing components. In fact, fraction B was also detected in the undialysed BC juice pectin-rich fraction of previous work (Chapter 4) and was completely removed following its dialysis with an 8 kDa M_w cut-off dialysis tubing. The peak at 52-55 min of the initial feeds may have represented small pectin species that are associated with UV absorbing components and/or unbound components, like phenolic compounds and small plant proteins. An extensive database on plant proteomes has been published by Mohanta et al. (2019) reporting that the M_w of plant proteins could range from ≈0.54 kDa to ≈2236.8 kDa. For example, the wild strawberry (*Fragaria vesca*) and wild cherry (*Prunus avium*) had proteins that ranged from ≈3 kDa to ≈600 kDa (Mohanta et al., 2019), therefore there is a possibility that the low M_w components correspond to small plant proteins.

Fraction A of pH 2 and pH 3 feeds (inset figures of Figure 5.3) demonstrate comparable LS, RI, and UV signals. However, the LS signal at pH 4.5 is slightly stronger than at pH 3, possibly representing slightly more and/or slightly larger components at retention time 40-45 min. Additionally, fraction A at pH 4.5 has an RI peak area (0.0175 RIU min) that is slightly larger than at pH 3 (0.0125 RIU min), indicating that more components are present in fraction A of pH 4.5 feed.

As the pH increases, the chromatogram displays stronger RI and UV signals at region B (52-55 min)—pH 2 < pH 3 < pH 4.5. The weaker RI and UV signals of fraction B may indicate that there are lower amount of low M_w and UV absorbing compounds in pH 2 feed than in pH 3 and pH 4.5 feeds. Sawayama et al. (1988) reported that adjusting the pH of citrus pectin (0.05% w/v) from pH 3.6 to pH 2 caused the increase of M_w and pectin-pectin aggregation. It is likely that the BC pectin lost majority of its negative charges at pH 2 as it was close to its pK_a of ≈1.7 (Chapter 4). Consequently, this could have weakened the electrostatic repulsion forces between the pectin molecules, leading to pectin-pectin aggregation. Moreover, some of the plant proteins present in the juice might also aggregate and sediment at pH 2. A wide variety of plant proteins will have a wide range of isoelectric points, and according to Mohanta et al. (2019) work, their isoelectric point could range between pH 2 and pH 14.

Aggregation and sedimentation of some of the juice components are probably the reason behind the overall low RI and UV signals of pH 2 feed.

On the contrary, fraction B at pH 4.5 has strong RI and UV signals, denoting the abundance of juice components, specifically those with low M_w and UV absorbing ability. This observation likely signifies the effect of pH 4.5 on: (i) the dissociation of bound ACNs from juice components, (ii) fragmentation of pectin and plant proteins into smaller units that might be associated to each other or ACNs and/or (iii) ionic dissociation of the plant proteins from pectin.

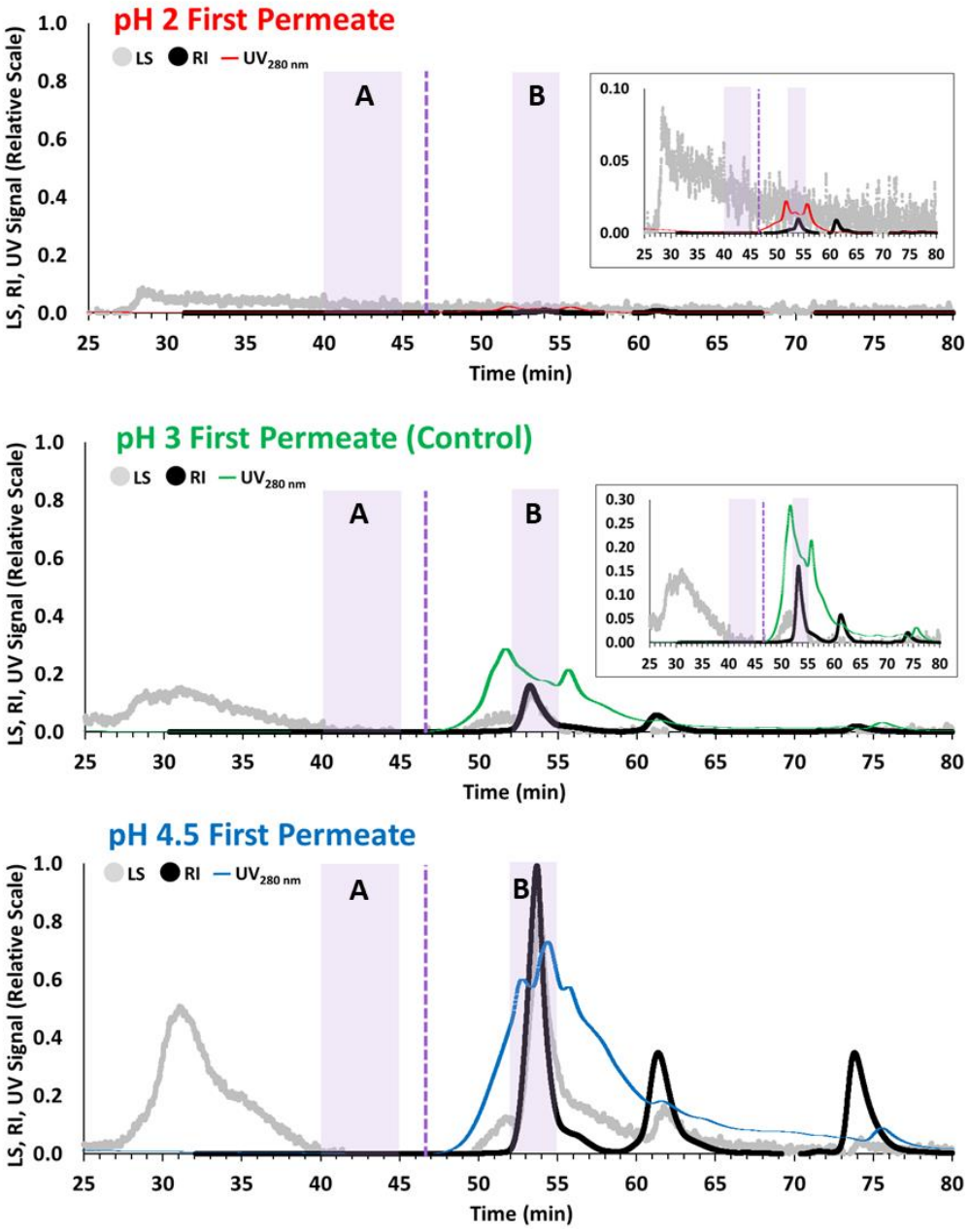

Figure 5.4 SEC-MALLS chromatogram of first permeate at pH 2, pH 3 (control) and pH 4.5 showing light scattering (LS), differential refractive index (RI), and ultra-violet ($UV_{280\ nm}$) signal.

The collected PM would contain low M_w and fragmented juice components that were <5 kDa. The SEC-MALLS chromatogram of PM1 at pH 2, pH 3 (control) and pH 4.5 is shown in Figure 5.4. Overall, the LS, RI, and UV signals for fraction A (40-45 min) are not detected in any of the PM1 chromatograms, confirming the complete size segregation by the UF system. Visible RI and UV peaks are seen in the chromatograms starting from 47 min onwards, and as expected PM1 at pH 4.5 displays the strongest RI and UV signals, while the PM1 at pH 2 shows the weakest signals (inset figure), agreeing with the observation made previously that there was greater quantity of low M_w and UV absorbing components in pH 4.5 BC juice.

Deductions on the identity of low M_w compounds (47 min onwards) were made by comparing the chromatogram of PM1s against major BC sugars—sucrose, fructose, and glucose—and GalUA (Figure 5.5). Comparisons between Figure 5.4 and Figure 5.5 at 52-65 min revealed that the fraction might contain GalUA and very small species of pectin that were associated with proteins and/or phenolic compounds like ACNs. This is because the retention time of the GalUA standard (54-63 min of Figure 5.5) is overlapped with the retention time of the unknown fraction (52-65 min of Figure 5.4). The UV signal observed in the GalUA standard is expected to represent remnants of plant protein and/or phenolic compounds—such as eriocitrin, ferulic and *p*-coumaric acid (Andersson et al., 2017; Fathy et al., 2022; Holser, 2012; Miyake et al., 1997; Saeidi et al., 2011)—of the initial material that is likely to be apple or citrus pectin. The peak at 59-65 min of Figure 5.4 may represent the peak of the unbound sugars of BC juice (59-68 min of Figure 5.5), which are not completely removed during ethanol washings. Since the M_w of sugars—sucrose (≈342 Da), fructose (≈180 Da) and glucose (≈180 Da) (PubChem, 2022g, 2022i, 2022k)—and GalUA (≈194 Da) (PubChem, 2022h) are much lower than the ACNs (≈449 Da to ≈611 Da) (PubChem, 2022e, 2022f, 2022j, 2022l), there is a possibility that fraction B contains dissociated ACNs, though the presence of fragmented pectin and/or protein that are associated with ACNs and other phenolic compounds should also be considered.

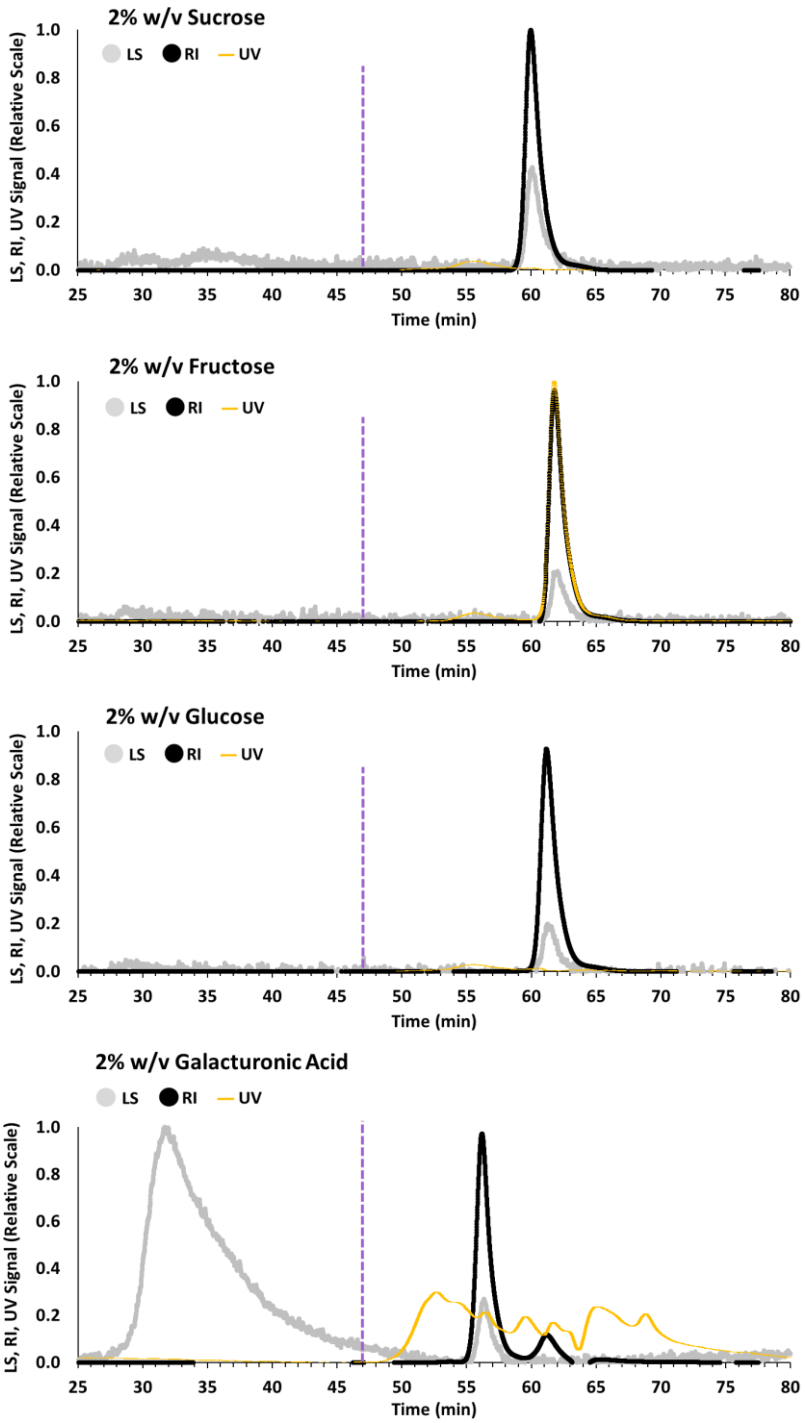

Figure 5.5 SEC-MALLS chromatogram of sucrose, fructose, glucose and galacturonic acid (2% w/v) showing light scattering (LS), differential refractive index (RI), and ultra-violet ($UV_{280\ nm}$) signal.

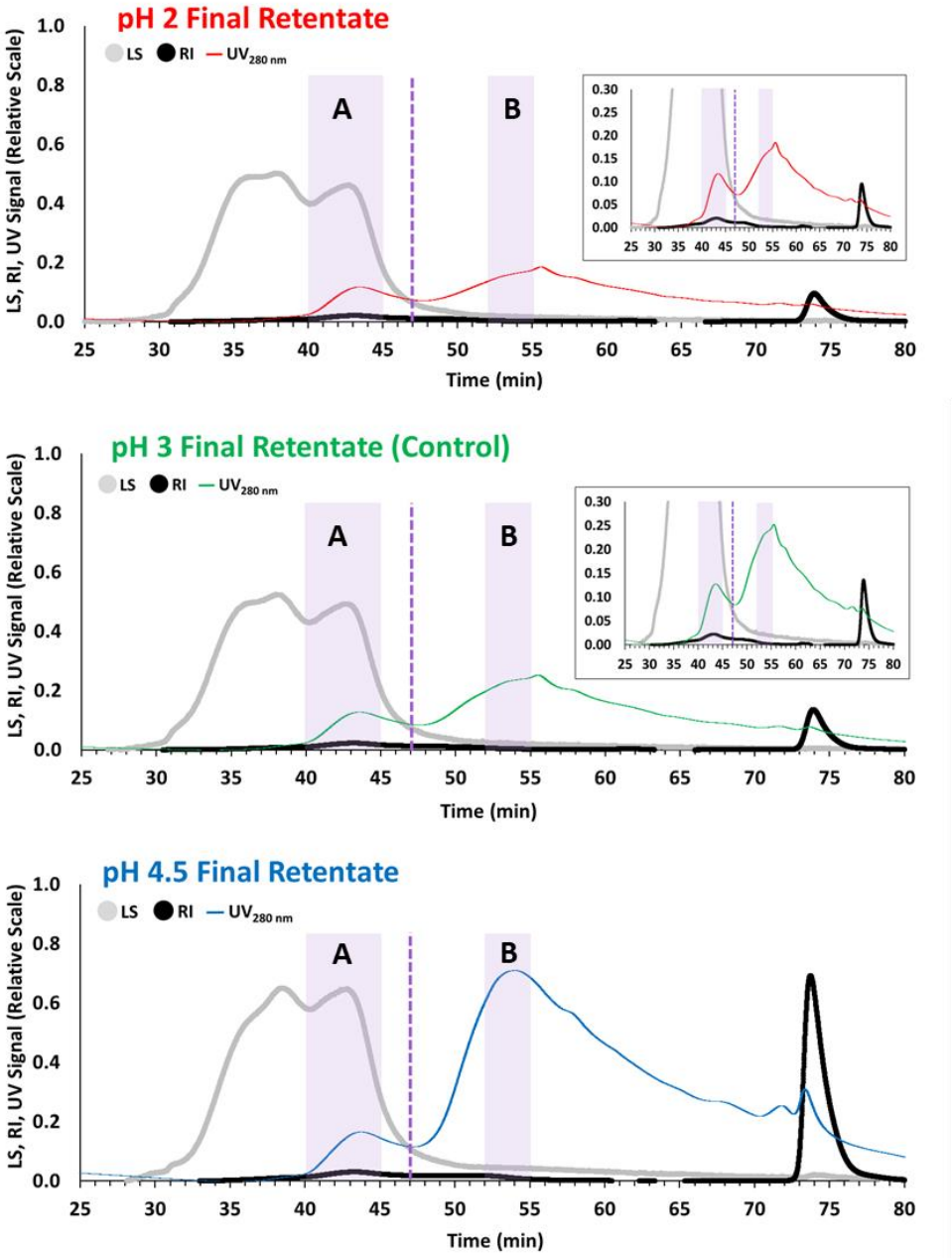

Figure 5.6 SEC-MALLS chromatogram of final retentate at pH 2, pH 3 (control) and pH 4.5 showing light scattering (LS), differential refractive index (RI), and ultra-violet ($UV_{280\ nm}$) signal.

The juice components that were >5 kDa were captured and concentrated in the RTT. This is shown in the SEC-MALLS chromatogram of the final RTT at pH 2, pH 3 (control) and pH 4.5 (Figure 5.6) as they demonstrate the increase of RI and UV peak areas of fraction A, following four cycles of UF. Fraction A at pH 4.5 has greater LS signal and larger RI peak area (0.0369 RIU min) than pH 3 (0.0272 RIU min), confirming the observation made previously on pH 4.5 feed that it has more juice components. This may suggest that tightly bound pectin was released from the residual hemicelluloses and cellulose (<0.1% w/w) that were present in the BC juice when the pH was increased (Andersson et al., 2017;

Hilz et al., 2005; Izydorczyk, 2005). There is minimal RI signal at 52-55 min of pH 2 and pH 3 final RTT (fraction B, inset figures of Figure 5.6), though an apparent shoulder peak was observed before the 52nd min, signifying the presence of slightly higher M_w components with the ability of UV absorption. In contrast, fraction B is much more visible in the main chromatogram of the final RTT at pH 4.5, indicating that it contains much more lower M_w components than the other two RTTs.

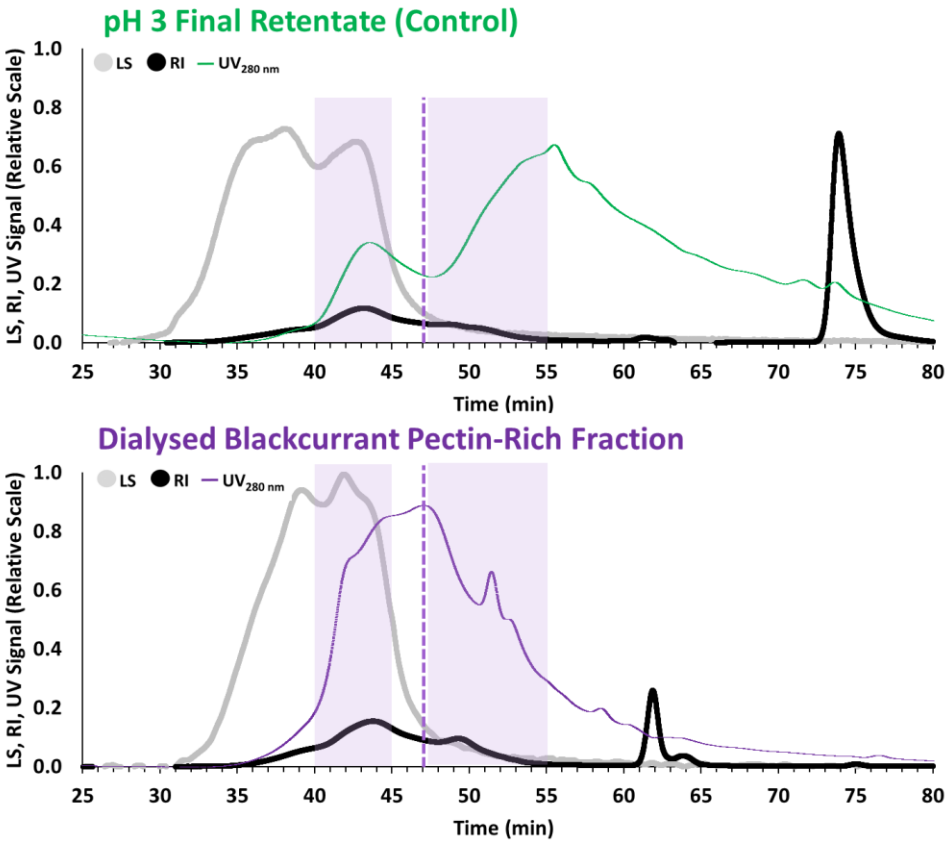

Figure 5.7 SEC-MALLS chromatogram of final retentate at pH 3 (control) and dialysed blackcurrant pectin-rich fraction showing light scattering (LS), differential refractive index (RI), and ultra-violet ($UV_{280\ nm}$) signal.

Figure 5.7 shows the SEC-MALLS chromatogram of pH 3 final RTT and dialysed BC pectin-rich fraction that was isolated and discussed in Chapter 4 (scaled to suit the comparison). Both samples had undergone ethanol washings and membrane separation—UF and dialysis for RTT and pectin-rich fraction, respectively. Comparison between the two, shows that both chromatograms are relatively comparable due to: (i) obvious LS, RI, and UV signals at 40-45 min that correspond to large quantity of high M_w components with high UV absorption and (ii) apparent RI and UV signals at 47 min onwards, which indicate lower M_w components with strong UV absorption. The only difference between them is the two small peaks (61-65 min) shown in the chromatogram of the BC pectin-rich fraction, which may represent some of the unbound plant proteins, BC sugars and/or GalUA units that were not removed during the ethanol washings and dialysis.

Table 5.1 Average molecular weight[a] of fraction A (40-45 min) and fraction B (52-55 min) of blackcurrant juice (initial feed) and its final retentate at pH 2, pH 3 (control) and pH 4.5.

	Initial Feed		Final Retentate	
	Fraction A	**Fraction B**	**Fraction A**	**Fraction B**
	M_w (kDa)	**M_w (kDa)**	**M_w (kDa)**	**M_w (kDa)**
pH 2	83.5 ± 4.10	13.1 ± 8.84	92.6 ± 1.06	32.2 ± 0.14
pH 3 (Control)	76.7 ± 2.33	0.65 ± 0.35	89.6 ± 6.36	26.5 ± 12.2
pH 4.5	88.3 ± 0.78	0.50 ± 0.00	88.3 ± 0.49	17.0 ± 0.78

[a]Results are reported as mean ± standard deviation (n = 2).

The M_w of fraction A and B of the initial feed and final RTT at pH 2, pH 3 (control) and pH 4.5 is presented in Table 5.1. Generally, the M_w of fraction A was larger than fraction B for initial feeds and final RTTs. At pH 3 (≈76.7 kDa), the M_w of fraction A appeared to be slightly smaller than the ones at pH 2 (≈83.5 kDa) and pH 4.5 (≈88.3 kDa). The larger M_w at pH 2 was probably due to pectin-pectin aggregation, since the environmental pH was close to the pK_a (≈1.7) of BC juice pectin, while the larger M_w at pH 4.5 might be due to the release of pectin that was initially bound to the residual hemicelluloses and cellulose found in the BC juice. The M_w of fraction B was higher at pH 2 (≈13.1 kDa) than at other pH levels—≈0.50 and ≈0.65 kDa for pH 3 and pH 4.5, respectively—possibly another indication of pectin-pectin aggregation at very low pH. After four cycles of filtration, there was a slight increase in the M_w of fraction A of final RTTs, but they were comparable to each other. The increase in M_w had also occurred in fraction B, but higher M_w was observed at lower pH levels—≈32.2 kDa, ≈26.5 kDa and ≈17.0 kDa for pH 2, pH 3 and pH 4.5, respectively—likely due to aggregation and fragmentation of juice components at low and high pH, respectively.

5.3.3. Distribution of Protein, Anthocyanin and Pectin in Filtered Blackcurrant Juice

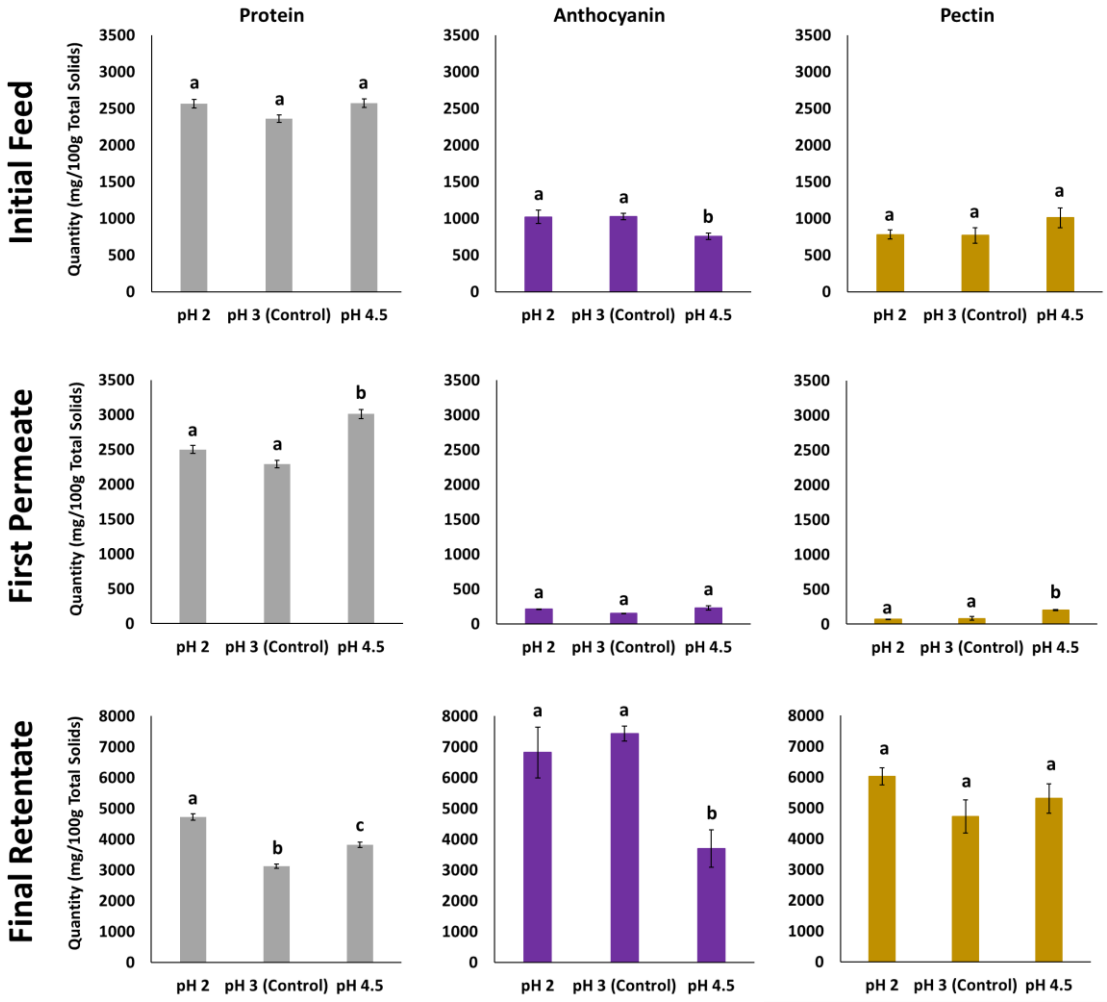

Figure 5.8 Quantity (mg/100 g total solids, mean ± standard deviation) of protein, anthocyanin (expressed as cyanidin-3-*O*-glucoside) and pectin (expressed as galacturonic acid) in blackcurrant juice (initial feed) and its filtered products (first permeate and final retentate) at pH 2, pH 3 (control) and pH 4.5. Means within a group are not significantly different if the letters (a-c) are the same.

The molecular profile of the initial feeds and PM1s showed some indication of ACN dissociation at pH 4.5, therefore the amount of protein, ACN, and pectin in the initial feeds and their filtered products were determined and shown in Figure 5.8. Overall, the amount of protein in all feeds was considerably larger than the amount of ACN and pectin, complementing the proportion of protein (≈2894 mg/100 g TS), ACN (≈1780 mg/100 g TS) and pectin (≈771 mg /100 g TS) in fresh BC juice that was presented in Chapter 3 and Chapter 4. Adjusting the pH of BC juice (pH 3) to pH 2 and pH 4.5 did not significantly affected the concentration of protein and pectin in feed, but it reduced the amount of ACN at pH 4.5 significantly—from 1029 ± 44 mg /100 g TS at pH 3 to 757 ± 45.9 mg /100 g TS at pH 4.5—likely as a result of unavoidable ACN degradation at that pH. At pH 4.5 and in the presence of

water, the ACNs existed as a mixture of blue quinoidal base and colourless carbinol pseudobase with minor flavylium cation. The carbinol pseudobase was likely tautomerized to chalcone form when there was a slight change in temperature before, during and after the UF, which could lead to hydrolytic and auto-oxidative reactions, permanently altering the structure of ACN.

In PM1, the protein remained as the dominant component at all pH levels and was most likely to be low M_w plant proteins or fragmented protein units. The quantity of protein was comparable at pH 2 (2500 ± 56.3 mg/100 g TS) and pH 3 (2292 ± 51.6 mg/100 g TS), but significant increase in protein was detected at pH 4.5 (3009 ± 67.7 mg/100 g TS). Similar trend was also observed in the amount of pectin—70.2 ± 3.9 mg/100 g TS, 83.4 ± 25.6 mg/100 g TS and 201 ± 6.1 mg/100 g TS for pH 2, pH 3 and pH 4.5, respectively. The increase of protein and pectin was probably due to their fragmentation into smaller units as a result of pH adjustment to pH 4.5, allowing them to pass through the 5 kDa membrane and be captured as the PM. Surprisingly, the amount of ACN in PM1 was comparable across all pH levels—212 ± 2.2 mg/100 g TS, 154 ± 1.7 mg/100 g TS and 228 ± 32.1 mg/100 g TS at pH 2, pH 3 and pH 4.5, respectively. The amount of ACN in PM1 was expected to be higher at pH 2 than those at pH 3 because at such low pH BC pectin would have lost most of its negative charges, hence the likelihood of freeing the positively charged ACNs from ionic association. However, the anticipated effect was not observed, likely because the ACNs were bound together with the low M_w pectin and/or protein through various interactive forces and not just ionic bonds. The amount of ACNs at pH 4.5 PM1 was also expected to be greater than the control due to the effect of pH on structural (loss of planar surface) and charge (loss of positive charge) manipulation of ACNs that could dissociate them from the biopolymers. Yet the expected effect was not observed here, possibly because the freed monomeric ACNs might have degraded due to their instability at pH 4.5. The ACNs that were detected in pH 4.5 PM1 could have been those that remained bound to the low M_w pectin and/or protein as biopolymers are known to provide protective effect on ACNs by shielding them from nucleophilic attack of water (Chung et al., 2015; Hubbermann et al., 2006).

The amount of protein in the final RTTs was significantly different across all pH levels—4722 ± 106.3 mg/100 g TS, 3125 ± 70.3 mg/100 g TS and 3819 ± 85.9 mg/100 g TS at pH 2, pH 3 and pH 4.5, respectively. The increase of protein at pH 2 was probably due to aggregation of the proteins and/or proteins that are bound to the pectin, such as extensin (Nuñez et al., 2009), which was then captured in the RTT. Whereas the increase of protein at pH 4.5 might be due to the release of plant glycoproteins from residual hemicelluloses and cellulose at higher pH (Andersson et al., 2017; Hilz et al., 2005; Izydorczyk, 2005). Despite pectin-pectin aggregation at pH 2 and pectin fragmentation at pH 4.5, the amount of pectin in all final RTTs was statistically not different. As for the ACNs, they have

very low M_w (<1 kDa) and therefore they should be able to pass through the 5 kDa membrane and be collected in PM, however in this case high quantity of ACNs was trapped in the final RTT. These ACNs were probably bound to the pectin and protein of the juice via pectin-ACN and protein-ACN interactions. The amount of ACNs in the final RTT was comparable at pH 2 (6823 ± 823.9 mg/100 g TS) and pH 3 (7428 ± 241.8 mg/100 g TS), however significant decrease of ACN was observed in pH 4.5 RTT (3702 ± 613 mg/100 g TS). The decrease was probably attributed to: (i) fragmentation of the pectin and/or protein that released bound ACNs and (ii) degradation of majority of the freed ACNs due to the non-ideal pH of 4.5.

5.3.4. Effect of pH on Anthocyanins and Other Phenolic Compounds

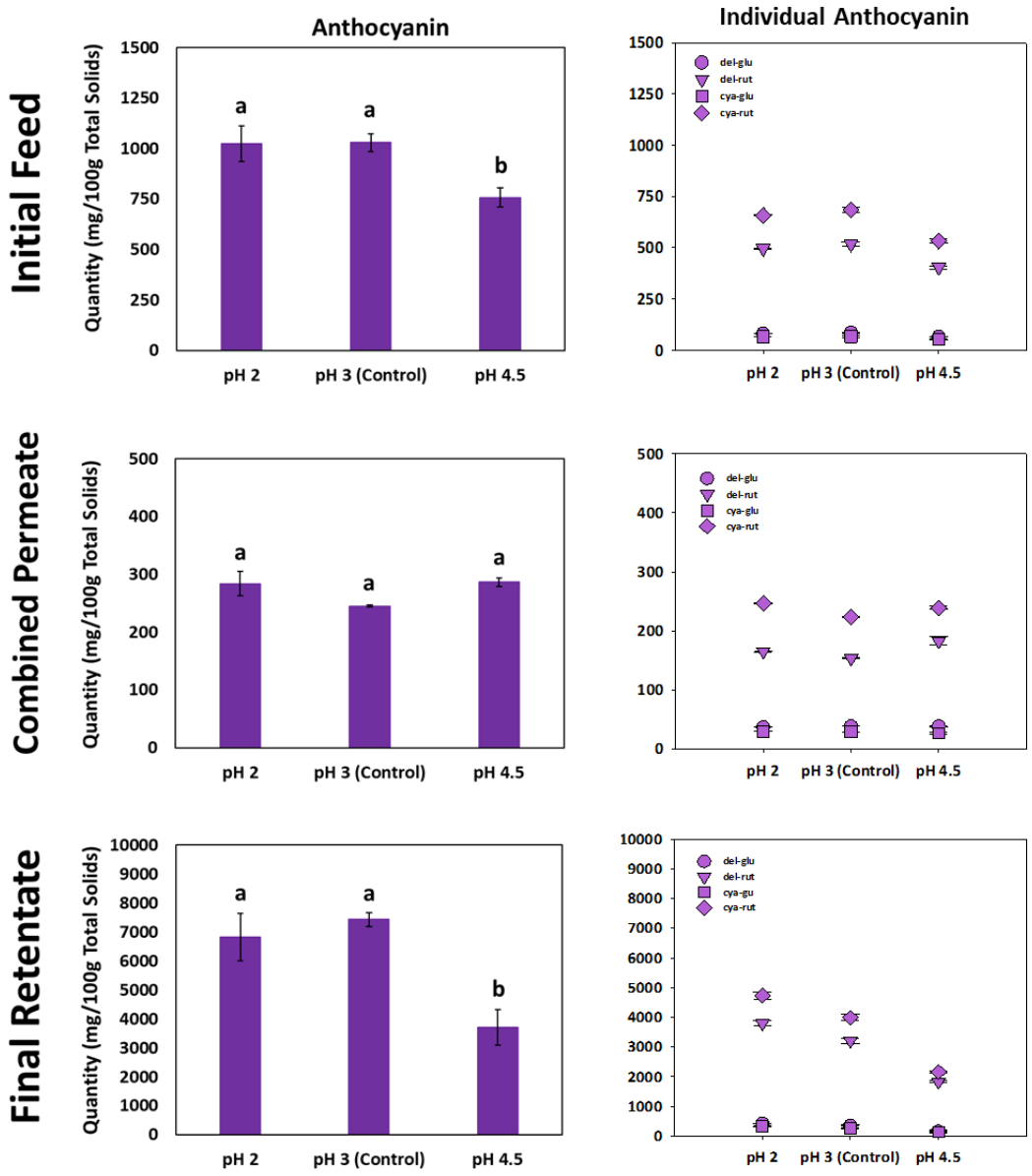

Figure 5.9 Quantity (mg/100 g total solids, mean ± standard deviation) of anthocyanin from pH differential method (expressed as cyanidin-3-*O*-glucoside) and individual anthocyanins from reversed-phase ultra-performance liquid chromatography (del-glu, delphinidin 3-*O*-glucoside; del-rut, delphinidin 3-*O*-rutinoside; cya-glu, cyanidin-3-*O*-glucoside; cya-rut, cyanidin-3-*O*-rutinoside) of blackcurrant juice (initial feed) and its filtered products (combined permeates and final retentate) at pH 2, pH 3 (control) and pH 4.5. Means within a group are not significantly different if the letters (a-c) are the same.

Figure 5.9 shows the overall quantity of ACNs—expressed as cya-glu—and the individual ACNs found in the initial feeds, combined PMs and final RTTs at pH 2, pH 3 (control) and pH 4.5. As expected, the initial feeds and filtered products were dominated by two major ACNs of BC: cyanidin 3-*O*-rutinoside (cya-rut) and delphinidin 3-*O*-rutinoside (del-rut). The cya-rut contributed the most ACNs (≈49-52%),

while the del-rut contributed ≈35-43% of the total ACNs. Collectively, the two minor ACNs—cya-glu (≈3-6%) and delphinidin 3-*O*-glucoside (del-glu, ≈4-9%)—contributed <15% to the total ACNs. When comparing the effect of pH, the result revealed similar trend as the overall ACN quantity that was determined by the pH differential method, where ACNs in pH 4.5 initial feed and final RTT were significantly lower than those at pH 2 and pH 3. Regardless of the pH, the proportion of individual ACNs was comparable amongst the initial feeds,—6%, 38%, 5% and 51% for del-glu, del-rut, cya-glu and cya-rut, respectively, but a slight change in ratio was observed in the combined PMs and final RTT at pH 4.5 as there was increase in the amount of del-rut.

The non-ACN phenolic compounds of the initial feeds, combined PMs and final RTT are presented in Figure 5.10. The first section of the plot shows the flavonols of the BC juice, followed by the phenolic acids and the minor flavanols. In the initial feed, the non-ACN phenolic compounds were at least ten times lower than ACNs and they were dominated by three flavonols (myricetin 3-*O*-galactoside/ glucoside, quercetin 3-*O*-glucoside, and que-rut) and two phenolic acids (3-caffeoylglucoside and neochlorogenic acids), irrespective of the pH. After filtration, about a quarter of the initial flavonols were captured in the PMs, but almost all the 3-caffeoylglucoside and neochlorogenic acids (≈92% and ≈99% of the initial amount in feed, respectively) were transferred to the PMs, likely because these phenolic acids were not bound to the juice components. However, the final RTTs show the opposite trend; they contained small amount of 3-caffeoylglucoside and neochlorogenic acids (averaging to ≈26% and ≈34% of the initial amount in feed, respectively) but large amounts of flavonols that were 3.5 times more concentrated than the initial feed, possibly signifying that the major flavonols were bound to the large M_w juice components. Furthermore, the flavonols at pH 4.5 were significantly lower than those at more acidic pH, likely because they were structurally altered and degraded at higher pH, as shown by Yao et al. (2014) and Wang and Zhao (2016).

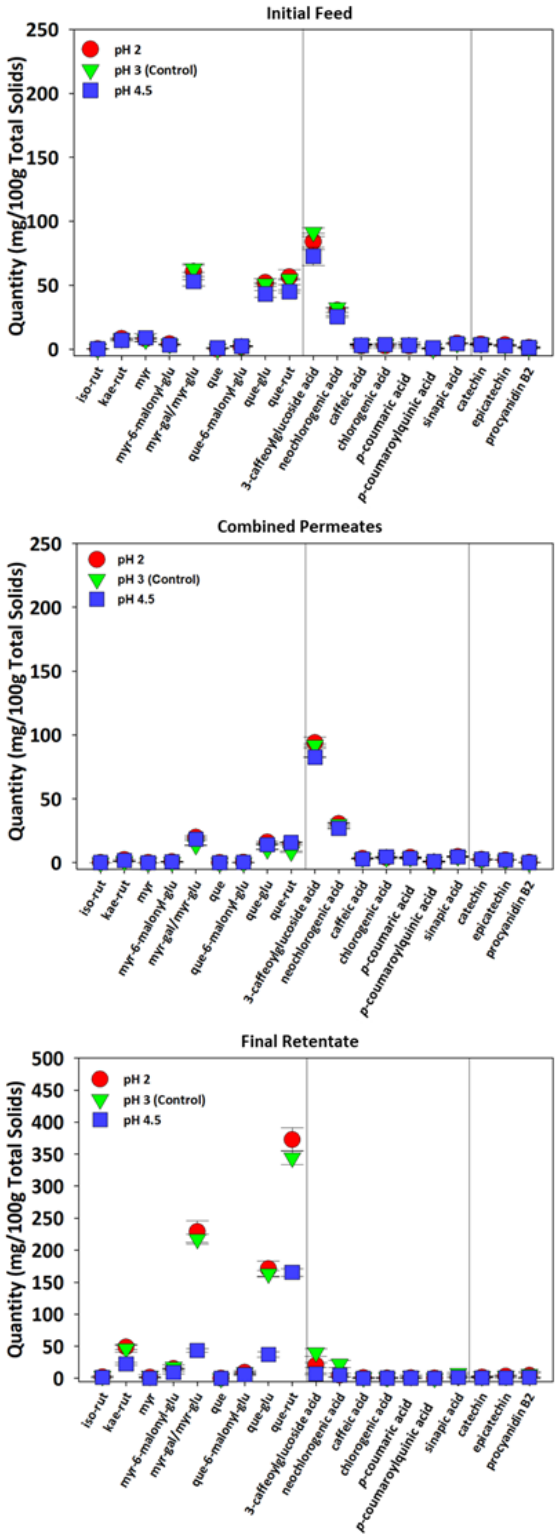

Figure 5.10 Quantity (mg/100 g total solids, mean ± standard deviation) of flavonols (iso-rut, isorhamnetin 3-*O*-rutinoside; kae-rut, kaempferol 3-*O*-rutinoside; myr, myricetin; myr-6-malonyl-glu, myricetin 3-*O*-(*6*-malonyl)-glucoside; myr-gal, myricetin 3-*O*-galactoside; myr-glu, myricetin 3-*O*-glucoside; que, quercetin; que-6-malonyl-glu, quercetin 3-*O*-(*6*-malonyl)-glucoside; que-glu, quercetin 3-*O*-glucoside; que-rut, quercetin 3-*O*-rutinoside), phenolic acids and flavanols in blackcurrant juice (initial feed) and its filtered products (combined permeates and final retentate) at pH 2, pH 3 (control) and pH 4.5.

5.4. Conclusions

- The study demonstrated that the BC juice is a complex system with multiple components.
- Segregation of juice components based on size was only partially effective as the bulk of the ACNs were still trapped in the RTT along with the BC pectin and other large M_w compounds, hence obtaining an ACN-free BC pectin fraction could not be achieved based on the current separation methods.
- The molecular profile of the final RTT at pH 3 was similar to the dialysed BC pectin-rich fraction that was isolated in Chapter 4.
- The effect of pH was seen clearly in the molecular profile of the BC juice. It altered the molecular properties of the juice components, demonstrating aggregation and fragmentation at pH 2 and pH 4.5, respectively.
- Lowering the juice pH to 2 did not show any indication of ACNs dissociation, likely because the ACNs were associated with the BC biopolymers by interactive forces other than the ionic bonds.
- Adjusting the juice pH to 4.5 could have released some of the ACNs from BC biopolymers via electrostatic dissociation and change in ACN planarity, though the likelihood of freed monomeric ACNs to degrade at pH 4.5 was high. Thus, the detected ACNs in pH 4.5 PM1 were highly likely to be bound and protected by the low M_w pectin and protein that had diffused through the 5 kDa membrane.
- Overall, the study demonstrated that electrostatic forces were not the only bonds involved in pectin-ACN interactions and that the ACNs were also likely to be associated to the BC proteins through protein-ACN interactions.

The bound ACNs made the BC pectic fraction visually distinctive and unique in comparison to the commercial apple and citrus pectins. This provided opportunities for a combined interaction study between pectin, protein, and polyphenols. The following chapter describes the investigation work on pectin-protein interactions between the isolated ACN-rich pectin fraction and whey protein in an attempt to elucidate the cause of physical instability of a mixed system containing BC juice and milk.

MASSEY UNIVERSITY
TE KUNENGA KI PŪREHUROA
UNIVERSITY OF NEW ZEALAND

GRADUATE RESEARCH SCHOOL

STATEMENT OF CONTRIBUTION DOCTORATE WITH PUBLICATIONS/MANUSCRIPTS

We, the student and the student's main supervisor, certify that all co-authors have consented to their work being included in the thesis and they have accepted the student's contribution as indicated below in the Statement of Originality.

Student name:	Nurhazwani Salleh
Name and title of main supervisor:	Associate Professor Lara Matia-Merino
In which chapter is the manuscript/published work?	Chapter 6
What percentage of the manuscript/published work was contributed by the student?	85%

Describe the contribution that the student has made to the manuscript/published work:

The experimental work and writing were carried out fully by the student with some input from the supervisors on the draft version.

Please select one of the following three options:

- (●) **The manuscript/published work is published or in press**

  Please provide the full reference of the research output:

  Salleh, N., Goh, K. K. T., Waterland, M. R., Huffman, L. M., Weeks, M., & Matia-Merino, L. (2022). Complexation of Anthocyanin-Bound Blackcurrant Pectin and Whey Protein: Effect of pH and Heat Treatment. Molecules, 27(13), 4202. https://doi.org/10.3390/molecules27134202

- ( ) **The manuscript is currently under review for publication**

  Please provide the name of the journal:

- ( ) **It is intended that the manuscript will be published, but it has not yet been submitted to a journal**

Student's signature:	Nurhazwani Salleh Digitally signed by Nurhazwani Salleh Date: 2023.03.01 10:33:19 +13'00'	Main supervisor's signature:	Lara Matia-Merino Digitally signed by Lara Matia-Merino DN: cn=Lara Matia-Merino, c=NZ, ou=School of Food and Advanced Technology, email=l.matia-merino@massey.ac.nz Date: 2023.02.28 17:29:42 +13'00'

This form should be placed at the beginning of each relevant thesis chapter.

Chapter 6 Complexation Between Anthocyanin-Bound Blackcurrant Pectin and Whey Protein: Effect of pH and Heat Treatment

6.1. Introduction

Interaction between polysaccharides, proteins and polyphenols occurs in various food systems and can affect the physical stability (Chevalier et al., 2019; Thongkaew et al., 2014), appearance (Chung et al., 2015; Millet et al., 2017), texture (Chevalier et al., 2019; Lin et al., 2018) and taste of food (Jauregi et al., 2016; Rinaldi et al., 2010). The components (polysaccharides, proteins, and polyphenols) that interact may be from natural ingredients—such as milk, egg, flour, and fruit puree—or isolated functional ingredients—such as whey protein (WP), plant extracts, gelatine, and pectin. These ingredients may interact with each other through covalent and/or non-covalent bonds. Covalent interaction is highly specific to certain biopolymers and polyphenols, and it tends to be stable against pH and ionic changes. In contrast, the non-covalent interactions can be affected by pH and ionic changes. The types of non-covalent interactions that can happen between the interactive components are (i) electrostatic, (ii) hydrophobic and (iii) hydrogen bonding interactions, although usually a multitude of interactive forces is responsible for the association of different functional groups of the components, and they have been discussed in various review papers (Dangles & Dufour, 2006; Dangles & Fenger, 2018; McClements, 2006; Schmitt et al., 1998; Siebert et al., 1996; Spencer et al., 1988; Yildirim-Elikoglu & Erdem, 2018).

In a binary polysaccharide-protein system, an anionic pectin is able to complex with WPs via electrostatic interactions as a result of opposite charges between the carboxyl groups of pectin (negative) and the amino groups of protein (positive) (Dumay et al., 1999; Girard et al., 2004; Girard et al., 2002, 2003a, 2003b; Wang & Qvist, 2000). However, the interaction depends heavily on the environmental pH as protein is amphoteric (Sperber et al., 2009), while pectin can lose its negative charges at pH below its pK_a value. Unlike the pectin-WP system, a polyphenol-protein system between anthocyanins (ACN) and WPs is less documented, especially at the molecular level. The ACNs may associate with WPs via various modes of interaction, depending on the structure of the ACN that

changes according to its environmental pH. Due to the alterations in ACN structure, it is believed that at different pH levels ACN exhibits different biopolymer affinities, where some reports have shown that flavylium cation binds more to biopolymers in comparison to carbinol pseudobase, especially when present at high concentration (Dangles & Fenger, 2018; Fernandes et al., 2014; Lin et al., 2016; Vuong & Hongsprabhas, 2021).

In addition to pH effects, heating also plays an important role in pectin-WP and ACN-WP interactions because the process of manufacturing food usually involves heat treatment. It is well known that heating at temperatures >60 °C causes the unfolding of the globular WPs and exposure of its hydrophobic and charged amino acids (AA) (Anema, 2017; Dannenberg & Kessler, 1988; Law & Leaver, 2000), which increase the binding sites for pectin-WP and ACN-WP interactions. Furthermore, heating can alter the structure of ACNs to chalcones, which can further develop into the derivatives of aldehyde or benzoic acid (Oancea, 2021).

It has been reported that the capacity of polyphenols—grape seed extract, hibiscus extract, tannic acid and catechin—to precipitate WPs was reduced significantly when WPs were complexed with apple pectin, indicating that the associated pectin provided the protein with some stability against precipitation (Thongkaew et al., 2014). Many researchers have worked on similar interaction work following the study above by exploring the interaction between other types of polysaccharides, proteins, and polyphenols for various research purposes (Cheng et al., 2018; Lin et al., 2021; Oliveira et al., 2016; Stănciuc et al., 2018; Stănciuc et al., 2017; Zhang et al., 2022). Undeniably, these studies contributed useful insights to the current field of work, but the sole use of isolated ingredients may not be comparable to the use of a natural ingredient. Thus, a less refined composite material like the one used in the present work may offer a different approach. A recent study by Chevalier et al. (2019) found that a blueberry pectic material (containing pectin, protein and polyphenols) that was extracted from blueberry puree was able to complex with WPs, and attributed the complexation to electrostatic interaction between the pectic and proteic components. However, investigation on the influence of blueberry polyphenols on the blueberry pectin-protein complexes was not pursued as the focus was given to the study of rheological and textural properties of a blueberry-WP smoothie drink (Chevalier et al., 2019). In another study, protein-polyphenol mesostructures were formed by complexing WPs with berry juice concentrates that were rich in polyphenols (mainly ACNs) and the authors attributed the complexation to protein-polyphenol interaction only, without addressing the possible interaction with the pectin found in the juice concentrates (Schneider et al., 2016).

Research gap from the above publications presented a bridging opportunity for a polysaccharide, protein, and polyphenol interaction study. Thus, a study between a composite pectic material known

as the ACN-bound blackcurrant pectin (BCP) and WPs was carried out as it allowed us to address the combined effect of pectin and ACNs when complexing with WPs. We hypothesise that the impact of bound ACNs on BCP-WP complexation can be studied through pH influence (pH 3.5 and pH 4.5) and heat treatment (85 °C for 15 min). The two pH levels were chosen based on: (i) the pH range of acidified milk drinks, which is between pH 3.6 and pH 4.6 (Wu et al., 2014) and (ii) the equilibrium of ACN structures at the two pH levels—more flavylium cations at pH 3.5 and less flavylium cations at pH 4.5. Heat treatment was carried out at 85 °C for 15 min to simulate the conditions of ultra-high temperature (UHT) treatment where ≥90% of the WPs are denatured (Anema, 2017). The current work involved: (i) preparation of BCP-WP mixtures at various conditions—pH 3.5 and pH 4.5, without and with heating, and different heating sequences (mixed-heated vs. heated-mixed); (ii) physical stability, particle size and zeta-potential measurements of the mixtures; (iii) determination of BCP in the sedimented fraction of the mixtures; (iv) investigation on the changes that occur in the functional groups of BCP and WPs using Fourier-Transform Infrared (FTIR) spectroscopy.

6.2. Materials and Methods

6.2.1. Materials

A dialysed high methoxyl BCP (65.2 ± 10.2%) was isolated from the blackcurrant juice and prepared according to the method described in our earlier work (Chapter 4) and its composition can also be obtained in that chapter.

The WP powder (Whey Protein Isolate 895) containing 94.2% w/w of protein was obtained from Fonterra, Auckland, New Zealand. As mentioned in Chapter 2, protein aggregates can affect the size distribution of complexes that are formed via electrostatic interaction (Schmitt et al., 2000). Therefore, aggregate-reduced WP powder was prepared based on Schmitt et al. (2000) method with some modifications. The protein powder was first hydrated with distilled water (20% w/w) and left stirring overnight at 4 °C. The pH of the solution was adjusted to pH 4.5 using 3 M and 6 M hydrochloric acid. Aggregate removal was carried out by high-speed ultra-centrifugation (78,702 x *g* for 1 h at 20 °C) using a Sorvall WX Ultra 100, T-865 motor (Thermo Fisher Scientific Inc., Waltham, Massachusetts, U.S.A). The supernatant was then carefully separated from the sediment, filtered using a 0.45 µm Durapore hydrophilic polyvinylidene fluoride vacuum filter (Merck Group, Darmstadt, Germany) and finally freeze-dried. The freeze-dried material contained 89.8% w/w of protein on dry weight basis.

Analytical grade D-(+)-galacturonic acid (GalUA) monohydrate (Sigma-Aldrich, St. Louis, Missouri, U.S.A) and 3-phenylphenol (Sigma-Aldrich, St. Louis, Missouri, U.S.A) were used as the standard and colorimetric reagent in GalUA analysis, respectively. A HPLC grade of cyanidin 3-*O*-rutinoside chloride and delphinidin 3-*O*-rutinoside chloride (Extrasynthese, Lyon, France) were used in zeta-potential measurements and FTIR analyses. All other chemicals were also of analytical grade and purchased from local companies. Chemical, stock, and buffer solutions were prepared using Milli-Q® water (Merck Group, Darmstadt, Germany) and stored in dust-free bottles.

6.2.2. Complexation of Blackcurrant Pectin and Whey Protein

In the current study, the chosen concentrations of BCP and WP were similar to those previously used by Sperber et al. (2009). Pectin and protein stocks (0.5% w/v) were prepared using distilled water and hydrated overnight at 4 °C under gentle stirring. Mixtures were kept in dust-free opaque bottles to avoid interference from dust particles during size measurements and to minimise light degradation of the ACNs. Appropriate amounts of BCP and WP stocks were measured to achieve a final concentration of 0.02% w/v BCP and a Pectin:Protein ratio of 1:1. Pectin concentration in BCP and, protein concentration in the aggregate-reduced WP, were calculated based on the amount of total carbohydrates (78% w/w) and protein (90% w/w) contained in the powders, respectively.

Firstly, the BCP stock solution was added to the pH 3.5 sodium citrate buffer (1 mM) or pH 4.5 sodium acetate buffer (1 mM). Under gentle stirring, the protein stock was then added to the buffered pectin solution and then mixed at 20 °C for 30 min. This mixture is referred as the "**non-heated BCP-WP" (NH BCP-WP)** system (Figure 6.1). For a **"mixed-heated BCP-WP" (MH BCP-WP) system** (Figure 6.1), the mixture was heated at 85 °C for 15 min to achieve ≥90% protein denaturation (Anema, 2017) and then cooled down in an ice bath. Preparation of the "**heated-mixed BCP-WP" (HM BCP-WP)** system required the 0.5% w/v protein stock to be hydrated in buffered solution (Figure 6.2) instead of distilled water. The buffered protein stock was then heated at 85 °C for 15 min and cooled down in an ice bath before adding it to the buffered pectin solution.

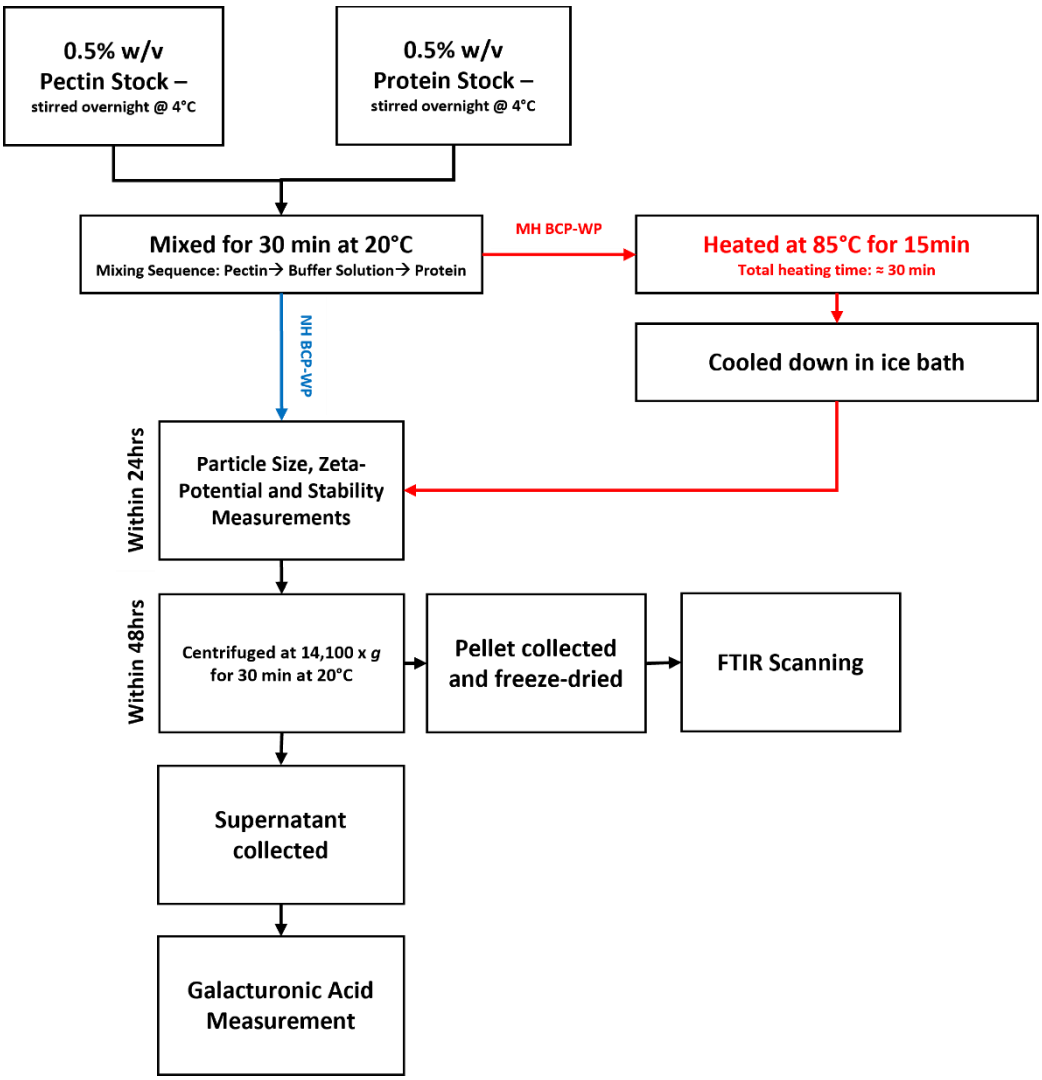

Figure 6.1 Preparation steps for non-heated (NH) and mixed-heated (MH) blackcurrant pectin-whey protein (BCP-WP) mixtures and the measurement techniques used.

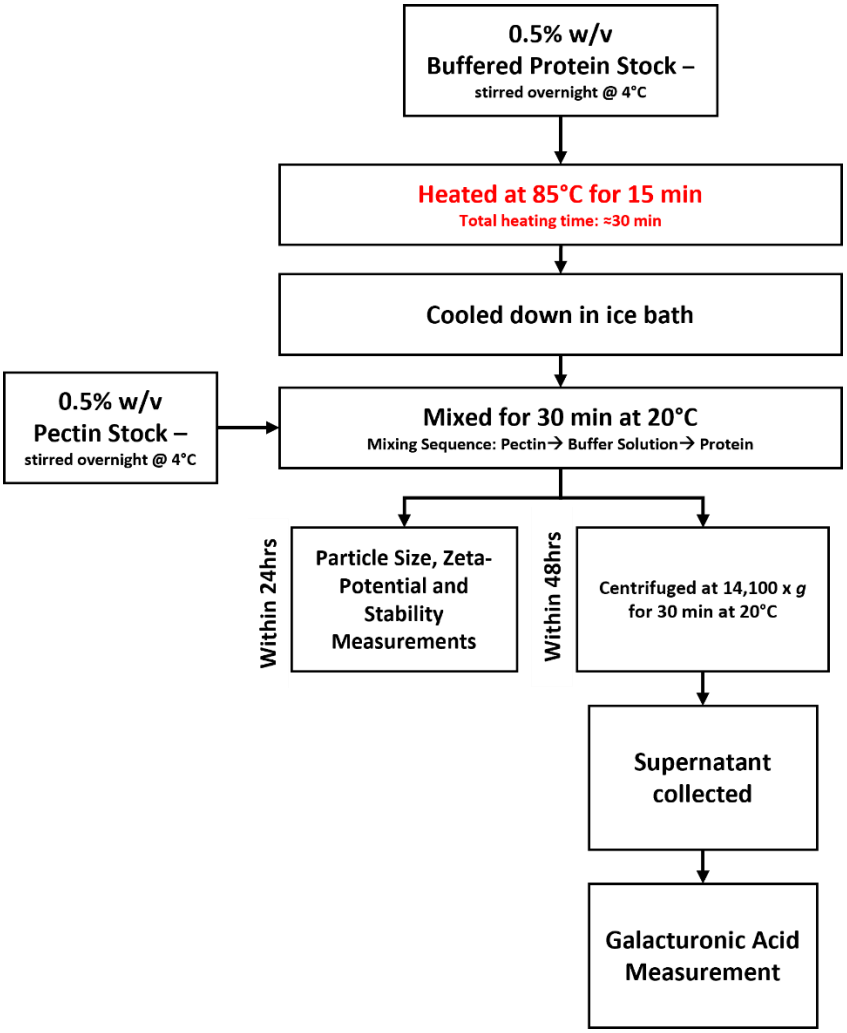

Figure 6.2 Preparation steps for heated-mixed blackcurrant pectin-whey protein mixture and the measurement techniques used.

6.2.3. Physical Stability Measurement

The stability of the mixtures was qualitatively determined by the Turbiscan Lab (Formulaction, Toulouse, France) at regular intervals over a sample height of 30 mm. A clear cylindrical glass cell was used to contain the sample (4 mL) immediately after sample preparation, and data were collected every 30 s for 24 h at 20 °C to simulate the environment of a typical UHT product. The TSI values are reported as the mean of two readings.

6.2.4. Particle Size and Zeta-Potential Measurements

The particle size (Z-average size) and zeta-potential of the controls (BCP and WP) and their mixtures were determined using a Zetasizer Pro (Malvern Panalytical Ltd., Malvern, United Kingdom). A low volume cuvette (ZEN0040) and folded capillary cell DTS1070 (Malvern Panalytical Ltd., Malvern, United Kingdom) were used for their size and surface charge measurements, respectively. Sample

filtration was not performed prior to size measurement to avoid exclusion of the formed complexes. The zeta-potential values of ACN mix containing cyanidin 3-*O*-rutinoside (52%) and delphinidin 3-*O*-rutinosides (48%) were also determined by preparing a stock solution (1.73 x 10^{-1} w/v) and diluting it to 9 x 10^{-4} % w/v using a pre-chilled pH 3.5 sodium citrate (1 mM) or pH 4.5 sodium acetate (1 mM) buffer. Detailed information on that ACN zeta-potential measurements can be found in Chapter 3. Three measurement readings were taken for each sample at 20 °C. The Z-average and zeta-potential values are reported as the mean and standard deviation of at least two readings.

6.2.5. Quantification of Galacturonic Acid

Uronic acid was determined by Blumenkrantz and Asboe-Hansen (1973) colorimetric method that was modified to fit a 96-well microplate (O'Donoghue et al., 2017). Details on the test can be obtained from Chapter 3. The mixtures were centrifuged after 24 h (14,100 x *g* for 30 min at 20 °C) and the supernatant was separated from the pellet. Centrifugation of the pectin control was also carried out, but no sedimentation was observed. The amount of GalUA in the supernatants was measured (regarded as the soluble complexes) and the percentage of GalUA in the pellet (regarded as insoluble complexes) was calculated by difference, based on the initial amount of GalUA in BCP. The assay was carried out twice and the samples were each measured in triplicate. The amount of uronic acid is reported as % (w/w) of GalUA equivalents and the mean and standard deviation of three readings.

6.2.6. Fourier-Transform Infrared Spectroscopy

Pellets (insoluble complexes) obtained after centrifugation of the mixtures were freeze-dried and placed on an iD7 ATR (Thermo Fisher Scientific Inc., Waltham, Massachusetts, U.S.A) diamond stage that was attached to a Nicolet™ iS™ 5 FTIR Spectrometer (Thermo Fisher Scientific Inc., Waltham, Massachusetts, U.S.A). Since no sedimentation was observed in the BCP and WP controls at both pH values, dried powders of the controls were used for the scanning. In addition, the dried form of cyanidin 3-*O*-rutinoside chloride and delphinidin 3-*O*-rutinoside chloride were also scanned for comparison with BCP. The FTIR scanning was done at 20 °C and each sample was only replicated twice (n=2)—controls and freeze-dried insoluble fractions—as the recorded spectra between the duplicated scans and samples were highly reproducible. The infrared spectra were recorded within the range of 400 cm^{-1} to 4000 cm^{-1} and band positions were identified by the Omnic™ Spectra software (Thermo Fisher Scientific Inc., Waltham, Massachusetts, U.S.A). The results were averaged, normalised, and plotted using SigmaPlot 14.5 (Systat Software, Inc., Chicago, Illinois, U.S.A). A consolidated table on band assignments can be obtained from Chapter 3.

6.2.7. Statistical Analysis

Statistical analyses were performed using SigmaPlot 14.5 (Systat Software, Inc., Chicago, Illinois, U.S.A). Comparison between samples and controls was carried out using the One-Way Analysis of Variance. Values of $p < 0.05$ were considered statistically significant and Tukey's multiple comparisons test was used to identify significant differences among the different samples.

6.3. Results and Discussion

6.3.1. Visual Appearance and Physical Stability of Blackcurrant Pectin-Whey Protein Mixtures

Despite containing equal amounts and types of ACNs (delphinidin 3-*O*-glucoside, delphinidin 3-*O*-rutinoside, cyanidin 3-*O*-glucoside and cyanidin 3-*O*-rutinoside), colour variation was observed between the two BCP controls at pH 3.5 (vivid pink) and pH 4.5 (pale purple) (Figure 6.3). This is likely due to the slight change in the molecular structure of the ACNs as their colour depends on several factors: (i) the number of hydroxy and methoxy groups on the aglycone unit, (ii) the type of sugar on the aglycone unit, and (iii) the amount of positive charges found at the pyrylium ring (Rivas-Gonzalo, 2003; Schwartz et al., 2008). The BCP control at pH 3.5 appeared pink because a proportion of the ACNs present were in the flavylium cationic form (red) and since water was present, some of the ACNs might also exist as the carbinol pseudobase (colourless) form. In contrast, the BCP control at pH 4.5 appeared to be pale purple because the ACNs were mainly in quinoidal base (blue) and carbinol pseudobase (colourless) form. Similar colour variation was also observed in the NH and HM BCP-WP mixtures.

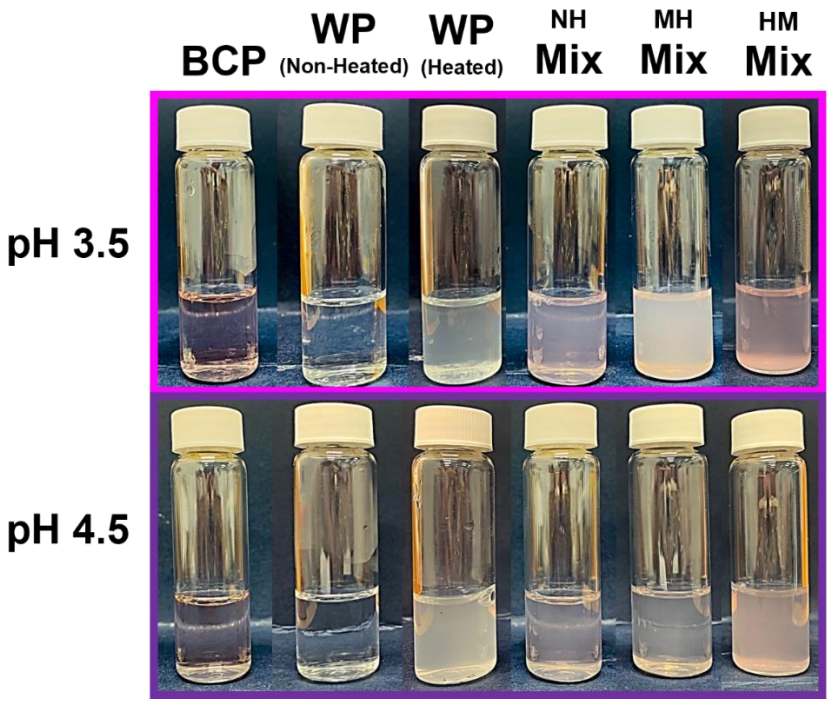

Figure 6.3 Blackcurrant pectin (BCP), whey protein (WP) and their mixtures (NH, Non-Heated; MH, Mixed-Heated; HM, Heated-Mixed) at pH 3.5 and pH 4.5.

Regardless of the environmental pH, both the BCP and non-heated WP controls were transparent. When the two materials were mixed, they complexed with each other causing the mixtures to be

turbid (NH mixtures), indicative of possible pectin-protein interactions. Applying heat caused the colour of the MH mixtures to fade away. This is likely because the high heat (85 °C) can irreversibly change the structures of the ACNs by opening the pyrylium ring to form chalcones, which are colourless (Oancea, 2021; Patras et al., 2010). Further thermal degradation will then ensue separating the ACNs from their sugar glycosyl molecules (Oancea, 2021) and permanently disabling the ability of ACN to generate colour. The turbid state of the heated WP control in Figure 6.3 clearly indicates that protein denaturation and protein-protein interactions had already occurred during the initial heating. Therefore, the turbidity observed in both HM mixtures might be contributed by the turbidity of the heated WP control and the complexes from pectin-protein interactions. Since heating was applied only to the WP, the HM samples were able to retain the colour of the ACNs.

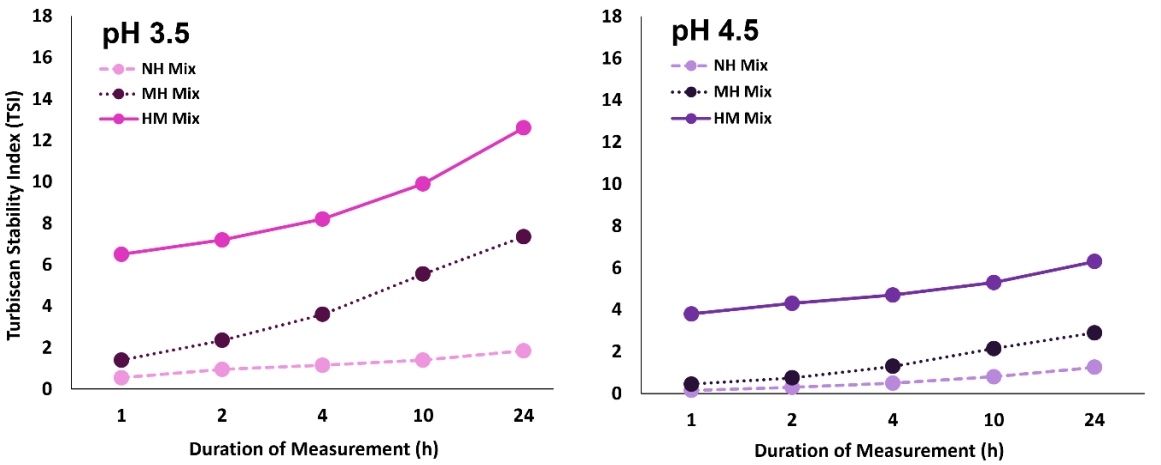

Figure 6.4 Turbiscan Stability Index (TSI) of blackcurrant pectin-whey protein mixtures (NH, Non-Heated; MH, Mixed-Heated; HM, Heated-Mixed) at pH 3.5 and pH 4.5 measured across 24-h timeframe.

Based on stability measurements, both the NH mixtures (pH 3.5 and pH 4.5) had comparable low TSI values that were difficult to be differentiated visually (Figure 6.3 and Figure 6.4, respectively). However, when heated at pH 3.5, the destabilisation of MH mixture increased drastically, matching its high turbidity shown in Figure 6.3. In contrast, the effect of heat on pH 4.5 MH mixture was less impactful. Heating increased the TSI value of pH 4.5 MH mixture slightly, but it did not affect its weak destabilised state nor its turbidity as it remained visually comparable to its NH counterpart. This could suggest that the heat treatment caused the increase in BCP-WP interactions at pH 3.5, but not so much at pH 4.5. On the other hand, the heating sequence (MH vs. HM mixtures) produced mixtures with very different stability. Heating WP solution separately before mixing with the BCP (HM mixture) led to a much greater instability at both pH levels, and at pH 3.5, the extent of turbidity was substantially worse. Heating the pectin-protein mixture (as opposed to heating the protein before mixing) seemed to improve the stability of the complexes substantially.

6.3.2. Particle Size and Zeta-Potential of Blackcurrant Pectin-Whey Protein Complexes

In order to elucidate the trends seen on the turbidity and stability of the pH 3.5 and pH 4.5 BCP-WP mixtures, data on particle size and zeta-potential was recorded. Figure 6.5 shows the Z-average size of the controls (BCP and WP) and their mixtures (NH, MH, HM) at pH 3.5 and pH 4.5. The particle size of the BCP was significantly smaller at pH 3.5 (300 nm) than at pH 4.5 (422 nm). This is likely owing to weaker BCP intramolecular repulsion (less negative charge) (Schmidt et al., 2017) at pH 3.5 as the pH is closer to the BCP pK_a of 1.7. The Z-average values for the non-heated WP controls at pH 3.5 and pH 4.5 were not significantly different (149 nm at pH 3.5 and 171 nm at pH 4.5) and although the Z-average size—based on scattering light intensity—were >100 nm, based on the number and volume distributions of both aggregate-reduced WPs (Figure 6.6), majority of the protein particles that are scattering the light—and interacting with pectin—are very small, falling within the 4.5 to 5.1 nm range.

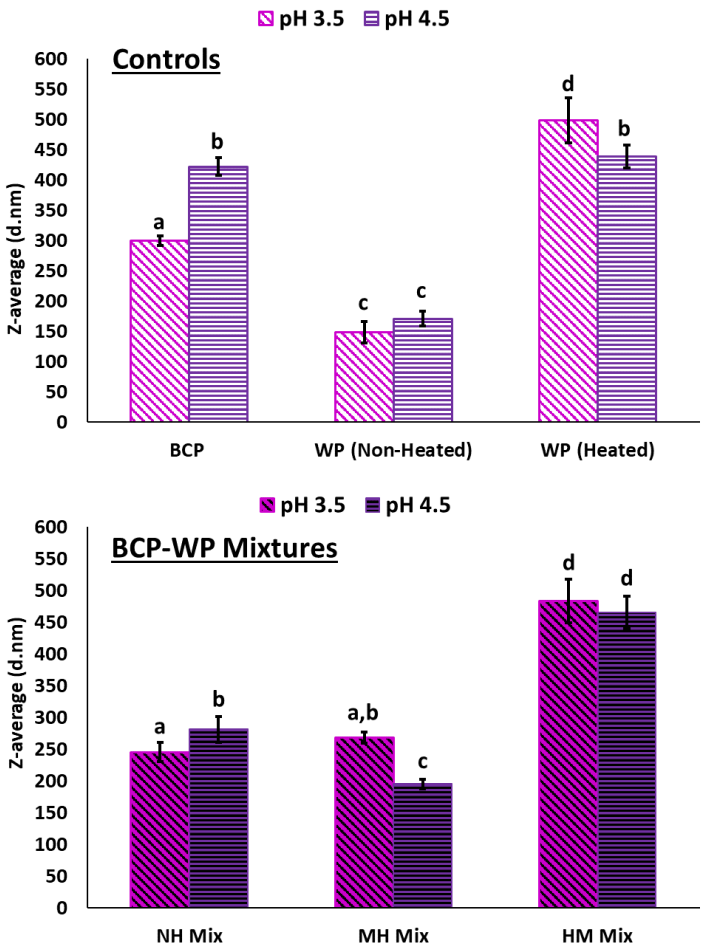

Figure 6.5 Particle size (nm, Z-averages mean ± standard deviation) of controls (BCP, blackcurrant pectin; WP, whey protein) and their mixtures (NH, Non-Heated; MH, Mixed-Heated; HM, Heated-Mixed) at pH 3.5 and pH 4.5. Means within a group are not significantly different if the letters are same.

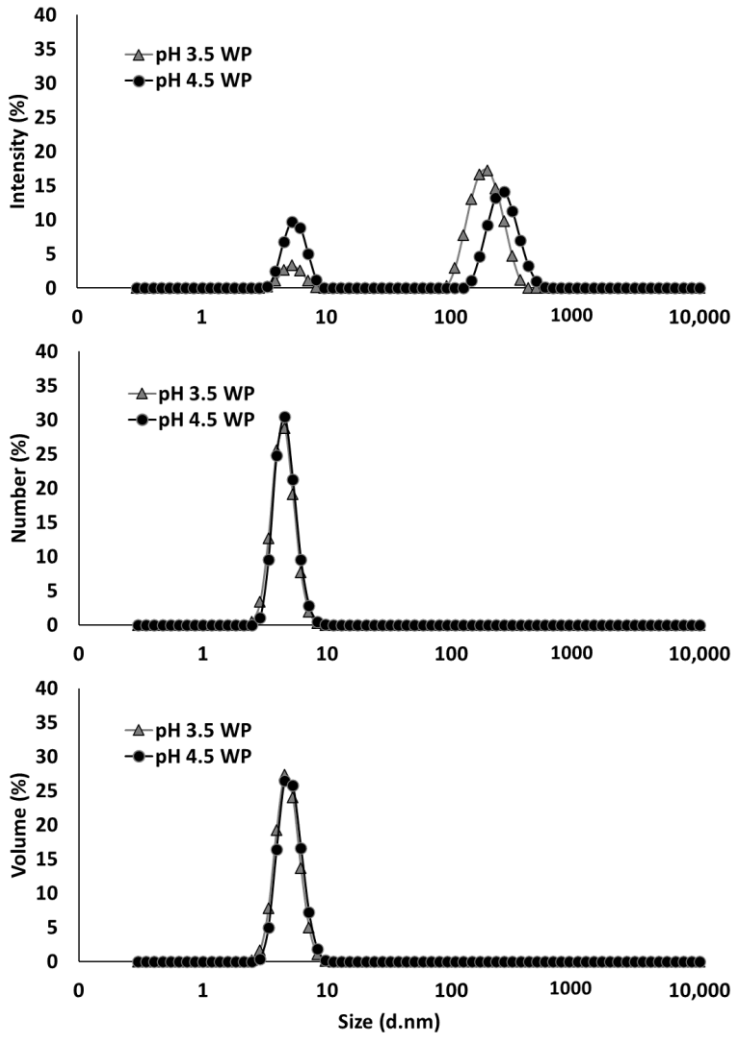

Figure 6.6 Average size distribution of aggregate-reduced whey protein (WP) at pH 3.5 and pH 4.5 based on intensity, number, and volume weighting mechanisms.

At both pH levels, the heat treatment increased the particle size of the WPs considerably (Figure 6.5). It is well known that heat treatment of 85 °C unfolds globular proteins allowing aggregation via disulphide bonds and non-covalent bonds like hydrophobic and hydrogen bonding interactions, significantly increasing their particle size (Donovan & Mulvihill, 1987; Spiegel & Huss, 2002). However, the aggregate size was significantly bigger at pH 3.5 (498 nm) as compared to pH 4.5 (439 nm). Spiegel and Huss (2002) also reported bigger aggregate size when WPs were heated at a pH lower than pH 4.5. A likely explanation is that during heating at pH 3.5, the greater positive net charge of the WPs provides the dominant β-lactoglobulin with more intramolecular repulsion that facilitates its unfolding (Donovan & Mulvihill, 1987) and subsequent aggregation with α-lactalbumin and bovine serum albumin. In contrast, the less positive net charge of the WPs at pH 4.5 weakens the intramolecular

repulsion of β-lactoglobulin and tightening its protein conformation, subsequently reducing the degree of unfolding and the resultant Z-average size of heated WPs.

Regarding the size of complexes (Figure 6.5), without heat treatment, the NH complexes at pH 3.5 (245 nm) and pH 4.5 (281 nm) had smaller particle sizes than their BCP controls (300 nm and 422 nm at pH 3.5 and pH 4.5, respectively). The size reduction can be attributed to the association of protein to the BCP, which reduced the intramolecular repulsion and compacted the conformation of BCP (Sperber et al., 2009). The complexes at pH 3.5 (245 nm) were significantly smaller than those at pH 4.5 (281 nm), but the Z-average size needs to be interpreted in conjunction with their particle size distributions as the presence of large particles can affect the reported Z-average size, and this will be discussed later.

When heating was introduced to the BCP-WP system at pH 4.5, the MH mixture experienced a significant size decrease from 281 nm to 195 nm, without and with heat, respectively, yet no significant change in size was observed at pH 3.5—245 nm without heat versus 268 nm with heat (Figure 6.5). Between the MH mixtures, pH 3.5 (268 nm) seemed to form significantly larger complexes than pH 4.5 (195 nm) and this comparison will be confirmed later along with their particle size distributions. On the contrary, if the heating sequence was changed to HM, it produced complexes that were significantly larger—483 nm and 465 nm, at pH 3.5 and pH 4.5, respectively—than the NH and MH complexes. The HM complexes at both pH levels were not significantly different, and they seemed to follow the size of their respective aggregated WP controls (498 nm and 439 nm at pH 3.5 and pH 4.5, respectively).

Figure 6.7 shows the particle size distribution of NH, MH, and HM mixtures at pH 3.5 and pH 4.5. Based on light scattering intensity (Figure 6.7A), the NH system at pH 4.5 has two populations of complexes (small peak: ≈68 nm and large peak: ≈346 nm) whereas at pH 3.5 only one population is seen (≈276 nm). According to the number distribution of NH mixtures (Figure 6.7B), the majority (99%) of the complexes at pH 4.5 (≈53 nm) were much smaller than the complexes at pH 3.5 (≈199 nm), however, a small number of large complexes (≈261 nm) was detected at pH 4.5, as shown in the inset figure of Figure 6.7B, represented by the minor peak. Large particles can affect the Z-average size of a system because they scatter light with greater intensity that overshadows the intensity from the smaller particles. This renders the calculated Z-average size to be less precise as it is not depicting the actual population of the complexes. This was the case for the pH 4.5 NH system where its Z-average size (281 nm) was larger than that of pH 3.5 (245 nm), yet, based on number distribution, the majority of its complexes were smaller (<100 nm) than the pH 3.5 complexes (>100 nm). A likely reason behind the

larger NH complexes at pH 3.5 is that they may be associated with more WP molecules than those at pH 4.5.

As mentioned previously, heating the NH mixtures changed the Z-average size of MH complexes at pH 4.5 but not at pH 3.5, and this size trend is also reflected in their intensity and number distribution shown in Figure 6.7A and Figure 6.7B. The small peak seen in the inset figure of NH mixture at pH 4.5 had disappeared after heat was applied (see inset figure of MH mixture at pH 4.5 in Figure 6.7B), indicating that the heat had altered or broken up the large complexes at pH 4.5. The number distribution plot also confirmed that the MH complexes at pH 3.5 were larger (≈237 nm) than those at pH 4.5 (≈44 nm), matching the Z-average size trend. A possible reason behind the larger MH complexes at pH 3.5 is that they may be associated with more WP molecules than those at pH 4.5, which corresponded with the more turbid pH 3.5 MH mixture shown in Figure 6.3.

Based on Figure 6.7A of HM mixtures, (i) the presence of an additional peak in pH 3.5 mixture, (ii) the increase of peak intensity in pH 4.5 mixture, and (iii) the shifting of overall peaks to the right side of the distribution plot indicates that there was a major change in the particle size of the HM mixtures. The number distribution plot revealed that there was an increase in particle size and the population of large aggregates—≈79 nm (96%) and ≈359 nm (4%) at pH 3.5, and ≈86 nm (93%) and ≈483 nm (7%) at pH 4.5—in comparison to the NH systems. The increase in size and population of large aggregates is likely to be the reason for the instability of the HM mixtures shown in Figure 6.4.

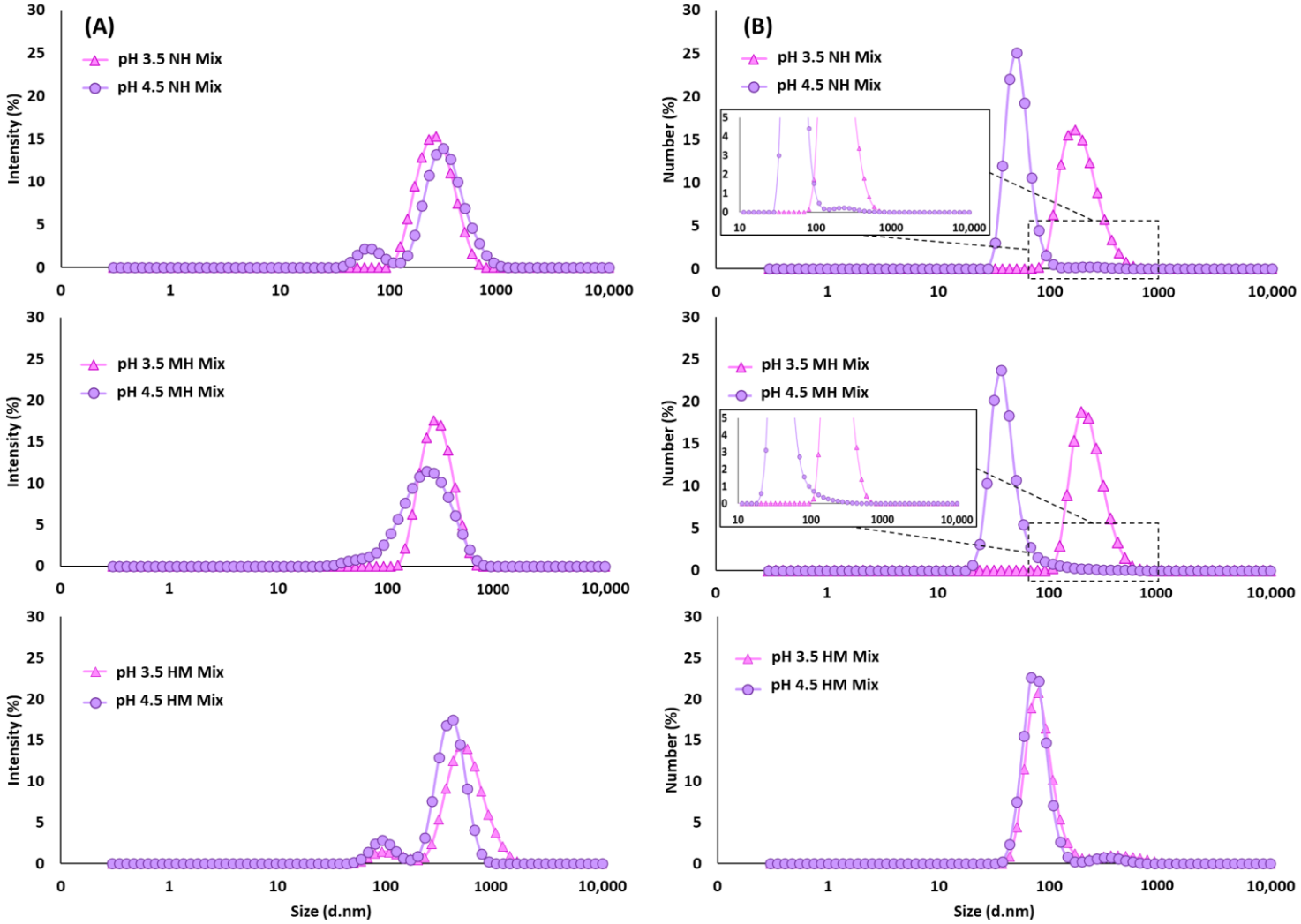

Figure 6.7 Average size distribution of blackcurrant pectin-whey protein mixtures (NH, Non-Heated; MH, Mixed-Heated; HM, Heated-Mixed) at pH 3.5 and pH 4.5 based on (A) intensity and (B) number weighting mechanisms.

The polydispersity index (PDI)—calculated based on intensity distribution—of the NH, MH, and HM mixtures at pH 3.5 and pH 4.5 is shown in Table 6.1. Mixtures that were not heated seemed to be medium polydisperse (0.1 to 0.4) with pH 4.5 having significantly higher PDI (0.39 ± 0.05), possibly due to the presence of two population peaks in the pH 4.5 NH system, as shown in Figure 6.7A. When heat was applied, it caused the size distribution of the MH mixtures to significantly narrow down to 0.12 ± 0.03 and 0.26 ± 0.01 at pH 3.5 and pH 4.5, respectively, because the heat might have compacted the pectin and its associated proteins (Masuelli, 2011). The described changes can be seen in Figure 6.7A, where the peak in pH 3.5 MH mixture was narrower than its NH counterpart and the two population peaks seen in pH 4.5 NH mixture were reduced to just a single peak after heating, thus the reduced PDI. In contrast to the MH mixtures, the PDI of both HM mixtures were significantly higher (0.52 ± 0.03 and 0.37 ± 0.03 at pH 3.5 and pH 4.5, respectively), probably due to a wider population of complexes that consisted of larger aggregates.

Table 6.1 Polydispersity index (mean ± standard deviation) of blackcurrant pectin-whey protein mixtures (NH, Non-Heated; MH, Mixed-Heated; HM, Heated-Mixed) at pH 3.5 and pH 4.5. Means with same letter are not significantly different.

	Polydispersity Index	
	pH 3.5	**pH 4.5**
NH Mix	0.21 ± 0.02^{a}	0.39 ± 0.05^{b}
MH Mix	0.12 ± 0.03^{c}	0.26 ± 0.01^{a}
HM Mix	0.52 ± 0.03^{e}	0.37 ± 0.03^{b}

Figure 6.8 shows the zeta-potential values of the ACN mix (cyanidin 3-*O*-rutinoside and delphinidin 3-*O*-rutinoside), BCP, WP and their mixtures (NH, MH, HM) at both pH levels. The concentration of the ACN mix (9×10^{-4} % w/v) represented the amount of ACNs present in the BCP (0.02% w/v) of the pectin-protein mixtures. The counter ions contributed by the ACNs at pH 3.5 (+1.56 mV) and pH 4.5 (-6.72 mV) were not significant for the BCP-WP mixtures and the slight negative charges observed at pH 4.5 were probably contributed by the chloride ions. At pH 3.5, the BCP control had a moderate amount of negative charge that significantly increased as the pH became less acidic—from -17.6 mV at pH 3.5 to -23.4 mV at pH 4.5—because as the pH was further away from its pK_a of 1.7 more carboxyl groups would be dissociated. The WP controls had significantly different zeta-potential values at pH 3.5 (+19.7 mV) and pH 4.5 (+7.84 mV). At the isoelectric point of the WPs (pH 5.3) (Anema, 2009), the proteins carry charged basic amino groups (NH_3^+) and acidic carboxylate groups (COO^-) on their backbone and these functional groups can be deprotonated to NH_2 or be protonated to COOH, respectively, depending on the pH of the system (Damodaran, 2008). As the pH decreases further to pH 3.5, more COO^- groups are protonated to COOH, increasing the overall positive charge of the WPs, thus, the higher zeta-potential at pH 3.5 as compared to pH 4.5. Heating the WP

controls revealed hidden AAs that carry side chains with ionizable groups and thereby, increasing the overall surface charge of the heated WPs (+37.5 mV and +16.1 mV at pH 3.5 and pH 4.5, respectively) as previously observed by Jiang et al. (2018) and Zhao and Xiao (2017).

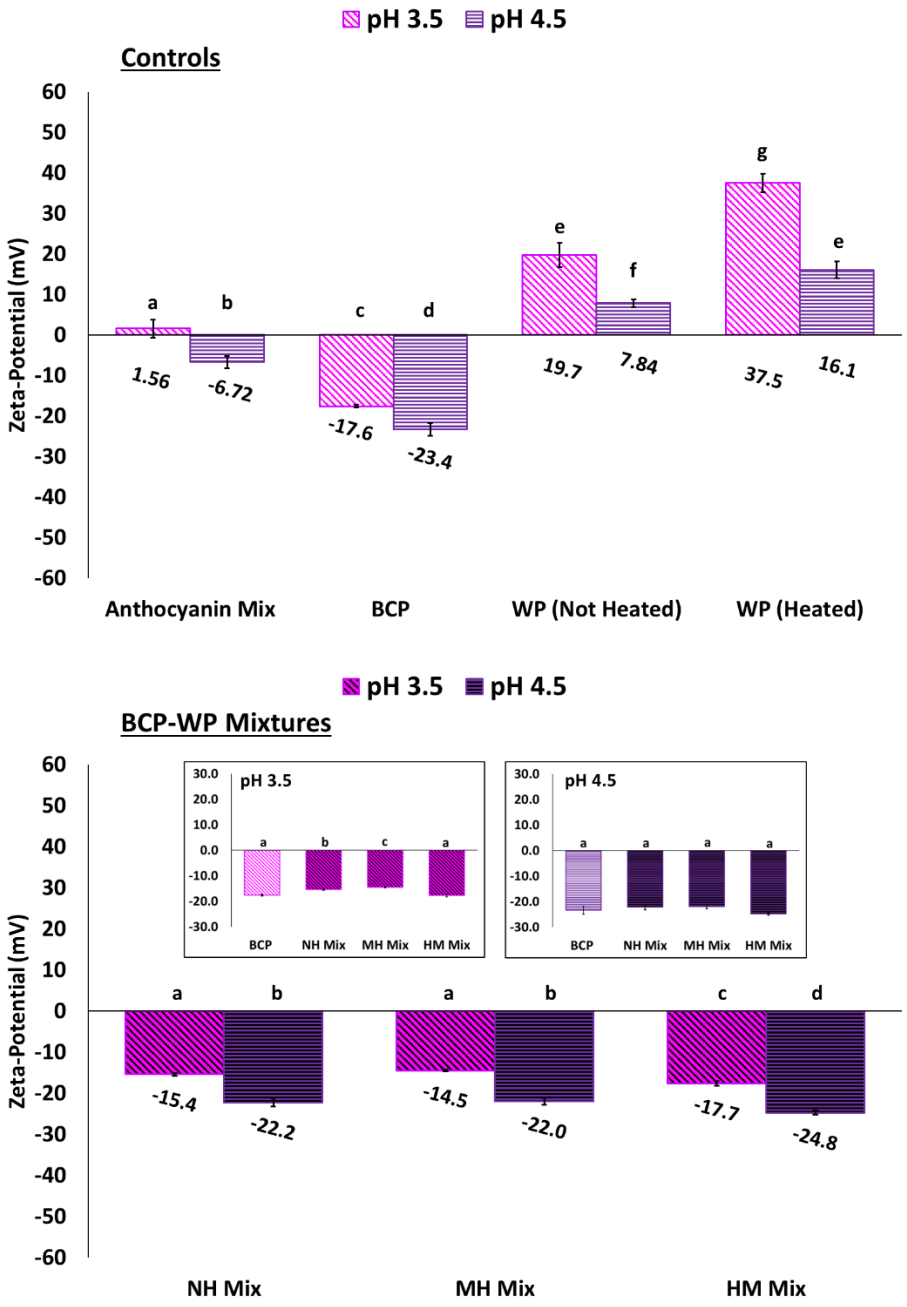

Figure 6.8 Zeta-potential (mV, mean ± standard deviation) of controls—anthocyanin mix (cyanidin 3-*O*-rutinoside and delphinidin 3-*O*-rutinoside), blackcurrant pectin (BCP) and whey protein (WP)—and their mixtures (NH, Non-Heated; MH, Mixed-Heated; HM, Heated-Mixed) at pH 3.5 and pH 4.5. Means within a group are not significantly different if the letters are same.

The zeta-potential plot of the NH, MH, and HM mixtures at pH 3.5 and pH 4.5 (Figure 6.8) shows that there was a minor decrease of surface charge in two of the mixtures (NH and MH), but not in the HM

mixtures. At pH 3.5, the zeta-potential value of NH (-15.4 mV) and MH (-14.5 mV) mixtures were significantly different from the zeta-potential value of BCP (-17.6 mV, inset figure of Figure 6.8), indicating that the reduction of surface charge was likely to be caused by pectin-protein interactions. Yet at pH 4.5, the surface charge of NH, MH, and HM mixtures (-22.2 mV, -22.0 mV and -24.8 mV, respectively) were comparable to the pH 4.5 BCP (-23.4 mV, inset figure of Figure 6.8), suggesting that complexation at higher pH had a minor impact on the surface charge of BCP. Nevertheless, the zeta potential values of all the pectin-protein mixtures (NH, MH, HM) seemed to be governed by the BCP, irrespective of their pH levels and heat treatment. This might suggest that the excess BCP in the mixtures or unoccupied binding sites in the BCP, rendered the overall mixed particles as negatively charged particles. Based on the surface charge of the complexes, systems at pH 3.5 and pH 4.5 can be considered as having relatively (±10-20 mV) and moderately (±20-30 mV) electrostatic stability, respectively (Bhattacharjee, 2016).

Overall, NH and MH BCP-WP mixtures at pH 3.5 seemed to form larger complexes (>100 nm) than those at pH 4.5 (<100 nm), a probable indication that the interactive forces between BCP and WPs at pH 3.5 are stronger, leading to more polymer association. Even though, the NH and MH complexes at both pH points were negatively charged, the aggregates at pH 4.5 had stronger electrostatic stability (>20 mV) than those at pH 3.5 (<20 mV). The weaker electrostatic stability at pH 3.5 was probably insufficient to keep the denser MH complexes suspended and stable as more WPs were associated to it. Furthermore, the effect of heat on the turbidity of the MH mixture was also more pronounced in pH 3.5, coupling this observation with the large complexes size (>100 nm) and the weaker electrostatic stability (<20 mV) led to the overall instability of the pH 3.5 MH mixture.

6.3.3. Insoluble Complexes in Blackcurrant Pectin-Whey Protein Mixtures

Besides characterising the complexes in the BCP-WP mixtures, it is also necessary to evaluate the sedimented insoluble fractions. Figure 6.9 shows the amount of pectin detected in the insoluble complexes of NH, MH, and HM mixtures at pH 3.5 and pH 4.5. Insoluble complexes were captured as the fraction that sedimented during centrifugation; neither BCP nor WP at both pH levels showed any sign of sedimentation. Both insoluble fractions of NH mixtures had a comparable amount of pectin (61% and 60% w/w at pH 3.5 and pH 4.5, respectively). Despite the comparable amount of sedimented pectin, the larger complexes of pH 3.5 NH mixture (≈199 nm)—seen in the number distribution of Figure 6.7B—may suggest that there is greater amount of WPs associated with the pH 3.5 BCP, probably owing to the combined effect of (i) greater positive charge of WPs at pH 3.5 (+19.7 mV) and (ii) the presence of more flavylium cations in the BCP. In contrast, the lower positive charge of WPs

(+7.84 mV) and the less flavylium cations at pH 4.5 could have led to lesser WPs association, and therefore the smaller NH complexes at pH 4.5 (≈53 nm based on Figure 6.7B).

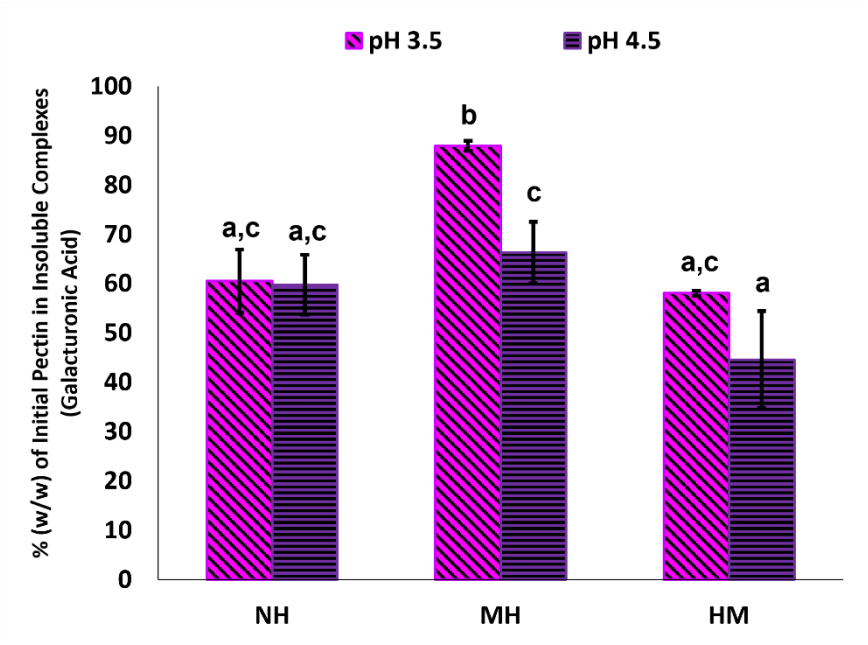

Figure 6.9 Percentage of the initial pectin (w/w, expressed as mean galacturonic acid ± standard deviation) found as part of the insoluble complexes of blackcurrant pectin-whey protein mixtures (NH, Non-Heated; MH, Mixed-Heated; HM, Heated-Mixed) at pH 3.5 and pH 4.5. Means with same letter are not significantly different.

When heat was applied to the pectin-protein mixtures, a significant increase of pectin in MH insoluble fraction was detected at pH 3.5 (88% w/w of the initial pectin), revealing the enhancement of complexation at this pH upon heating. The amplified complexation could be attributed to the interaction of pectic carboxyl groups and bound ACNs with the newly exposed AAs of unfolded WPs. In addition to hydrophobic and hydrogen bonding interactions, flavylium cations of pH 3.5 BCP might also interact with the WPs electrostatically via AAs with acidic side chains (aspartic and glutamic acids), and this was likely because aspartic and glutamic acids are the two most abundant AAs of WPs (Peña-Ramos et al., 2004). Furthermore, the comparable size of the NH and MH complexes at pH 3.5 (245 nm and 268 nm, respectively in Figure 6.5) probably suggests that more WPs were associated with the pH 3.5 BCP, yet size difference was not observed because the heat had compacted the complexes, causing the particle size to be similar.

On the contrary, heating at pH 4.5 was not enough to show the enhancement effect of bound ACNs as the increase of pectin in MH insoluble complexes (66% w/w) was not statistically different than its NH counterpart (60% w/w). This coincides with the significant size decrease observed between the NH and MH complexes at pH 4.5 (281 nm and 195 nm, respectively in Figure 6.5), suggesting that the lower positive charge of WPs (+16.1 mV) and the lesser flavylium cations made the complexation

between the pectin and protein at this pH to be less intense that allowed the heat to compact the complexes into smaller particles size.

In comparison to the NH mixtures, mixing BCP with the heated WP—presumably, unfolded protein with interactive sides exposed—did not increase the amount of pectin in the insoluble complexes of HM mixtures at pH 3.5 (58% w/w) and pH 4.5 (45% w/w) and were regarded as not significantly different. The protein-protein interactions might have dominated when WP solution was heated before mixing, leading to a decrease of available binding sites for interaction with BCP.

FTIR spectroscopy was used to identify the functional groups of blackcurrant ACNs, BCP and WP, before comparing them against the insoluble fraction of the BCP-WP mixtures. The FTIR spectrum of BCP was first compared against the spectrum of the two major ACNs of blackcurrant (Figure 6.10). The overall broadness of BCP peaks is an indication that there are various intermolecular interactions happening within the BCP, and this is because the pectic material contained bound components like ACNs, proteins and minerals, as it has been shown and discussed in Chapter 4. Choong et al. (2019) reported a similar spectrum with broad region around 2500 to 3800 cm^{-1} for *Hibiscus sabdariffa* (Roselle) plant extract that contained pectin and ACNs. The first broad peak of BCP (3327 cm^{-1}) is comparable to the broad peak (Peak A) seen in both ACN spectra. The smoothness and broadness of the region between 2400 and 3600 cm^{-1} of the BCP are probably characteristic of an ACN-rich material. This region was assigned to: (i) the O-H stretch of carboxylic and phenolic groups of the pectin and ACNs, respectively and (ii) the C-H stretch of the alkyl and aromatic groups of the pectin and ACNs, respectively (Pretsch et al., 2009; Zaleska et al., 2000).

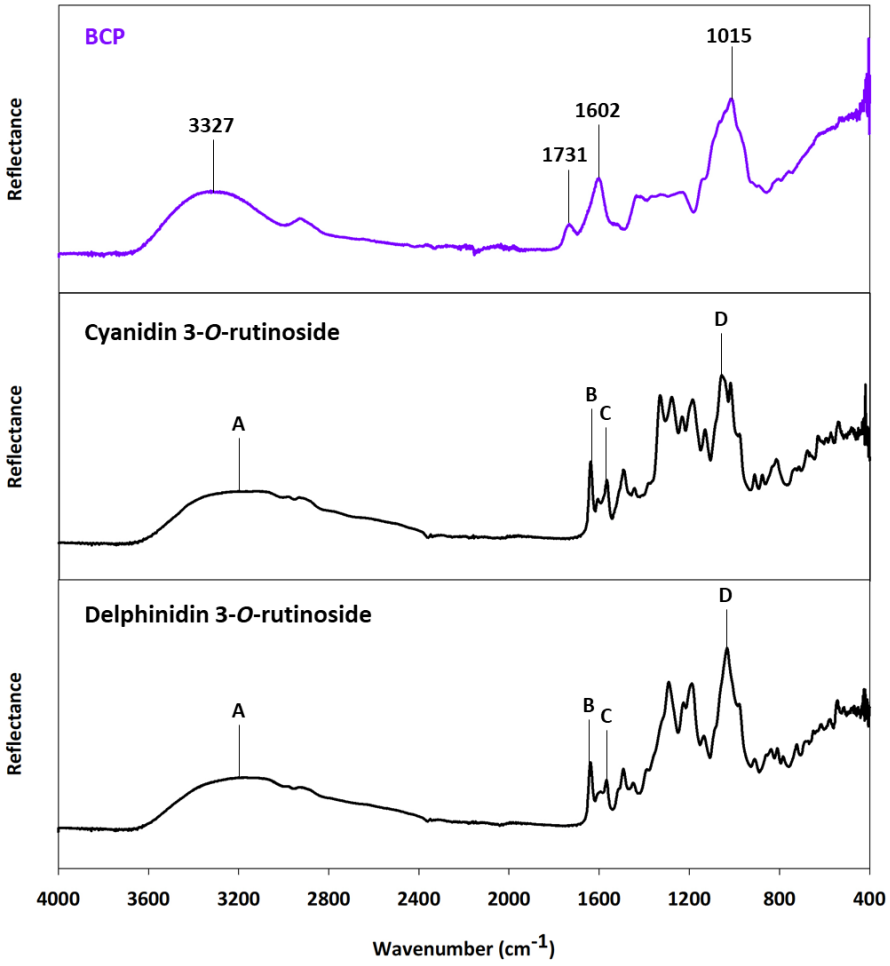

Figure 6.10 FTIR spectra of blackcurrant pectin (BCP), and the two major anthocyanins found in blackcurrant.

The second (1731 cm^{-1}) and third (1602 cm^{-1}) peaks of the BCP corresponded to the C=O stretching of the esterified and non-esterified carboxyl groups of the pectin chain, respectively (Mierczynska et al., 2017; Zaleska et al., 2000). The region of the third peak (1550 to 1700 cm^{-1}) coincided with the fingerprint region of the two ACNs, likely representing the C=C stretch of alkenes and aromatic C-C groups (Peak B and Peak C, respectively) (Pretsch et al., 2009; Wahyuningsih et al., 2017). The final distinct peak (1015 cm^{-1}) of the BCP between 800 and 1200 cm^{-1} might represent the various functional groups of the BCP components such as the C-O stretch of the carboxylic acids, ethers, esters and alcohol groups of the pectin or its bound protein. Within that same region, both ACNs also showed a strong peak (Peak D) that could correspond to the C-C backbone (stretches, bends, and torsions) and the many C-O stretches and C-H bends of ACNs. Due to the overlapping region of interest, it was difficult to distinguish the peaks and make definitive assignments of the ACN functional groups. This was expected as the BCP is a complex material, and therefore only approximate location of the ACN functional groups was used for the complexation study.

Further study was carried out on NH and MH mixtures as they showed better physical stability. FTIR spectra were recorded for the insoluble complexes of the two systems to investigate the changes that occurred in the functional groups of the BCP and WP following their complexation. The WP spectrum was used as a reference because the spectrum of the sedimented fractions resembled the WP spectrum more than the BCP (Figure 6.11). Note that some of the spectra in Figure 6.11 show carbon dioxide band (≈2340 cm^{-1}) and artefacts from the ATR diamond—between 2000 to 2400 cm^{-1}.

Irrespective of the pH, peak shifts are seen throughout the spectrum of NH and MH insoluble complexes, indicating that the complexation between BCP and WP had affected their functional groups (Figure 6.11). The first broad peak of the sedimented fractions—between 3000 and 3600 cm^{-1}–has shifted slightly away from the first reference peak of WP (3275 cm^{-1}). Peak shift within that region is attributed to pectin and protein interacting via hydrogen bonding and electrostatic interactions as the region signifies the polymeric interaction between the O-H groups of carboxylic acids—originating from BCP and WP—and the N-H groups of amides and amines that originate from WPs (Zaleska et al., 2000; Zhao et al., 2020). As mentioned earlier, the O-H groups of the bound ACNs were also assigned to this region (Choong et al., 2019; Pretsch et al., 2009; Wahyuningsih et al., 2017), however based on these results, the extent of their contribution to the complexation is not clear due to the undistinguishable region.

Shifting of peaks is also detected on the two prong-like peaks of the sedimented fractions—between 1460 and 1680 cm^{-1}. The two peaks (1627 and 1518 cm^{-1}) were originally identified in the WP spectrum corresponding to the C=O stretching of amides and the N-H bend of WP amines, respectively (Pretsch et al., 2009; Raei et al., 2018; Zaleska et al., 2000). As mentioned previously, this region also coincided with the non-esterified C=O groups of BCP (Mierczynska et al., 2017), and the C=C stretch of alkenes and aromatic C-C groups of bound ACNs (Pretsch et al., 2009; Wahyuningsih et al., 2017). Similar spectral shifts were observed in the complexation between ACN-free high methoxyl apple pectin and WP, signifying the impact of electrostatic interaction on the two prong-like peaks (Zaleska et al., 2000). However, in this study, the presence of ACN functional groups in the same region means that other interactive forces such as hydrogen bonding and hydrophobic interactions can also contribute to the peak shifts.

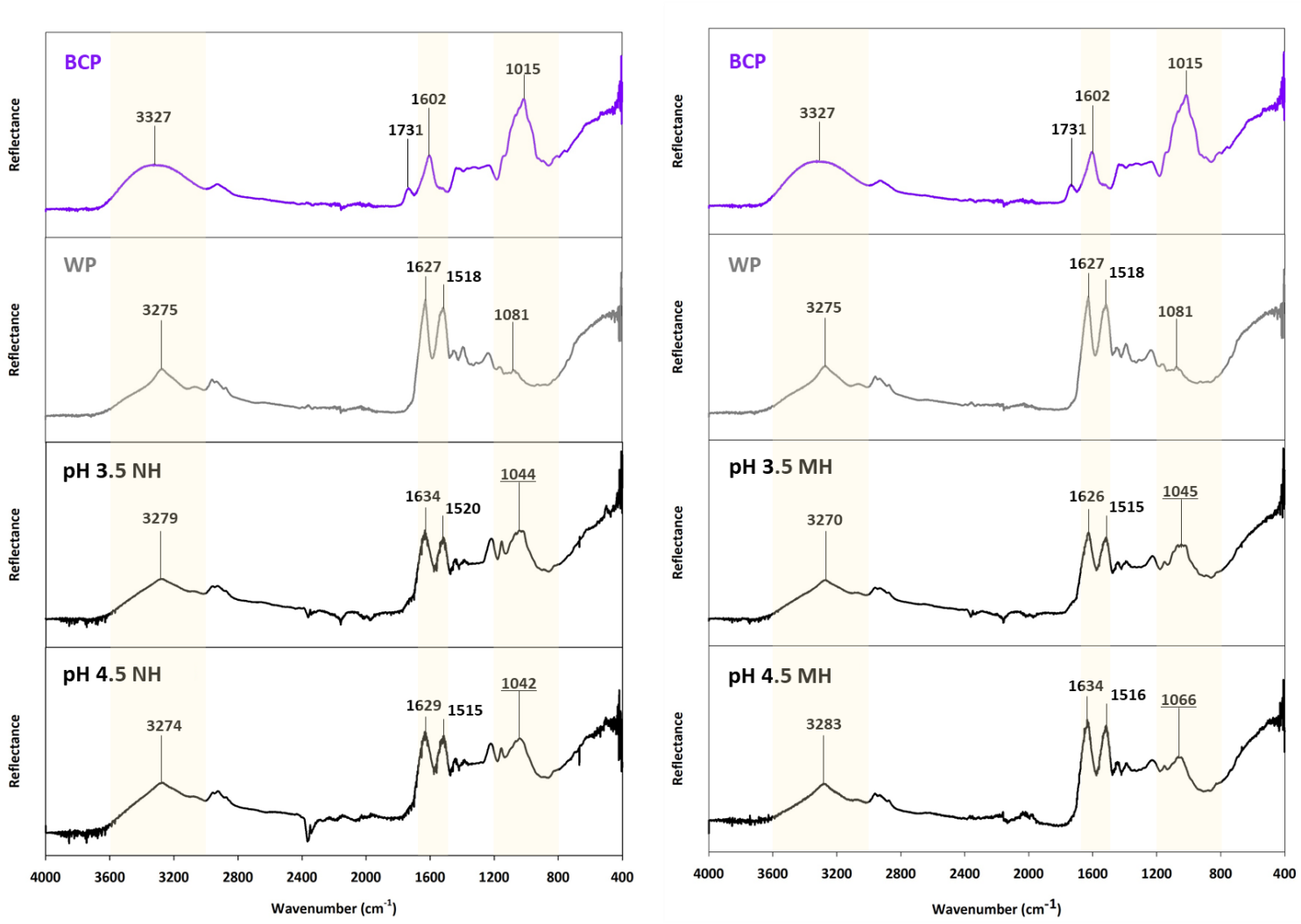

Figure 6.11 FTIR spectra of blackcurrant pectin (BCP), whey protein (WP) and the insoluble complexes of their mixtures (NH, Non-Heated; MH, Mixed-Heated; HM, Heated-Mixed) at pH 3.5 and pH 4.5.

In addition to the spectral shifts, a new peak—between 800 to 1200 cm^{-1}—was also identified in the spectra of the sedimented fractions. The new peak coincided with the location of aliphatic amines of WPs and various functional groups of the BCP (pectic and ACN components). Based on the nature of these functional groups, the new peak might be related to hydrogen bonding and hydrophobic interactions, confirming that an additional type of interaction other than electrostatic had occurred. At pH 4.5, the spectrum of MH insoluble complexes shows that the new peak has shifted to 1066 cm^{-1} as opposed to the rest of the insoluble complexes that peaked at 1042 to 1045 cm^{-1}. This is likely due to the interaction of WP with thermally altered bound ACNs of BCP. The molecular structure of ACNs at pH 4.5 is more susceptible to thermal changes, therefore, thermal degradation accelerates at less acidic pH (Loypimai et al., 2016), producing derivatives of aldehyde or benzoic acid (Oancea, 2021). These compounds are likely to interact with the WPs as they have aromatic ring on their molecular structure, and their interaction with WPs may have impacted the location of that new peak.

6.3.4. Overall Discussion: Possible Mechanism of Complexation between Blackcurrant Pectin and Whey Protein

Based on the results described earlier, a schematic diagram in Figure 6.12, illustrates the possible NH and MH complexation of BCP and WP at pH 3.5 and pH 4.5. The first component of the diagram shows the negatively charged BCP and its bound ACNs at both pH levels. The BCP is negatively charged at pH 3.5 and its bound ACNs appear pink because majority of the ACNs are protonated as the flavylium cation. When the pH increases to pH 4.5, the BCP becomes more negative and turns purple as majority of its bound ACNs are deprotonated to the blue quinoidal base. The net charge of the WPs increases as the pH moves away from the isoelectric point of the WPs (pH 5.3), therefore the WPs at pH 3.5 were more positively charge than at pH 4.5 as shown in Figure 6.12.

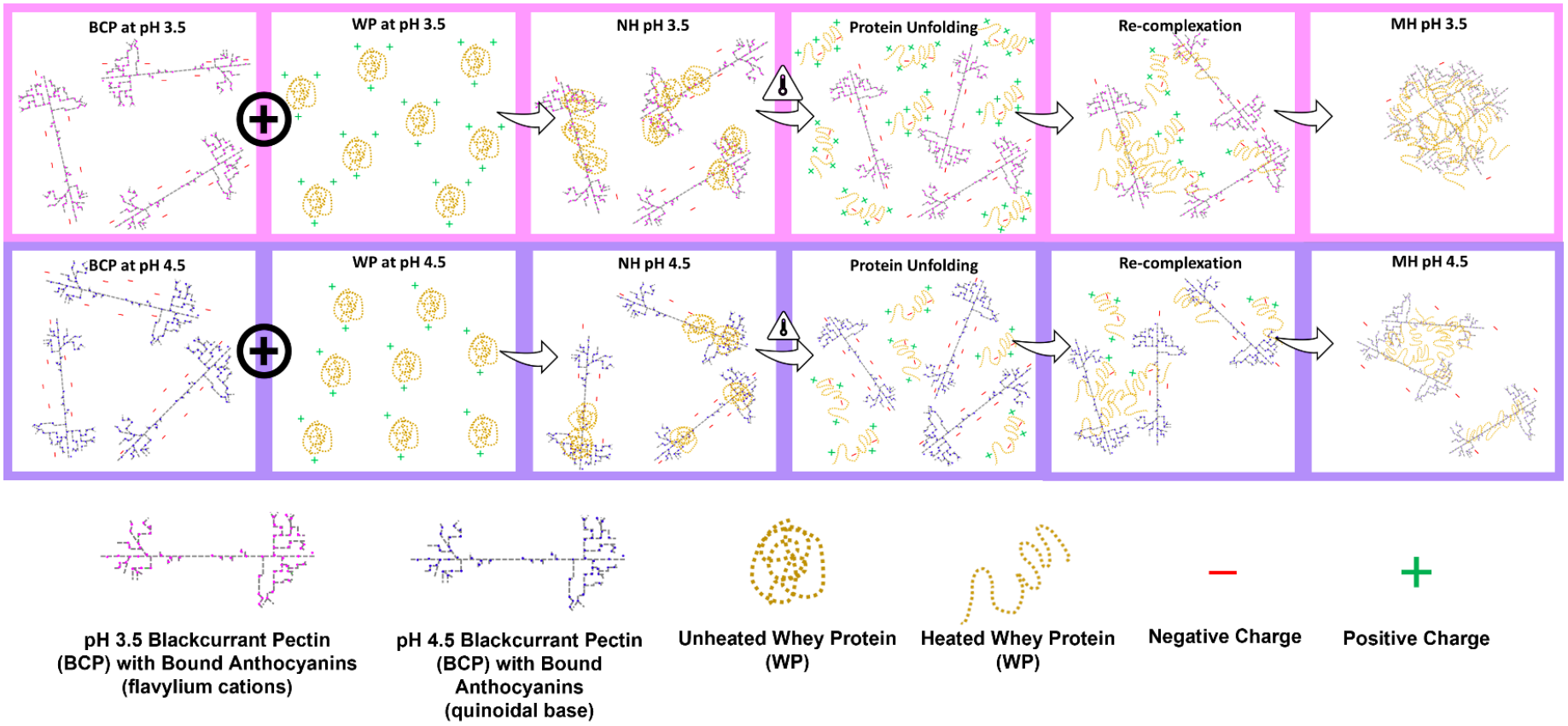

Figure 6.12 Schematic diagram of non-heated (NH) and mixed-heated (MH) blackcurrant pectin-whey protein mixtures at pH 3.5 and pH 4.5.

The complexation starts when the oppositely charged BCP and globular WPs are mixed, forming complexes that carry net negative charges at both pH levels, probably due to excess or unoccupied binding sites of BCP. In the absence of heat, findings from FTIR indicated that the complexation occur as a result of combinative interactions: (i) electrostatic interactions between the negatively charged BCP and positively charge WPs, (ii) hydrogen bonding of amino and hydroxy groups from the BCP components (pectin, ACNs and protein) with amino and hydroxy groups of the WPs, as well as (iii) hydrophobic interactions between the ACNs and hydrophobic AAs such as tryptophan61 and tryptophan134 that can be found on the surface of β-lactoglobulin and bovine serum albumin, respectively (Albani et al., 2014; Edwards et al., 2009; Topală et al., 2014). More WPs may associate with the BCP at pH 3.5 as the WPs are more positively charged and that there are more flavylium cations on the BCP resulting in larger complexes. At pH 4.5, the WPs are less positively charged and less flavylium cations are available on the BCP, therefore the complexes formed are generally smaller.

When the mixtures are heated at 85 °C, the complexes are likely to undergo a simultaneous restructuring of components, involving the partial unfolding of the WPs and its re-complexation with the BCP via the mechanism described earlier before assuming the 'core shell arrangement' (Jones & McClements, 2011; Santipanichwong et al., 2008). At pH 3.5, the intramolecular charges of the globular WPs aid in the unfolding of its protein structures, exposing the hydrophobic AAs and other charged AAs that are once hidden. The newly exposed AAs can now act as available sites for the pectin, ACNs, and possibly the nearby soluble complexes to cross-link with, which eventually permit more pectin-protein and ACN-protein complexation to occur. The ACNs at pH 3.5 are most likely to interact with the exposed AAs via hydrogen bonding, hydrophobic and ionic interactions, depending on the side chains of the AAs (Vuong & Hongsprabhas, 2021), and hydrogen bonding will eventually ensue to reinforce their associations (Spencer et al., 1988). The acidity of the system may have provided the BCP with flexibility (Schmidt et al., 2017), which makes it advantageous during the re-complexation process as it allows more contact between the binding sites. These occurrences proved that heating intensified the interaction between the BCP and WP at pH 3.5, causing the increase of turbidity (Figure 6.3) in MH mixture and the increase of pectin percentage (Figure 6.9) in MH insoluble complexes that adversely affected its stability (Figure 6.4). The lower percentage of pectin in MH insoluble complexes at pH 4.5 may be owing to a combination of factors: (i) the lesser positive charges of WPs, (ii) the unfolding resistance of the WPs that may have reduced the exposure of concealed AAs, (iii) fewer binding sites of ACNs and (iv) the reduced flexibility of the BCP. These reasonings correspond well with the turbidity and stability of the pH 4.5 MH system observed in Figure 6.3 and Figure 6.4.

6.4. Conclusions

- The present study demonstrated that bound ACNs of BCP could affect the complexation of BCP and WP.
- The BCP-WP complexation was heightened upon heating at pH 3.5 mainly due to the combined effect of (i) greater positive charge of WPs at pH 3.5 and (ii) additional mode of interaction presented by the bound ACNs at pH 3.5, that is, electrostatic interactions between the flavylium ACNs and the two dominant AAs of WPs that carried acidic side chains—aspartic and glutamic acids.
- The overall stability of the NH and MH mixtures at pH 4.5 was probably conferred by steric stabilisation and their relatively higher net surface charges, which provided the complexes with some electrostatic stability.
- The remarkable stability of the pH 4.5 MH system that was comparable to its NH version could be attributed to the following reasons: (i) the markedly lower extent of BCP-WP interactions that led to smaller particle sizes, (ii) the relatively low polydispersity and (iii) the moderate electrostatic stability.
- A noteworthy finding is that sequence of heating demonstrated a huge impact on the stability of the mixtures. Heating of WP at pH ≤4.5 produced aggregates that were not favourable for protein-rich beverages, especially if the mixture contains fruit or berry materials that are packed with polyphenols such as ACNs.
- Although, definitive FTIR bands were not assigned due to overlapping regions of interest, findings from the FTIR spectroscopy clearly showed that the complexation between BCP and WP had altered their functional groups and that electrostatic interaction was not the only mode of interaction between the ACN-bound BCP and WP.
- The emergence of a new peak in the spectrum of BCP-WP insoluble fractions strongly suggests that the additional mode of interaction could be related to hydrogen bonding and hydrophobic interactions.

The following chapter is a comparative study on pectin-protein complexation between the ACN-rich BCP pectin and an ACN-free pectin. The work aimed to establish differences between them and expand the knowledge of ACNs' influence on pectin-protein interactions.

MASSEY UNIVERSITY
TE KUNENGA KI PŪREHUROA
UNIVERSITY OF NEW ZEALAND

GRADUATE RESEARCH SCHOOL

STATEMENT OF CONTRIBUTION DOCTORATE WITH PUBLICATIONS/MANUSCRIPTS

We, the student and the student's main supervisor, certify that all co-authors have consented to their work being included in the thesis and they have accepted the student's contribution as indicated below in the Statement of Originality.

Student name:	Nurhazwani Salleh
Name and title of main supervisor:	Associate Professor Lara Matia-Merino
In which chapter is the manuscript/published work?	Chapter 7
What percentage of the manuscript/published work was contributed by the student?	85%

Describe the contribution that the student has made to the manuscript/published work:

The experimental work was conducted by the student, except the proximate analysis of protein, ash and calcium, which was performed by the accredited Nutrition Lab at Massey University. The writing was done fully by the student with some input from the supervisors on the draft version.

Please select one of the following three options:

- ○ **The manuscript/published work is published or in press**
  Please provide the full reference of the research output:
- ◉ **The manuscript is currently under review for publication**
  Please provide the name of the journal:
  Food Hydrocolloids
- ○ **It is intended that the manuscript will be published, but it has not yet been submitted to a journal**

Student's signature:	Nurhazwani Salleh Digitally signed by Nurhazwani Salleh Date: 2023.03.01 10:35:37 +13'00'	Main supervisor's signature:	Lara Matia-Merino Digitally signed by Lara Matia-Merino DN: cn=Lara Matia-Merino, c=NZ, ou=School of Food and Advanced Technology, email=l.matia-merino@massey.ac.nz Date: 2023.02.28 17:31:12 +13'00'

This form should be placed at the beginning of each relevant thesis chapter.

Chapter 7 Comparison on Pectin-Protein Complexation Between Blackcurrant and Citrus Pectins

7.1. Introduction

Commercial pectin is typically extracted from the by-products of fruit juice and essential oil industry, either from the apple pomace or citrus fruit peel (Picot-Allain et al., 2022). Structurally, pectin is a heteropolysaccharide with high complexity and diversity that consists of three main structures: (i) homogalacturonan (HG)—an unbranched linear chain of α-(1,4)-linked D-galacturonic acids (GalUA) that can be methylated and acetylated, (ii) rhamnogalacturonan-I (RG-I)— a highly branched chain of alternating rhamnose and GalUA residues with neutral sugar side chains, and (iii) rhamnogalacturonan-II (RG-II)—a complex side chain of HG, consisting of 13 different sugars and 21 glycosidic linkages (Ropartz & Ralet, 2020). Despite the structural complexity, pectin can be classified by its degree of methyl-esterification (DE), as low methoxyl pectin (DE <50%) and high methoxyl pectin (DE ≥50%) (Gawkowska et al., 2018; Thakur et al., 1997). The presence of methoxy groups and functional oxygen atoms from the GalUA residues means that hydrophobic interactions and hydrogen bonds can happen amongst the pectin molecules (Oakenfull & Scott, 1984; Van Buren et al., 1988; Walkinshaw & Arnott, 1981). Regardless of the DE, both types of pectin are anionic due to the presence of carboxyl group in their GalUA units, which gives the pectin the ability to interact electrostatically with molecules that are of opposite charges, such as between a negatively charged pectin and a positively charged protein.

It has been widely established that a suitable pH range—above the acid dissociation constant (pK_a) value of the pectin and below the isoelectric point of the protein—is required for the attractive electrostatic interaction to occur between pectin and protein (Goh et al., 2009; Schmitt et al., 2009; Schmitt et al., 1998). Girard et al. (2002) had demonstrated that β-lactoglobulin interaction with either a low or high methoxyl pectin at 4 °C and 40 °C was primarily driven by electrostatic interaction, and to a lesser extent, by hydrogen bonding. However, the possibility of hydrophobic interactions cannot be disregarded if the pectin-protein complexation occurs at a temperature that is near to the denaturation temperature (>60 °C) of the whey protein (WP) (Law & Leaver, 2000). This is particularly relevant when high methoxyl pectin is involved, as the methoxy groups may interact hydrophobically

with the exposed hydrophobic amino acids of the WPs (Girard et al., 2002, 2003a, 2003b; Jones et al., 2009).

Due to the source and purification process of commercial pectins—acidic extraction between pH 1 and pH 3 at 50 °C to 90 °C (Izydorczyk, 2005)—apple and citrus pectin (CP) powders have very low, or no antioxidant capacity, indicating that there is negligible amount of phenolic compounds in the powders (Rubio-Senent et al., 2015). As it was reported in Chapter 4, characterisation work on the blackcurrant juice pectin-rich fraction revealed that the material was highly pigmented and comprised of carbohydrate (78% w/w), GalUA (21% w/w), protein (4.8% w/w), calcium (2.2% w/w) and anthocyanins (ACN) (3.9% w/w)—predominantly cyanidin 3-*O*-rutinoiside. Physical separation like dialysis and solvent extraction using ethanol and methanol failed to remove the ACNs from the fraction, and therefore it was concluded that the ACNs were interacting with the biopolymers. Existing publications have attributed the association of ACNs to both, pectin and protein, to non-covalent interactive forces, like electrostatic and hydrophobic interactions, as well as hydrogen bonding (Asen et al., 1970; Buchweitz et al., 2013; Dangles & Dufour, 2006; Fernandes et al., 2014; Hagerman, 2012; Lin et al., 2016; Mazzaracchio et al., 2004; Ozdal et al., 2013; Phan et al., 2017; Siebert et al., 1996; Spencer et al., 1988; Stănciuc et al., 2018; Stănciuc et al., 2017). As a result of its low GalUA content (21% w/w), the isolated blackcurrant pectin (BCP) does not qualify as a commercial pectin (≥65% w/w of GalUA) (FAO, 2016; Freitas et al., 2021). Nonetheless, the fraction behaved like an anionic polysaccharide due to the negative charges present (ca. -23mV at pH 4.8). Fourier-Transform Infrared (FTIR) analyses from Chapter 6 revealed that all key interactive components—pectin, ACN and protein—were involved in the complexation between the BCP and WP at slightly acidic medium (pH 3.5 and pH 4.5), signifying the occurrence of both pectin-protein and polyphenol-protein interactions.

The involvement of ACNs in the BCP-WP complexation in the previous study indicated that the ACNs had provided the WP with additional binding sites. Hence, the current study was conducted to validate ACN participation by comparing pectin-WP systems made with the ACN-rich BCP and ACN-free CP. The effect of increasing WP ratios was also analysed as well as the effect of heat treatment. We hypothesise that the bound ACNs in BCP provided the WPs with additional binding sites through non-electrostatic interactions. The investigation work consisted of: (i) preparation of BCP-WP and CP-WP mixtures at pH 4.5, without heat at 1:1 pectin:protein ratio and with heat treatment at 1:1, 1:5 and 1:10 pectin:protein ratios; (ii) measurements of turbidity, physical stability, particle size and zeta-potential of the mixtures; (iii) quantification of pectin and protein in the suspended and sedimented fractions of the mixtures; (iv) assessment on the functional groups of BCP, CP and WP using FTIR spectroscopy.

7.2. Materials and Methods

7.2.1. Materials

Two types of pectin were used in this complexation study: (i) a commercial ACN-free CP (GRINDSTED® Pectin MRS 351, International Flavors & Fragrances, New York, U.S.A) and (ii) a dialysed ACN-rich BCP that was prepared following the method described in Chapter 4. An aggregate-reduced WP powder was used as the protein component, and its preparation method had been described in Chapter 6. The analytical grade D-(+)-GalUA monohydrate (Sigma-Aldrich, St. Louis, Missouri, U.S.A) and 3-phenylphenol (Sigma-Aldrich, St. Louis, Missouri, U.S.A) were used as the standard and colorimetric reagent in GalUA analysis, respectively. Other chemicals were of analytical grade and purchased from local companies. All solutions were prepared using Milli-Q® water (Merck Group, Darmstadt, Germany) and stored in dust-free bottles.

7.2.2. Characterisation of Pectins

The physico-chemical and molecular properties of the CP were collected based on the techniques described in Chapter 3 and Chapter 4. The total carbohydrate and GalUA content of the CP were measured via colorimetric method by Nielsen (2017b) and Blumenkrantz and Asboe-Hansen (1973), respectively. Determination of crude protein (AOAC 968.06), ash (AOAC.05), and calcium (Inductively Coupled Plasma-Optical Emission Spectrometry) were carried out by the accredited Nutrition Laboratory in the School of Food and Advanced Technology at Massey University, Palmerston North (AOAC, 2023). Moisture analysis was done according to AOAC 925.10 (AOAC, 2023). Titration method was used to estimate the pK_a value of the CP, by titrating 0.25% w/v of CP with 0.1 M NaOH. The molecular characteristics—molecular weight (M_w) and root mean squared (RMS) radius—of the CP (0.7% w/v), were determined via size-exclusion chromatography that was coupled to a multi-angle laser light scattering (SEC-MALLS) detector using three polymer-based aqueous columns that were connected in series: Shodex SB-805 (8.0 mm × 300 mm, 13 µm), SB-803 (8.0 mm × 300 mm, 6 µm), and SB-802.5 (8.0 mm × 300 mm, 6 µm) (Showa Denko, Tokyo, Japan). All results are reported as the mean and standard deviation of at least two readings.

The viscosities of BCP and CP were measured at 20 °C using an Anton Paar MCR 302 rheometer (Anton-Paar, Graz, Austria). Dialysed BCP and commercial CP solutions containing 0.42% w/v of GalUA were prepared in pH 4.5 sodium acetate buffer (1 mM) and allowed to hydrate overnight at 4 °C under gentle stirring. The shear rate was set to increase from 0.01 to 1000 s^{-1} with a log ramp time setting that started from 30 s and ended at 2 s. A double gap geometry (DG 26.7 and C-PTD 200) was used for

all analyses. Each sample was prepared in duplicate with at least three measurements, and the viscosity is reported as a mean average.

7.2.3. Preparation of Pectin-Protein Mixtures

The working concentration of biopolymers and the preparation method of pectin-protein mixtures were kept identical to those described in Chapter 6, with the exception that the present study was done at three pectin:protein ratios (1:1, 1:5 and 1:10). The 1:1 ratio and biopolymer concentrations are originally based on the work of Sperber et al. (2009). The pectin-protein ratio was then increased to 1:5 as this corresponds to the pectin:protein ratio of a typical beverage that is stabilised by pectin (Wilbanks et al., 2022), with the subsequent 1:10 ratio representing a sample with a much higher protein concentration. Since the order of heating greatly impacted the stability of the mixtures (Chapter 6), two mixtures with good physical stability were prepared at pH 4.5: non-heated (NH) and mixed-heated (MH) mixtures. Figure 7.1 shows the preparation steps of these mixtures and the measurement techniques used. Firstly, 0.5% w/v solutions of the BCP, CP and WP powders were prepared with distilled water at 4 °C under gentle stirring overnight. Appropriate amounts of the biopolymer stock solutions were then aliquoted to achieve a final concentration of pectin (0.02% w/v) and protein (0.02%, 0.1% and 0.2% w/v)—determined based on the total amount of carbohydrate (BCP: 78% w/w, CP: 62% w/w) and protein (90% w/w) present in the powders. The pectin stock was first mixed with the pH 4.5 sodium acetate buffer (1 mM) followed by the protein stock under gentle stirring for 30 min at 20 °C; this is referred to as the NH mixture. For the preparation of the MH mixture, a heat treatment of 85 °C for 15 min was applied, followed by a rapid cooling in an ice bath. The stocks and mixtures were kept in dust-free bottles to avoid interference from dust particles during size measurements and stored at 4 °C. Solutions that contained ACNs were kept in dust-free opaque bottles at 4 °C to minimize their degradation.

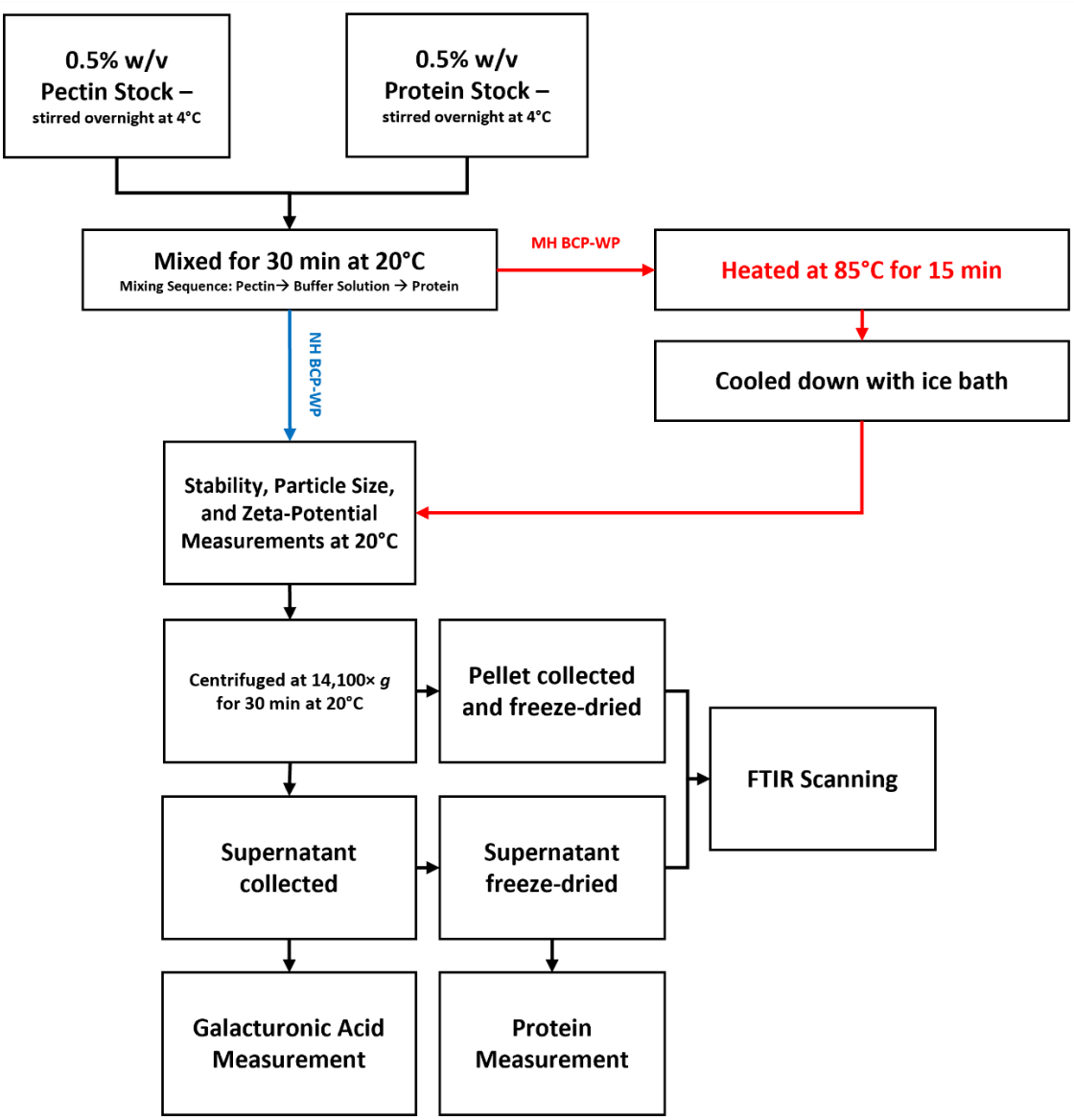

Figure 7.1 Preparation steps for blackcurrant pectin-whey protein (BCP-WP) and citrus pectin-whey protein (CP-WP) mixtures (NH, Non-Heated; MH, Mixed-Heated) at pH 4.5 and the measurement techniques used.

7.2.4. Physical Stability Measurement

Immediately after sample preparation, physical stability measurements of the controls (BCP and CP at 0.02% w/v; Non-Heated WP at 0.02% and 0.2% w/v) and the mixtures (BCP-WP and CP-WP, NH at 1:1 pectin:protein ratio and MH at 1:1, 1:5 and 1:10 pectin:protein ratios) were carried out as per the method described in Chapter 6 using a Turbiscan Lab (Formulaction, Toulouse, France). The percentage of light transmission was determined from the collected data at time 0 s and was used to describe the turbidity. The Turbiscan Stability Index (TSI) and percentage of light transmission are reported as the mean of two samples.

7.2.5. Particle Size and Zeta-Potential Measurements

Particle size measurement of controls and mixtures at pectin:protein ratios of 1:1 and 1:5 was determined using a Zetasizer Pro (Malvern Panalytical Ltd., Malvern, United Kingdom) based on the method described in Chapter 6. Prior to measurement, mixtures at 1:5 pectin:protein ratio were diluted with pH 4.5 sodium acetate buffer (1 mM) to achieve an overall protein concentration of 0.02% w/v. As for the mixture with the highest protein concentration (1:10), majority of the particles were >10 µm; therefore, particle size was determined using a Mastersizer 2000 (Malvern Panalytical Ltd., Malvern, United Kingdom) that was connected to a Hydro SM attachment used for analysing small volume samples. Zeta-potential values were measured for all the controls and mixtures using the Zetasizer Pro following the method described in Chapter 6. For accurate readings, heated mixtures at 1:5 and 1:10 pectin:protein ratios were diluted with the same buffer to achieve the overall protein concentration of 0.02% w/v. All particle size and zeta-potential measurements were carried out at 20 °C with three readings taken for each sample and reported as the mean and standard deviation of at least two samples.

7.2.6. Quantification of Galacturonic Acid and Protein

After particle size and zeta-potential analyses, the remaining samples were centrifuged (14,100 x *g*, 30 min, 20 °C) and collected separately as the supernatant (soluble complexes) and pellet (insoluble complexes) of the mixtures. No sedimentation was seen in BCP, CP and WP (0.02% and 0.2% w/v) solutions. Quantification of uronic acid was carried out as the method described in Chapter 3 and Chapter 6. The amount of uronic acid is reported as the % (w/w total solids) of GalUA equivalents and the mean and standard deviation of at least two samples. Protein was quantified via Dumas method (AOAC 968.06) by the same accredited Nutrition Laboratory at Massey University, Palmerston North (AOAC, 2023). Due to the dilute condition of the supernatants, they were freeze-dried before protein analysis. Similar to the GalUA analysis, the amount of protein in the supernatants was measured and the percentage of protein in the pellet was calculated by difference based on the initial amount of protein in WP. The amount of protein is reported as the mean % (w/w total solids) and standard deviation of two samples.

The molar ratio of pectin and protein for all types of insoluble complexes was calculated using the M_w information of the controls and the collected GalUA and protein data. The M_w of BCP (109,600 kDa) was determined based on the SEC-MALLS results in Chapter 4, while the M_w of the CP (0.7% w/v; 228,800 kDa) and WP (0.5% w/v; 32, 050 kDa) were acquired as per the method described in the same chapter. Firstly, the number of moles for pectin (0.02% w/v) and protein (0.02%, 0.1% and 0.2% w/v) added to the mixture were determined, followed by the number of moles for pectin and protein

present in the insoluble complexes. Then, the molar ratio was obtained by dividing the number of moles of protein with the number of moles of pectin detected in the insoluble complexes.

7.2.7. Fourier-Transform Infrared Spectroscopy

The freeze-dried supernatant and pellet of the mixtures (NH and MH mixtures of BCP-WP and CP-WP at 1:1 pectin:protein ratio) were scanned by a Nicolet™ iS™ 5 FTIR Spectrometer (Thermo Fisher Scientific Inc., Waltham, Massachusetts, U.S.A) using the method described in Chapter 6. The results were averaged (n = 2), normalized, and plotted using the SigmaPlot 14.5 (Systat Software, Inc., Chicago, Illinois, U.S.A). A consolidated table on band assignments can be obtained from Chapter 3.

7.2.8. Statistical Analysis

Statistical analyses were performed using SigmaPlot 14.5 (Systat Software, Inc., Chicago, Illinois, U.S.A). Comparison between samples and controls was carried out using the One-Way Analysis of Variance. Values of p <0.05 were considered statistically significant and Tukey's multiple comparisons test was used to identify significant differences among the different samples.

7.3. Results and Discussion

7.3.1. Characterisation of Blackcurrant and Citrus Pectins

The physico-chemical and molecular properties of the dialysed BCP and commercial CP powders are shown in Table 7.1. The BCP and CP were high methoxyl pectins with a comparable DE (65 ± 10% and 67-71%, respectively). Both pectin powders had comparable moisture content (12.2 ± 0.32% and 10.7 ± 0.03% for BCP and CP, respectively) and contained structural proteins (4.8% w/w in BCP and 6.6 ± 0.2% w/w in CP), which are inherent in plant cell wall materials (Andersson et al., 2017). The BCP (78 ± 4.8 % w/w) contained substantially more carbohydrate than the CP (62 ± 4.6% w/w) of which ≈27% and ≈53% is GalUA, respectively. Based on previous work (Chapter 4), the carbohydrates in BCP comprised mainly of GalUA and neutral sugars—galactose, arabinose and rhamnose—signifying that it was rich in RG-I. Although, specific sugars of RG-II were not analysed in the previous work, traces of fucose and glucuronic acid were also detected, indicating the presence of RG-II as it has been shown by Hilz, Williams, et al. (2006). In contrast to this, pectic fraction that was isolated from citrus peels, via acid extraction, was found to contain more HG (88%) than RGs (12%) (Yapo et al., 2007). This coincided with the greater amount of GalUA in the CP powder (33 ± 4.4% w/w) than in the BCP powder (21 ± 2.9% w/w), likely because the CP was predominantly made of HG with a lot more GalUA units. The structural difference between the two pectins can be ascribed to the origin of the plant material and the method of isolation (Yapo et al., 2007).

Table 7.1 Physico-chemical and molecular properties of dialysed blackcurrant pectin (BCP) and commercial citrus pectin (CP) powder.

Properties		BCP	CP
Degree of Esterification	%	65 ± 10[b]	67-71[c]
Moisture[a]	% w/w	12.2 ± 0.32	10.7 ± 0.03
Crude Protein[a]	% w/w	4.5 ± 0.16[b]	6.6 ± 0.2
Total Carbohydrate[a]	% w/w	78 ± 4.8[b]	62 ± 4.6
Galacturonic Acid[a]	% w/w	21 ± 2.9[b]	33 ± 4.4
Ash[a]	% w/w	5.1 ± 0.2[b]	2.0 ± 0.1
Calcium[a]	% w/w	2.2 ± 0.1[b]	0.018 ± 0.001
Anthocyanin (pH differential method)[a]	% w/w	3.9 ± 0.1[b]	not detected
Acid Dissociation Constant, pK_a		1.7 ± 0.17[b]	1.8 ± 0.06
Range of Molecular Weight, M_w	kDa	97-283[b]	85-381
Range of root mean square (RMS) radius	nm	30-34[b]	29-50
Physical Appearance			

[a] Results are expressed as % of the component in the pectin powder (mean ± standard deviation).
[b] Data from Chapter 4.
[c] Provided by the manufacturer.

One of the isolation steps of BCP involved extensive dialysis that removed majority of the unbound small molecules, yet the amount of ash remained was much higher in BCP (5.1 ± 0.2% w/w) than in CP (2.0 ± 0.1% w/w), particularly the calcium content (2.2 ± 0.1% w/w and 0.018 ± 0.001% w/w, respectively). The large difference in ash and calcium content can have different causes, such as variations due to plant origin and possible calcium supplementation during the blackcurrant growth. Equally, it could be attributed to the milder extraction process of the BCP—water and ethanol extraction at 4 °C—which probably kept the calcium intact within the pectic fraction. The calcium ions detected in the BCP could be those stabilising the borate-dimeric-RG-II (dRG-II-B) fractions, via calcium bridges between the carboxyl groups of the HG segments covalently linked to the RG-II regions (Kobayashi et al., 1999). Shi et al. (2017) have shown that borate—bound to the dRG-II-B—and calcium, were essential components of plant cell wall that helped maintaining the integrity of the pectin network, and might be protected from chelation through steric hindrance, rendering chelating agents such as EDTA less effective. Therefore, the higher quantity of calcium in BCP could be justified by: (i) the high amount of RG-II in the commercial blackcurrant juice (Hilz, Williams, et al., 2006), and the

presence of sugars associated with RG-II in the mildly extracted BCP. In comparison, the extraction process of a commercial CP is usually done at harsher conditions—acidic extraction (pH 1-3) between 50 °C and 90 °C (Izydorczyk, 2005)—that may strip away or release the bound calcium. The low calcium content of CP might also be related to its minor RG-II fraction (Yapo et al., 2007). Overall, the chances of BCP calcium participating or affecting the pectin-protein complexation was low as the calcium ions were likely to be trapped among the RG-II regions and made unavailable via steric hindrance.

The crucial difference between the two pectins was the presence of ACNs, rich in BCP (3.9 ± 0.1% w/w) but absent in CP (yellowish powder). The orange and yellow colour of citrus fruits are attributed to the presence of carotenoids and eriocitrin, respectively and ACN is not a common phenolic compound of citrus fruits except in blood red orange (Curl & Bailey, 1956; Miyake et al., 1997; Singh et al., 2020). The highly processed CP might contain some phenolic compounds, but the quantity would be negligible compared to the amount of ACNs in the BCP. Rubio-Senent et al. (2015) reported that commercial apple pectin and CP have very low, or no antioxidant capacity and attributed it to the purification process of the commercial pectins, which may have removed and decreased their phenolic compounds. The similarity in the pK_a value of the BCP and CP (1.7 ± 0.17 and 1.8 ± 0.06, respectively) indicated that both pectins were negatively charged at the experimental pH of 4.5; this is important as one of the major mechanisms of pectin-protein interactions is via electrostatic forces. Generally, the BCP had a lower M_w and RMS radius (97-283 kDa and 30-34 nm, respectively) than the CP (85-381 kDa and 29-50 nm, respectively) and it displayed lower viscosity than the CP (Figure 7.2), despite comparing them at similar levels of GalUA. The lower viscosity of BCP was likely due to its (i) branched structure—based on its greater total carbohydrate content and the findings of Hilz, Williams, et al. (2006) on the presence of RG-II fraction in blackcurrant juice—and (ii) lower M_w. Similar relationship between the M_w, RMS radius, and viscosity has been reported in the extraction study of lime and orange pectin, where lower M_w and smaller RMS radius corresponded to the development of lower viscosities (Fishman et al., 2003). The relationship between M_w, size of polysaccharides and the viscosity properties of their solutions has been extensively studied (Lopes da Silva & Rao, 2006; Masuelli, 2011; Owens et al., 1944).

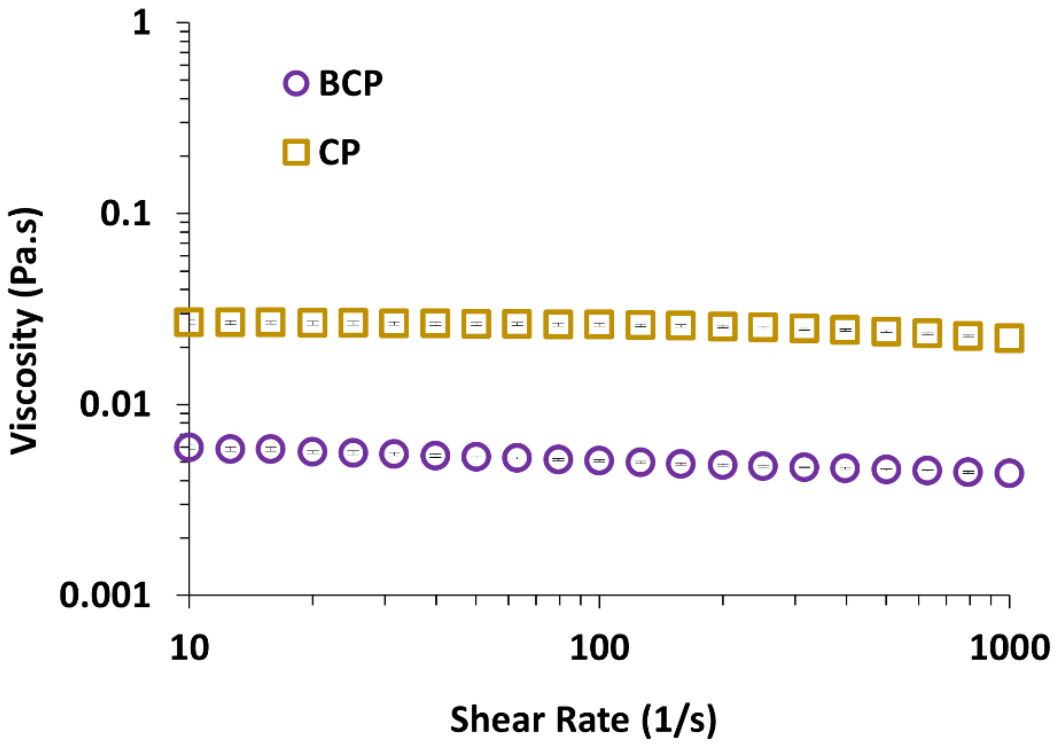

Figure 7.2 Viscosity (Pa.s) versus shear rate (1/s) of blackcurrant pectin (BCP) and citrus pectin (CP) at pH 4.5 based on 0.42% w/v galacturonic acid content.

7.3.2. Visual Appearance and Physical Stability of Pectin-Protein Mixtures

Turbidity can be measured by the amount of light that passes through a medium or is scattered by suspended solids (Ahmad Fairuz & Mohd Zubir Mat, 2013). In this study, the amount of light transmitted through the sample was used as a turbidity indicator. Figure 7.3 shows the amount of near-infrared light being transmitted through the controls and mixtures of BCP-WP and CP-WP (NH and MH at pectin:protein ratios of 1:1, 1:5 and 1:10). Mixing the BCP with WP caused the transmission of light in NH BCP-WP (1:1) mixture (62.8 ± 0.44%) to be lower than its BCP and WP controls (64.4 ± 0.04% and 65.0 ± 0.03%, respectively), signifying an increase of turbidity, likely because of complexes formation as a result of pectin-protein interactions. However, this was not observed in the NH CP-WP (1:1) mixture as the light transmission was insignificant as compared to its CP and WP controls. The contrast in turbidity between the images of NH BCP-WP and NH CP-WP mixtures at 1:1 ratio matches the trend in light transmission, suggesting that there were greater interactions happening in ACN-rich environment (BCP) than in ACN-free environment (CP).

Heating and increasing the protein ratio significantly reduced the light transmission of MH BCP-WP mixtures at 1:1 and 1:5 ratios—55.1 ± 0.67% and 9.26 ± 0.06%, respectively. Yet, heating did not

strongly affect the light transmission of MH CP-WP (1:1) mixture (61.9 ± 0.54%) as it was comparable to the light transmission of its NH equivalent (63.4 ± 1.76%). The reduction in light transmission became apparent only when the protein ratio of the MH CP-WP mixture was increased to 1:5 (52.3 ± 0.28%).

At higher protein ratio (1:10), the MH BCP-WP (0.09 ± 0.00%) mixture shows lower light transmission than the MH CP-WP (2.04 ± 0.25%) mixture. The high turbidity observed in both mixtures was likely the result of increased pectin-protein interaction at higher protein ratio as compared to the WP solution at 0.2% w/v which was relatively clear. It should be noted that the CP-WP mixture at 1:10 ratio was very unstable, and its complexes were sedimenting as soon as the mixture was poured into the measurement cell. Thus, the higher light transmission recorded for the MH CP-WP (1:10) mixture was because some of its complexes had sedimented, causing the mixture to appear less turbid than the MH BCP-WP (1:10) mixture. Overall, increasing protein concentration in the presence of heat led to increased turbidity in both MH BCP-WP and CP-WP systems, signifying greater pectin-protein interactions.

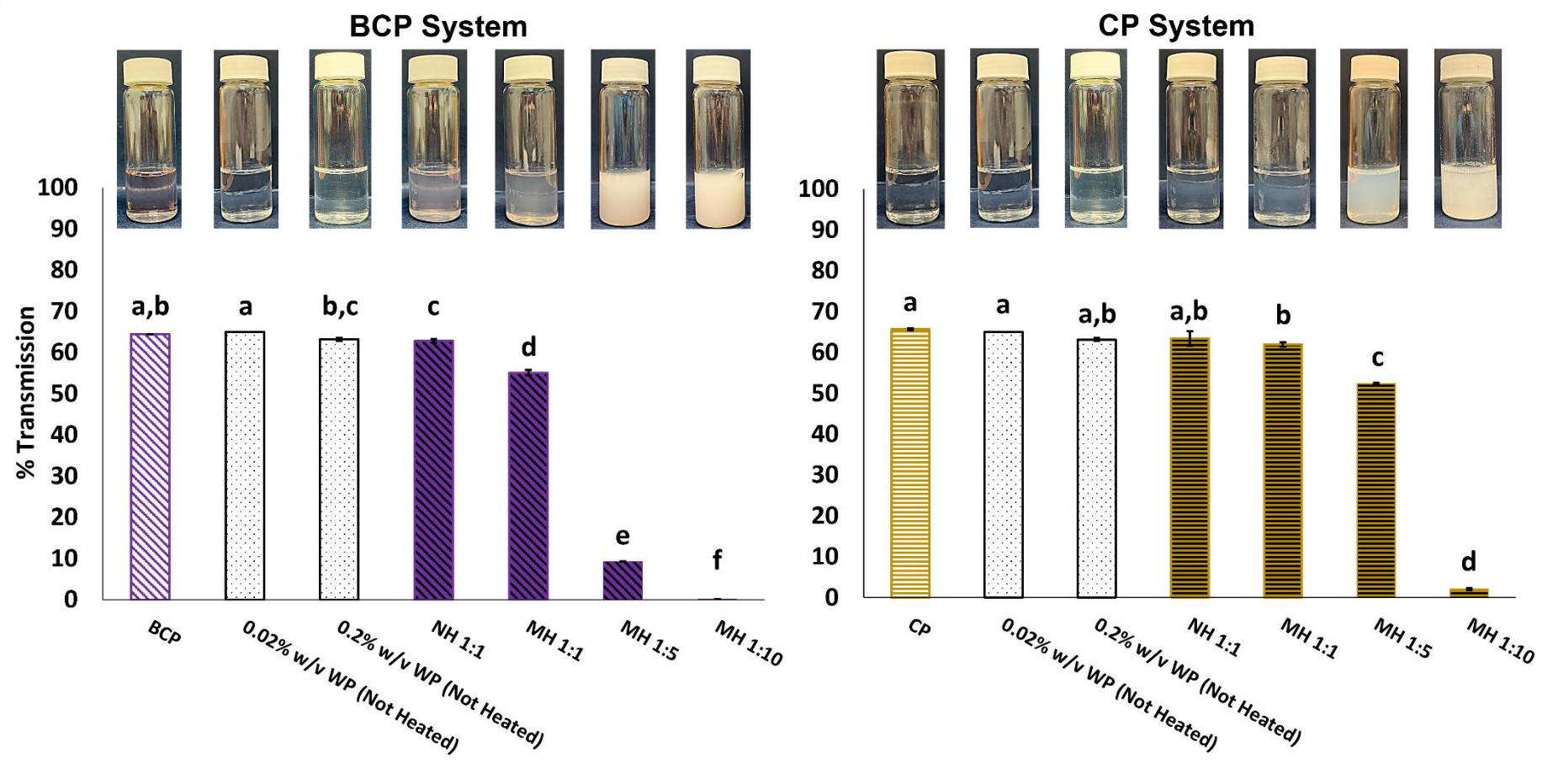

Figure 7.3 Percentage transmission of near-infrared LED (λ_{air}=880 nm, time 0 s) of blackcurrant and citrus pectin systems consisting of controls (BCP, blackcurrant pectin; CP, citrus pectin; 0.02% and 0.2% w/v WP, whey protein) and their mixtures (NH, Non-heated; MH, Mixed-Heated) at 1:1, 1:5 and 1:10 pectin:protein ratios (mean ± standard deviation). Means within a group are not significantly different if the letters (a-f) are the same.

The stability measurement of BCP-WP and CP-WP mixtures at 1:1 pectin:protein ratio (NH and MH) is shown in Figure 7.4. According to the TSI scale, at 24 h the NH mixtures of BCP-WP and CP-WP had weak (TSI of 1.25 ± 0.07) to significant (TSI of 3.05 ± 0.92) destabilisation, respectively. Based on the image of the NH CP-WP at 1:1 ratio, the mixture was comparably clear as its CP and WP controls with no visible sedimentation (Figure 7.3). However, the sudden increase of TSI at the tenth hour—from 1.65 ± 0.49 to 3.05 ± 0.92—is likely due to aggregates sedimenting, which could not be seen visually but detectable by the Turbiscan. Heating caused the final TSI value of the MH BCP-WP (1:1) mixture to slightly increase from ≈1.25 to 2.90 ± 0.14, yet visually, the MH mixture was comparable to its NH counterpart (Figure 7.3). In contrast, the stability of the MH CP-WP (1:1) mixture had improved markedly upon heating, reducing the TSI value from ≈3.05 to 1.90 ± 0.00. Observations from the two MH systems suggested that the heat treatment could have affected the conformation of both complexes that eventually changed their physical stability.

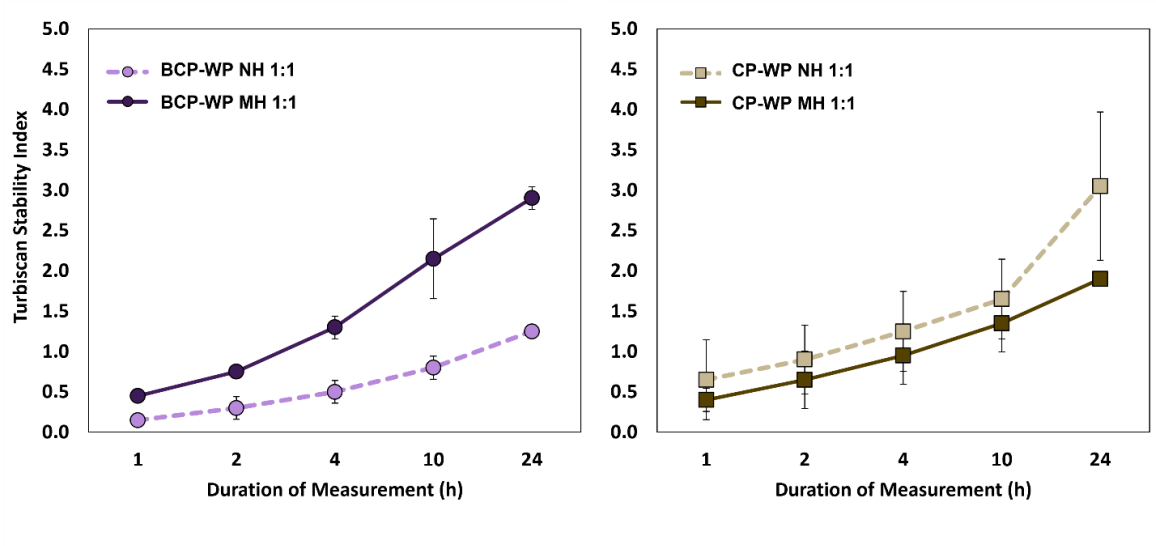

Figure 7.4 Turbiscan Stability Index of blackcurrant pectin-whey protein (BCP-WP) and citrus pectin-whey protein (CP-WP) mixtures (NH, Non-heated; MH, Mixed-Heated) at pectin:protein ratio of 1:1 measured across 24-h timeframe.

Figure 7.5A shows the stability measurements between MH BCP-WP and MH CP-WP mixtures at increasing pectin:protein ratios (1:1, 1:5, 1:10). Raising the protein ratio to 1:5 increased the final TSI value of both systems—BCP-WP mixture: ≈2.90 to 7.60 ± 4.38 and CP-WP mixture: ≈1.90 to 2.35 ± 0.07 (inset image of Figure 7.5A)—but the stability of BCP-WP mixture was severely impacted as its final TSI value was considered as significantly unstable (TSI 3 to 10). When the protein ratio was increased further to 1:10, the instability worsened and the final TSI value increased drastically for both mixtures—tripling to 21.1 ± 11.7 and increasing 24-fold to 57.8 ± 4.10 for MH BCP-WP and MH CP-WP, respectively. As described above, some of the MH CP-WP complexes at 1:10 ratio might have

sedimented as soon as it was aliquoted into the measurement cell and this instability is evident in the TSI plot of Figure 7.5B. Figure 7.5B shows the increasing TSI values of MH BCP-WP and MH CP-WP at 1:10 pectin:protein ratio in minutes. At time 2 to 10 min, the BCP-WP system shows gradual increase of TSI value as opposed to the rapid increase for CP-WP system. This highlights that the complexes formed in the CP-WP system were the least stable and likely to be large. The increase of protein ratio in the presence of heat did not only increase the turbidity of the mixtures, but also aggravated their instability, probably indicating amplified pectin-protein association. In order to understand the trend in light transmission and physical stability, information on the complexes size and surface charge is needed, and therefore presented in the next section.

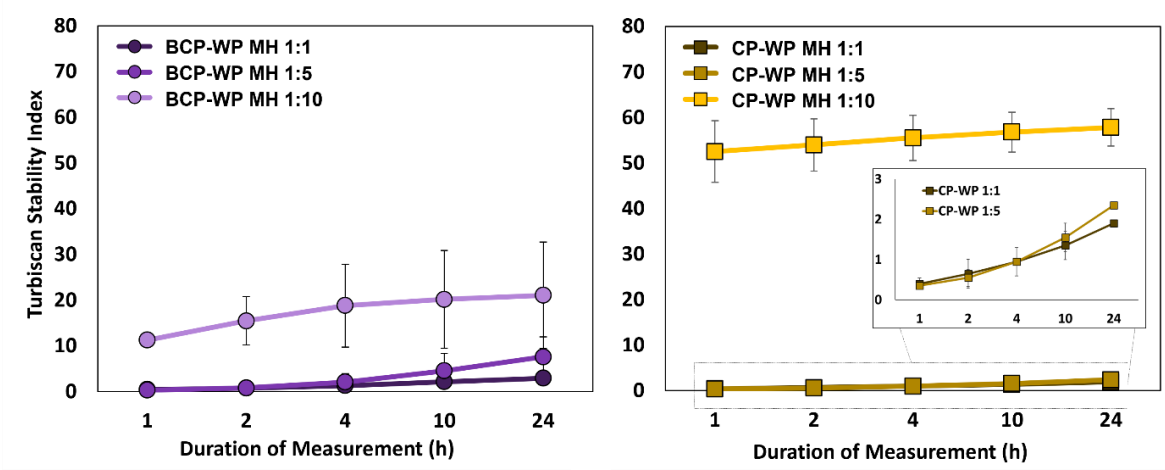

(A)

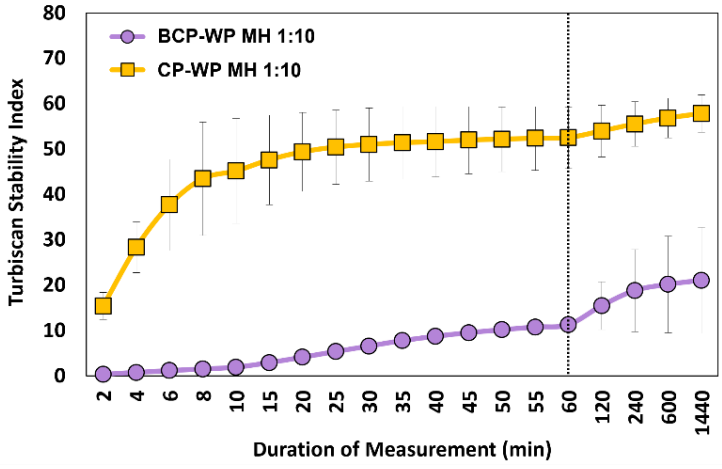

(B)

Figure 7.5 Turbiscan Stability Index of mixed-heated (MH) blackcurrant pectin-whey protein (BCP-WP) and citrus pectin-whey protein (CP-WP) mixtures at (A) 1:1, 1:5 and 1:10 pectin:protein ratios measured across 24-h timeframe and (B) 1:10 pectin:protein ratio showing time in minutes.

7.3.3. Particle Size and Zeta-Potential of Pectin-Protein Complexes

The Z-average size of the controls and the mixtures of BCP-WP and CP-WP is shown in Figure 7.6A. The BCP (422 ± 14.5 nm) was significantly smaller than the CP (772 ± 43.2 nm)—supported by the light intensity, number, and volume particle size distributions (Appendix B)—this was expected as the BCP had lower M_w (97-283 kDa) than the CP (85-381 kDa) and probably adopted a more branched conformation due to its RG regions. Furthermore, the lower quantity of GalUA in BCP—≈21% w/w and ≈33% w/w in BCP and CP, respectively—meant that a lower amount of dissociated carboxylic groups was present to extend the BCP structure. Thus, the reduced intramolecular repulsion could have also led to the smaller Z-average size of BCP in comparison to CP (Morris et al., 2000). Although the Z-average size of the non-heated WP was above 100 nm, based on its number and volume distributions, majority of the protein particles were actually very small, falling within the 4.5 to 5.1 nm range, as reported in Chapter 6.

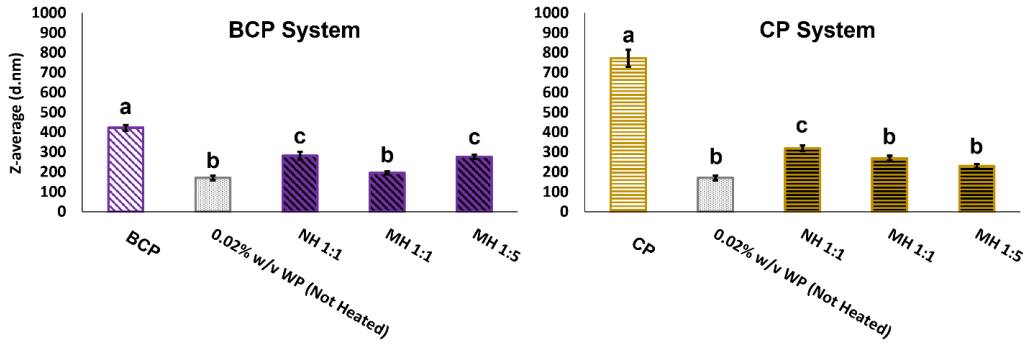

(A)

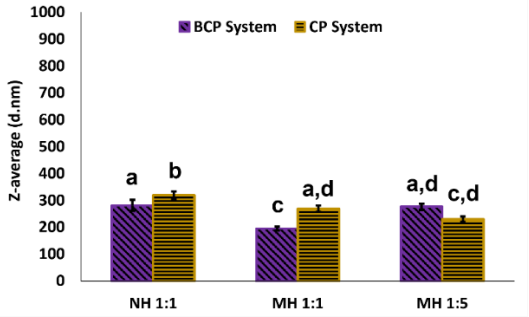

(B)

Figure 7.6 (A) Z-average size (nm) of blackcurrant and citrus pectin systems consisting of controls (BCP, blackcurrant pectin; CP, citrus pectin; 0.02% w/v WP, whey protein) and their mixtures (NH, Non-heated; MH, Mixed-Heated) at 1:1 and 1:5 pectin:protein ratios (mean ± standard deviation). Means within a group are not significantly different if the letters (a-c) are the same. (B) Z-average size (nm) of blackcurrant pectin-whey protein and citrus pectin-whey protein mixtures (NH, Non-heated; MH, Mixed-Heated) at 1:1 and 1:5 pectin:protein ratios (mean ± standard deviation). Means with the same letter (a–d) are not significantly different.

When either pectins were mixed with the WP at 1:1 ratio, the Z-average size of the NH BCP-WP (281 ± 20.2 nm) and NH CP-WP (319 ± 19.3 nm) complexes became considerably smaller than their pectin controls (≈422 nm and ≈772 nm, for BCP and CP respectively). The association of WPs to BCP or CP caused the pectin charges to be screened and the intramolecular repulsion of the pectin to be reduced, resulting in a more compacted conformation as it has been shown by Sperber et al. (2009).

When heat was applied, the Z-average of both MH 1:1 mixtures were further reduced—195 ± 7.31 nm and 269 ± 12.2 nm, for MH BCP-WP and MH CP-WP, respectively. The transition towards smaller particle size upon heating is likely due to the partial dissociation of the complexes—partial unfolding of the WP and disruption of hydrogen bonds at high temperature—and the re-complexation of the complexes to a more compacted conformation—via electrostatic and hydrophobic interactions, as well as hydrogen bonding upon cooling of the mixtures (Jones et al., 2010; Jones et al., 2009; Jones & McClements, 2011; Santipanichwong et al., 2008). Although the Z-average size of MH BCP-WP (1:1) complexes had reduced from ≈281 nm to ≈195 nm with heat treatment (Figure 7.6B), the instability of the mixture was slightly increased, from TSI value of ≈1.25 to ≈2.90. This is likely attributed to the complexes becoming slightly denser and heavier due to (i) the association of more WPs to the BCP and/or (ii) the compacting of the complexes during heating. It is worth noting that turbidity is not only affected by the size of the particles, but it also changes according to the number and conformation of the particles (Linke & Drusch, 2016; Niskanen et al., 2019).

When the pectin:protein ratio was increased to 1:5, the mixture produced larger MH BCP-WP complexes (276 ± 11.4 nm) than those at 1:1 ratio (≈195 nm), likely indicating that more WPs were associated to the BCP. However, raising the pectin:protein ratio in MH CP-WP mixture resulted in a statistically comparable complexes with Z-average size of 230 ± 10.2 nm. There is a possibility that more WPs were complexing with the CP, but it can only be confirmed by checking its particle size distribution. Based on Figure 7.6B, there was no difference between the Z-average size of MH BCP-WP and MH CP-WP at 1:5 ratio, as well as between MH CP-WP complexes at 1:1 and 1:5 ratios, yet the light transmission data and image of the mixtures show otherwise (Figure 7.3).

In order to ensure that the Z-average size is describing the complexes size correctly, it was interpreted along with the particle size distribution. The (A) light intensity and (B) number distributions of BCP-WP and CP-WP complexes (NH and MH at pectin:protein ratios of 1:1 and 1:5) are shown in Figure 7.7. The intensity distribution (Figure 7.7A) shows that the NH mixtures of BCP-WP (small peak: ≈68 nm and large peak: ≈346 nm) and CP-WP (small peak: ≈95 nm and large peak: ≈568 nm) had two complexes populations, with the BCP-WP mixture having the overall smaller complexes. This trend is similar to the number distribution (Figure 7.7B) of both NH mixtures, consisting of: (i) a major peak

representing small complexes (BCP-WP: ≈53 nm and CP-WP: ≈66 nm) and (ii) a shoulder peak representing large complexes (BCP-WP: ≈261 nm and CP-WP: ≈417 nm), as shown in the inset figure of the NH mixtures. The number distribution shows that both types of NH complexes were mostly (≥98%) <100 nm and that BCP-WP complexes were slightly smaller than the CP-WP complexes, matching the trend in the Z-average size.

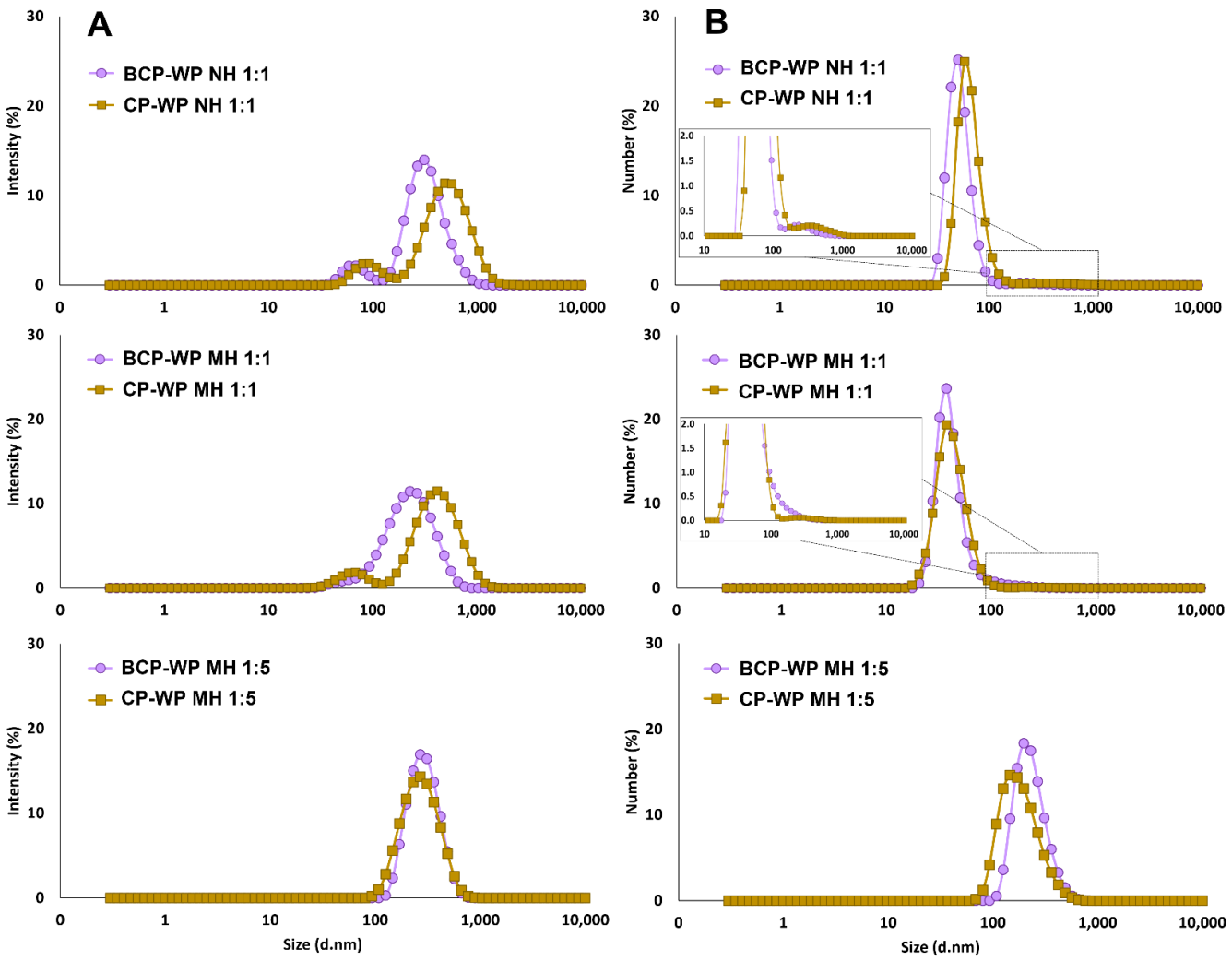

Figure 7.7 Average size distribution of blackcurrant pectin-whey protein (BCP-WP) and citrus pectin-whey protein (CP-WP) mixtures (NH, Non-Heated; MH, Mixed-Heated) at 1:1 and 1:5 pectin:protein ratios, based on (A) light scattering intensity and (B) number weighting mechanisms.

The larger aggregates in the NH CP-WP (1:1) mixture—≈417 nm, based on number distribution—is likely the reason for its sudden increase of TSI value at the tenth hour (Figure 7.4). According to a study by Xu et al. (2015), the interaction between β-lactoglobulin and ACN-free pectin at 25 °C—DE of 37% to 86%—occurred via a two-stage process: (i) the association of proteins to pectin via electrostatic interaction forming small complexes and (ii) the development of the associated proteins into seeding proteins that promoted the nucleated growth of protein aggregates on top of the seeding proteins. It is likely that the large aggregates of NH CP-WP (1:1) mixture were formed via the mechanism proposed by Xu et al. (2015)

Upon heating, the complexes in the MH BCP-WP (1:1) mixture (≈246 nm) were reduced to a single population peak, yet no major peak change was observed in the MH CP-WP (1:1) mixture (small peak: ≈67 nm and large peak: ≈457 nm) (Figure 7.7A). According to the number distribution, heating reduced the particle size of both MH 1:1 mixtures (Figure 7.7B). There are two indications: (i) the major peak of MH mixtures representing small complexes (BCP-WP: ≈44 nm and CP-WP: ≈45 nm) was shifted to the left side of the distribution plot and was almost overlapping with each other, and (ii) the shoulder peak which represents large complexes had disappeared from MH BCP-WP mixture but remained present in the MH CP-WP mixture. The changes observed in the shoulder peak of the MH 1:1 mixtures highlighted the conformational changes of the pectin-protein complexes upon heating, possibly from the disruption of hydrogen bonds. Overall, number distribution indicates that majority (≥99.5%) of the complexes in both MH mixtures were <50 nm and were of comparable size, but due to the presence of minute large complexes in MH CP-WP (1:1) mixture (≈314 nm) its reported Z-average size was greater than the size of MH BCP-WP (1:1) mixture (Figure 7.6B).

Heating the mixtures at 1:5 pectin:protein ratio produced bigger complexes that are of comparable size—≈301 nm and ≈286 nm for MH BCP-WP and MH CP-WP, respectively, based on light intensity distribution (Figure 7.7A)—and the number distribution (Figure 7.7B) corresponds well with the complexes growth as more protein was added. The importance of interpretating the Z-average size along with the particle size distributions is evident. It is especially relevant when the Z-average size between two samples appeared comparable, yet the number distributions indicate that their dominant particles were of different size, such as between the mixtures of MH CP-WP at 1:1 and 1:5 ratios of Figure 7.6B and Figure 7.7B.

The polydispersity index (PDI) of BCP-WP and CP-WP mixtures is shown in Table 7.2. All the BCP-WP mixtures have moderate (0.1 to 0.4) polydispersity, while two of the CP-WP mixtures (NH and MH at 1:1 pectin:protein ratio) were categorized as broadly polydisperse (>0.4). In the absence of heating, the NH BCP-WP (1:1) mixture (0.39 ± 0.05) was significantly less polydisperse than the NH CP-WP (1:1)

mixture (0.49 ± 0.02). Heating these, reduced the PDI of MH BCP-WP to 0.26 ± 0.01, while the PDI of MH CP-WP (0.45 ± 0.04) remained comparable. This significant decrease was probably due to the complete disappearance of large aggregates in the MH BCP-WP (1:1) mixture observed in Figure 7.7B. Increasing the protein ratio to 1:5 almost halved the PDI value of both mixtures (0.15 ± 0.03 and 0.24 ± 0.01, for MH BCP-WP and MH CP-WP, respectively), and this can be seen clearly in the narrowness of the peaks in Figure 7.7A.

Table 7.2 Polydispersity index (mean ± standard deviation) of blackcurrant pectin-whey protein (BCP-WP) and citrus pectin-whey protein (CP-WP) mixtures (NH, Non-Heated; MH, Mixed-Heated) at 1:1 and 1:5 pectin:protein ratios. Means with the same letter (a-d) are not significantly different.

	Polydispersity Index	
	BCP-WP	**CP-WP**
NH 1:1	0.39 ± 0.05^{a}	0.49 ± 0.02^{d}
MH 1:1	0.26 ± 0.01^{b}	$0.45 \pm 0.04^{a,d}$
MH 1:5	0.15 ± 0.03^{c}	$0.24 \pm 0.01^{b,c}$

Since the complexes at 1:10 pectin:protein ratio were above the size limit of dynamic light scattering (3×10^{-4} µm to 10 µm), static light scattering (Mastersizer with a size range 0.02 µm–1000 µm) was used as the particle size technique. Figure 7.8 shows the particle size distributions and the mean size diameters of these mixtures, with the CP-WP complexes (D [4,3]: 92.1 ± 16.2 and D [3,2]: 63.6 ± 10.3) being much larger than the BCP-WP complexes (D [4,3]: 21.3 ± 2.76 and D [3,2]: 15.4 ± 2.00). The increase in particle size of both mixtures indicated that more protein association had occurred, as well as the possibility of complex association. Majority of the CP-WP complexes were >100 µm while most of the BCP-WP complexes were <100 µm. This accounts for the extremely high turbidity and instability of both MH 1:10 mixtures shown in Figure 7.3 and Figure 7.5, respectively, with the CP-WP mixture being the least stable. The size difference could be likely attributed to structural variations like larger M_w and higher GalUA content of CP that accommodated more binding sites for protein and possibly other complexes.

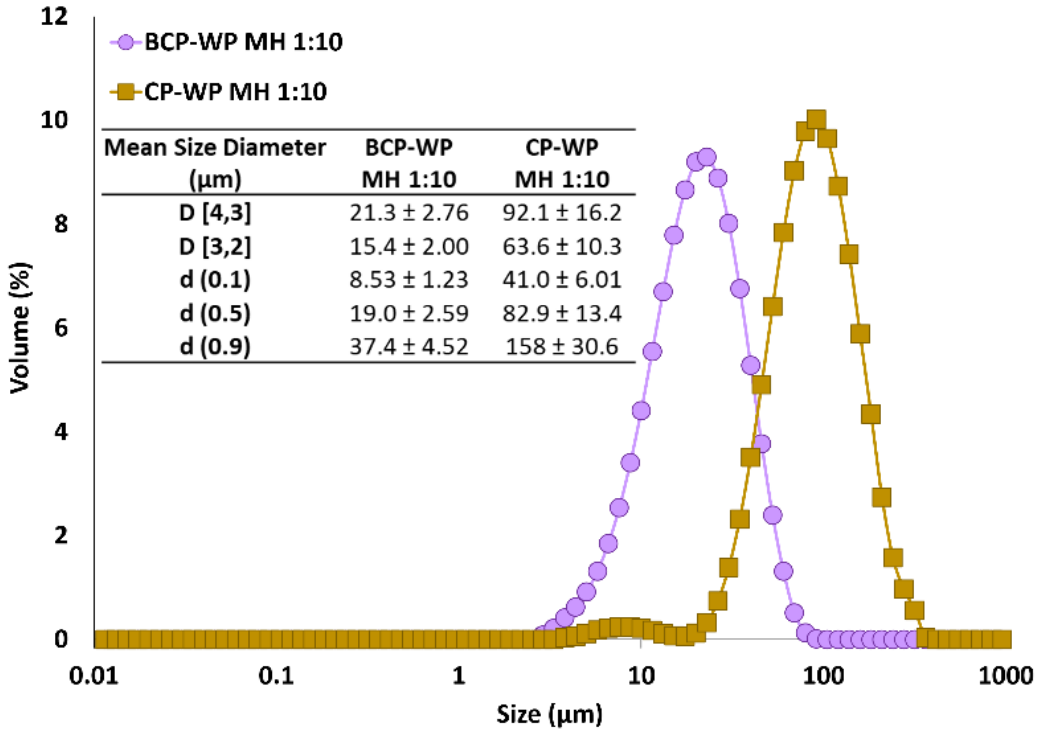

Figure 7.8 Average size distribution of mixed-heated (MH) blackcurrant pectin-whey protein (BCP-WP) and citrus pectin-whey protein (CP-WP) mixtures at 1:10 pectin:protein ratio, based on volume weighting mechanism.

The zeta-potential of the controls and the mixtures of BCP-WP and CP-WP is presented in Figure 7.9. Despite having comparable DE, the CP (-33.2 ± 3.66 mV) was more negatively charged than the BCP (-23.4 ± 1.57 mV) and this was expected as the CP carries more carboxyl groups due to its higher content of GalUA, as described earlier. When the negatively charged pectin was mixed with the positively charged WP (+7.84 ± 0.96 mV), the surface charge of the resultant NH BCP-WP (-22.2 ± 1.00 mV) and NH CP-WP (-34.6 ± 1.74 mV) mixtures appeared to be similar as their pectin controls (≈-23.4 mV and ≈-33.2 mV, for BCP and CP respectively). This trend was also observed in both MH mixtures at pectin:protein ratios of 1:1 and 1:5, where their surface net charge was comparable to the surface charge of their respective pectin controls.

The zeta-potential value of both pectins was not significantly affected by the association of WPs at pectin:protein ratio below 1:5. Obvious surface charge reduction was only seen in the MH CP-WP mixture at 1:10 pectin:protein ratio (-19.1 ± 2.91 mV). Surprisingly, regardless of the heating and the increasing of protein ratio, the surface charge of MH BCP-WP (1:10) mixture (-20.6 ± 0.88 mV) remained similar as the surface charge of the BCP and other MH BCP-WP mixtures, signifying that most of the electrostatic binding sites of the BCP were unoccupied. This reveals the presence of other non-electrostatic interactions between the BCP and WP with heat treatment, such as hydrophobic and

hydrogen bonding forces. It is possible that the negatively charged carboxyl groups of the BCP were not significantly reduced, despite the increased pectin-protein association at increasing protein ratios, as shown in Figure 7.3. In contrast, the carboxyl groups of the CP were screened significantly when more WPs were added to the mixture, hence the significantly reduced zeta-potential value at 1:10 pectin:protein ratio.

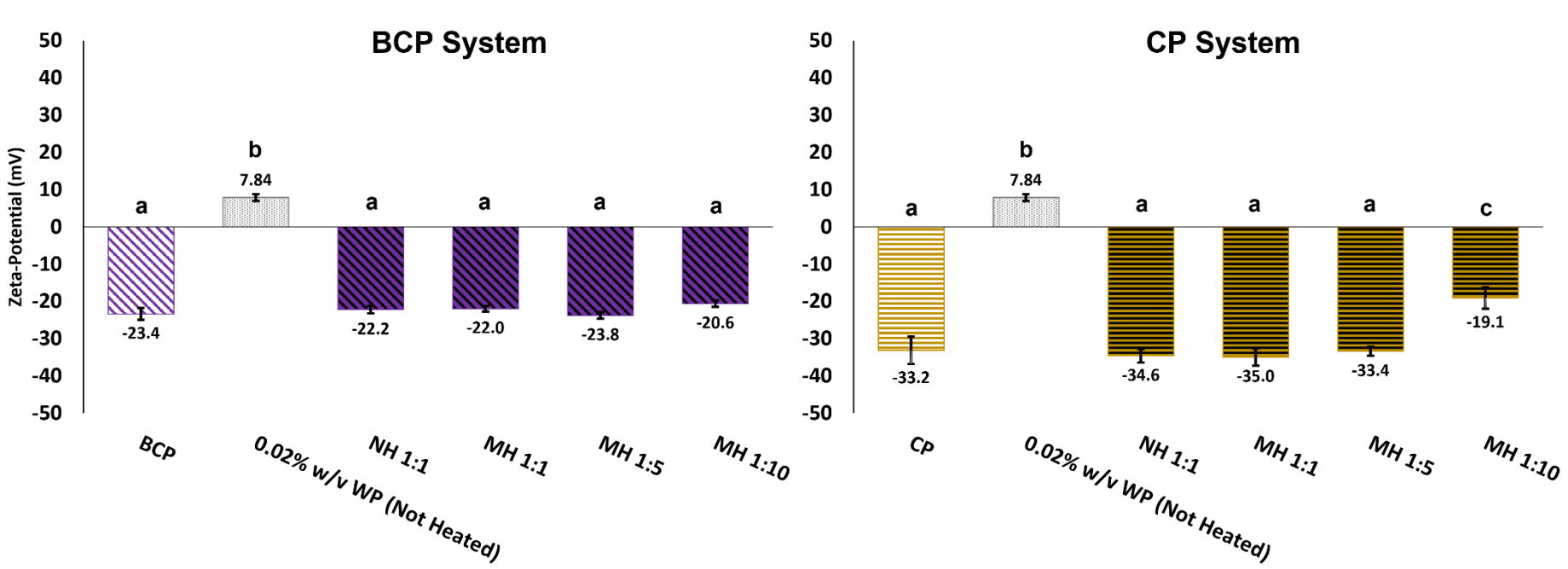

Figure 7.9 Zeta-potential (mV, mean ± standard deviation) of controls (BCP, blackcurrant pectin; CP, citrus pectin; 0.02% w/v WP, whey protein) and their mixtures (NH, Non-Heated; MH, Mixed-Heated) at 1:1, 1:5 and 1:10 pectin:protein ratios. Means within a group are not significantly different if the letters (a-c) are the same.

7.3.4. Distribution of Pectin and Protein in Soluble and Insoluble Fractions

Quantifying the amount of pectin and protein in the soluble and insoluble fractions provided information on (i) the distribution of biopolymers in the two phases and (ii) the yield of soluble and insoluble complexes—estimated from the total quantity of biopolymers. Since centrifuging the controls at the studied concentration did not show any sign of sedimentation, the fraction that had sedimented from the mixture was regarded as the insoluble complexes, while the fraction that remained in the supernatant was deemed as the soluble complexes.

Figure 7.10 shows the distribution of pectin and protein within the complexes (soluble and insoluble) of BCP-WP and CP-WP mixtures at 1:1 pectin:protein ratio (NH and MH). Chapter 6 has shown that pH influenced the interaction between BCP, its bound ACNs and WP, and that the BCP-WP complexation was weaker at pH 4.5 than at pH 3.5. Comparison between the BCP-WP and CP-WP systems at pH 4.5 showed that more insoluble complexes were produced when ACNs were present in the system (Figure 7.10), regardless of heat treatment. In an ACN-rich environment, almost half of the pectin (59.8 ± 6.09% w/w) and protein (48.6 ± 0.96% w/w) added were found in the NH BCP-WP sedimented fraction, but in the absence of ACNs, much lower amounts of pectin (16.7 ± 0.84% w/w) and protein (13.1 ± 2.95% w/w) were detected in the NH CP-WP sedimented fraction. This observation can be interpreted as (i) the WPs were more associative or reactive towards the BCP than the CP due to the presence of ACNs, (ii) the electrostatic stability conferred by the BCP (<-25 mV) was weaker than the CP (>-30 mV), thus sedimenting more BCP-WP complexes despite their comparable particle size and/or (iii) the viscosity conferred by the BCP was too low to prevent any sedimentation of the complexes.

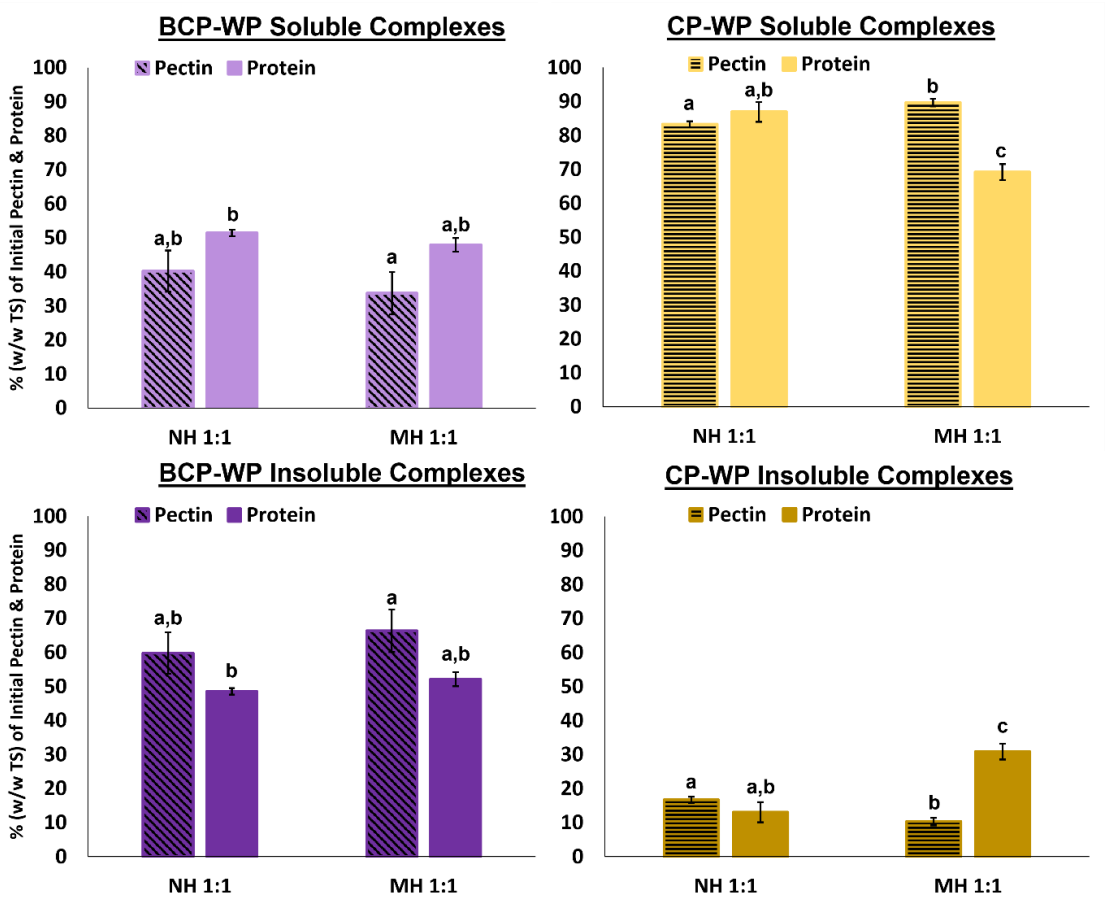

Figure 7.10 Percentage of initial pectin and protein (w/w total solids, mean ± standard deviation) found as part of the soluble and insoluble complexes of non-heated (NH) and mixed-heated (MH) mixtures of blackcurrant pectin-whey protein (BCP-WP) and citrus pectin-whey protein (CP-WP) at pectin:protein ratio of 1:1. Means within a group are not significantly different if the letters (a-c) are the same.

The amount of pectin (66.3 ± 6.26% w/w) and protein (52.1 ± 2.03% w/w) in the MH BCP-WP insoluble complexes was comparable to its NH equivalent. As indicated in Chapter 6, heating might have altered the initial conformation of the BCP-WP complexes by partially unfolding the globular WPs and re-complexing it with the BCP. As a result of the re-structuring during heating, the MH BCP-WP complexes might appear more compact than the NH BCP-WP complexes, possibly making the sedimentation of the MH complexes easier than the NH complexes. However, based on Figure 7.7B, their size difference was not big enough to cause more sedimentation, thus the comparable biopolymer amount in the sedimented complexes. Unlike the BCP-WP systems, the amount of pectin and protein in the MH CP-WP insoluble complexes was significantly different from its NH equivalent—lesser pectin (10.3± 1.10% w/w) and more protein (30.8 ± 2.33% w/w). This indicates that heating might have caused structural changes that altered the distribution of biopolymers between the NH and MH CP-WP insoluble complexes.

When the pectin:protein ratio was increased from 1:1 to 1:10, more biopolymers were captured in the sedimented fraction of MH BCP-WP and MH CP-WP mixtures (Figure 7.11) (i.e., more insoluble complexes were produced), signifying that the pectin-protein interactions were greater when additional protein was made available, irrespective of the ACNs presence. This increasing trend also coincided with the increasing turbidity of both types of mixtures shown in Figure 7.3. Yet, heated mixtures that contained BCP at 1:1 and 1:5 pectin:protein ratios had considerably more sedimented biopolymers and insoluble complexes than those made with CP, and this was probably the reason for the more turbid appearance of the BCP-WP systems (Figure 7.3).

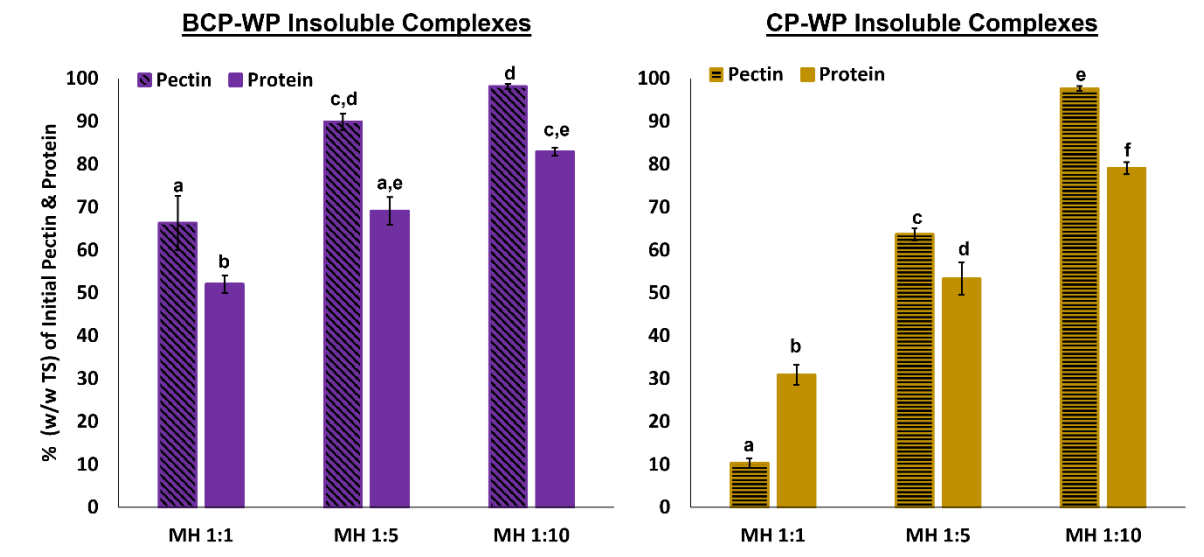

Figure 7.11 Percentage of initial pectin and protein (w/w total solids, mean ± standard deviation) found as part of the insoluble complexes of mixed-heated (MH) mixtures of blackcurrant pectin-whey protein (BCP-WP) and citrus pectin-whey protein (CP-WP) at pectin:protein ratio of 1:1, 1:5 and 1:10. Means within a group are not significantly different if the letters (a-f) are the same.

The molar ratio of the sedimented pectin and protein for all the mixtures is presented in Table 7.3. The NH BCP-WP (1:1) insoluble complexes had molar ratio that was comparable to its MH counterpart—1:2.79 and 1:2.69, respectively. In comparison, the CP-WP (1:1) insoluble complexes had molar ratios that were much higher and different from each other—1:5.63 and 1:21.5, for NH and MH, respectively. The higher molar ratio for both CP-WP insoluble complexes meant that the CP had greater capacity for WP association, likely because the CP is a larger pectin (85-381 kDa) with more GalUA content (33 ± 4.4% w/w) than the BCP (M_w: 97-283 kDa and GalUA content: 21 ± 2.9% w/w). A larger polysaccharide can facilitate the formation of complexes allowing the interaction with more proteins (Schmitt et al., 2009). When heating was involved, the capacity of CP complexing with the WP became higher—tripled to 1:21.5—yet the capacity of the BCP remained similar (1:2.69) as its NH equivalent. In this situation, it is likely that the WP molecules were fully distributed and associated to

the BCP molecules as both soluble and insoluble complexes, therefore heating the BCP-WP mixture at 1:1 ratio could not increase the amount of associated WPs, unless there were un-associated WPs in the mixture or more WP was added. Increasing the WP ratio to 1:5 and 1:10, raised the molar ratio considerably for both types of insoluble complexes—MH BCP-WP (1:13.2 and 1:28.9, respectively) and MH CP-WP (1:29.9 and 1:57.8, respectively)—revealing that both pectins were associated with more WPs and were not saturated.

Table 7.3 Molar ratio of pectin (BCP, blackcurrant pectin; CP, citrus pectin) and whey protein (WP) for the insoluble complexes of non-heated (NH) and mixed-heated (MH) BCP-WP and CP-WP mixtures at 1:1, 1:5 and 1:10 pectin:protein ratios.

	BCP-WP Insoluble Complexes	SD	CP-WP Insoluble Complexes	SD
NH 1:1	1 : 2.79	0.34	1 : 5.63	1.54
MH 1:1	1 : 2.69	0.15	1: 21.5	3.90
MH 1:5	1 : 13.2	0.89	1: 29.9	1.45
MH 1:10	1 : 28.9	0.13	1 : 57.8	1.35

Overall, sedimentation of BCP-WP complexes could be ascribed to a combination of reasons. Although there was a possibility that the WPs were more associative towards the BCP, sedimentation of BCP-WP complexes could also be driven by the weaker electrostatic stability and the low viscosity of the BCP, indicating weaker resistance against the centrifugal force. In order to verify the effect of ACNs on pectin-protein interactions, FTIR spectroscopy was used to assess the functional groups of the pectins and WP upon their complexation.

7.3.5. FTIR Assessment of Soluble and Insoluble Fractions

Figure 7.12 shows the FTIR spectrum of controls and the soluble fractions of BCP-WP and CP-WP mixtures at 1:1 pectin:protein ratio (NH and MH). The presence of bound ACNs caused the peaks of BCP to appear broader than the peaks of the ACN-free CP, signifying the various intermolecular interactions happening within the BCP. The spectrum of BCP and CP has two peaks corresponding to the esterified (1731 cm^{-1}) and non-esterified (BCP: 1602 cm^{-1} CP: 1601 cm^{-1}) carboxyl groups of pectin, while the distinct peak at the end (BCP: 1015 cm^{-1} CP: 1012 cm^{-1}) indicates that they are GalUA-rich polysaccharides (Mierczynska et al., 2017; Posé et al., 2015).

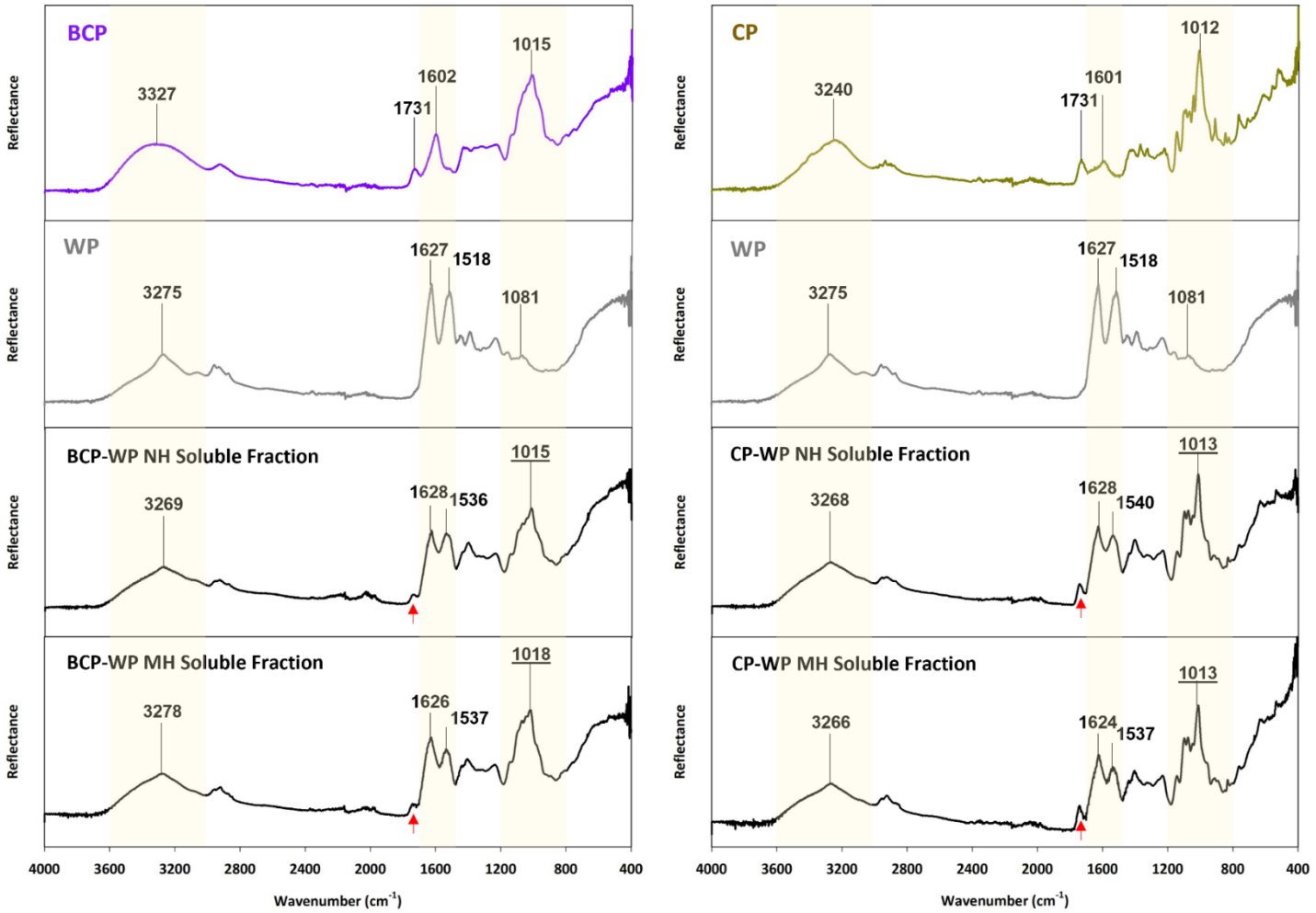

Figure 7.12 FTIR spectrum of controls (BCP, blackcurrant pectin; CP, citrus pectin; WP, whey protein) and the soluble fraction of their mixtures (NH, Non-Heated; MH, Mixed-Heated) at pH 4.5. Bands between 2000 cm^{-1} and 2400 cm^{-1} are artefacts from the ATR diamond.

The spectrum of BCP-WP and CP-WP soluble fractions retained the profile of WP and their respective pectin control. The first three identified peaks of the soluble fractions—from (i) 3000 to 3600 cm^{-1} and (ii) 1460 to 1680 cm^{-1}—resemble the peaks of WP and comparison between them indicates that the peaks have shifted away from the WP peaks, suggesting slight perturbations to the bond strengths as a result of pectin-protein interactions. The first region is assigned to the polymeric interaction between the O-H groups of carboxylic acids—originating from the BCP, CP and WP—and the N-H groups of amides and amines from the WPs, indicative of hydrogen bonding and electrostatic interactions (Zaleska et al., 2000; Zhao et al., 2020). The second region corresponds to three functional groups that are also likely to be involved in electrostatic interactions: (i) C=O stretching of non-esterified carboxyl groups of the pectin chain (≈1600 cm^{-1}), (ii) the C=O stretching of WP amides (1627 cm^{-1}), and (iii) the N-H bend of WP amines (1518 cm^{-1}) (Mierczynska et al., 2017; Zaleska et al., 2000). Major peak shift is observed on the band assigned to the N-H bend of amines (1518 cm^{-1}) in comparison to the one assigned to C=O stretching of amides (1627 cm^{-1}). This is probably because electrostatic interaction occurs mainly between the non-esterified carboxyl groups of pectin (COO^-) and the N-H bend of WP amines (NH_3^+) as they carry opposite charges at pH 4.5 (Zhao et al., 2020).

Previous work (Chapter 6) has shown that the IR bands of the functional groups of ACNs and BCP were overlapping, hence, there is a possibility that the bound ACNs of BCP are also contributing to the peak shifts mentioned in the above regions. Moreover, the peak that represents the esterified carboxyl group of pectin (1731 cm^{-1}) can be seen in all soluble fractions—indicated by the red arrow—suggesting that the functional group was not that affected by the complexation, irrespective of ACNs presence.

The final identified region of BCP-WP and CP-WP soluble fractions—between 800 and 1200 cm^{-1}—is similar to the signature peak of the BCP (1015 cm^{-1}) and CP (1012 cm^{-1}), respectively, corresponding to the C-O stretch of the carboxylic acids, ethers, esters, and alcohol groups of the pectin molecule, as shown in Chapter 6. Remarkably, no substantial shift is observed in this region, except for a minor shift in the peak of MH BCP-WP soluble fraction (1018 cm^{-1}). Based on the discussion in Chapter 6, this region also represents the functional groups of the ACNs, thus there is a possibility that the minor peak shift is related to the bound ACNs of BCP interacting with WP upon heating, which is lacking in CP. Overall, it is likely that the formation of BCP-WP and CP-WP soluble complexes was governed by electrostatic interaction and to a lesser extent, hydrogen bonding.

The FTIR analysis of the BCP-WP and CP-WP insoluble fractions at 1:1 pectin:protein ratio (NH and MH) is shown in Figure 7.13. The spectrum of the insoluble fractions shares similar profile as the WP, but not their respective pectin control. Similar to the soluble fractions, minor peak shift seen in the first

three peaks of the NH BCP-WP and NH CP-WP insoluble fractions proves that the functional groups of WP have been altered due to pectin-protein interactions. When heating was involved, larger peak shifts are observed in the MH BCP-WP insoluble fraction, indicating that heating affects pectin-protein complexation more when ACNs are present.

As mentioned previously, the location of the final peak—between 800 and 1200 cm^{-1}—can be assigned to various functional groups of the pectin (BCP or CP) and ACNs. Comparison between the final peak of CP and CP-WP insoluble fractions reveals that the peak has shifted slightly from 1012 cm^{-1} to 1017 cm^{-1} and 1018 cm^{-1} in NH and MH CP-WP, respectively. The slight shift may indicate minor hydrogen bonding and/or hydrophobic interactions that occurred within the CP-WP systems. Although, the primary mode of CP-WP interaction is by electrostatic interaction, some hydrogen bonding and hydrophobic interactions can still occur, depending on the experimental conditions (Girard et al., 2002, 2003a, 2003b; Jones et al., 2009). On the contrary, the BCP-WP insoluble fractions have a new peak with a very distinct peak number as compared to the final peak of BCP—1015 cm^{-1} versus 1042 cm^{-1} and 1066 cm^{-1} in NH and MH BCP-WP, respectively. The new peak may be related to the substantial amounts of hydrophobic interactions and hydrogen bonds occurring between the WPs and the bound ACNs and other functional groups of the BCP. Moreover, the peak of WP aliphatic amines—assigned at 1081 cm^{-1} (Zaleska et al., 2000) and indicated by the red arrow—can be seen in the spectrum of both CP-WP insoluble fractions but not apparent at all in the BCP-WP insoluble fractions, suggesting that the aliphatic amines of the WPs were altered when they complexed with BCP.

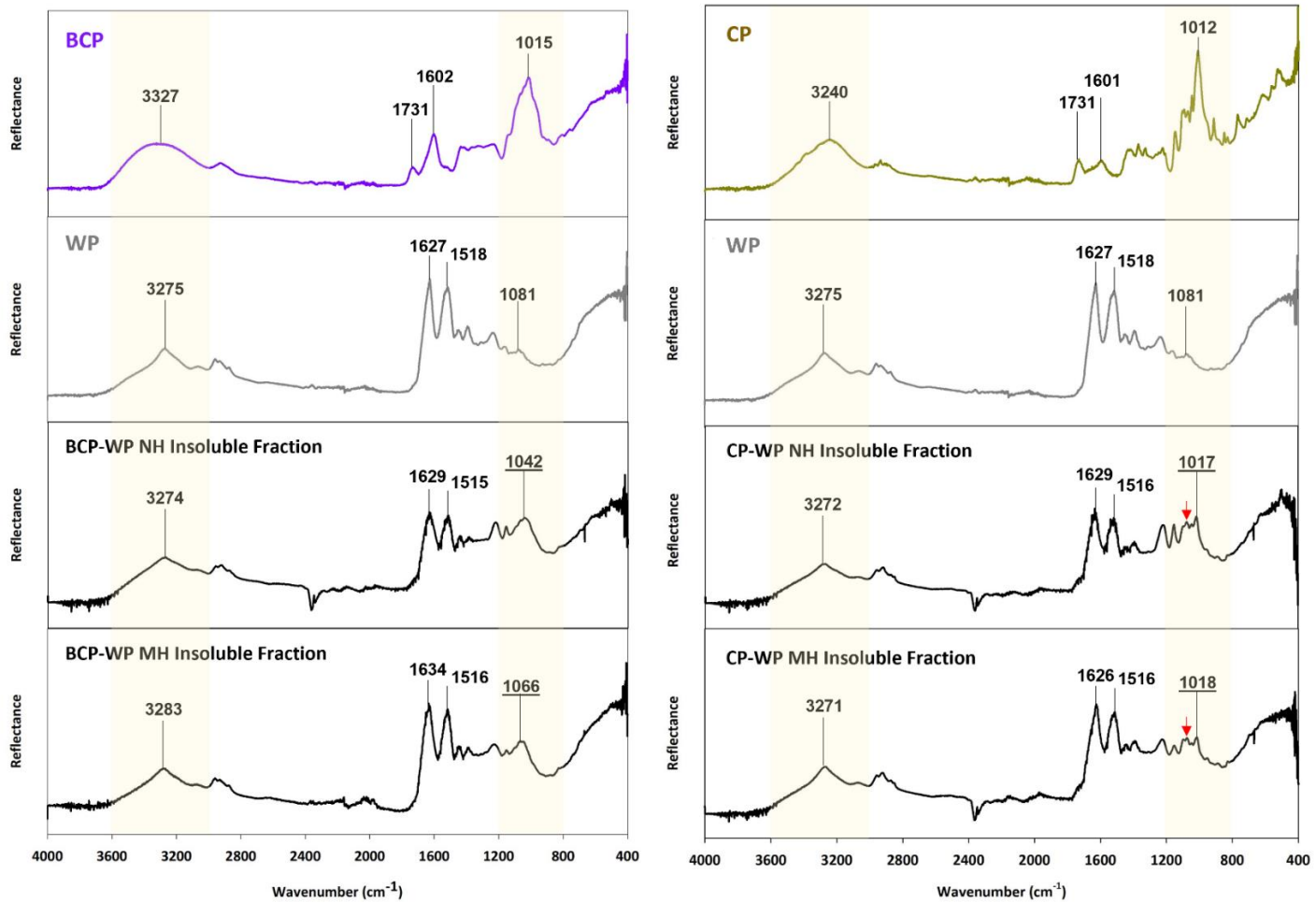

Figure 7.13 FTIR spectrum of controls (BCP, blackcurrant pectin; CP, citrus pectin; WP, whey protein) and the insoluble fraction of their mixtures (NH, Non-Heated; MH, Mixed-Heated) at pH 4.5. Some of the spectra show a carbon dioxide band (≈2340 cm^{-1}) and artefacts from the ATR diamond between 2000 cm^{-1} and 2400 cm^{-1}.

7.4. Conclusions

- The considerable peak changes seen in the FTIR analysis of the ACN-rich insoluble complexes had validated the interference and participation of ACNs in pectin-protein complexations, likely by providing a large quantity of non-electrostatic binding sites to the WP.
- In the absence of heat, the interaction between BCP and WP was probably initiated by the attractive electrostatic force—between the negatively charged carboxyl groups of BCP and the positively charged amino groups of the WPs. It was likely that hydrogen bonding and hydrophobic interactions were also occurring at the binding sites found on the surface of the globular WPs and the BCP (i.e., the ACNs, O-H and N-H groups and methoxy groups of the BCP).
- The CP might have interacted with the globular WPs mainly via electrostatic and some hydrogen bonding forces. Due to ACNs absence there was little opportunity for hydrophobic interactions to occur, although minor hydrophobic interactions might arise between the CP methoxy groups, and the hydrophobic amino acids found on the surface of the WPs.
- The development of turbidity and the distribution of pectin and protein amongst the soluble and insoluble complexes offered valuable information that suggested the influence of ACNs in pectin-protein interactions. However, several factors could contribute to the trends seen in both measurement techniques, such as the impact of particle size, number, and conformation on turbidity, and the impact of electrostatic stability and viscosity on complexes sedimentation and physical stability.
- Particle size data correlated well with physical stability results, but they did not illustrate the influence of ACNs on pectin-protein interactions.
- Under heating, ratios of pectin (BCP or CP) to WP above 1:5 substantially affected the physical stability of the mixed system.
- Surface charge data demonstrated that with heat treatment, the BCP-WP interaction was likely governed by non-electrostatic interactions.
- FTIR analyses revealed that the functional groups of BCP-WP soluble fractions were mostly affected by electrostatic interactions, whereas in the insoluble fractions, the functional groups were affected by a combination of interactive forces, confirming that the bound ACNs provided additional binding sites for the WPs to interact with.

Chapter 8 Overall Conclusions and Future Work Recommendations

8.1. Overall Conclusions

The instability mechanisms of blackcurrant juice-milk system were studied by characterising the key interactive components of the blackcurrant juice and investigating their complexations with whey proteins (WP) using a model system. This study provided answers to the research questions presented in Figure 1.2. The followings show the three main research questions:

8.1.1. What are the components of blackcurrant juice that can potentially interact with milk proteins?

- The key interactive components were identified to be pectin, polyphenols (mainly anthocyanins), and proteins (Figure 8.1). These components were likely to be associated with one another at the early processing stages of the puree and juice, such as during crushing, mashing, and enzyme maceration. Due to the disruption of the cell wall, various plant constituents were liberated and exposed, allowing interactions such as pectin-anthocyanin, pectin-protein, and polyphenol-protein interactions to occur between the blackcurrant components.

- The highly pigmented pectin-rich fraction that was obtained after multiple ethanol washes and dialyses indicated that the anthocyanins were bound to the fraction. The unsuccessful attempt to quantify the bound anthocyanins via liquid chromatography reinforced the deduction that high quantity of anthocyanins was tightly bound to the blackcurrant biopolymers. Further analyses by SEC-MALLS demonstrated that the lower molecular weight pectic components had UV signals, suggesting that UV absorbing compounds like polyphenols and protein were present in the fraction and/or associated to the pectic components.

- An attempt to dissociate blackcurrant anthocyanins from the blackcurrant biopolymers through (i) disruption of electrostatic forces, (ii) change of anthocyanins planarity and (iii) ultra-filtration also failed to show substantial difference as majority of the anthocyanins remained associated with the large molecular weight biopolymers. Hence, it has been suggested that the association

of anthocyanins with the blackcurrant biopolymers likely involved a combination of interactive forces: electrostatic, hydrophobic, hydrogen bonding and possibly covalent bonding.

- Despite their association, the fraction that was isolated from the blackcurrant juice had net negative charges which could electrostatically complex with WPs. In addition, the high content of bound anthocyanins meant that they could participate as additional binding sites for the WPs, increasing the likelihood of physical destabilisation in blackcurrant juice-milk system. The blackcurrant protein was considered as one of the interactive components, but more information is needed to understand its characteristics.

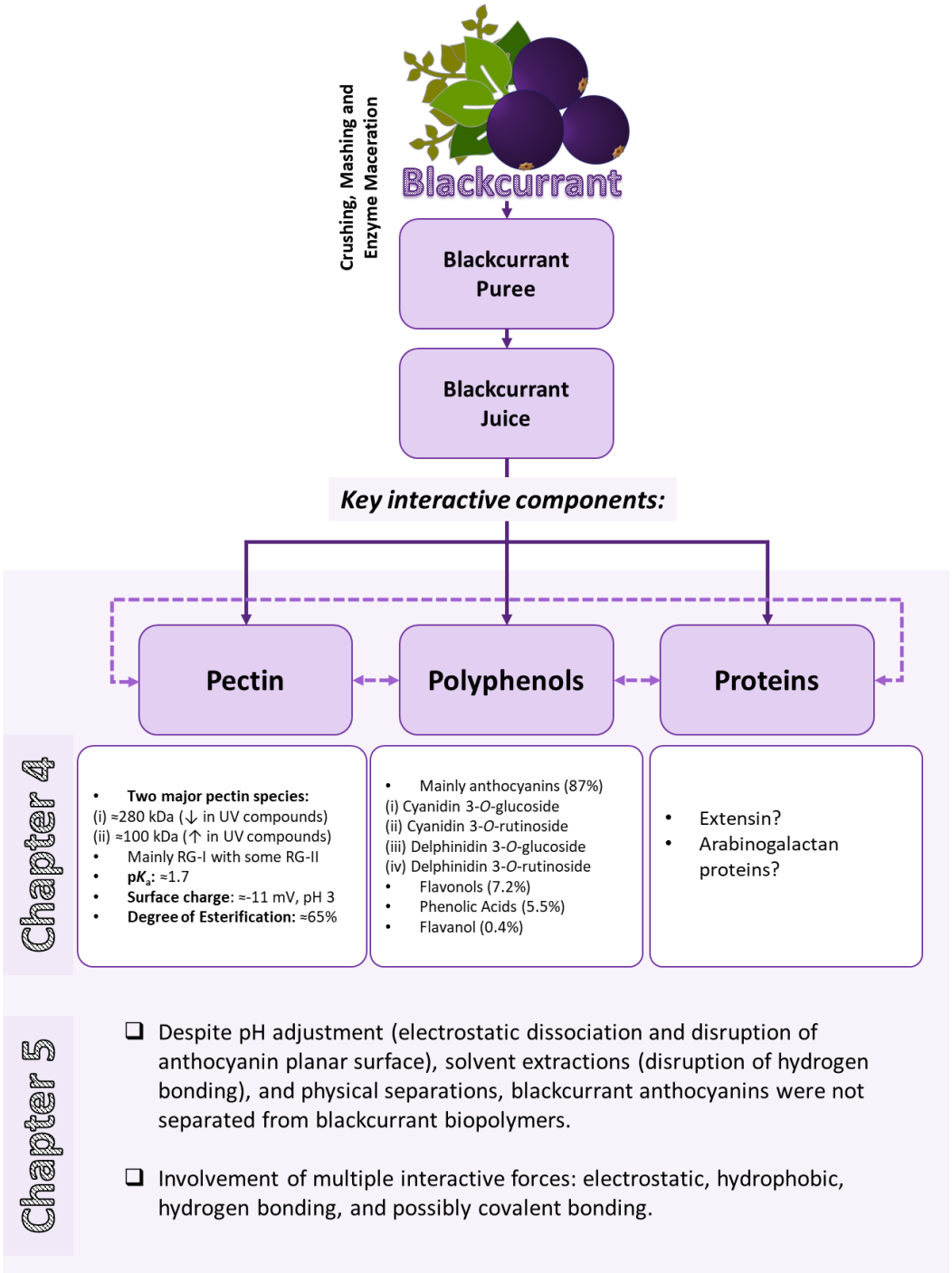

Figure 8.1 Overview of Chapter 4 and Chapter 5.

8.1.2. How do whey proteins interact with the identified blackcurrant juice components?

- The WPs interacted with anthocyanins and pectin through multiple associative mechanisms (Figure 8.2). In the absence of heat, the electrostatic forces between the oppositely charged WPs and blackcurrant pectin (BCP) caused the two biopolymers to be drawn to each other. The close approximation of the two biopolymers would then trigger the occurrence of other interactive forces like hydrophobic forces (i.e., between the hydrophobic amino acids found on the surface of β-lactoglobulin and bovine serum albumin and the methoxy groups of pectin and its bound anthocyanins) and hydrogen bonding (i.e., between the O-H and N-H groups of the blackcurrant components and O-H and N-H groups of the WPs). In the presence of heat, the above associative mechanisms would be amplified due to the exposure of amino acids from the unfolded WPs, increasing the number of binding sites for the blackcurrant components to interact with.

- Different anthocyanin structures conferred different associative mechanisms. At pH 3.5, majority of the anthocyanins were positively charged (flavylium form), thus they provided three binding modes for the WPs: (i) electrostatic, (ii) hydrophobic, and (iii) hydrogen bonding. In contrast, at pH 4.5 majority of the anthocyanins were neutrally charged (quinonoidal base and carbinol pseudobase form), hence only two binding modes were available for the WPs: (i) hydrophobic and (ii) hydrogen bonding. This shows that the initial pH of the blackcurrant juice plays a crucial role as this will not only determine the structure of the anthocyanins, but also the intensity of anthocyanins complexation with protein.

- Mixing the BCP with WPs at pH 3.5 and pH 4.5 produced mixtures that were different in colour (pink at pH 3.5 and purple at pH 4.5), but similar in physical stability. However, complexes at pH 3.5 were much larger (>100 nm) than the ones at pH 4.5 (≈50 nm). Poor phase stability started to develop when heat was introduced. Regardless of the pH, heating affected the colour intensity and physical stability of both mixtures. The impact was prominent on pH 3.5 system as it became very turbid and less stable than its heated pH 4.5 counterpart. The decrease in the stability of pH 3.5 system was contributed by the growth of complexes—from >100 nm to >200 nm—signifying the intensification of complexation at lower pH. One of the reasons for the intensified complexation was the ability of positively charged anthocyanins to electrostatically interact with the exposed negatively charged amino acids. Since heating is one of the key processing steps of a beverage production, the possibility of weakening the physical stability of the blackcurrant juice-milk system via heating is elevated, especially at pH <4.5.

- The sequence of heating also plays an important role in the preparation of blackcurrant juice-milk system. Heating the WPs before the addition of blackcurrant components caused protein-protein interactions to occur, producing large protein aggregates. When these aggregates interacted with the blackcurrant components, they formed even larger complexes that eventually sedimented, worsening the instability of the mixture. Despite the negative impact on physical stability, the colour of the mixture and probably the functionality of the anthocyanins were preserved.

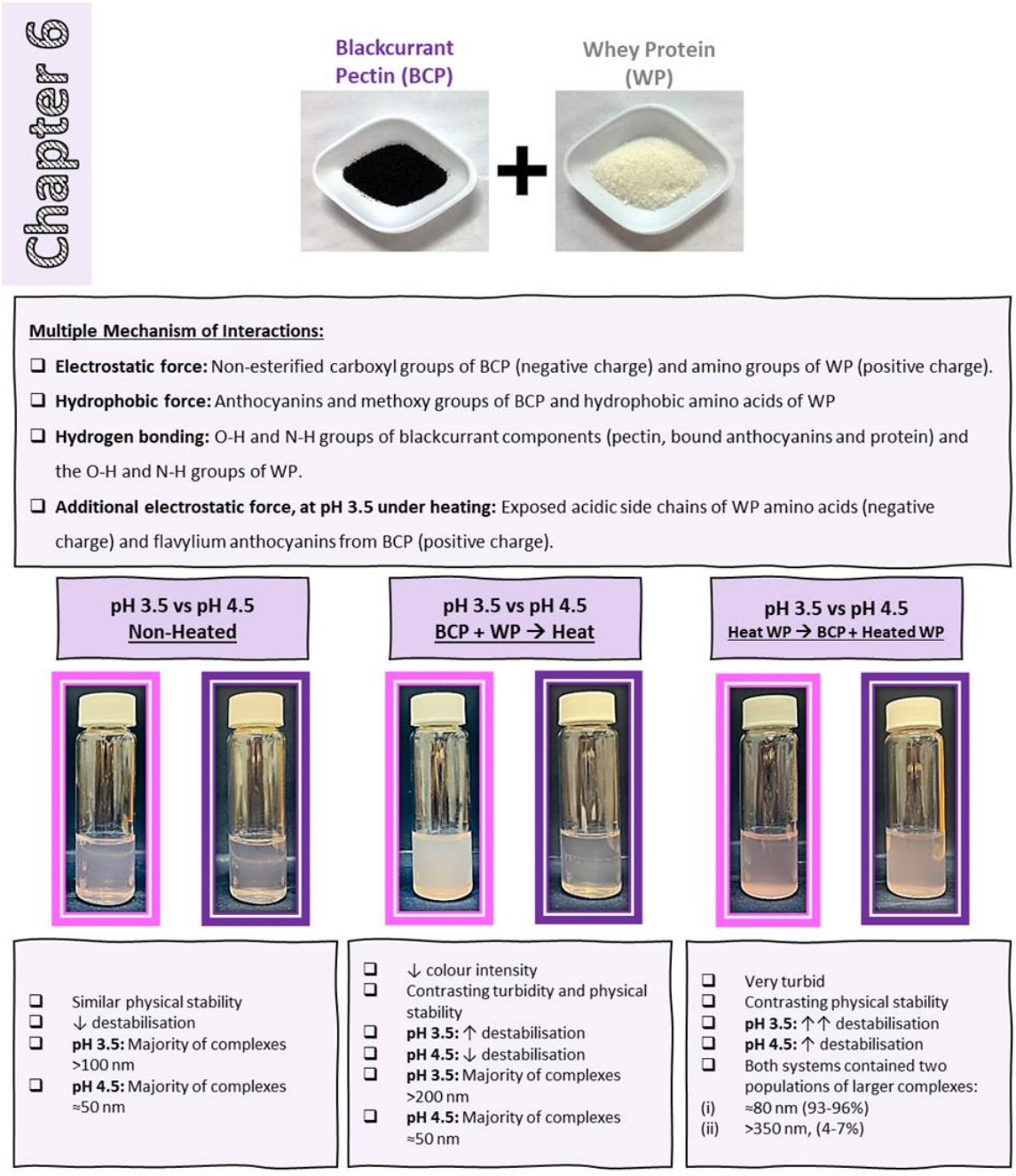

Figure 8.2 Overview of Chapter 6.

8.1.3. How do blackcurrant pectin-whey protein interactions differ from citrus pectin-whey protein interactions?

- The bound anthocyanins in BCP-rich fraction provided the WPs with additional binding sites that citrus pectin (CP) could not offer (Figure 8.3). In the unheated state, both pectins interacted with WPs through identical associative mechanisms—electrostatic, hydrophobic, and hydrogen bonding—but vary in the association intensity. The CP in this study had greater surface charge than the BCP, owing to its higher content of galacturonic acids and therefore, more ionic interactions had occurred in the CP-WP systems. Due to the abundance of O-H groups in the BCP (contributed by the anthocyanins and other blackcurrant components) the amount of hydrogen bonding occurring in the BCP-WP systems were likely a lot more than the hydrogen bonding interactions in CP-WP systems. Similarly, hydrophobic interactions in the anthocyanin-rich systems were probably greater because the aromatic rings of anthocyanins provided plenty of hydrophobic binding sites along with the BCP methoxy groups, while the CP had only methoxy groups as its hydrophobic sites. When heating was introduced, the intensity of interactions was amplified in both pectin-protein systems, but overall, hydrogen bonding and hydrophobic interactions were likely to be more intense in the anthocyanin-rich systems due to the reasons mentioned above.

- In the absence of heat, the pectin-protein systems were very different in colour and turbidity, though they were similar in physical stability (low destabilisation) and complexes size (≈50-60 nm). Raising the WP concentration in the presence of heat increased the turbidity and complexes size that resulted in the declining of physical stability of both systems. Differences in turbidity, complexes size and physical stability were observed between the anthocyanin-rich and anthocyanin-free systems, yet their differences were not attributed to the presence of anthocyanins as various factors could also influence them, like the impact of particle size, particle number, and conformation on turbidity, and the impact of electrostatic stability and viscosity on physical stability. Overall, heating the pectin-protein systems at ratios above 1:5 substantially affected the physical stability of the mixed system.

- The surface charge of the CP-WP systems was comparable to the CP and was not significantly different up to pectin:protein ratio of 1:5. Such trend was also observed in the BCP-WP systems but at all pectin:protein ratios, likely signifying that the anthocyanin-rich systems were mainly governed by non-electrostatic interactions.

- Comparison between the BCP-WP and CP-WP systems demonstrated that the physical stability of a pectin-protein mixture was governed by a combination of factors, such as the physico-chemical and molecular properties of the biopolymers, absence or presence of heat, and pectin:protein ratio. Physical instability was not attributed exclusively to the presence of bound polyphenols, though they might aggravate it.

Based on the findings of this thesis, physical instability in blackcurrant juice-milk system will likely be caused by: (i) the complexation between the interactive blackcurrant components and milk proteins, (ii) the pH of the blackcurrant juice (pH 3) that supports the intense binding of free and bound flavylium anthocyanins to milk proteins, (iii) the low viscosity and relatively weak charge of the BCP, and (iv) the heat treatment that denatures the proteins, amplifying the complexations between milk proteins and key blackcurrant components.

The knowledge presented in this thesis is far from complete, though it provides an overview on the cause of instability in blackcurrant juice-milk system, as well as the missing information on blackcurrant components that no researcher has mentioned or worked on. The discovery of the anthocyanin-bound pectin-rich fraction unlocks the prospect for a unique type of functional pectin. There is a possibility that the pectic material has emulsifying and encapsulation properties as it contains components with different surface activity (i.e., protein and bound anthocyanins). These components may drive the adsorption at the oil-and-water interface and make it surface active, while the pectic component can confer steric stabilisation and provide longer term stability against flocculation and coalescence.

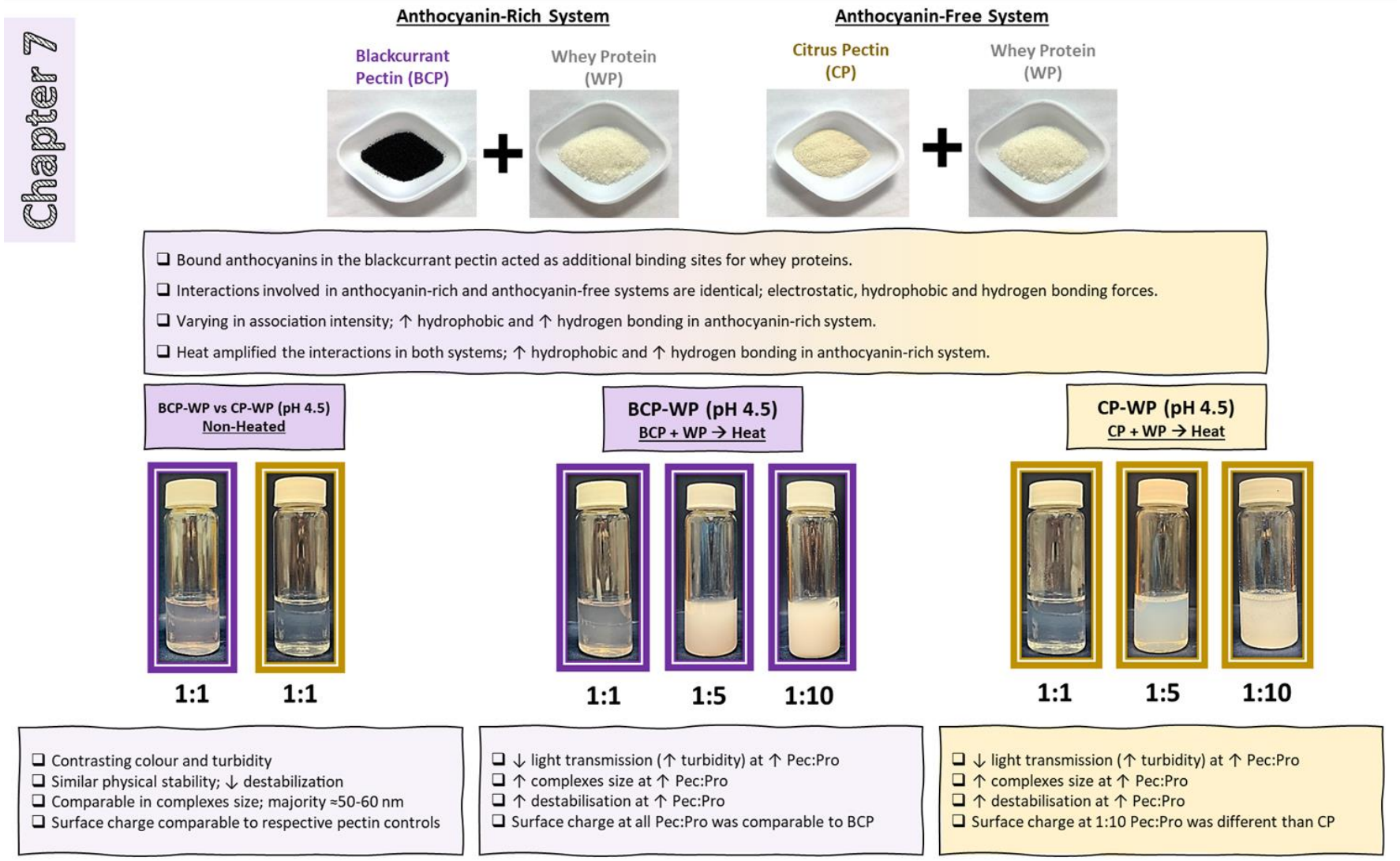

Figure 8.3 Overview of Chapter 7

8.2. Future Work Recommendations

8.2.1. Further Work on Anthocyanins Dissociation

Further work on the dissociation of anthocyanins from blackcurrant biopolymers (Chapter 5) can be continued through enzymatic studies using pectinases. Measurement techniques like size-exclusion chromatography that is coupled to multi-angle laser light scattering (SEC-MALLS) detector can be used to study the change in molecular weight and UV signals of the blackcurrant pectin-rich fraction, while reversed-phase ultra-performance liquid chromatography (RP-UPLC) can be used to study the release of anthocyanins.

8.2.2. Investigation on Blackcurrant Protein

Knowledge on blackcurrant protein is needed to complete the study on blackcurrant components. Based on Chapter 4 findings, the isolated fraction contained biopolymers with mostly arabinan, and/or type II arabinogalactan side chains, thus the likelihood of having arabinogalactan proteins as one of the components is high. Typically, plant proteins are hydroxyproline-rich and are known to complex with polyphenols. The presence of hydroxyproline-rich proteins can be confirmed and quantified using the Yariv reagent (β-glucosyl Yariv phenylglycoside). Investigative work on dissociation of blackcurrant polyphenols from blackcurrant proteins can be done through enzymatic studies using proteases, where change in molecular weight and UV signal of the blackcurrant pectin-rich fraction can be observed. The liberation of anthocyanins can be evaluated using chromatographic method.

8.2.3. Isolation and Characterisation of Pectin from Blackcurrant Puree

Subsequent work shall involve the isolation of pectin from blackcurrant puree as its pectin content is higher, as shown in (Chapter 3). Following that, identical characterisation work of the pectin can be carried out, and comparisons can be made against the blackcurrant juice pectin. This can help to establish the presence of bound anthocyanins in other blackcurrant pectic fractions.

8.2.4. Effect of Ionic Strength on Blackcurrant Pectin-Whey Protein System

The effect of ionic strength on BCP-WP mixtures needs to be investigated as free ions can leave a negative impact on physical stability of the mixed system, and this is particularly relevant as the blackcurrant juice is rich in minerals, as shown in Chapter 3.

8.2.5. Interaction Study Between Blackcurrant Pectin and Milk Proteins

Interaction study between the blackcurrant pectin and overall milk proteins (casein and whey proteins) can be conducted using milk protein isolates. Milk protein isolates contain micellar caseins that are representative of the casein proteins found in milk, but without the interference of other milk components like lactose, minerals, and milk fat. This can provide a clearer picture and understanding of the blackcurrant juice-milk system.

References

Ahmad Fairuz, O., & Mohd Zubir Mat, J. (2013). *Optical System in Measurement of Water Turbidity: Design and Analytical Approach*. Penerbit USM.

Alba, K., MacNaughtan, W., Laws, A. P., Foster, T. J., Campbell, G. M., & Kontogiorgos, V. (2018). Fractionation and Characterisation of Dietary Fibre From Blackcurrant Pomace. *Food Hydrocolloids*, *81*, 398-408. https://doi.org/10.1016/j.foodhyd.2018.03.023

Albani, J. R., Vogelaer, J., Bretesche, L., & Kmiecik, D. (2014). Tryptophan 19 residue is the origin of bovine β-lactoglobulin fluorescence. *Journal of Pharmaceutical and Biomedical Analysis*, *91*, 144-150. https://doi.org/10.1016/j.jpba.2013.12.015

Aleixandre-Tudo, J. L., & du Toit, W. (2018). The Role of UV-Visible Spectroscopy for Phenolic Compounds Quantification in Winemaking. In R. L. Solís-Oviedo & Á. D. L. C. Pech-Canul (Eds.), *Front. New Trends Sci. Fermented Food Beverages* (pp. 1-21). https://doi.org/10.5772/intechopen.79550

Andersson, R., Westerlund, E., & Åman, P. (2017). Cell-Wall Polysaccharides: Structural, Chemical, and Analytical Aspects. In A.-C. Eliasson (Ed.), *Carbohydrates in Food* (3 ed., pp. 147-191). CRC Press. https://doi.org/10.1201/9781315372822

Anema, S. G. (2009). The whey proteins in milk: thermal denaturation, physical interactions and effects on the functional properties of milk. In A. Thompson, M. Boland, & H. Singh (Eds.), *Milk Proteins: from Expression to Food* (1st ed., pp. 239-281). Academic Press. https://doi.org/10.1016/B978-0-12-374039-7.X0001-3

Anema, S. G. (2017). The thermal denaturation of the total whey protein in reconstituted whole milk [Article]. *International Journal of Dairy Technology*, *70*(3), 332-338. https://doi.org/10.1111/1471-0307.12356

Aneta, W., Jan, O., Magdalena, M., & Joanna, W. (2013). Phenolic Profile, Antioxidant and Antiproliferative Activity of Black and Red Currants (*Ribes* spp.) from Organic and Conventional Cultivation [Article]. *International Journal of Food Science and Technology*, *48*, 715-726. https://doi.org/10.1111/ijfs.12019

Anttonen, M. J., & Karjalainen, R. O. (2006). High-Performance Liquid Chromatography Analysis of Black Currant (*Ribes nigrum* L.) Fruit Phenolics Grown Either Conventionally or Organically. *Journal of Agricultural and Food Chemistry*, *54*, 7530-7538. https://doi.org/10.1021/jf0615350

AOAC, I. (2023). *Official Methods of Analysis of AOAC INTERNATIONAL 22nd Edition* (G. W. Latimer, Jr., Ed.). Oxford University Press. https://doi.org/10.1093/9780197610145.001.0001

Arts, I. C. W., Venema, D. P., & Hollman, P. C. H. (2003). Quantitative Determination of Flavonols in Plant Foods and Biological Fluids. In C. Santos-Buelga & G. Williamson (Eds.), *Methods in Polyphenol Analysis* (1st ed., pp. 214-228). The Royal Society of Chemistry.

Asen, S., Stewart, R. N., Norris, K. H., & Massie, D. R. (1970). A Stable Blue Non-Metallic Co-Pigment Complex of Delphanin and C-Glycosylflavones in Prof. Blaauw Iris. *Phytochemistry*, *9*, 619-627. https://doi.org/10.1016/S0031-9422(00)85702-7

Bae, R.-N., Kim, K.-W., Kim, T.-C., & Lee, S.-K. (2006). Anatomical Observations of Anthocyanin Rich Cells in Apple Skins. *HortScience: Horticultural Science*, *41*(3), 733-736. https://doi.org/10.21273/hortsci.41.3.733

Banerjee, S., & Mazumdar, S. (2012). Electrospray Ionization Mass Spectrometry: A Technique to Access the Information beyond the Molecular Weight of the Analyte. *International Journal of Analytical Chemistry*, *2012*, 282574. https://doi.org/10.1155/2012/282574

Barbieri, S. F., da Costa Amaral, S., Ruthes, A. C., de Oliveira Petkowicz, C. L., Kerkhoven, N. C., da Silva, E. R. A., & Silveira, J. L. M. (2019). Pectins From the Pulp of Gabiroba (*Campomanesia Xanthocarpa* Berg): Structural Characterization and Rheological Behavior. *Carbohydrate Polymers*, *214*, 250-258. https://doi.org/10.1016/j.carbpol.2019.03.045

Barth, H. G., Boyes, B. E., & Jackson, C. (1996). Size Exclusion Chromatography. *Analytical Chemistry*, *68*(12), 445-466. https://doi.org/10.1021/a19600193

Baxter, N. J., Lilley, T. H., Haslam, E., & Williamson, M. P. (1997). Multiple interactions between polyphenols and a salivary proline-rich protein repeat result in complexation and precipitation [Article]. *Biochemistry*, *36*(18), 5566-5577. https://doi.org/10.1021/bi9700328

BCNZ. (2017). *New Zealand Blackcurrants a UK superfood*. Blackcurrants NZ Incorporated. Retrieved 13 September from https://www.blackcurrant.co.nz/new-zealand-blackcurrants-a-uk-superfood/

BCNZ. (2022). *The NZ Blackcurrant Industry*. Blackcurrants NZ Incorporated. Retrieved 8th September from https://www.blackcurrant.co.nz/blackcurrants/the-nz-industry/

Beart, J. E., Lilley, T. H., & Haslam, E. (1985). Polyphenol interactions. Part 2. Covalent binding of procyanidins to proteins during acid-catalysed decomposition; observations on some polymeric proanthocyanidins. *Journal of the Chemical Society, Perkin Transactions 2*(9), 1439-1443.

Bhattacharjee, S. (2016). DLS and zeta potential – What they are and what they are not? *Journal of Controlled Release*, *235*, 337-351. https://doi.org/10.1016/j.jconrel.2016.06.017

Blumenkrantz, N., & Asboe-Hansen, G. (1973). New method for quantitative determination of uronic acids. *Analytical Biochemistry*, *54*, 484-489. https://doi.org/10.1016/0003-2697(73)90377-1

Boeing, J. S., Barizão, É. O., e Silva, B. C., Montanher, P. F., de Cinque Almeida, V., & Visentainer, J. V. (2014). Evaluation of Solvent Effect on the Extraction of Phenolic Compounds and Antioxidant Capacities From the Berries: Application of Principal Component Analysis. *Chemistry Central Journal*, *8*, 48-57. https://doi.org/10.1186/s13065-014-0048-1

Brett, C., & Waldron, K. (1990a). Cell Wall Structure and the Skeletal Functions of the Wall. In *Physiology and Biochemistry of Plant Cell Walls* (pp. 4-57). Springer https://doi.org/10.1007/978-94-010-9641-6_2

Brett, C., & Waldron, K. (1990b). The Role of the Cell Wall in the Life of the Plant. In *Physiology and Biochemistry of Plant Cell Walls* (pp. 1-3). Springer https://doi.org/10.1007/978-94-010-9641-6_2

Brouillard, R. (1988). Flavonoids and Flower Colour. In J. B. Harborne (Ed.), *The Flavonoids : Advances in Research since 1980* (pp. 525-538). Chapman and Hall.

Buchert, J., Koponen, J. M., Suutarinen, M., Mustranta, A., Lille, M., Törrönen, R., & Poutanen, K. (2005). Effect of enzyme-aided pressing on anthocyanin yield and profiles in bilberry and blackcurrant juices [Article]. *Journal of the Science of Food and Agriculture*, *85*(15), 2548-2556. https://doi.org/10.1002/jsfa.2284

Buchweitz, M., Speth, M., Kammerer, D. R., & Carle, R. (2013). Impact of Pectin Type on the Storage Stability of Black Currant (*Ribes nigrum* L.) Anthocyanins in Pectic Model Solutions. *Food Chemistry*, *139*, 1168-1178. https://doi.org/10.1016/j.foodchem.2013.02.005

Calvo, M. M., Leaver, J., & Banks, J. M. (1993). Influence of other whey proteins on the heat-induced aggregation of α-lactalbumin. *International Dairy Journal*, *3*(8), 719-727. https://doi.org/10.1016/0958-6946(93)90085-E

Chaplin, L. C., & Lyster, R. L. J. (1986). Irreversible heat denaturation of bovine a-lactalbumin. *Journal of Dairy Research*, *2*(53), 249-258. https://doi.org/10.1017/S0022029900024857

Chen, D., Harris, P. J., Sims, I. M., Zujovic, Z., & Melton, L. D. (2017). Polysaccharide Compositions of Collenchyma Cell Walls From Celery (*Apium Graveolens* L.) Petioles. *BMC Plant Biology*, *17*, 104-117. https://doi.org/10.1186/s12870-017-1046-y

Chen, H.-M., Fu, X., & Luo, Z.-G. (2016). Effect of Molecular Structure on Emulsifying Properties of Sugar Beet Pulp Pectin. *Food Hydrocolloids*, *54*, 99-106. https://doi.org/10.1016/j.foodhyd.2015.09.021

Chen, L., Xin, X. L., Yuan, Q. P., Su, D. H., & Liu, W. (2014). Phytochemical Properties and Antioxidant Capacities of Various Colored Berries [Article]. *Journal of the Science of Food and Agriculture*, *94*, 180-188. https://doi.org/10.1002/jsfa.6216

Cheng, H., Fang, Z., Liu, T., Gao, Y., & Liang, L. (2018). A study on β-lactoglobulin-triligand-pectin complex particle: Formation, characterization and protection. *Food Hydrocolloids*, *84*, 93-103. https://doi.org/10.1016/j.foodhyd.2018.05.055

Cheng, J., Liu, J.-H., Prasanna, G., & Jing, P. (2017). Spectrofluorimetric and molecular docking studies on the interaction of cyanidin-3-O-glucoside with whey protein, β-lactoglobulin. *International Journal of Biological Macromolecules*, *105*, 965-972. https://doi.org/10.1016/j.ijbiomac.2017.07.119

Chevalier, L. M., Rioux, L.-E., Angers, P., & Turgeon, S. L. (2019). Study of the interactions between pectin in a blueberry puree and whey proteins: Functionality and application. *Food Hydrocolloids*, *87*, 61-70. https://doi.org/10.1016/j.foodhyd.2018.07.038

Choong, Y. K., Mohd Yousof, N. S. A., Jamal, J. A., & Wasiman, M. I. (2019). Determination of anthocyanin content in two varieties of *Hibiscus Sabdariffa* from Selangor, Malaysia using a combination of chromatography and spectroscopy. *Journal of Plant Science and Phytopathology*(3), 067-075. https://doi.org/10.29328/journal.jpsp.1001034

Chung, C., Rojanasasithara, T., Mutilangi, W., & McClements, D. J. (2015). Enhanced stability of anthocyanin-based color in model beverage systems through whey protein isolate complexation [Article]. *Food Research International*, *76*, 761-768. https://doi.org/10.1016/j.foodres.2015.07.003

Corredig, M., Kerr, W., & Wicker, L. (2000). Molecular Characterization of Commercial Pectins by Separation With Linear Mix Gel Permeation Columns In-Line With Multi-Angle Light Scattering Detection. *Food Hydrocolloids*, *14*, 41-47. https://doi.org/10.1016/S0268-005X(99)00044-2

Cosmulescu, S., Trandafir, I., & Nour, V. (2015). Mineral composition of fruit in black and red currant. *South Western Journal of Horticulture, Biology and Environment*, *6*(1), 45-51. http://biozoojournals.ro/swjhbe/v6n1/04_swjhbe_v6n1_Cosmulescu.pdf

Curl, A., & Bailey, G. (1956). Orange Carotenoids, Part I-Comparison of Carotenoids of Valencia Orange Peel and Pulp, Part II-Carotenoids Aged Canned Valencia Orange Juice. *Journal of Agricultural and Food Chemistry*, *4*(2), 156-162. https://doi.org/10.1021/jf60060a007

Currie, A., Langford, G., McGhie, T., Apiolaza, L. A., Snelling, C., Braithewaite, B., & Vather, R. (2006, 18-21 April 2006). *Inheritance of Antioxidants in a New Zealand Blackcurrant (Ribes nigrum L.) Population* 13th Australasian Plant Breeding Conference, Christchurch, New Zealand. https://ir.canterbury.ac.nz/handle/10092/2032

Damodaran, S. (2008). Amino acids, peptides, and proteins. In S. Damodaran, K. L. Parkin, & O. R. Fennema (Eds.), *Fennema's Food Chemistry* (4th ed., pp. 217-329). CRC Press. https://doi.org/10.1201/9781420020526

Dangles, O., & Dufour, C. (2006). Flavonoid-protein interactions. In Ø. M. Andersen & K. R. Markham (Eds.), *Flavonoids : Chemistry, Biochemistry and Applications* (1st ed., pp. 443-469). CRC Press. https://doi.org/10.1201/9781420039443

Dangles, O., & Fenger, J.-A. (2018). The chemical reactivity of anthocyanins and its consequences in food science and nutrition. *Molecules*, *23*(8), 1970. https://doi.org/10.3390/molecules23081970

Dannenberg, F., & Kessler, H.-G. (1988). Reaction kinetics of the denaturation of whey proteins in milk. *Journal of Food Science*, *53*(1), 258-263. https://doi.org/10.1111/j.1365-2621.1988.tb10223.x

Di Primo, C., & Lebars, I. (2007). Determination of refractive index increment ratios for protein–nucleic acid complexes by surface plasmon resonance. *Analytical Biochemistry*, *368*(2), 148-155. https://doi.org/10.1016/j.ab.2007.06.016

Dixon, R. A., & Paiva, N. L. (1995). Stress-Induced Phenylpropanoid Metabolism. *The Plant Cell*, *7*(7), 1085-1097. https://doi.org/10.1105/tpc.7.7.1085

Donovan, M., & Mulvihill, D. M. (1987). Thermal denaturation and aggregation of whey proteins. *Irish Journal of Food Science and Technology*, *11*(1), 87-100. http://www.jstor.org/stable/25558155

DuBois, M., Gilles, K. A., Hamilton, J. K., Rebers, P. A., & Smith, F. (1956). Colorimetric Method for Determination of Sugars and Related Substances. *Analytical Chemistry*, *28*(3), 350-356. https://doi.org/10.1021/ac60111a017

Dumay, E., Laligant, A., Zasypkin, D., & Cheftel, J. C. (1999). Pressure- and heat-induced gelation of mixed β-lactoglobulin/polysaccharide solutions: scanning electron microscopy of gels. *Food Hydrocolloids*, *13*(4), 339-351. https://doi.org/10.1016/S0268-005X(99)00016-8

Edwards, P. B., Creamer, L. K., & Jameson, G. B. (2009). Structure and stability of whey proteins In A. Thompson, M. Boland, & H. Singh (Eds.), *Milk Proteins: from Expression to Food* (pp. 163-203). Academic Press. https://doi.org/10.1016/B978-0-12-374039-7.X0001-3

Fan, D., Alamri, Y., Liu, K., MacAskill, M., Harris, P., Brimble, M., Dalrymple-Alford, J., Prickett, T., Menzies, O., Laurenson, A., Anderson, T., & Guan, J. (2018). Supplementation of Blackcurrant Anthocyanins Increased Cyclic Glycine-Proline in the Cerebrospinal Fluid of Parkinson Patients: Potential Treatment to Improve Insulin-Like Growth Factor-1 Function. *Nutrients*, *10*(6), 714. https://doi.org/10.3390/nu10060714

FAO. (2016). *Pectins* https://www.fao.org/3/bq695e/bq695e.pdf

FAO. (2022). *Production Quantities of Currants by Country* http://www.fao.org/faostat/en/#data/QC/visualize

Fathy, H. M., Abd El-Maksoud, A. A., Cheng, W., & Elshaghabee, F. M. F. (2022). Value-Added Utilization of Citrus Peels in Improving Functional Properties and Probiotic Viability of Acidophilus-bifidus-thermophilus (ABT)-Type Synbiotic Yoghurt during Cold Storage. *Foods*, *11*(17), 2677. https://doi.org/10.3390/foods11172677

Fátima Barroso, M., Carvalho, A. P., Correia, M., Ramalhosa, M. J., Delerue-Matos, C., & Grosso, C. (2019). Characterization of Bioactive Compounds in Flavored Waters and Fruit Juices. In A. M. Grumezescu & A. M. Holban (Eds.), *Bottled and Packaged Water* (pp. 311-366). Woodhead Publishing. https://doi.org/10.1016/B978-0-12-815272-0.00012-X

Fernandes, A., Brás, N. F., Mateus, N., & de Freitas, V. (2014). Understanding the molecular mechanism of anthocyanin binding to pectin. *Langmuir*, *30*, 8516-8527. https://doi.org/10.1021/la501879w

Fishman, M., Chau, H., Coffin, D., & Hotchkiss, A. (2003). A comparison of lime and orange pectin which were rapidly extracted from albedo. In *Advances in pectin and pectinase research* (pp. 107-122). Springer. https://doi.org/10.1007/978-94-017-0331-4

Fishman, M. L., Chau, H. K., Kolpak, F., & Brady, J. (2001). Solvent Effects on the Molecular Properties of Pectins. *Journal of Agricultural and Food Chemistry*, *49*, 4494-4501. https://doi.org/10.1021/jf001317l

Formulaction. (2018). *Turbiscan Lab User Guide* (5th ed.). Formulation Scientific Instruments.

Fox, M. (2022). 6 Brands Dominating The Explosive Functional Beverages Market. https://www.forbes.com/sites/meimeifox/2022/03/26/6-brands-dominating-the-explosive-functional-beverages-market/?sh=5997541451cf

Fox, P. F. (2009). Milk: an overview. In A. Thompson, M. Boland, & H. Singh (Eds.), *Milk Proteins: from Expression to Food* (pp. 1-54). Academic Press. https://doi.org/10.1016/B978-0-12-374039-7.X0001-3

Fox, P. F., & McSweeney, P. L. H. (2013). *Advanced dairy chemistry, Proteins: Basic Aspects* (P. F. Fox & P. L. H. McSweeney, Eds. 4th ed ed., Vol. 1A). Springer. https://doi.org/10.1007/978-1-4614-4714-6

Freitas, C. M. P., Coimbra, J. S. R., Souza, V. G. L., & Sousa, R. C. S. (2021). Structure and Applications of Pectin in Food, Biomedical, and Pharmaceutical Industry: A Review. *Coatings*, *11*(8), 922. https://doi.org/10.3390/coatings11080922

Fry, S. C. (1982). Phenolic Components of the Primary Cell Wall Feruloylated Disaccharides of D-Galactose and L-Arabinose From Spinach Polysaccharide. *Biochemical Journal*, *203*, 493-504. https://doi.org/10.1042/bj2030493

Gawkowska, D., Cybulska, J., & Zdunek, A. (2018). Structure-Related Gelling of Pectins and Linking with Other Natural Compounds: A Review. *Polymers (Basel)*, *10*(7). https://doi.org/10.3390/polym10070762

Gerwig, G. J. (2021). Detection of Carbohydrates by Colorimetric Methods. In G. J. Gerwig (Ed.), *The Art of Carbohydrate Analysis* (pp. 61-88). Springer International Publishing. https://doi.org/10.1007/978-3-030-77791-3_4

Girard, M., Sanchez, C., Laneuville, S. I., Turgeon, S. L., & Gauthier, S. F. (2004). Associative phase separation of β-lactoglobulin/pectin solutions: a kinetic study by small angle static light scattering. *Colloids and Surfaces B: Biointerfaces*, *35*(1), 15-22. https://doi.org/10.1016/j.colsurfb.2004.02.002

Girard, M., Turgeon, S. L., & Gauthier, S. F. (2002). Interbiopolymer complexing between β-lactoglobulin and low- and high-methylated pectin measured by potentiometric titration and ultrafiltration. *Food Hydrocolloids*, *16*(6), 585-591. https://doi.org/10.1016/S0268-005X(02)00020-6

Girard, M., Turgeon, S. L., & Gauthier, S. F. (2003a). Quantification of the interactions between β-lactoglobulin and pectin through capillary electrophoresis analysis. *Journal of Agricultural and Food Chemistry*, *51*(20), 6043-6049. https://doi.org/10.1021/jf034266b

Girard, M., Turgeon, S. L., & Gauthier, S. F. (2003b). Thermodynamic parameters of β-lactoglobulin–pectin complexes assessed by isothermal titration calorimetry. *Journal of Agricultural and Food Chemistry*, *51*(15), 4450-4455. https://doi.org/10.1021/jf0259359

Goh, K. K. T., Sarkar, A., & Singh, H. (2009). Milk protein–polysaccharide interactions. In A. Thompson, M. Boland, & H. Singh (Eds.), *Milk Proteins: from Expression to Food* (1st ed., pp. 347-376). Academic Press. https://doi.org/10.1016/B978-0-12-374039-7.X0001-3

Gopalan, A., Reuben, S. C., Ahmed, S., Darvesh, A. S., Hohmann, J., & Bishayee, A. (2012). The health benefits of blackcurrants [Review]. *Food and Function*, *3*(8), 795-809. https://doi.org/10.1039/c2fo30058c

Goulas, V., Vicente, A. R., & Manganaris, G. A. (2012). Structural Diversity of Anthocyanins in Fruits. In N. Motohashi (Ed.), *Anthocyanins Structure, Biosynthesis and Health Benefits* (pp. 225-250). Nova Science Publishers, Inc.

Günther, C. S., Dare, A. P., McGhie, T. K., Deng, C., Lafferty, D. J., Plunkett, B. J., Grierson, E. R. P., Turner, J. L., Jaakola, L., Albert, N. W., & Espley, R. V. (2020). Spatiotemporal Modulation of Flavonoid Metabolism in Blueberries [Original Research]. *Frontiers in Plant Science*, *11*, 1-17. https://doi.org/10.3389/fpls.2020.00545

Guo, M. (2019). *Whey protein production, chemistry, functionality and applications* (1st edition ed.). Wiley. https://doi.org/10.1002/9781119256052

Guo, M., & Wang, C. (2019). Chemistry of Whey Proteins. In M. Guo (Ed.), *Whey protein production, chemistry, functionality and applications* (First edition ed., pp. 39-65). Wiley. https://doi.org/10.1002/9781119256052

Guo, X., Meng, H., Zhu, S., Tang, Q., Pan, R., & Yu, S. (2016). Stepwise Ethanolic Precipitation of Sugar Beet Pectins From the Acidic Extract. *Carbohydrate Polymers*, *136*, 316-321. https://doi.org/10.1016/j.carbpol.2015.09.003

Hagerman, A. E. (2012). Fifty Years of Polyphenol-Protein Complexes. In *Recent Advances in Polyphenol Research, Volume 3* (Vol. 3, pp. 71-97). https://doi.org/10.1002/9781118299753.ch3

Hagerman, A. E., & Butler, L. G. (1978). Protein precipitation method for the quantitative determination of tannins. *Journal of Agricultural and Food Chemistry*, *26*(4), 809-812. https://doi.org/10.1021/jf60218a027

Heiberg, N., & Maage, F. (2003). CURRANTS AND GOOSEBERRIES A2 - Caballero, Benjamin. In *Encyclopedia of Food Sciences and Nutrition* (2nd ed., pp. 1708-1712). Academic Press. https://doi.org/10.1016/B0-12-227055-X/00317-5

Henry-Kirk, R. A., Plunkett, B., Hall, M., McGhie, T., Allan, A. C., Wargent, J. J., & Espley, R. V. (2018). Solar UV Light Regulates Flavonoid Metabolism in Apple (Malus x domestica). *Plant, Cell & Environment*, *41*(3), 675-688. https://doi.org/10.1111/pce.13125

Hiller, B., & Lorenzen, P. C. (2010). Functional properties of milk proteins as affected by Maillard reaction induced oligomerisation. *Food Research International*, *43*(4), 1155-1166. https://doi.org/10.1016/j.foodres.2010.02.006

Hilz, H., Bakx, E. J., Schols, H. A., & Voragen, A. G. J. (2005). Cell Wall Polysaccharides in Black Currants and Bilberries - Characterisation in Berries, Juice, and Press Cake [Article]. *Carbohydrate Polymers*, *59*, 477-488. https://doi.org/10.1016/j.carbpol.2004.11.002

Hilz, H., de Jong, L. E., Kabel, M. A., Schols, H. A., & Voragen, A. G. J. (2006). A Comparison of Liquid Chromatography, Capillary Electrophoresis, and Mass Spectrometry Methods to Determine Xyloglucan Structures in Black Currants. *Journal of Chromatography A*, *1133*, 275-286. https://doi.org/10.1016/j.chroma.2006.08.024

Hilz, H., Williams, P., Doco, T., Schols, H. A., & Voragen, A. G. J. (2006). The Pectic Polysaccharide Rhamnogalacturonan II is Present as a Dimer in Pectic Populations of Bilberries and Black Currants in Muro and in Juice. *Carbohydrate Polymers*, *65*, 521-528. https://doi.org/10.1016/j.carbpol.2006.02.011

Ho, C. S., Lam, C. W., Chan, M. H., Cheung, R. C., Law, L. K., Lit, L. C., Ng, K. F., Suen, M. W., & Tai, H. L. (2003). Electrospray ionisation mass spectrometry: principles and clinical applications. *Clinical Biochemist Reviews*, *24*(1), 3-12.

Hofmann, T., Glabasnia, A., Schwarz, B., Wisman, K. N., Gangwer, K. A., & Hagerman, A. E. (2006). Protein Binding and Astringent Taste of a Polymeric Procyanidin, 1,2,3,4,6-Penta-O-galloyl-β-d-glucopyranose, Castalagin, and Grandinin. *Journal of Agricultural and Food Chemistry*, *54*(25), 9503-9509. https://doi.org/10.1021/jf062272c

Holser, R. A. (2012). Principal Component Analysis of Phenolic Acid Spectra. *ISRN Spectroscopy*, *2012*, 493203. https://doi.org/10.5402/2012/493203

Hubbermann, E. M., Heins, A., Stöckmann, H., & Schwarz, K. (2006). Influence of acids, salt, sugars and hydrocolloids on the colour stability of anthocyanin rich black currant and elderberry concentrates [journal article]. *European Food Research and Technology*, *223*(1), 83-90. https://doi.org/10.1007/s00217-005-0139-2

Huglin, M. B. (1965). Specific Refractive Index Increments of Polymer Solutions. Part I. Literature Values. *Journal of Applied Polymer Science*, *9*, 3963-4001. https://doi.org/10.1002/app.1965.070091219

Izydorczyk, M. (2005). Understanding the chemistry of food carbohydrates. In S. W. Cui (Ed.), *Food Carbohydrates: Chemistry, Physical Properties, and Applications* (1st ed., pp. 1-65). CRC Press. https://doi.org/10.1201/9780203485286

Jarvis, M. C. (1984). Structure and Properties of Pectin Gels in Plant Cell Walls. *Plant, Cell & Environment*, *7*, 153-164. https://doi.org/10.1111/1365-3040.ep11614586

Jauregi, P., Olatujoye, J. B., Cabezudo, I., Frazier, R. A., & Gordon, M. H. (2016). Astringency reduction in red wine by whey proteins [Article]. *Food Chemistry*, *199*, 547-555. https://doi.org/10.1016/j.foodchem.2015.12.052

Jiang, S., Altaf hussain, M., Cheng, J., Jiang, Z., Geng, H., Sun, Y., Sun, C., & Hou, J. (2018). Effect of heat treatment on physicochemical and emulsifying properties of polymerized whey protein concentrate and polymerized whey protein isolate. *LWT*, *98*, 134-140. https://doi.org/10.1016/j.lwt.2018.08.028

Jones, O., Decker, E. A., & McClements, D. J. (2010). Thermal analysis of β-lactoglobulin complexes with pectins or carrageenan for production of stable biopolymer particles. *Food Hydrocolloids*, *24*(2), 239-248. https://doi.org/10.1016/j.foodhyd.2009.10.001

Jones, O. G., Decker, E. A., & McClements, D. J. (2009). Formation of biopolymer particles by thermal treatment of β-lactoglobulin–pectin complexes. *Food Hydrocolloids*, *23*(5), 1312-1321. https://doi.org/10.1016/j.foodhyd.2008.11.013

Jones, O. G., & McClements, D. J. (2011). Recent progress in biopolymer nanoparticle and microparticle formation by heat-treating electrostatic protein–polysaccharide complexes. *Advances in Colloid and Interface Science*, *167*(1), 49-62. https://doi.org/10.1016/j.cis.2010.10.006

Kalantar, M. (2021). Do we know what "clean label" food products are? https://www.ifis.org/blog/clean-label-food-products

Kapasakalidis, P. G., Rastall, R. A., & Gordon, M. H. (2006). Extraction of Polyphenols From Processed Black Currant (*Ribes Nigrum* L.) Residues [Article]. *Journal of Agricultural and Food Chemistry*, *54*, 4016-4021. https://doi.org/10.1021/jf0529991

Karjalainen, R., Anttonen, M., Saviranta, N., Hilz, H., Törrönen, R., Stewart, D., McDougall, G. J., & Mattila, P. (2009). A Review on Bioactive Compounds in Black Currants (Ribes Nigrum L.) and Their Potential Health-Promoting Properties [Conference Paper]. *Acta Horticulturae*, *839*, 301-307. https://doi.org/10.17660/ActaHortic.2009.839.38

Kasapoğlu, K. N., Daşkaya-Dikmen, C., Yavuz-Düzgün, M., Karaça, A. C., & Özçelik, B. (2019). In A. M. Grumezescu & A. M. Holban (Eds.), *Value-Added Ingredients and Enrichments of Beverages* (pp. 63-99). Academic Press. https://doi.org/10.1016/B978-0-12-816687-1.00003-5

Kashyap, D. R., Vohra, P. K., Chopra, S., & Tewari, R. (2001). Applications of pectinases in the commercial sector: a review. *Bioresource Technology*, *77*(3), 215-227. https://doi.org/10.1016/S0960-8524(00)00118-8

Kobayashi, M., Nakagawa, H., Asaka, T., & Matoh, T. (1999). Borate-Rhamnogalacturonan II Bonding Reinforced by Ca^{2+} Retains Pectic Polysaccharides in Higher-Plant Cell Walls. *Plant physiology*, *119*, 199-204. https://doi.org/10.1104/pp.119.1.199

Koponen, J. M., Happonen, A. M., Auriola, S., Kontkanen, H., Buchert, J., Poutanen, K. S., & Törrönen, A. R. (2008). Characterization and Fate of Black Currant and Bilberry Flavonols in Enzyme-Aided Processing. *Journal of Agricultural and Food Chemistry*, *56*(9), 3136-3144. https://doi.org/10.1021/jf703676m

Krüger, E., Dietrich, H., Hey, M., & Patz, C.-D. (2012). Effects of Cultivar, Yield, Berry Weight, Temperature and Ripening Stage on Bioactive Compounds of Black Currants. *Journal of Applied Botany and Food Quality*, *84*(1), 40. https://ojs.openagrar.de/index.php/JABFQ/article/view/1694

Laneuville, S. I., Sanchez, C., Turgeon, S. L., Hardy, J., & Paquin, P. (2005). Small-Angle Static Light Scattering Study of Associative Phase Separation Kinetics in β-lactoglobulin + Xanthan Gum Mixtures Under Shear. In E. Dickinson (Ed.), *Food Colloids : Interactions, Microstructure and Processing* (pp. 443-465). Royal Society of Chemistry. https://doi.org/10.1039/9781847552389-00443

Law, A. J. R., & Leaver, J. (2000). Effect of pH on the thermal denaturation of whey proteins in milk. *Journal of Agricultural and Food Chemistry*, *48*(3), 672-679. https://doi.org/10.1021/jf981302b

Lee, J., Durst, R. W., & Wrolstad, R. E. (2005). Determination of Total Monomeric Anthocyanin Pigment Content of Fruit Juices, Beverages, Natural Colorants, and Wines by the pH Differential Method: Collaborative Study [Article]. *Journal of AOAC International*, *88*, 1269-1278. https://doi.org/10.1093/jaoac/88.5.1269

Levoguer, C. (2013). Using laser diffraction to measure particle size and distribution. *Metal Powder Report*, *68*(3), 15-18. https://doi.org/10.1016/S0026-0657(13)70090-0

Lim, J., Yeap, S. P., Che, H. X., & Low, S. C. (2013). Characterization of magnetic nanoparticle by dynamic light scattering. *Nanoscale Research Letters*, *8*(1), 381. https://doi.org/10.1186/1556-276X-8-381

Lin, D., Xiao, L., Wen, Y., Qin, W., Wu, D., Chen, H., Zhang, Q., & Zhang, Q. (2021). Comparison of apple polyphenol-gelatin binary complex and apple polyphenol-gelatin-pectin ternary complex: Antioxidant and structural characterization. *LWT*, *148*, 111740. https://doi.org/10.1016/j.lwt.2021.111740

Lin, J., Tan, Y. X. G., Leong, L. P., & Zhou, W. (2018). Steamed bread enriched with quercetin as an antiglycative food product: Its quality attributes and antioxidant properties [10.1039/C8FO00818C]. *Food & Function*, *9*(6), 3398-3407. https://doi.org/10.1039/C8FO00818C

Lin, Z., Fischer, J., & Wicker, L. (2016). Intermolecular binding of blueberry pectin-rich fractions and anthocyanin [Article]. *Food Chemistry*, *194*, 986-993. https://doi.org/10.1016/j.foodchem.2015.08.113

Linke, C., & Drusch, S. (2016). Turbidity in oil-in-water-emulsions — Key factors and visual perception. *Food Research International*, *89*, 202-210. https://doi.org/10.1016/j.foodres.2016.07.019

Lopes da Silva, J. A., & Rao, M. A. (2006). Pectins: Structure, Functionality, and Uses. In A. M. Stephen, G. O. Phillips, & P. A. Williams (Eds.), *Food polysaccharides and their applications* (2 ed., pp. 353-411). Boca Raton : CRC/Taylor & Francis. https://doi.org/10.1201/9781420015164

Loypimai, P., Moongngarm, A., & Chottanom, P. (2016). Thermal and pH degradation kinetics of anthocyanins in natural food colorant prepared from black rice bran. *Journal of Food Science and Technology*, *53*(1), 461-470. https://doi.org/10.1007/s13197-015-2002-1

Makarova, E. N., Shakhmatov, E. G., & Belyy, V. A. (2016). Structural Characteristics of Oxalate-Soluble Polysaccharides of Sosnowsky's Hogweed (*Heracleum Sosnowskyi* Manden). *Carbohydrate Polymers*, *153*, 66-77. https://doi.org/10.1016/j.carbpol.2016.07.089

Makila, L., Laaksonen, O., Kallio, H., & Yang, B. R. (2017). Effect of processing technologies and storage conditions on stability of black currant juices with special focus on phenolic compounds and sensory properties [Article]. *Food Chemistry*, *221*, 422-430. https://doi.org/10.1016/j.foodchem.2016.10.079

Malawer, G. E., & Senak, L. (2003). Introduction to Size Exclusion Chromatography. In C. -s. Wu (Ed.), *Handbook of Size Exclusion Chromatography and Related Techniques* (2nd ed., rev. and expanded ed.). CRC Press. https://doi.org/10.1201/9780203913321

Malvern Panalytical Ltd. (2007). *Mastersizer 2000 User Manual* https://www.malvernpanalytical.com/en/assets/Mastersizer-2000-user-manual-English-MAN0384-1-0_tcm50-11674.pdf

Malvern Panalytical Ltd. (2022). *Zetasizer Advance Range*. Retrieved 22/12/22 from https://www.malvernpanalytical.com/en/products/product-range/zetasizer-range/zetasizer-advance-range

Marcarelli, R. (2016). Functional Refreshments. Consumers want better-for-you beverages that taste great and can replace a meal when needed. http://www.winsightgrocerybusiness.com/functional-refreshments

Maroziene, A., & de Kruif, C. G. (2000). Interaction of pectin and casein micelles. *Food Hydrocolloids*, *14*(4), 391-394. https://doi.org/10.1016/S0268-005X(00)00019-9

Masuelli, M. A. (2011). Viscometric study of pectin. Effect of temperature on the hydrodynamic properties. *International Journal of Biological Macromolecules*, *48*(2), 286-291. https://doi.org/10.1016/j.ijbiomac.2010.11.014

Matia-Merino, L., Lau, K., & Dickinson, E. (2004). Effects of low-methoxyl amidated pectin and ionic calcium on rheology and microstructure of acid-induced sodium caseinate gels. *Food Hydrocolloids*, *18*(2), 271-281. https://doi.org/10.1016/S0268-005X(03)00083-3

Mattila, P. H., Hellstrom, J., Karhu, S., Pihlava, J. M., & Vetelainen, M. (2016). High variability in flavonoid contents and composition between different North-European currant (Ribes spp.) varieties. *Food Chemistry*, *204*, 14-20. https://doi.org/10.1016/j.foodchem.2016.02.056

Mazzaracchio, P., Pifferi, P., Kindt, M., Munyaneza, A., & Barbiroli, G. (2004). Interactions Between Anthocyanins and Organic Food Molecules in Model Systems [Article]. *International Journal of Food Science & Technology*, *39*, 53-59. https://doi.org/10.1111/j.1365-2621.2004.00747.x

McClements, D. J. (2006). Non-covalent interactions between proteins and polysaccharides. *Biotechnology Advances*, *24*(6), 621-625. https://doi.org/10.1016/j.biotechadv.2006.07.003

McKenna, C., Al-Assaf, S., Phillips, G. O., & Funami, T. (2006). The Protein Component in Pectin-Is it an AGP? *Foods and Food Ingredients Journal of Japan*, *211*, 264-271.

McKenzie, H. A. (1970). *Milk proteins; chemistry and molecular biology*. Academic Press. https://doi.org/10.1002/ange.19720840845

Mierczynska, J., Cybulska, J., & Zdunek, A. (2017). Rheological and chemical properties of pectin enriched fractions from different sources extracted with citric acid [Article]. *Carbohydrate Polymers*, *156*, 443-451. https://doi.org/10.1016/j.carbpol.2016.09.042

Miller, R., Putnam, S., Edwards, M., Woodward, G., & Kay, C. (2013). Potential Health Benefits of Blackcurrants. In *Bioactives in Fruit* (pp. 215-250). https://doi.org/10.1002/9781118635551.ch10

Millet, M., Poupard, P., Le Quéré, J.-M., Bauduin, R., & Guyot, S. (2017). Haze in apple-based beverages: Detailed polyphenol, polysaccharide, protein, and mineral compositions. *Journal of Agricultural and Food Chemistry*, *65*(31), 6404-6414. https://doi.org/10.1021/acs.jafc.6b05819

Mishra, S., Mann, B., & Joshi, V. K. (2001). Functional improvement of whey protein concentrate on interaction with pectin. *Food Hydrocolloids*, *15*(1), 9-15. https://doi.org/10.1016/S0268-005X(00)00043-6

Miyake, Y., Yamamoto, K., & Osawa, T. (1997). Isolation of Eriocitrin (Eriodictyol 7-rutinoside) from Lemon Fruit (<I>Citrus limon</I> BURM. f.) and Its Antioxidative Activity. *Food Science and Technology International, Tokyo*, *3*(1), 84-89. https://doi.org/10.3136/fsti9596t9798.3.84

Mohanta, T. K., Khan, A., Hashem, A., Abd_Allah, E. F., & Al-Harrasi, A. (2019). The molecular mass and isoelectric point of plant proteomes. *BMC Genomics*, *20*(1), 631. https://doi.org/10.1186/s12864-019-5983-8

Mohnen, D. (2008). Pectin Structure and Biosynthesis. *Current Opinion in Plant Biology*, *11*, 266-277. https://doi.org/10.1016/j.pbi.2008.03.006

Money, R. W., & Christian, W. A. (1950). Analytical data of some common fruits. *Journal of the Science of Food and Agriculture*, *1*(1), 8-12. https://doi.org/10.1002/jsfa.2740010105

Moore, E. (2016). *Fourier Transform Infrared Spectroscopy (FTIR) : Methods, Analysis, and Research Insights* [Book]. Nova Science Publishers, Inc.

Moraes, I., & Archer, M. (2015). Methods for the Successful Crystallization of Membrane Proteins. In R. J. Owens (Ed.), *Structural Proteomics: High-Throughput Methods* (pp. 211-230). Springer New York. https://doi.org/10.1007/978-1-4939-2230-7_12

Morris, G. A., Foster, T. J., & Harding, S. E. (2000). The effect of the degree of esterification on the hydrodynamic properties of citrus pectin. *Food Hydrocolloids*, *14*(3), 227-235. https://doi.org/10.1016/S0268-005X(00)00007-2

Muhammad, K., Mohd. Zahari, N. I., Gannasin, S. P., Mohd. Adzahan, N., & Bakar, J. (2014). High Methoxyl Pectin From Dragon Fruit (*Hylocereus Polyrhizus*) Peel. *Food Hydrocolloids*, *42*, 289-297. https://doi.org/10.1016/j.foodhyd.2014.03.021

Naczk, M., Grant, S., Zadernowski, R., & Barre, E. (2006). Protein precipitating capacity of phenolics of wild blueberry leaves and fruits. *Food Chemistry*, *96*(4), 640-647. https://doi.org/10.1016/j.foodchem.2005.03.017

Neirynck, N., Van der Meeren, P., Bayarri Gorbe, S., Dierckx, S., & Dewettinck, K. (2004). Improved emulsion stabilizing properties of whey protein isolate by conjugation with pectins. *Food Hydrocolloids*, *18*(6), 949-957. https://doi.org/10.1016/j.foodhyd.2004.03.004

Nep, E. I., Carnachan, S. M., Ngwuluka, N. C., Kontogiorgos, V., Morris, G. A., Sims, I. M., & Smith, A. M. (2016). Structural Characterisation and Rheological Properties of a Polysaccharide From Sesame Leaves (*Sesamum Radiatum* Schumach. & Thonn.). *Carbohydrate Polymers*, *152*, 541-547. https://doi.org/10.1016/j.carbpol.2016.07.036

New Zealand Horticulture Export Authority. (2022). *Blackcurrants*. https://hea.co.nz/2012-05-11-03-05-28/blackcurrant-trade

Nielsen, S. S. (2017a). Protein Nitrogen Determination. In *Food Analysis Laboratory Manual* (pp. 131-135). Springer International Publishing. https://doi.org/10.1007/978-3-319-44127-6_13

Nielsen, S. S. (2017b). Total Carbohydrate by Phenol-Sulfuric Acid Method. In *Food Analysis Laboratory Manual* (pp. 137-141). Springer International Publishing. https://doi.org/10.1007/978-3-319-44127-6_14

Nielsen, S. S., & Talcott, T. S. (2017). High-Performance Liquid Chromatography. In *Food Analysis Laboratory Manual* (pp. 77-85). Springer International Publishing. https://doi.org/10.1007/978-3-319-44127-6_7

Niskanen, I., Forsberg, V., Zakrisson, D., Reza, S., Hummelgård, M., Andres, B., Fedorov, I., Suopajärvi, T., Liimatainen, H., & Thungström, G. (2019). Determination of nanoparticle size using Rayleigh approximation and Mie theory. *Chemical Engineering Science*, *201*, 222-229. https://doi.org/10.1016/j.ces.2019.02.020

Nunes, C., Rocha, S. M., Saraiva, J., & Coimbra, M. A. (2006). Simple and Solvent-Free Methodology for Simultaneous Quantification of Methanol and Acetic Acid Content of Plant Polysaccharides Based on Headspace Solid Phase Microextraction-Gas Chromatography (Hs-Spme-Gc-Fid). *Carbohydrate Polymers*, *64*, 306-311. https://doi.org/10.1016/j.carbpol.2005.11.039

Nuñez, A., Fishman, M. L., Fortis, L. L., Cooke, P. H., & Hotchkiss, A. T., Jr. (2009). Identification of Extensin Protein Associated with Sugar Beet Pectin. *Journal of Agricultural and Food Chemistry*, *57*(22), 10951-10958. https://doi.org/10.1021/jf902162t

Nyanhanda, T., Gould, E. M., McGhie, T., Shaw, O. M., Harper, J. L., & Hurst, R. D. (2014). Blackcurrant Cultivar Polyphenolic Extracts Suppress CCL26 Secretion From Alveolar Epithelial Cells [10.1039/C3FO60568J]. *Food & Function*, *5*, 671-677. https://doi.org/10.1039/C3FO60568J

O'Donoghue, E. M., Somerfield, S. D., Deroles, S. C., Sutherland, P. W., Hallett, I. C., Erridge, Z. A., Brummell, D. A., & Hunter, D. A. (2017). Simultaneous knock-down of six beta-galactosidase genes in petunia petals prevents loss of pectic galactan but decreases petal strength. *Plant Physiology and Biochemistry*, *113*, 208-221. https://doi.org/10.1016/j.plaphy.2017.02.005

O'Mahony, J. A., & Fox, P. F. (2013). Milk Proteins: Introduction and Historical Aspects. In P. L. H. McSweeney & P. F. Fox (Eds.), *Advanced Dairy Chemistry, Proteins: Basic Aspects* (Vol. 1A, pp. 43-95). Springer. https://doi.org/10.1007/978-1-4614-4714-6_2

O'Mahony, J. A., & McSweeney, P. L. H. (2016). *Advanced dairy chemistry, Proteins: Applied Aspects* (J. A. O'Mahony & P. L. H. McSweeney, Eds. Fourth edition ed., Vol. 1B). Springer. https://doi.org/10.1007/978-1-4939-2800-2

Oakenfull, D., & Scott, A. (1984). Hydrophobic Interaction in the Gelation of High Methoxyl Pectins. *Journal of Food Science*, *49*(4), 1093-1098. https://doi.org/10.1111/j.1365-2621.1984.tb10401.x

Oancea, S. (2021). A review of the current knowledge of thermal stability of anthocyanins and approaches to their stabilization to heat. *Antioxidants*, *10*(9), 1337. https://doi.org/10.3390/antiox10091337

Ochmian, I. D., Dobrowolska, A., & CheŁPiŃSki, P. (2014). Physical Parameters and Chemical Composition of Fourteen Blackcurrant Cultivars (Ribes nigrum L.). *Notulae Botanicae Horti Agrobotanici Cluj-Napoca*, *42*(1). https://doi.org/10.15835/nbha4219103

Oldfield, D. J., Singh, H., & Taylor, M. W. (1998). Association of β-Lactoglobulin and β-Lactalbumin with the Casein Micelles in Skim Milk Heated in an Ultra-high Temperature Plant. *International Dairy Journal*, *8*(9), 765-770. https://doi.org/10.1016/S0958-6946(98)00127-7

Oliveira, A. L., von Staszewski, M., Pizones Ruiz-Henestrosa, V. M., Pintado, M., & Pilosof, A. M. R. (2016). Impact of pectin or chitosan on bulk, interfacial and antioxidant properties of (+)-catechin and β-lactoglobulin ternary mixtures. *Food Hydrocolloids*, *55*, 119-127. https://doi.org/10.1016/j.foodhyd.2015.11.007

Otter, D. (2003). MILK | Physical and Chemical Properties A2 - Caballero, Benjamin. In *Encyclopedia of Food Sciences and Nutrition (Second Edition)* (pp. 3957-3963). Academic Press. https://doi.org/10.1016/B0-12-227055-X/00786-0

Owens, H., Lotzkar, H., Merrill, R., & Peterson, M. (1944). Viscosities of pectin solutions. *Journal of the American Chemical Society*, *66*(7), 1178-1182.

Owuor, P. O. (2003). In B. Caballero (Ed.), *Encyclopedia of Food Sciences and Nutrition (Second Edition)* (pp. 5743-5752). Academic Press. https://doi.org/10.1016/B0-12-227055-X/01182-2

Ozdal, T., Capanoglu, E., & Altay, F. (2013). A review on protein–phenolic interactions and associated changes. *Food Research International*, *51*(2), 954-970. https://doi.org/10.1016/j.foodres.2013.02.009

Padayachee, A., Netzel, G., Netzel, M., Day, L., Zabaras, D., Mikkelsen, D., & Gidley, M. J. (2012a). Binding of polyphenols to plant cell wall analogues – Part 1: Anthocyanins. *Food Chemistry*, *134*(1), 155-161. https://doi.org/10.1016/j.foodchem.2012.02.082

Padayachee, A., Netzel, G., Netzel, M., Day, L., Zabaras, D., Mikkelsen, D., & Gidley, M. J. (2012b). Binding of polyphenols to plant cell wall analogues – Part 2: Phenolic acids. *Food Chemistry*, *135*(4), 2287-2292. https://doi.org/10.1016/j.foodchem.2012.07.004

Parkar, S. G., Redgate, E. L., McGhie, T. K., & Hurst, R. D. (2014). In Vitro Studies of Modulation of Pathogenic and Probiotic Bacterial Proliferation and Adhesion to Intestinal Cells by Blackcurrant Juices. *Journal of Functional Foods*, *8*, 35-44. https://doi.org/10.1016/j.jff.2014.02.021

Patras, A., Brunton, N. P., O'Donnell, C., & Tiwari, B. K. (2010). Effect of thermal processing on anthocyanin stability in foods; mechanisms and kinetics of degradation. *Trends in Food Science & Technology*, *21*(1), 3-11. https://doi.org/10.1016/j.tifs.2009.07.004

Pecket, R. C., & Small, C. J. (1980). Occurrence, location and development of anthocyanoplasts. *Phytochemistry*, *19*(12), 2571-2576. https://doi.org/10.1016/S0031-9422(00)83921-7

Pelegrine, D. H. G., & Gasparetto, C. A. (2005). Whey proteins solubility as function of temperature and pH. *LWT - Food Science and Technology*, *38*(1), 77-80. https://doi.org/10.1016/j.lwt.2004.03.013

Peña-Ramos, E. A., Xiong, Y. L., & Arteaga, G. E. (2004). Fractionation and characterisation for antioxidant activity of hydrolysed whey protein. *Journal of the Science of Food and Agriculture*, *84*(14), 1908-1918. https://doi.org/10.1002/jsfa.1886

Petit, J., Moreau, A., Ronse, G., Debreyne, P., Bouvier, L., Blanpain-Avet, P., Jeantet, R., & Delaplace, G. (2016). Role of Whey Components in the Kinetics and Thermodynamics of β-Lactoglobulin Unfolding and Aggregation. *Food and Bioprocess Technology*, *9*(8), 1367-1379. https://doi.org/10.1007/s11947-016-1726-x

Pettolino, F. A., Walsh, C., Fincher, G. B., & Bacic, A. (2012). Determining the Polysaccharide Composition of Plant Cell Walls. *Nature Protocols*, *7*, 1590-1607. https://doi.org/10.1038/nprot.2012.081

Phan, A. D. T., Flanagan, B. M., D'Arcy, B. R., & Gidley, M. J. (2017). Binding Selectivity of Dietary Polyphenols to Different Plant Cell Wall Components: Quantification and Mechanism. *Food Chemistry*, *233*, 216-227. https://doi.org/10.1016/j.foodchem.2017.04.115

Picot-Allain, M. C. N., Ramasawmy, B., & Emmambux, M. N. (2022). Extraction, Characterisation, and Application of Pectin from Tropical and Sub-Tropical Fruits: A Review. *Food Reviews International*, *38*(3), 282-312. https://doi.org/10.1080/87559129.2020.1733008

Pike, A. C. W., Brew, K., & Acharya, K. R. (1996). Crystal structures of guinea-pig, goat and bovine α-lactalbumin highlight the enhanced conformational flexibility of regions that are significant for its action in lactose synthase. *Structure*, *4*(6), 691-703. https://doi.org/10.1016/S0969-2126(96)00075-5

Posé, S., Kirby, A. R., Paniagua, C., Waldron, K. W., Morris, V. J., Quesada, M. A., & Mercado, J. A. (2015). The nanostructural characterization of strawberry pectins in pectate lyase or polygalacturonase silenced fruits elucidates their role in softening. *Carbohydrate Polymers*, *132*, 134-145. https://doi.org/10.1016/j.carbpol.2015.06.018

Pretsch, E., Bühlmann, P., & Badertscher, M. (2009). IR spectroscopy. In *Structure Determination of Organic Compounds: Tables of Spectral Data* (4th ed., pp. 1-67). Springer. https://doi.org/10.1007/978-3-540-93810-1_7

Prigent, S. V. E., Gruppen, H., Visser, A. J. W. G., van Koningsveld, G. A., de Jong, G. A. H., & Voragen, A. G. J. (2003). Effects of Non-covalent Interactions with 5-O-Caffeoylquinic Acid (Chlorogenic Acid) on the Heat Denaturation and Solubility of Globular Proteins. *Journal of Agricultural and Food Chemistry*, *51*(17), 5088-5095. https://doi.org/10.1021/jf021229w

Prior, R. L., & Wu, X. (2012). Analysis of Methods of Anthocyanins. In Z. Xu & L. R. Howard (Eds.), *Analysis of Antioxidant-Rich Phytochemicals*. Wiley-Blackwell.

PubChem. (2022a). *2D-Structure of Chrysanthemin* https://pubchem.ncbi.nlm.nih.gov/compound/44256715#section=2D-Structure

PubChem. (2022b). *2D-Structure of Cyanidin 3-O-rutinoside* https://pubchem.ncbi.nlm.nih.gov/compound/441674#section=2D-Structure

PubChem. (2022c). *2D-Structure of Delphinidin 3-O-glucoside* https://pubchem.ncbi.nlm.nih.gov/compound/443650#section=2D-Structure

PubChem. (2022d). *2D-Structure of Tulipanin* https://pubchem.ncbi.nlm.nih.gov/compound/5492231#section=2D-Structure

PubChem. (2022e). *Compound Summary of Chrysanthemin* https://pubchem.ncbi.nlm.nih.gov/compound/44256715

PubChem. (2022f). *Compound Summary of Cyanidin 3-O-rutinoside* https://pubchem.ncbi.nlm.nih.gov/compound/441674

PubChem. (2022g). *Compound Summary of D-Fructose* https://pubchem.ncbi.nlm.nih.gov/compound/2723872

PubChem. (2022h). *Compound Summary of D-Galacturonic Acid* https://pubchem.ncbi.nlm.nih.gov/compound/439215

PubChem. (2022i). *Compound Summary of D-Glucose* https://pubchem.ncbi.nlm.nih.gov/compound/5793

PubChem. (2022j). *Compound Summary of Delphinidin 3-O-glucoside* https://pubchem.ncbi.nlm.nih.gov/compound/443650

PubChem. (2022k). *Compound Summary of Sucrose* https://pubchem.ncbi.nlm.nih.gov/compound/5988

PubChem. (2022l). *Compound Summary of Tulipanin* https://pubchem.ncbi.nlm.nih.gov/compound/5492231

Qi, W., Ye, T., Xiaolong, Z., Xiaoying, D., Jixing, X., Renfang, S., & Xiaofang, Z. (2022). Pectin Methylesterases Enhance Root Cell Wall Phosphorus Remobilization in Rice. *Rice Science*, *29*(2), 179-188. https://doi.org/10.1016/j.rsci.2022.01.006

Raei, M., Rafe, A., & Shahidi, F. (2018). Rheological and structural characteristics of whey protein-pectin complex coacervates. *Journal of Food Engineering*, *228*, 25-31. https://doi.org/10.1016/j.jfoodeng.2018.02.007

Ralet, M.-C., Dronnet, V., Buchholt, H. C., & Thibault, J.-F. (2001). Enzymatically and chemically de-esterified lime pectins: characterisation, polyelectrolyte behaviour and calcium binding properties. *Carbohydrate Research*, *336*(2), 117-125. https://doi.org/10.1016/S0008-6215(01)00248-8

Ralet, M. C., Crépeau, M. J., Buchholt, H. C., & Thibault, J. F. (2003). Polyelectrolyte Behaviour and Calcium Binding Properties of Sugar Beet Pectins Differing in Their Degrees of Methylation and Acetylation [Article]. *Biochemical Engineering Journal*, *16*, 191-201. https://doi.org/10.1016/S1369-703X(03)00037-8

Ranque, C. (2022). Electrospray Ionization (ESI) Mass Spectrometry In R. Faller (Ed.), *UCD Biophysics 241: Membrane Biology*. LibreTexts. https://phys.libretexts.org/Courses/University_of_California_Davis/UCD%3A_Biophysics_241_-_Membrane_Biology/06%3A_Experimental_Characterization_-_Mass_Spectrometry_and_Atomic_Force_Microscopy/6.03%3A_Electrospray_Ionization_(ESI)_Mass_Spectrometry

Reijenga, J., van Hoof, A., van Loon, A., & Teunissen, B. (2013). Development of Methods for the Determination of pK_a Values. *Analytical chemistry insights*, *8*, 53-71. https://doi.org/10.4137/ACI.S12304

Rinaldi, A., Gambuti, A., Moine-Ledoux, V., & Moio, L. (2010). Evaluation of the astringency of commercial tannins by means of the SDS–PAGE-based method. *Food Chemistry*, *122*(4), 951-956. https://doi.org/10.1016/j.foodchem.2010.03.105

Rivas-Gonzalo, J. C. (2003). Analysis of anthocyanins. In C. Santos-Buelga & G. Williamson (Eds.), *Methods in Polyphenol Analysis* (1st ed., pp. 338-358). The Royal Society of Chemistry.

Rodríguez-Carvajal, M. A., Hervé du Penhoat, C., Mazeau, K., Doco, T., & Pérez, S. (2003). The Three-Dimensional Structure of the Mega-Oligosaccharide Rhamnogalacturonan II Monomer: A Combined Molecular Modeling and NMR Investigation. *Carbohydrate Research*, *338*, 651-671. https://doi.org/10.1016/S0008-6215(03)00003-X

Rombouts, F. M., & Thibault, J. F. (1986). Sugar Beet Pectins: Chemical Structure and Gelation through Oxidative Coupling. In *Chemistry and Function of Pectins* (Vol. 310, pp. 49-60). American Chemical Society. https://doi.org/10.1021/bk-1986-0310.ch005

Ropartz, D., & Ralet, M.-C. (2020). Pectin Structure. In V. Kontogiorgos (Ed.), *Pectin: Technological and Physiological Properties* (pp. 17-36). Springer International Publishing. https://doi.org/10.1007/978-3-030-53421-9_2

Rubio-Senent, F., Rodríguez-Gutiérrez, G., Lama-Muñoz, A., García, A., & Fernández-Bolaños, J. (2015). Novel pectin present in new olive mill wastewater with similar emulsifying and better biological properties than citrus pectin. *Food Hydrocolloids*, *50*, 237-246. https://doi.org/10.1016/j.foodhyd.2015.03.030

Russell, W. R., Labat, A., Scobbie, L., Duncan, G. J., & Duthie, G. G. (2009). Phenolic acid content of fruits commonly consumed and locally produced in Scotland. *Food Chemistry*, *115*(1), 100-104. https://doi.org/10.1016/j.foodchem.2008.11.086

Saeidi, I., Hadjmohammadi, M. R., Peyrovi, M., Iranshahi, M., Barfi, B., Babaei, A. B., & Dust, A. M. (2011). HPLC determination of hesperidin, diosmin and eriocitrin in Iranian lime juice using polyamide as an adsorbent for solid phase extraction. *Journal of Pharmaceutical and Biomedical Analysis*, *56*(2), 419-422. https://doi.org/10.1016/j.jpba.2011.05.015

Santipanichwong, R., Suphantharika, M., Weiss, J., & McClements, D. J. (2008). Core-shell biopolymer nanoparticles produced by electrostatic deposition of beet pectin onto heat-denatured β-lactoglobulin aggregates. *Journal of Food Science*, *73*(6), N23-N30. https://doi.org/10.1111/j.1750-3841.2008.00804.x

Santos-Buelga, C., Garcia-Viguera, C., & Tomas-Barberan A., F. (2003). On-Line Identification of Flavonoids by HPLC Coupled to Diode Array Detection. In C. Santos-Buelga & G. Williamson (Eds.), *Methods in Polyphenol Analysis* (pp. 92-127). The Royal Society of Chemistry.

Satoh, A., Chantrell, R. W., & Coverdale, G. N. (1999). Brownian Dynamics Simulations of Ferromagnetic Colloidal Dispersions in a Simple Shear Flow. *Journal of Colloid and Interface Science*, *209*(1), 44-59. https://doi.org/10.1006/jcis.1998.5826

Saulnier, L., & Thibault, J.-F. (1999). Ferulic acid and diferulic acids as components of sugar-beet pectins and maize bran heteroxylans. *Journal of the Science of Food and Agriculture*, *79*(3),

396-402. https://doi.org/10.1002/(SICI)1097-0010(19990301)79:3<396::AID-JSFA262>3.0.CO;2-B

Sawayama, S., Kawabata, A., Nakahara, H., & Kamata, T. (1988). A light scattering study on the effects of pH on pectin aggregation in aqueous solution. *Food Hydrocolloids*, *2*(1), 31-37. https://doi.org/10.1016/S0268-005X(88)80035-3

Scalzo, J., Currie, A., Stephens, J., Alspach, P., & McGhie, T. (2008). The anthocyanin composition of different Vaccinium, Ribes and Rubus genotypes. *BioFactors*, *34*(1), 13-21. https://doi.org/10.1002/biof.5520340103

Schmidt, U. S., Schütz, L., & Schuchmann, H. P. (2017). Interfacial and emulsifying properties of citrus pectin: Interaction of pH, ionic strength and degree of esterification. *Food Hydrocolloids*, *62*, 288-298. https://doi.org/10.1016/j.foodhyd.2016.08.016

Schmitt, C., Aberkane, L., & Sanchez, C. (2009). Protein–polysaccharide complexes and coacervates. In G. O. Phillips & P. A. Williams (Eds.), *Handbook of Hydrocolloids (Second edition)* (Second ed., pp. 420-476). Woodhead Publishing. https://doi.org/10.1533/9781845695873.420

Schmitt, C., Sanchez, C., Desobry-Banon, S., & Hardy, J. (1998). Structure and technofunctional properties of protein-polysaccharide complexes: A review. *Critical Reviews in Food Science and Nutrition*, *38*(8), 689-753. https://doi.org/10.1080/10408699891274354

Schmitt, C., Sanchez, C., Despond, S., Renard, D., Thomas, F., & Hardy, J. (2000). Effect of protein aggregates on the complex coacervation between β-lactoglobulin and acacia gum at pH 4.2. *Food Hydrocolloids*, *14*(4), 403-413. https://doi.org/10.1016/S0268-005X(00)00022-9

Schneider, M., Esposito, D., Lila, M. A., & Foegeding, E. A. (2016). Formation of whey protein-polyphenol mesostructures as a natural means of creating functional particles [Article]. *Food & Function*, *7*(3), 1306-1318. https://doi.org/10.1039/c5fo01499a

Schrage, B., Stevenson, D., Wells, R. W., Lyall, K., Holmes, S., Deng, D., & Hurst, R. D. (2010). Evaluating the Health Benefits of Fruits for Physical Fitness: A Research Platform [Article]. *Journal of Berry Research*, *1*, 35-44. https://doi.org/10.3233/BR-2010-004

Schwartz, S. J., von Elbe, J. H., & Giusti, M. M. (2008). Colorants. In S. Damodaran, K. L. Parkin, & O. R. Fennema (Eds.), *Fennema's Food Chemistry* (4th ed., pp. 571-638). CRC Press. https://doi.org/10.1201/9781420020526

Selvendran, R. R. (1985). Developments in the Chemistry and Biochemistry of Pectic and Hemicellulosic Polymers. *Journal of Cell Science*, *1985*, 51-88. https://doi.org/10.1242/jcs.1985.Supplement_2.4

Shakhmatov, E. G., Toukach, P. V., & Makarova, E. N. (2020). Structural Studies of the Pectic Polysaccharide From Fruits of *Punica Granatum*. *Carbohydrate Polymers*, *235*, 115978. https://doi.org/10.1016/j.carbpol.2020.115978

Shaw, O. M., Nyanhanda, T., McGhie, T. K., Harper, J. L., & Hurst, R. D. (2017). Blackcurrant anthocyanins modulate CCL11 secretion and suppress allergic airway inflammation. *Molecular Nutrition & Food Research*, *61*(9), 1600868. https://doi.org/10.1002/mnfr.201600868

Shi, D.-c., Wang, J., Hu, R.-b., Zhou, G.-k., O'Neill, M. A., & Kong, Y.-z. (2017). Boron-bridged RG-II and calcium are required to maintain the pectin network of the Arabidopsis seed mucilage ultrastructure. *Plant Molecular Biology*, *94*(3), 267-280. https://doi.org/10.1007/s11103-017-0606-8

Siebert, K. J., Troukhanova, N. V., & Lynn, P. Y. (1996). Nature of polyphenol-protein interactions [Article]. *Journal of Agricultural and Food Chemistry*, *44*(1), 80-85. https://doi.org/10.1021/jf9502459

Siew, C. K., & Williams, P. A. (2008). Role of Protein and Ferulic Acid in the Emulsification Properties of Sugar Beet Pectin. *Journal of Agricultural and Food Chemistry*, *56*(11), 4164-4171. https://doi.org/10.1021/jf073358o

Sims, I. M., & Furneaux, R. H. (2003). Structure of the Exudate Gum From *Meryta Sinclairii*. *Carbohydrate Polymers*, *52*, 423-431. https://doi.org/10.1016/S0144-8617(02)00326-0

Singh, B., Singh, J. P., Kaur, A., & Singh, N. (2020). Phenolic Composition, Antioxidant Potential and Health Benefits of Citrus Peel. *Food Research International*, *132*, 109114. https://doi.org/10.1016/j.foodres.2020.109114

Slimestad, R., & Solheim, H. (2002). Anthocyanins from Black Currants (*Ribes nigrum* L.). *Journal of Agricultural and Food Chemistry*, *50*, 3228-3231. https://doi.org/10.1021/jf011581u

Spencer, C. M., Cai, Y., Martin, R., Gaffney, S. H., Goulding, P. N., Magnolato, D., Lilley, T. H., & Haslam, E. (1988). Polyphenol Complexation - Some thoughts and observations [Review]. *Phytochemistry*, *27*, 2397-2409. https://doi.org/10.1016/0031-9422(88)87004-3

Sperber, B. L. H. M., Schols, H. A., Cohen Stuart, M. A., Norde, W., & Voragen, A. G. J. (2009). Influence of the overall charge and local charge density of pectin on the complex formation between pectin and β-lactoglobulin [Article]. *Food Hydrocolloids*, *23*, 765-772. https://doi.org/10.1016/j.foodhyd.2008.04.008

Spiegel, T., & Huss, M. (2002). Whey protein aggregation under shear conditions – effects of pH-value and removal of calcium. *International Journal of Food Science & Technology*, *37*(5), 559-568. https://doi.org/10.1046/j.1365-2621.2002.00612.x

Stănciuc, N., Oancea, A. M., Aprodu, I., Turturică, M., Barbu, V., Ioniţă, E., Râpeanu, G., & Bahrim, G. (2018). Investigations on binding mechanism of bioactives from elderberry (*Sambucus nigra L.*) by whey proteins for efficient microencapsulation. *Journal of Food Engineering*, *223*, 197-207. https://doi.org/10.1016/j.jfoodeng.2017.10.019

Stănciuc, N., Turturică, M., Oancea, A. M., Barbu, V., Ioniţă, E., Aprodu, I., & Râpeanu, G. (2017). Microencapsulation of anthocyanins from grape skins by whey protein isolates and different polymers. *Food and Bioprocess Technology*, *10*(9), 1715-1726. https://doi.org/10.1007/s11947-017-1938-8

Stefania, I., Beatrice, G., Giuseppe, V., & Francesco, B. (1996). Modifications Occur at Different Structural Levels During the Heat Denaturation of β - Lactoglobulin. *European Journal of Biochemistry*, *237*(1), 106-112. https://doi.org/10.1111/j.1432-1033.1996.0106n.x

Swaisgood, H. E. (2008). Characteristics of Milk. In S. Damodaran, K. L. Parkin, & O. R. Fennema (Eds.), *Fennema's Food Chemistry, Fourth Edition* (4 ed., pp. 885-921). CRC Press. https://doi.org/10.1201/9781420020526

Tabart, J., Kevers, C., Pincemail, J., Defraigne, J.-O., & Dommes, J. (2006). Antioxidant Capacity of Black Currant Varies with Organ, Season, and Cultivar. *Journal of Agricultural and Food Chemistry*, *54*(17), 6271-6276. https://doi.org/10.1021/jf061112y

Takaki, K., Takahashi, K., Guionet, A., & Ohshima, T. (2021). Pulsed Power Applications for Protein Conformational Change and the Permeabilization of Agricultural Products. *Molecules*, *26*(20), 6288. https://doi.org/10.3390/molecules26206288

Tamiello-Rosa, C. S., Cantu-Jungles, T. M., Iacomini, M., & Cordeiro, L. M. C. (2019). Pectins From Cashew Apple Fruit (*Anacardium Occidentale*): Extraction and Chemical Characterization. *Carbohydrate Research*, *483*, 107752. https://doi.org/10.1016/j.carres.2019.107752

Tang, W., Liu, D., Li, Y., Zou, M.-Y., Shao, Y.-C., Yin, J.-Y., & Nie, S.-P. (2021). Structural Characteristics of a Highly Branched and Acetylated Pectin From *Portulaca Oleracea* L. *Food Hydrocolloids*, *116*, 106659. https://doi.org/10.1016/j.foodhyd.2021.106659

Thakur, B. R., Singh, R. K., Handa, A. K., & Rao, M. A. (1997). Chemistry and uses of pectin — A review. *Critical Reviews in Food Science and Nutrition*, *37*(1), 47-73. https://doi.org/10.1080/10408399709527767

Thompson, A., Boland, M., & Singh, H. (2009). *Milk Proteins: from Expression to Food* (1st ed.). Academic Press. https://doi.org/10.1016/B978-0-12-374039-7.X0001-3

Thongkaew, C., Gibis, M., Hinrichs, J., & Weiss, J. (2014). Polyphenol interactions with whey protein isolate and whey protein isolate–pectin coacervates. *Food Hydrocolloids*, *41*, 103-112. https://doi.org/10.1016/j.foodhyd.2014.02.006

Topală, T., Bodoki, A., Oprean, L., & Oprean, R. (2014). Bovine Serum Albumin Interactions with Metal Complexes. *Clujul Medical*, *87*(4), 215-219. https://doi.org/10.15386/cjmed-357

Townsend, A.-A., & Nakai, S. (1983). Relationships Between Hydrophobicity and Foaming Characteristics of Food Proteins. *Journal of Food Science*, *48*(2), 588-594. https://doi.org/10.1111/j.1365-2621.1983.tb10796.x

Uhrínová, S., Smith, M. H., Jameson, G. B., Uhrín, D., Sawyer, L., & Barlow, P. N. (2000). Structural Changes Accompanying pH-Induced Dissociation of the β-Lactoglobulin Dimer. *Biochemistry*, *39*(13), 3565-3574. https://doi.org/10.1021/bi992629o

Vagiri, M., Ekholm, A., Andersson, S. C., Johansson, E., & Rumpunen, K. (2012). An Optimized Method for Analysis of Phenolic Compounds in Buds, Leaves, and Fruits of Black Currant (Ribes nigrum L.). *Journal of Agricultural and Food Chemistry*, *60*(42), 10501-10510. https://doi.org/10.1021/jf303398z

Vagiri, M., Ekholm, A., Öberg, E., Johansson, E., Andersson, S. C., & Rumpunen, K. (2013). Phenols and Ascorbic Acid in Black Currants (Ribes nigrum L.): Variation Due to Genotype, Location, and Year. *Journal of Agricultural and Food Chemistry*, *61*(39), 9298-9306. https://doi.org/10.1021/jf402891s

Van Buren, J. P., Kean, W. P., & Wilkison, M. (1988). Influence Of Salts And Ph On The Firmness Of Cooked Snap Beans In Relation To The Properties Of Pectin. *Journal of Texture Studies*, *19*(1), 15-25. https://doi.org/10.1111/j.1745-4603.1988.tb00921.x

Verheul, M., Roefs, S. P. F. M., & de Kruif, K. G. (1998). Kinetics of Heat-Induced Aggregation of β-Lactoglobulin. *Journal of Agricultural and Food Chemistry*, *46*(3), 896-903. https://doi.org/10.1021/jf970751t

Verkempinck, S. H. E., Kyomugasho, C., Salvia-Trujillo, L., Denis, S., Bourgeois, M., Van Loey, A. M., Hendrickx, M. E., & Grauwet, T. (2018). Emulsion Stabilizing Properties of Citrus Pectin and its Interactions With Conventional Emulsifiers in Oil-In-Water Emulsions. *Food Hydrocolloids*, *85*, 144-157. https://doi.org/10.1016/j.foodhyd.2018.07.014

Vitality Wellness (NZ) Limited. (2020). *Breakthrough Key Brain Nutrient Discovery in New Zealand Blackcurrant Berries Essential for all Ages*. NutraIngredients-asia.com. Retrieved 13 September from https://www.nutraingredients-asia.com/News/Promotional-Features/What-superfood-s-best-New-Zealand-blackcurrants-key-for-brain-health

Vuong, T. T., & Hongsprabhas, P. (2021). Influences of pH on binding mechanisms of anthocyanins from butterfly pea flower (*Clitoria ternatea*) with whey powder and whey protein isolate. *Cogent Food & Agriculture*, *7*(1), 1889098. https://doi.org/10.1080/23311932.2021.1889098

Wahyuningsih, S., Wulandari, L., Wartono, M. W., Munawaroh, H., & Ramelan, A. H. (2017). The effect of pH and color stability of anthocyanin on food colorant. *IOP Conference Series: Materials Science and Engineering*, *193*, 012047. https://doi.org/10.1088/1757-899X/193/1/012047

Walker, P. G., Viola, R., Woodhead, M., Jorgensen, L., Gordon, S. L., Brennan, R. M., & Hancock, R. D. (2010). Ascorbic acid content of blackcurrant fruit is influenced by both genetic and environmental factors. *Functional Plant Science and Biotechnology*, *4*(1), 40-52. http://www.globalsciencebooks.info/Online/GSBOnline/images/2010/FPSB_4(SI1)/FPSB_4(SI1)40-52o.pdf

Walkinshaw, M. D., & Arnott, S. (1981). Conformations and interactions of pectins: II. Models for junction zones in pectinic acid and calcium pectate gels. *Journal of Molecular Biology*, *153*(4), 1075-1085. https://doi.org/10.1016/0022-2836(81)90468-X

Walstra, P. (2003). Bonds and Interaction Forces. In P. Walstra (Ed.), *Physical Chemistry of Foods* (First ed., pp. 46-58). CRC Press. https://doi.org/10.1201/9780203910436

Wang, G., & Guo, M. (2019a). History of Whey Production and Whey Protein Manufacturing. In M. Guo (Ed.), *Whey protein production, chemistry, functionality and applications* (First edition ed., pp. 1-12). Wiley. https://doi.org/10.1002/9781119256052

Wang, G., & Guo, M. (2019b). Manufacturing Technologies of Whey Protein Products. In M. Guo (Ed.), *Whey protein production, chemistry, functionality and applications* (First edition ed., pp. 13-37). Wiley. https://doi.org/10.1002/9781119256052

Wang, J., & Zhao, X.-H. (2016). Degradation kinetics of fisetin and quercetin in solutions as effected by pH, temperature and coexisted proteins. *Journal of the Serbian Chemical Society*, *81*(3), 243-253. https://doi.org/10.2298/JSC150706092W

Wang, Q., & Qvist, K. B. (2000). Investigation of the composite system of β-lactoglobulin and pectin in aqueous solutions. *Food Research International*, *33*(8), 683-690. https://doi.org/10.1016/S0963-9969(00)00113-7

Wang, T., & Lucey, J. A. (2003). Use of Multi-Angle Laser Light Scattering and Size-Exclusion Chromatography to Characterize the Molecular Weight and Types of Aggregates Present in Commercial Whey Protein Products. *Journal of Dairy Science*, *86*(10), 3090-3101. https://doi.org/10.3168/jds.S0022-0302(03)73909-5

Wargent, J. J., & Jordan, B. R. (2013). From ozone depletion to agriculture: understanding the role of UV radiation in sustainable crop production. *New Phytologist*, *197*(4), 1058-1076. https://doi.org/10.1111/nph.12132

Wijayanti, H. B., Bansal, N., & Deeth, H. C. (2014). Stability of Whey Proteins during Thermal Processing: A Review [Article]. *Comprehensive Reviews in Food Science and Food Safety*, *13*(6), 1235-1251. https://doi.org/10.1111/1541-4337.12105

Wijayanti, H. B., Waanders, J., Bansal, N., & Deeth, H. C. (2015). Identification of the binding of β-lactoglobulin (β-Lg) with sulfhydryl (–SH) blocking reagents by polyacrylamide gel electrophoresis (PAGE) and electrospray ionisation/time of flight-mass spectrometry (ESI/TOF-MS). *LWT - Food Science and Technology*, *63*(2), 934-938. https://doi.org/10.1016/j.lwt.2015.04.012

Wilbanks, D. J., Yazdi, S. R., & Lucey, J. A. (2022). Effects of varying casein and pectin concentrations on the rheology of high-protein cultured milk beverages stored at ambient temperature. *Journal of Dairy Science*, *105*(1), 72-82. https://doi.org/10.3168/jds.2021-20597

Wojciech, D., Minoru, K., Akio, S., & Yoshihiro, T. (2001). FTIR study on heat-induced and pressure-assisted cold-induced changes in structure of bovine α-lactalbumin: Stabilizing role of calcium ion. *Biopolymers*, *62*(1), 29-39. https://doi.org/10.1002/1097-0282(2001)62:1<29::AID-BIP50>3.0.CO;2-A

Wu, J., Du, B., Li, J., & Zhang, H. (2014). Influence of homogenisation and the degradation of stabilizer on the stability of acidified milk drinks stabilized by carboxymethylcellulose. *LWT - Food Science and Technology*, *56*(2), 370-376. https://doi.org/10.1016/j.lwt.2013.12.029

Wu, W., Zhu, S., Chen, Q., Lin, Y., Tian, J., & Liang, C. (2019). Cell Wall Proteins Play Critical Roles in Plant Adaptation to Phosphorus Deficiency. *International Journal of Molecular Sciences*, *20*(21). https://doi.org/10.3390/ijms20215259

Wu, X., Beecher, G. R., Holden, J. M., Haytowitz, D. B., Gebhardt, S. E., & Prior, R. L. (2006). Concentrations of Anthocyanins in Common Foods in the United States and Estimation of Normal Consumption. *Journal of Agricultural and Food Chemistry*, *54*(11), 4069-4075. https://doi.org/10.1021/jf060300l

Wyatt, P. J. (1993). Light scattering and the absolute characterization of macromolecules. *Analytica Chimica Acta*, *272*(1), 1-40. https://doi.org/10.1016/0003-2670(93)80373-S

Xiao, J., Cao, H., Wang, Y., Yamamoto, K., & Wei, X. (2010). Structure–affinity relationship of flavones on binding to serum albumins: Effect of hydroxyl groups on ring A. *Molecular Nutrition & Food Research*, *54*(S2), S253-S260. https://doi.org/10.1002/mnfr.200900454

Xu, A. Y., Melton, L. D., Jameson, G. B., Williams, M. A. K., & McGillivray, D. J. (2015). Structural mechanism of complex assemblies: characterisation of beta-lactoglobulin and pectin interactions [10.1039/C5SM01378J]. *Soft Matter*, *11*(34), 6790-6799. https://doi.org/10.1039/C5SM01378J

Xu, Z. (2012). Analysis Methods of Phenolic Acids. In Z. Xu & L. R. Howard (Eds.), *Analysis of Antioxidant-Rich Phytochemicals*. Wiley-Blackwell.

Yao, Y., Lin, G., Xie, Y., Ma, P., Li, G., Meng, Q., & Wu, T. (2014). Preformulation studies of myricetin: a natural antioxidant flavonoid. *Die Pharmazie - An International Journal of Pharmaceutical Sciences*, *69*(1), 19-26. https://doi.org/10.1691/ph.2014.3076

Yapo, B. M., Lerouge, P., Thibault, J.-F., & Ralet, M.-C. (2007). Pectins from citrus peel cell walls contain homogalacturonans homogenous with respect to molar mass, rhamnogalacturonan I and rhamnogalacturonan II. *Carbohydrate Polymers*, *69*(3), 426-435. https://doi.org/10.1016/j.carbpol.2006.12.024

Yildirim-Elikoglu, S., & Erdem, Y. K. (2018). Interactions between milk proteins and polyphenols: Binding mechanisms, related changes, and the future trends in the dairy industry. *Food Reviews International*, *34*(7), 665-697. https://doi.org/10.1080/87559129.2017.1377225

Young, J. C., & Abdel-Aal, E.-S. M. (2009). Anthocyanins. In P. R. Shewry & J. L. Ward (Eds.), *Healthgrain Methods - Analysis of Bioactive Components in Small Grain Cereals* (pp. 141-165). AACC International Press. https://doi.org/10.1016/B978-1-891127-70-0.50015-7

Yue, F., Zhang, J., Xu, J., Niu, T., Lü, X., & Liu, M. (2022). Effects of monosaccharide composition on quantitative analysis of total sugar content by phenol-sulfuric acid method. *Frontiers in Nutrition*, *9*, 963318. https://doi.org/10.3389/fnut.2022.963318

Yuliarti, O., Goh, K. K. T., Matia-Merino, L., Mawson, J., & Brennan, C. (2015). Extraction and Characterisation of Pomace Pectin From Gold Kiwifruit (*Actinidia Chinensis*). *Food Chemistry*, *187*, 290-296. https://doi.org/10.1016/j.foodchem.2015.03.148

Yuliarti, O., Matia-Merino, L., Goh, K. K. T., Mawson, J., Williams, M. A. K., & Brennan, C. (2015). Characterization of Gold Kiwifruit Pectin From Fruit of Different Maturities and Extraction Methods. *Food Chemistry*, *166*, 479-485. https://doi.org/10.1016/j.foodchem.2014.06.055

Yuris, A., Hardacre, A. K., Goh, K. K. T., & Matia-Merino, L. (2019). The Role of Calcium in Wheat Starch-*Mesona Chinensis* Polysaccharide Gels: Rheological Properties, in Vitro Digestibility and Enzyme Inhibitory Activities. *LWT*, *99*, 202-208. https://doi.org/10.1016/j.lwt.2018.09.041

Zaleska, H., Ring, S. G., & Tomasik, P. (2000). Apple pectin complexes with whey protein isolate. *Food Hydrocolloids*, *14*(4), 377-382. https://doi.org/10.1016/S0268-005X(00)00014-X

Zdzisław, E. S., Pokorny, J., & Damodaran, S. (2008). Physical and Chemical Interactions of Components in Food Systems. In S. Damodaran, K. L. Parkin, & O. R. Fennema (Eds.), *Fennema's Food Chemistry, Fourth Edition* (pp. 849-884). CRC Press. https://doi.org/10.1201/9781420020526

Zhang, Q., Zhao, X., & Qiu, H. (2013). Flavones and Flavonols: Phytochemistry and Biochemistry. In K. G. Ramawat & J.-M. Mérillon (Eds.), *Natural Products Phytochemistry, Botany and Metabolism of Alkaloids, Phenolics and Terpenes*. Springer. https://doi.org/10.1007/978-3-642-22144-6

Zhang, Y., Li, S., Yang, Y., Wang, C., & Zhang, T. (2022). Formation and characterization of noncovalent ternary complexes based on whey protein concentrate, high methoxyl pectin, and phenolic acid. *Journal of Dairy Science*, *105*(4), 2963-2977. https://doi.org/10.3168/jds.2021-21088

Zhao, Y., Wang, X., Li, D., Tang, H., Yu, D., Wang, L., & Jiang, L. (2020). Effect of anionic polysaccharides on conformational changes and antioxidant properties of protein-polyphenol binary covalently-linked complexes. *Process Biochemistry*, *89*, 89-97. https://doi.org/10.1016/j.procbio.2019.10.021

Zhao, Z., & Xiao, Q. (2017). Effect of chitosan on the heat stability of whey protein solution as a function of pH. *Journal of the Science of Food and Agriculture*, *97*(5), 1576-1581. https://doi.org/10.1002/jsfa.7904

Zheng, J., Yang, B., Ruusunen, V., Laaksonen, O., Tahvonen, R., Hellsten, J., & Kallio, H. (2012). Compositional Differences of Phenolic Compounds between Black Currant (Ribes nigrum L.) Cultivars and Their Response to Latitude and Weather Conditions. *Journal of Agricultural and Food Chemistry*, *60*(26), 6581-6593. https://doi.org/10.1021/jf3012739

Zheng, J., Yang, B., Tuomasjukka, S., Ou, S., & Kallio, H. (2009). Effects of Latitude and Weather Conditions on Contents of Sugars, Fruit Acids, and Ascorbic Acid in Black Currant (Ribes nigrum L.) Juice. *Journal of Agricultural and Food Chemistry*, *57*(7), 2977-2987. https://doi.org/10.1021/jf8034513

Appendices

Appendix A – Supplementary Information for Chapter 4

Table A.1 Chromatographic characteristics of identified anthocyanins in blackcurrant juice.

Compound	Juice			
	Peak No.	Retention Time (t_R), min	Dominant Wavelength, nm	Peak Area, % (530nm)
delphinidin 3-*O*-glucoside	1	6.14	522	7.04
delphinidin 3-*O*-rutinoside	2	6.61	524	40.12
cyanidin 3-*O*-glucoside	3	7.21	514	4.69
cyanidin 3-*O*-rutinoside	4	7.66	516	48.14

Table A.2 Chromatographic characteristics of identified anthocyanins in blackcurrant pectin-rich fractions.

Compound	Undialysed Pectin-Rich Fraction				Dialysed Pectin-Rich Fraction		
	Peak No.	Retention Time (t_R), min	Dominant Wavelength, nm	Peak Area, % (530nm)	Retention Time (t_R), min	Dominant Wavelength, nm	Peak Area, % (530nm)
delphinidin 3-*O*-glucoside	1	6.13	522	6.80	6.17	522	7.37
delphinidin 3-*O*-rutinoside	2	6.59	524	42.6	6.63	524	41.1
cyanidin 3-*O*-glucoside	3	7.20	514	4.22	7.22	514	5.22
cyanidin 3-*O*-rutinoside	4	7.63	516	46.4	7.67	516	46.4

Appendix B – Supplementary Information for Chapter 7

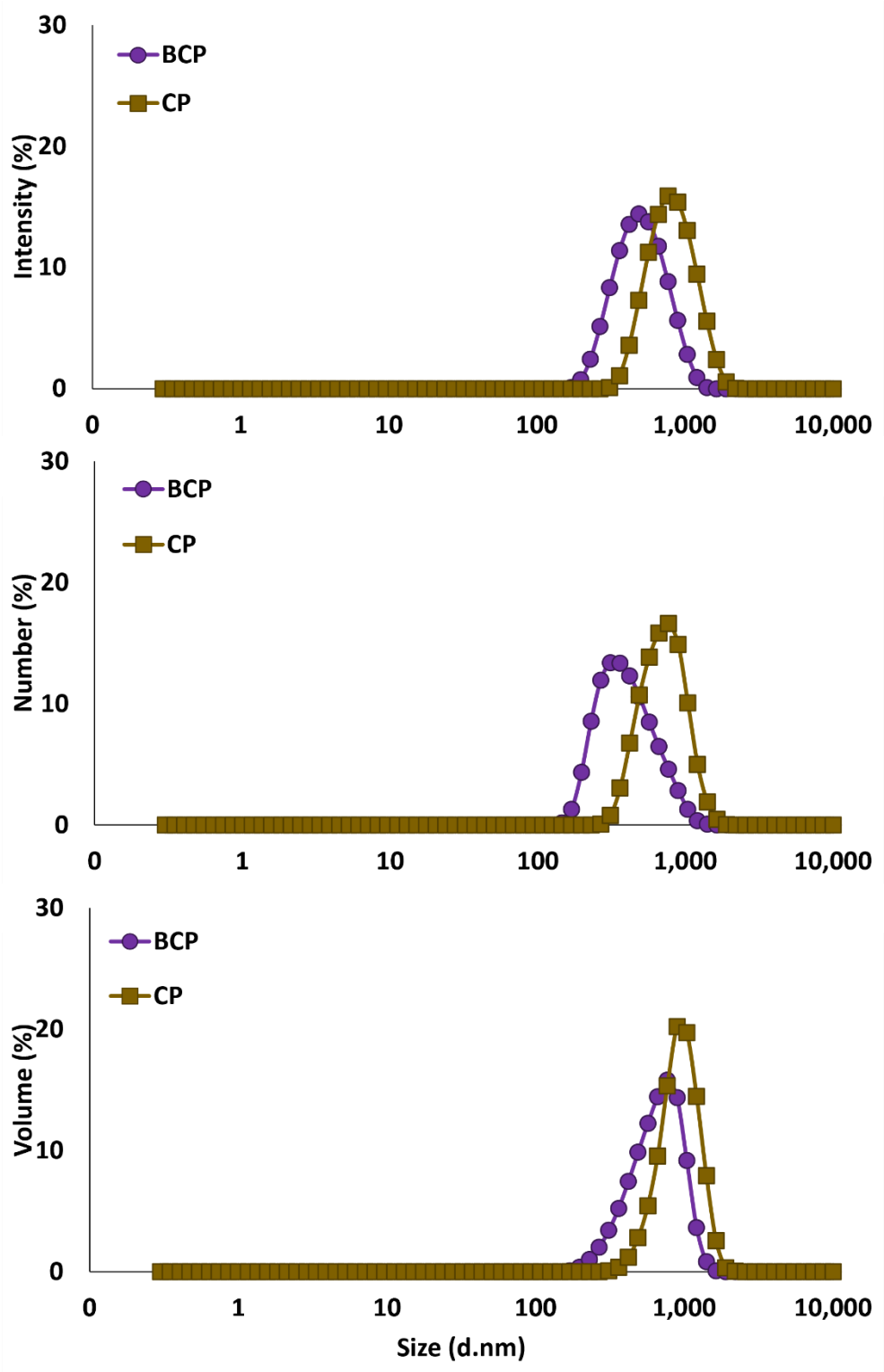

Figure B.1 Average size distribution of blackcurrant pectin (BCP) and citrus pectin (CP) at pH 4.5, based on intensity, number, and volume weighting mechanisms.